

Role of Fe-oxides for predicting phosphorus sorption in calcareous soils

Zur Erlangung des akademischen Grades eines

Doktors der Naturwissenschaften

An der Fakultät für Bauingenieur-, Geo- und Umweltwissenschaften

Der Universität Karlsruhe (TH)

genehmigte

DISSERTATION

von

Mehruinsa Memon

aus Pakistan

2008

Tag der mündlichen Prüfung: 7.5.2008

Referentin: Prof. Dr. Doris Stüben

Korreferent: Prof. Dr. Mohammad Saleem Akhtar

Abstract

The understanding of phosphorus-soil interactions is necessary for a high agronomic efficiency and for an environmentally profound management of P. The focus of this study was to characterize iron phases and P species in young alluvial and weathered residual soils to understand the contribution of these and further parameters in regard to P sorption in agricultural soils. Four surface horizons were sampled of nine different soils comprising five alluvial soils from arid/semi-arid region, one of loess, another one of shale origin (Pakistan), one of Muschelkalk origin and one of glacial loess origin (Germany). Soil clay minerals and iron oxides were examined by X-Ray diffraction, TG/DSC, TEM equipped with microanalysis, and by cyclic voltammetry. Soil P was sequentially extracted by NaHCO_3 , NH_4 -acetate, NH_4F , $\text{NaOH-Na}_2\text{CO}_3$, Na-dithionite, and remaining by digestion in H_2SO_4 solution. Phosphorus sorption isotherms were developed (1:10 soil solution ratio) and sorption parameters were derived from best-fit Langmuir and Freundlich models. The alluvial soils consist of silty loam to sand loam, with pH values higher than 8, CaCO_3 contents of 48 to 250 g kg^{-1} , and well crystalline goethite of 5 to 28 g kg^{-1} soil. The shale and loess derived soils consist of silty loam/silty clay characterized by pH value between 7.2 and 7.8, CaCO_3 contents of 2 to 30 g kg^{-1} and quantitatively higher contents but less well crystalline goethite and, in case of Murree soil hematite fractions, in addition. The Muschelkalk and glacial loess derived soils consist of silty clay characterized with pH value of 4.5 to 7.7, decalcified surface of 3 to 5 g kg^{-1} and CaCO_3 accumulation in the soil profile below 50 cm depth, and less crystallized but higher goethite content (17 to 34 g kg^{-1}). The soil clays were composed mostly of layered silicates. Apatite and octa-calcium phosphate contents were higher in the alluvial soils compared to the contents of residual soils where P adsorption and occlusion of iron oxides and organic P were higher. CBD and oxalate extractable iron and aluminum fractions and smectite and kaolinite contents were the dominant parameters for sorption selected through stepwise regression explaining 85 to 92% variation in the soil P fractions. The weathered soils showed higher sorption strength (k_f) and maximum sorption on high-affinity sites (b_1) while the alluvial soils showed higher maximum sorption on low-affinity sites (b_2). Modeling of this study indicates that soil CaCO_3 alone plays an insignificant role in explaining P sorption. Multiple regression calculations showed that the combination of various iron phases (Fe_d , Fe_o , Fe_{crst} , Gt_s), of soil clay, kaolinite, Al, exchangeable Ca, and CaCO_3 phases were the most important soil properties pertaining P.

Kurzfassung

Für eine hohe landwirtschaftliche Produktivität und einen umweltbewussten Umgang mit Phosphor ist es notwendig, die Wechselbeziehungen zwischen Phosphor und Bodenbestandteilen zu kennen und zu verstehen. Der Schwerpunkt dieser Arbeit lag auf der Charakterisierung von Eisenphasen und Phosphorspezies in jungen alluvialen, und verwitterten residualen Böden, um deren Beitrag sowie den Einfluss weiterer Parameter bezüglich der P-Sorption in landwirtschaftlich genutzten Böden zu verstehen. Vier oberflächennahe Bodenhorizonte von neun verschiedenen Böden wurden beprobt, davon fünf alluviale Böden aus ariden/semi-ariden Regionen, eine Boden aus einem Lössgebiet, ein weiterer auf Schiefertone (Pakistan), sowie jeweils ein Boden auf Muschelkalk und glazialen Löss (Deutschland). Tonminerale und Eisenoxide verschiedener Böden wurden mittels XRD (Röntgendiffraktometrie), TG/DSC (differential scanning calorimeter), TEM (Transmissions-Elektronenmikroskopie), das mit einer Mikroanalyse ausgestattet war, und mittels zyklischer Voltammetrie untersucht. Die Bindungsformen von Phosphor im Boden wurden anhand einer sequentiellen Extraktion mit NaHCO_3 , NH_4 -Acetat, NH_4F , $\text{NaOH-Na}_2\text{CO}_3$, Na-Dithionit bestimmt. Phosphor in der residualen Fraktion wurde durch einen H_2SO_4 -Aufschluss bestimmt. Zusätzlich wurden Sorptionsisothermen für Phosphor (1:10 Boden-Lösungs-Verhältnis) nach Langmuir und Freundlich aufgestellt.

Die alluvialen Böden bestehen aus schluffigem bis sandigem Lehm mit einem pH-Wert größer 8, einem CaCO_3 -Anteil von 48 – 250 g/kg und einem Anteil an kristallinem Goethit von 5 – 28 g/kg. Die Böden aus Löss und Schiefertone bestehen aus schluffigem Lehm bis schluffigem Ton, die einen pH-Wert zwischen 7,2 und 7,8, einen CaCO_3 Gehalt von 2 – 30 g/kg und quantitativ höhere Gehalte an allerdings schlechter kristallinem Goethit und im Fall des Bodens von Murree Hämatit aufweisen. Die Böden auf dem Muschelkalk und dem glazialen Löss bestehen aus schluffigem Ton und zeigen pH-Werte zwischen 4,5 und 7,7, einen entkalkten Oberboden mit 3 – 5 g/kg CaCO_3 und einer CaCO_3 Akkumulation im Bodenprofil unterhalb 50 cm Tiefe, sowie einem höheren Gehalt an schlechter kristallinem Goethit (17 – 34 g/kg). Die Tonminerale der Böden sind zumeist Schichtsilikate. Apatit und Oktacalciumphosphat sind in den alluvialen Böden im Vergleich zu den residualen Böden angereichert. In den residualen Böden hingegen, ist die P-Adsorption und der Einschluss (Okklusion) in Eisenoxiden und der Anteil an organischem P höher.

CBD (Citrate bicarbonate dithionite) und Oxalat-extrahierbare Eisen- und Aluminium-Fractionen, sowie die Gehalte an Smektit und Kaolinit sind die dominanten Parameter der P Sorption, die sich anhand einer schrittweisen Regression ergeben haben, und eine 85 – 92%ige Variation der P-Fractionen in den Böden erklärt. Die verwitterten Böden zeigen eine höhere Sorptionskraft (k_f) und eine maximale Sorption für die Stellen mit hoher Affinität (b_1), wohingegen die alluvialen Böden ein höheres Maximum für die Stellen mit schwacher Affinität (b_2) zeigen. Modellierungen in dieser Arbeit zeigen, dass CaCO_3 im Boden alleine eine eher untergeordnete Rolle bei der Erklärung der P Sorption spielt. Multiple Regressionsberechnungen verdeutlichen, dass die Kombination verschiedener Eisenphasen (Fe_d , Fe_0 , Fe_{crst} , G_{ts}), der Tonfraktion der Böden, Kaolinit, Aluminium, austauschbarem Ca und der CaCO_3 Phasen die wichtigsten Bodeneigenschaften in Bezug auf die P-Sorption sind.

Acknowledgements

I am grateful to Professor Dr. D. Stueben, for supervising my Ph.D research at the Institute of Mineralogy and Geochemistry, University of Karlsruhe. Her valuable suggestions, support throughout the research and critical review of the manuscript is highly appreciated.

Professor Dr. M. S. Akhtar, University of Arid, Agriculture Pakistan has been the core person for soil related information and techniques. His expertise, love and dedication in the subject with special reference to soil mineralogy helped me to improve this work. I appreciate his help.

I am thankful to the Ph.D committee members Dr. D. Bosbach, for his valuable questions during my presentations, Professor Dr. D. Burger for briefing on Weingarten location and specially Professor H.G. Stosch for his fair support in Ph.D registration, in particular his presence late in the evenings at the institute made it possible to continue my work.

Dr. Z. Berner contributed a lot to run this research smoothly. He was always there to encourage, guide, suggest, solve and sometimes just be there by saying “Every thing ok?, you will complete in time!”. I thank him for this support. I am thankful to Dr. Th. Neumann, Institute of Mineralogy and Geochemistry for the ICP-OAS measurements, with special reference to phosphorus, Professor E. Hoffmann, Institute für Wasser und Gewässerentwicklung, for allowing me to use the digestion unit at short notice, Dr. K. Emmerich and her students K. Petrick and A. Steudel, Institute for Technical Chemistry, Water Technology and Geotechnology Division, Forschungszentrum Karlsruhe for STA analysis, V. Zibat for microprobe and SEM analysis, and M. Fatouhi, for the TEM analysis.

Technical and analytical assistance throughout my Ph.D research was accorded from the institute by C. Haug, B. Oetzel, with special reference to G. Preuß, C. Mößner, K. Nikoloski, and P. Schaupp.

M. Tannhäuser, H. Nitz, R. Bender are acknowledged for their administrative support all along my Ph.D.

I am grateful to S. A. Shah, Director General, Soil Survey Pakistan, M. Gul, Deputy Director, Soil Survey, Regional Office, Peshawar, Professor Dr. K. S. Memon, Sindh Agriculture University Tando Jam and Mr. A. H. Ansari, for their help regarding soil maps, sampling and photography of Pakistan soils. Thanks to Dr. S. Norra for German soil maps.

I am thankful to my husband Ali Mohammad and my daughter Uswa who have given me the energies, love, and support to stay this far and complete the work, my parents Dr. Kazi Suleman and Mumtaz Memon, my brothers and sisters for their support, all my friends with special thanks to Abiz on computer help and Steffi, Eli and Nina for German translation of the Abstract.

Related publications

Papers published

Puno, H.K., K.S. Memon and **M. Memon**. 2004. Phosphorus fertility buildup under different cropping systems. Pak. J. Agri., Agril. Engg. Vet. Sc. 20(1):1-4.

Solangi, M.A., **M. Memon** and H.K. Puno. 2006. Assessment of phosphorus in soils of district Shikarpur, Pakistan. International J. of Agri. & Biol. 8(4):565-566.

Shaikh, K., K.S. Memon, M. Memon, M.S. Akhtar. 2007. Changes in mineral composition and bioavailable potassium under long-term fertilizer use in cotton-wheat system. Soil and Environ. 26(1):1-9.

Papers presented

- “Iron oxides characterization and quantification occurring in low concentration in soils” at 10th International Symposium on Soil and Plant Analysis, at Hotel Mercure Buda, Budapest, Hungary, June 11-15, **2007**.
- “Phosphorus uptake and yield response of wheat for evaluating the availability of residual and applied phosphorus” at 10th Congress of Soil Science for Management of Natural Resources for Food and Security at Sindh Agriculture University Tando Jam, March 16-19, **2004**.
- “Comparison of NaHCO₃, NH₄HCO₃-DTPA and CaCl₂ soil tests for available phosphorus”, at 7th National Symposium on Analytical and Environmental Chemistry, at Center of Excellence in Analytical Chemistry, University of Sindh Jamshoro, March 4-5, **2003**.

Papers submitted

- **Memon, M.**, K.S. Memon, M.S. Akhtar, D. Stüben. “Iron oxides characterization and quantification occurring in low concentration in soils”. Submitted to Communications in Soil Science and Plant Analysis. In year **2007**.
- Memon, K.S., A.J. Jarwar, **M. Memon** and Zia-ul-Hassan. Development of a correction factor to account for the effect of temperature on Olsen’s soil phosphorus. Submitted to Communications in Soil Science and Plant Analysis. In year **2007**.

Table of Contents

Abstract.....	i
Kurzfassung	ii
Acknowledgements.....	iii
Related publications.....	iv
Table of Contents.....	v
List of Figures.....	viii
List of Tables.....	xi
List of Appendices.....	xii
Abbreviations.....	xiii
1. Motivation.....	1
2. Introduction.....	3
2.1. Iron oxides.....	5
2.1.1. Goethite.....	5
2.1.2. Hematite.....	6
2.1.3. Formation of iron oxides.....	7
2.1.4. Nature of charge.....	9
2.1.5. Specific adsorption by phosphate on iron oxides.....	11
2.1.6. Identification and quantification of iron oxides.....	13
2.2. Soil phosphorus.....	14
2.2.1. Species in soil.....	14
2.2.2. Fertilizer P	16
2.2.3. Processes of soil P.....	16
2.2.4. Determination of P-Speciation.....	19
2.2.5. Phosphorus sorption isotherms.....	20
3. Materials and Methods.....	23
3.1. Study area	23
3.1.1. General profile description.....	33
3.1.2. Characteristics of the individual soil profiles	34
3.2. Basic soil properties.....	42

3.2.1. Iron and aluminum oxide determination by CBD method.....	42
3.2.2. Iron and aluminum oxide determination by ammonium oxalate method.....	42
3.2.3. Soil elemental Analysis by XRF.....	43
3.3. Soil fractionation and particle size analysis.....	43
3.3.1. Pretreatments.....	43
3.3.2. Separation into sand, silt and clay fractions.....	44
3.4. Soil mineralogy.....	44
3.4.1. Sand, silt and clay mineralogy by X-ray diffraction.....	44
3.4.2. Smectite and vermiculite quantification by CEC.....	45
3.4.3. Kaolinite quantification by STA.....	46
3.5. Iron oxide determination.....	47
3.5.1. Pre-concentration and phase identification by XRD	47
3.5.2. Iron oxide determination by cyclic voltammetry.....	48
3.6. Phosphorus determination.....	49
3.6.1. Total phosphorus.....	49
3.6.2. Sequential extraction of inorganic phosphorus.....	49
3.6.3. Phosphorus sorption isotherms.....	50
3.7. Transmission electron microscopy (TEM).....	51
3.8. Statistics.....	51
4. Results.....	52
4.1. Basic soil properties.....	52
4.2. Soil mineralogy.....	59
4.2.1. Sand and silt mineral composition by XRD.....	60
4.2.2. Clay (<2 μm) mineral composition by XRD.....	61
4.3. Iron Oxide.....	68
4.3.1. Iron Oxide phase identification by XRD.....	68
4.3.2. Quantification of iron oxide in clay by voltammetry.....	74
4.4. Phosphorus sorption.....	76
4.4.1. Freundlich sorption parameters.....	77
4.4.2. Langmuir sorption parameters.....	80
4.5. Phosphorous fractions.....	86
4.5.1. Total phosphorus.....	86
4.5.2. Total organic P.....	87

4.5.3. Total sum the of sequentially extracted inorganic fractions.....	88
4.5.4. Overall distribution of sequentially extracted P fractions.....	97
4.6. Microanalysis of P saturated clay.....	97
5. Discussion.....	103
5.1. The soils and their mineral composition.....	103
5.2. Soil iron oxides.....	105
5.3. Phosphorus sorption and its relation with soil matrix components...	109
5.4. Soil phosphorus fractions.....	115
6. Summary.....	124
7. References.....	128
8. Appendices.....	145

List of Figures

Figure 2.1:	Goethite structure.....	6
Figure 2.2:	Hematite structure.....	7
Figure 2.3:	Representation of competitive process of goethite and hematite formation and factors influencing it.....	9
Figure 2.4:	The reaction of surface groups of iron oxide particles with water.....	10
Figure 2.5:	The net variable charge on the surface (point zero charge, PZC).....	11
Figure 2.6:	Bidentate arrangement.....	12
Figure 2.7:	The soil P cycle in calcareous soil environment.....	15
Figure 2.8:	Adsorption, absorption and occlusion of P.....	18
Figure 3.1:	Map of Pakistan showing overall sampling areas.....	25
Figure 3.2:	Location map of Shahdara, Sultanpur, Pacca and Pitafi soils.....	26
Figure 3.3:	Location map of Peshawar soil.....	27
Figure 3.4:	Location map of Guliana soil.....	28
Figure 3.5:	Location map of Murree soil.....	29
Figure 3.6:	Map of Baden Wurttemberg, Germany showing the overall sampling sites for Prb-Ostb and Prb-Wein soils.....	30
Figure 3.7:	Location map of Prb-Ostb soil.....	31
Figure 3.8:	Location map of Prb-Wein soil.....	32
Figure 4.1:	Sand, silt and clay distribution on CaCO ₃ and organic matter free basis.....	53
Figure 4.2:	Soil CaCO ₃ distribution in the profiles.....	54
Figure 4.3:	Distribution of soil organic matter in the profiles.....	55
Figure 4.4:	Citrate bicarbonate dithionite extractable iron (Fe _d) and ammonium oxalate extractable iron (Fe _o) distribution in the soil profiles.....	56
Figure: 4.5:	Citrate bicarbonate dithionite extractable aluminum (Al _d) and ammonium oxalate extractable aluminum (Al _o) distribution in the soil profiles.....	57
Figure 4.6:	Zirconium/titanium (Zr/Ti) and sand/silt ratio in the soil profiles.....	59
Figure 4.7:	Sand and silt mineralogy of Sultanpur soil: Q, quartz; M, mica; Ch., chlorite, K-feld., K-feldspar.....	61
Figure 4.8:	X-ray diffraction pattern for clay (<2μm) (a) Shahdara C1, (b) Guliana Ap, (c) Murree from Ap horizon and (d) Prb-Ostb Bv: Mg-Gly., Mg saturated and glycolated; Mg-25, Mg saturated and air-dried; K-25, K saturated and air-dried; K-350, K saturated and heated at 350°C; and K-550, K saturated and heated at 550°C.....	63

Figure 4.9:	TG and DSC curves for Murree (Bt1), Guliana (Batac) and Prb-Wein (Bv) soil clays.....	65
Figure 4.10:	Clay mineral composition of the soils.....	67
Figure 4.11:	X-ray diffraction patterns of clay (<2 μ m) before (I) and after (II) pre-concentration treatment: (a) Shahdara C2 (32-63 cm), and (b) Prb-Wein Bv (4-25 cm) showing goethite, (c) Murree Bt1 (11-43 cm) showing hematite and (d) Peshawar Bt1 (11-43 cm) showing both goethite and hematite.....	70
Figure 4.12:	Transmission electron micrographs of alluvial soils showing well crystalline goethite particles.....	71
Figure 4.13:	Transmission electron micrographs of weathered residual soils showing less crystalline goethite particles.....	72
Figure 4.14:	Transmission electron micrographs of shale derived soils showing well to poorly crystalline goethite and hematite particles.....	73
Figure 4.15:	Goethite distribution in the soil profiles (hematite in case of Murree)...	75
Figure 4.16:	Phosphorus sorption isotherms.....	76
Figure 4.17:	Freundlich sorption parameters.....	78
Figure 4.18:	Profile distribution of the Freundlich parameters b and k_f	80
Figure 4.19:	Langmuir sorption parameters.....	82
Figure 4.20:	Maximum P sorption distribution in the soil profiles as determined by Langmuir equation: (a) related to high-affinity sorption sites b_1 and (b) related to low-affinity sites b_2	84
Figure 4.21:	Phosphorus binding affinity distribution in the soil profiles as determined by Langmuir equation: (a) related to high-affinity sorption sites k_1 and (b) related to low-affinity sites k_2	85
Figure 4.22:	Distribution of total P content determined by HClO ₄ acid digestion and total organic P by difference of the total P and sum of inorganic fractions of the soils.....	87
Figure 4.23:	Distribution of total inorganic P content (calculated from sum of inorganic P fractions), and the apatite P (extracted by H ₂ SO ₄ digestion) fraction of the soils.....	89
Figure 4.24:	Distribution of Fe-P fraction extracted by NaOH-Na ₂ CO ₃ and occluded-P extracted by Na-dithionite in soils.....	91
Figure 4.25:	Distribution of Ca ₂ -P extracted by NaHCO ₃ and Ca ₈ -P extracted by NH ₄ -acetate in the soils.....	94
Figure 4.26:	Distribution of the Fe co-extracted with P (a) in NaOH-Na ₂ CO ₃ and (b) Na-dithionite in the soils.....	95
Figure 4.27:	Comparative distribution of P and the co-extracted Fe in Na-dithionite and NaOH-Na ₂ CO ₃ in the (a) Guliana soil, (b) Pacca soil, and (c) Murree soil.....	96

Figure 4.28:	Distribution of proportion of various inorganic P fractions in the soils.....	98
Figure 4.29:	TEM images with relevant EDX spectra of P saturated goethite particles from alluvial soil clays.....	99
Figure 4.30:	TEM images with relevant EDX spectra of P saturated goethite particles from weathered soil clays.....	100
Figure 4.31:	TEM images with relevant EDX spectra of P saturated goethite particles from shale derived soil clays.....	101
Figure 5.1:	Schematic diagram depicting relationship between P sorption parameters and P fractions with soil properties: The inward arrows on both sides indicate negative relationship and the outward arrows on both sides indicate positive relationship.....	121

List of Tables

Table 3.1:	Soil classification and environment.....	33
Table 3.2:	Simultaneous thermal analysis measurement.....	47
Table 4.1:	Mean goethite calculated on clay content and soil bases in the profiles.....	75
Table 4.2:	Soil mean of Freundlich parameters.....	79
Table 4.3:	Mean values of two-surface Langmuir parameters.....	83
Table 4.4:	Total soil P (extracted by H ₂ SO ₄ digestion method), total inorganic P (sum of inorganic P fractions) and organic P (the difference between total P and inorganic P).....	88
Table 4.5:	Soil P fractions extracted by NaOH-Na ₂ CO ₃ (Fe-P), by sodium dithionite (occluded P) and extracted by NH ₄ -F (Al-P).....	90
Table 4.6:	Soil phosphorus fractions extracted by NaHCO ₃ (Ca ₂ -P) and NH ₄ -acetate (Ca ₈ -P).....	93
Table 5.1:	Stepwise multiple regression equations between soil properties and Freundlich parameters.....	111
Table 5.2:	Stepwise multiple regression equations between soil properties and the Langmuir parameters.....	114
Table 5.3:	Stepwise multiple regression equations between soil properties and total P, total inorganic P and apatite P.....	117
Table 5.4:	Stepwise multiple regression equations between soil properties and Fe-P and occluded P fractions.....	119
Table 5.5:	Stepwise multiple regression equations between soil properties and Ca ₂ -P and Ca ₈ -P fractions.....	120
Table 5.6:	Multiple regression equations between Olsen P and soil properties.....	123

List of Appendices

Appendix I:	Selected properties of the soils.....	145
Appendix II:	Major and trace elemental analysis of the soils as determined by XRF.....	146
Appendix III:	X-ray diffraction pattern of sand (>50 μm) and silt (2-50 μm) fractions from the profiles: Q, quartz; Feld, feldspar; K-feld, potassium feldspar; M, mica; Ch, chlorite.....	147
Appendix IV:	X-ray diffraction pattern for clay (<2 μm) size fraction from soil profile: Mg-Gly., Mg saturated and glycolated; Mg-25, Mg saturated and air dried; K-25, K saturated and air dried; K-350, K saturated and heated at 350°C; and K-550, K saturated and heated at 550°C. Sm, Smectite; Vm, vermiculite; Ch, chlorite; M, mica; K, kaolinite.....	157
Appendix V:	TG/DSC patterns for the soil clays.....	190
Appendix VI:	Vermiculite, smectite, kaolinite, goethite and hematite content of soil clays.....	200
Appendix VII:	X-ray diffraction pattern for clay (<2 μm) size fraction from soil profile: before (I) and after (II) pre-concentration treatment showing goethite/hematite. Gt, goethite; Hm; Q, quartz; and M, mica. Goethite is represented by diffraction lines at 4.18, 2.69, and 2.45 Å. Hematite is represented by diffraction lines 2.70, 2.52, 2.21, and 1.84 Å.....	201
Appendix VIII:	Phosphorus adsorption isotherms where P adsorbed, (x/m mg kg ⁻¹) is plotted against equilibrium concentration (mg L ⁻¹). The inset in each case depicts the initial part of isotherm.....	210
Appendix IX:	Phosphorus adsorption isotherms fitted to Freundlich equation.....	220
Appendix X:	Freundlich and Langmuir parameters.....	230
Appendix XI:	Phosphorus fractions (inorganic) as sequentially extracted, sum of inorganic P fractions, organic P and total P of the soils.....	231
Appendix XII:	Pearson coefficient correlation for seven best selected correlations.....	232

Abbreviations

Al_d	CBD extracted aluminum
Al_o	Oxalate extractable aluminum
Al_o/Al_d	Ratio of oxalate extractable aluminum to CBD aluminum
Al-OM	Aluminum-organic matter
Al-P	Aluminum phosphorus
b_1	Maximum sorption at high affinity sites (Langmuir parameter)
b_1/b_2	Ratio of maximum sorption at high affinity sites to low affinity sites
b_2	Maximum sorption at low affinity sites (Langmuir parameter)
b_f	Freundlich b parameter
b_{nonlin}	Maximum P sorption as fitted by non-linear Langmuir
Ca_{10-P}	Apatite phosphorus
Ca_2-P	Di-calcium phosphate
Ca_8-P	Octa-calcium phosphate
Ca_{ex}	Exchangeable calcium
Ca-P	Calcium phosphate
CBD	Citrate bicarbonate dithionite
CEC	Cation exchange capacity
$cmol_c$	Centi-mole of cation
CPEE	Carbon paste electroactive electrode
DRS	Diffuse reflectance spectroscopy
$dS\ m^{-1}$	Deci- Simon per meter
EC	Electrical conductivity
EDX	Energy dispersive X-ray analysis
FAO	Food and agriculture organization
Fe_{CBD}	Iron in occluded P fraction
Fe_{crs}	Crystalline iron
Fe_d	CBD extractable iron
Fe_{NaOH}	Iron in Fe-P fraction
Fe_o	Oxalate extractable iron
Fe_o/Fe_d	Ratio of oxalate extractable iron to CBD extractable iron
Fe-P	P adsorbed on iron oxide
Gt_c	Goethite on clay percent basis
Gt_s	Soil goethite
HIS/HIV	hydroxyinterlayer smectite/vermiculite
ICP-OES	Inductively coupled plasma optical emission spectrometer
k_1	Binding energy at high affinity sites (Langmuir parameter)
k_2	Binding energy at low affinity sites (Langmuir parameter)
k_f	Freundlich k parameter
Kl	Kaolinite

k_{nonlin}	Binding energy as fitted by non-linear Langmuir
OM	Organic matter
P	Phosphorus
$P_{2\text{ppm}}$	P sorbed to achieve 2 ppm solution P concentration
P_{ocl}	Occluded P (trapped into iron oxide coatings)
P_{olsen}	Phosphorus determined by Olsen's method
P_{om}	Organic P
Prb-Ostb	Parabraunerde from Osterburken
Prb-Wein	Parabraunerde from Weingarten
P_{T}	Total P
P_{tin}	Total inorganic P
PZC	Point of zero charge
Rpm	Rotations per minute
SAS	Statistical analysis system
Sm	Smectite
STA	Simultaneous thermal analysis
TEM	Transmission electron microscopy
TG/DSC	Thermogravimetry/differential scanning calorimetry
UV/Vis	Ultraviolet/visible
Vm	Vermiculite
WD-XRF	Wavelength dispersive X-ray fluorescence
XRD	X-ray diffraction
YR	Yellow red

1. Motivation

Plant available soil phosphorus (P) level in soil is generally too low for sustained crop yields; therefore, application of inorganic fertilizer P becomes necessary for commercial crop production (Fox and Kamprath, 1970). In soils, plants take up less than 20% of applied P and the remaining is immobilized (Bürkert et al., 2001). Phosphorus fertilizer use efficiency is especially low in calcareous soils (Memon et al., 1991).

The poor mobility of soil inorganic P is thought to be due to (1) low dissolution rate of inorganic P species, (2) sorption of phosphate ions onto iron and aluminum oxides in acidic and onto CaCO_3 in calcareous soils, and (3) conversion to relatively insoluble species; thus P becomes fixed in the soil matrix (Hinsinger, 2001). Calcareous soils have some level of iron oxides, either as discrete mono-mineralic phases or as aggregates with other phases as coatings on other mineral particles. Thus phosphate sorption in calcareous soils may also be controlled by the presence of iron oxides similar to that in acidic soils (Holford and Mattingly, 1975; Parfitt, 1978; Ryan et al., 1984; Ryan et al., 1985; Solis and Torrent 1989; Beauchemin et al., 2003; Manojlovic et al., 2007).

Phosphorus retention by iron oxides in calcareous system has been studied using synthetic samples (e.g. Bertrand et al., 2001; Yuji and Sparks, 2001; Karageorgiou et al., 2007), most probably due to the ease of the medium. Quantification of low contents of iron oxides in calcareous soils is still a challenge (Grygar et al., 2002; Memon et al., 2008). Much is to be explored regarding P sorption by natural iron oxides in calcareous environment.

The majority of soils of Pakistan are calcareous where crop production is done, fertilizer P efficiency is therefore low and fertilizer P is an expensive input for resource poor farmers. Fertilizer P use in developed countries may be cost effective, excessive use over the crop needs adversely affects ecosystem as P enters into the freshwater bodies through surface runoff carrying particulate and soluble P species from the P-enriched croplands.

The basic motivation comes from the fact that P fertilizer recommendations in these soils, as currently practiced, are not site specific, while level of P in solution is controlled by many factors including CaCO_3 , clay content and the quantities and type of iron oxide (e.g. goethite and hematite) present in soil. It is therefore essential to understand the processes and parameters contributing to P sorption in soils with wide ranging characteristics.

Phosphorus research on Pakistani soils has mainly focused on the soil-P test based on crop-response. Preliminary data regarding critical levels of P for some important crops have been presented (Memon et al., 1991). However, such information cannot be translated into P fertilizer recommendations unless additional data are also available on some measure of P sorption.

It is anticipated that this study will provide useful data and new dimension to the efforts for site-specific fertilizer recommendations and formulation of fertilizer management strategies.

2. Introduction

Bioavailability of phosphorus (P) has been a major research field of soil science. Small concentrations of phosphates in soil solution compared with plant requirement, and apparently small recovery of fertilizer phosphate stimulated tremendous research (Delgado et al., 2000; Beauchemin et al., 2003; von Wandruszka, 2006). Earlier P research focused on P nutrition in plants (Speter, 1935) while later work concentrated maximizing P supply for cultivated plants and attempting yield targets (Rajan, 1975; Memon and Fox, 1983; Fox, 1989). Today, an increasing number of scientists work on reducing the agricultural P inputs and balancing the production with environmental values (Hedley and Sharpley, 1998; Sims et al., 2000; Yuji and Sparks, 2001; Bertrand et al., 2001; Zhang et al., 2005). The studies have concentrated on the reactions of added phosphate with soil constituents and on mechanisms controlling the amount of phosphate in solution.

Researchers of the mid-nineteenth century related the retention of P to the presence of iron oxides in acidic soils and to CaCO_3 in neutral and alkaline calcareous environment (Borggard, 1983; Lindsay et al., 1989). Strong relationship between CaCO_3 and P was reported by Lajtha and Bloomer (1988) and phenomenon was ascribed to precipitation of P with Ca ions as dicalcium phosphate and surface precipitation on solid CaCO_3 (Mackay et al., 1986). It was also related to increased surface area of CaCO_3 particles (Holford and Mattingly, 1975).

Recent studies have shown that iron minerals play a dominant role in P sorption compared to Ca minerals (Matar et al., 1992; Hinsinger, 2001; Zhou and Li, 2001; Zhang et al., 2005). It has been further confirmed that relative quantities of P occluded to iron oxides are not necessarily related to the degree of P enrichment in soils (Dominguez et al., 2001). Hence smaller concentrations of either iron or phosphates are not valid criteria to negate P sorption in alkaline calcareous soils.

The role of iron oxides has been highlighted in wide range of calcareous soils (Ryan et al., 1985; Hamad et al., 1992; Shen et al., 2004; von Wandruszka, 2006). The stronger relationship on P sorption using hydrous iron oxides compared to soil CaCO_3 (Solis and Torrent, 1989; Hamad et al., 1992; Simard et al., 1994; Beauchemin et al., 2003; Manojlovic et al., 2007), and with quantity and type of iron oxides have been reported (Colombo et al., 1991; Frossard et al., 1995).

Phosphorus sorption on iron oxides explains the soil P behaviour better and precipitation becomes dominant only under high concentration of phosphate ions (Castro and Torrent, 1998), which is never the case in most calcareous soil systems (Delgado and Torrent, 2000; von Wandruszka, 2006). In low concentrations, P initially adsorbs on iron oxide surfaces through ligand exchange reaction and is later trapped through occlusion (Lindsay et al., 1989; Tunesi et al., 1999; Hinsinger, 2001; Parfitt et al., 1976; Goldberg and Sposito, 1985; Torrent et al., 1992).

Despite an increasing interest in P sorption on iron oxides, numerous sorption studies have been conducted using only synthetic iron oxides. Considerably less is known about natural systems (Bigham et al., 2002), especially in calcareous environment where the mechanisms of P sorption and strength and reversibility of sorption can differ substantially. Since build-up of P is affected by the nature of P species in soil varying widely with location, redox and pH conditions, soil type and management system (von Wandruszka, 2006), each soil may have different mechanisms for P mobility and transfer (Haygarth et al., 2000) and hence variable buffering coefficients.

The importance of P for crop production is obvious from the worldwide P fertilization. The chemistry of P has been investigated in developed countries on mostly highly weathered and acidic soils (Frossard et al., 1995; Sinaj et al., 1992; Said and Dakermanji, 1993). Parallel studies have not been carried out in developing countries where the P deficiency is wide spread and high cost of inorganic fertilizers limits its application. The serious gap in knowledge hinders improving fertilizer use efficiency while economy of these countries relies on the progress of the agriculture sector.

For complete understanding of bio-availability it is essential to elucidate the processes involved in P sorption. There is a need to indicate the relative association of P with soil minerals such as a suite of natural iron oxides in calcareous soil matrix at a nano-mineral level. Therefore, this study highlights the importance of iron oxides and hypothesises that “even the small fractions of iron oxides influence P sorption than actually the CaCO_3 itself“. The specific objectives are:

- Identification of different iron oxide phases (goethite and hematite) to assess their contribution of P sorption
- Investigation of the role of clays, especially iron oxides in regard to P sorption in calcareous soils
- Determination of the relationship of soil properties to P sorption.

2.1 Iron oxides

Iron oxides are the most abundant metallic oxides in soils. Iron oxides occur in most soils (Allen and Hajek, 1989). They are present in most soils of different climatic regions as very fine particles in one or more different mineral forms and at variable levels of concentrations. They may occur evenly dispersed throughout the soil in horizons with a friable or loose consistency or concentrated in discrete horizons or in particular morphological features as mottles, nodules, etc. Soil iron oxides have a high pigmenting power and determine the color of soils. Because iron oxide surfaces have a strong affinity for the oxyanions of P and for transition metals, they play a significant role in the environmental cycling of these elements (Schwertmann and Taylor, 1989; Cornell and Schwertmann, 1996; Kämpf et al., 2002). Beside, iron exists in primary minerals (biotite, pyroxene, amphibole, and olivine). Different names have been used such as “free” or “combined iron oxides” (Jackson, 1965). Here the term “iron oxides” is used which refers to oxides, hydroxides and oxyhydroxides of iron (Bigham et al., 2002). Of the 14 iron oxides, 10 are known to occur in nature. The most widespread iron oxides in soils, having high thermodynamic stability are crystalline (with an ordered arrangement of ions) goethite and hematite.

2.1.1 Goethite

Goethite (α -FeOOH), an oxy-hydroxide is named after the famous German poet (and mineralogist) Johann Wolfgang von Goethe (Schroeder, 1988). It is an abundant mineral in tropical and subtropical soils of the world and gives yellowish brown color to soils (Schwertmann, 1985). Goethite is often the sole pedogenic iron oxide in soils formed in cool and temperate climates and hematite often occurs in soils in warmer climates (Schwertmann and Taylor, 1989). Consequently it is either one of the first iron oxide to form or the final product of transformations (Fig. 2.3). In goethite structure, Fe (III) ions occupy one half of the octahedral positions within a layer to produce double chains of octahedral linked by corner-sharing and separated by double chains of vacant sites that appear as tunnels in polyhedral models. Fe-O-Fe and H bonds on binding the octahedra to neighboring double chain octahedra (Fig. 2.1).

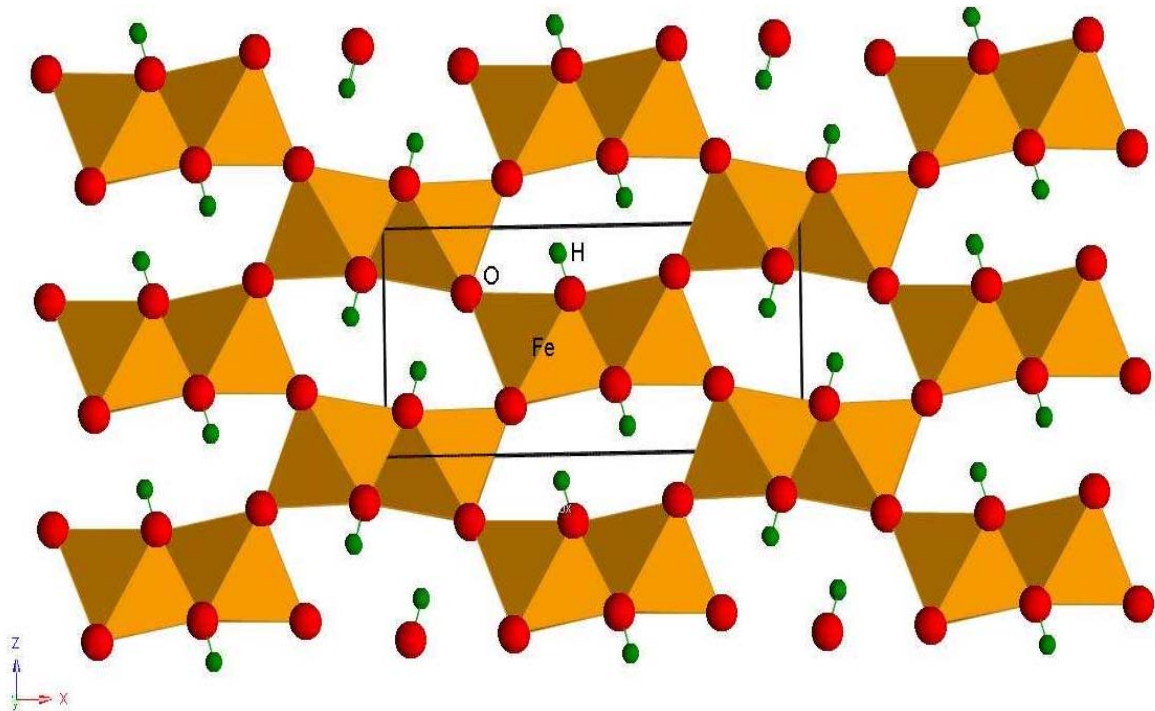


Figure 2.1: Goethite structure [CrystalMaker 1.4].

2.1.2 Hematite

Hematite ($\alpha\text{-Fe}_2\text{O}_3$), another well-developed crystalline iron oxide is wide spread in soils and has high thermodynamic stability. It is responsible for rich red color of soils (Schwertmann and Taylor, 1989). Hematite consists of a close-packed array of O atoms stacked along (011) with Fe (III) ions occupying two of every three octahedral sites. So the structure of hematite can be visualized as a stack of di-octahedral sheets with adjacent sheets having a common plane of oxygen. As a result, each FeO_6 octahedron shares edges with three neighboring octahedra in the same plane and a side is shared with an octahedron in an adjacent plane (Fig. 2.2).

Pedogenic hematite is abundant in arid and semi-arid regions as well as the humid and monsoonal tropics. It is also common in Mediterranean climates and elsewhere in the temperate zone with high carbonate parent material (Bigham et al. 2002). Hematite may also form in cooler climates, provided there is a marked dry period during the year (Bresson, 1974; Schwertmann et al., 1982).

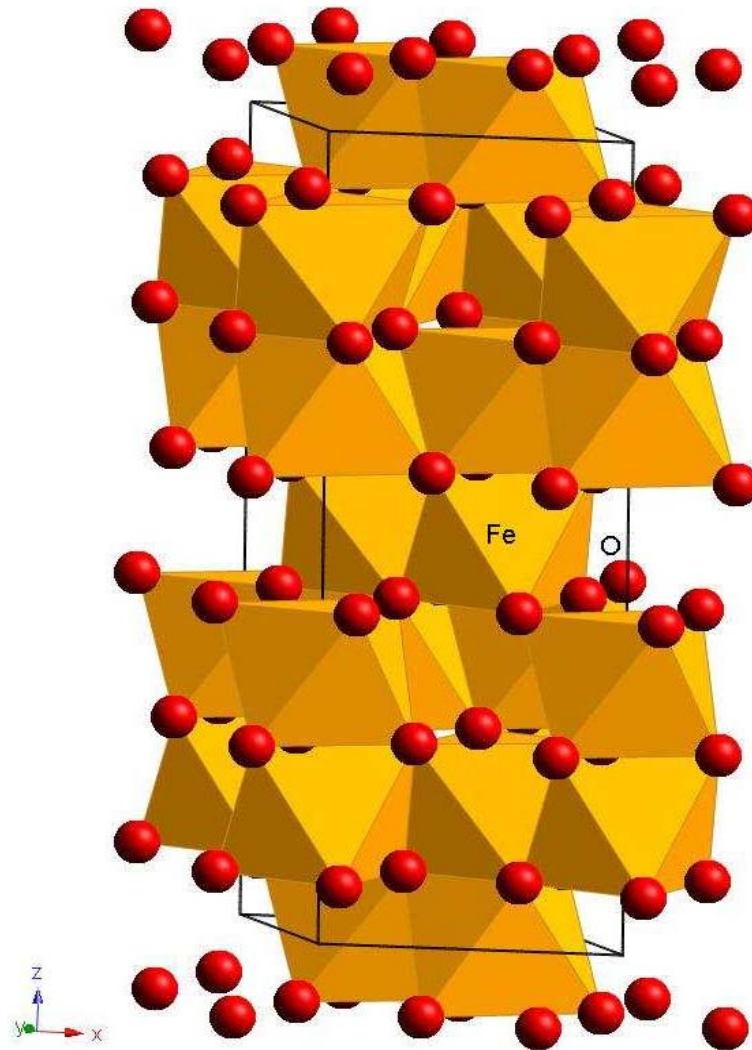


Figure 2.2: Hematite structure [Schwertmann and Taylor, 1989, CrystalMaker 1.4].

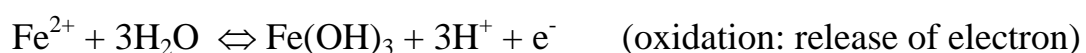
2.1.3 Formation of iron oxides

Iron in primary minerals occurs as divalent cation and is released after protonation or oxidation. The mechanism of Fe release is the breakdown of silicate by the following protonation reaction:

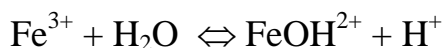


The released Fe^{2+} is oxidized immediately. When oxidation of Fe^{2+} occurs inside the mineral, it results in charge imbalance and weakening of the crystal structure, which facilitates breakdown.

The oxidation of Fe^{2+} to Fe^{3+} can be written as:



Once the Fe^{3+} is released, it will be hydrolyzed when it comes in contact with H_2O .



The resulting iron oxides have extremely low solubility products (Schwertmann and Taylor, 1989). The nature of iron oxides formed by weathering is more dependent on environmental conditions than on particular structure of the primary mineral from which iron has been released (Cornell and Schwertmann 1996).

Figure 2.3 shows that once ferrihydrite is formed, it can act as a source of hematite and goethite. The small arrows indicate that increasing or decreasing expression of the factor favours hematite formation (and vice versa for goethite). Higher soil temperature may induce dehydration of ferrihydrite and thereby reinforce hematite formation and accelerate iron release. Organic matter decomposition favours hematite formation. A study of tropical and subtropical soils showed a general lack of ferrihydrite alongside of hematite, which suggests that the direct transformation to hematite can also occur (Schwertmann and Taylor, 1989). Soil temperature and H_2O activity are acting directly on the dehydration and rearrangement of ferrihydrite to yield hematite. As pH rises from 4 to 8, the activity of the $\text{Fe}(\text{OH})_2^+$ ion decreases, reducing the rate of goethite formation in favor of hematite. These studies suggest that ferrihydrite can be a necessary precursor of hematite. This process appears likely because ferrihydrite already possesses a hematite-type structure, except that it is highly disordered and contains water (Feitknecht and Michaelis, 1962; Schwertmann and Fischer, 1966; Chukhrov et al., 1973).

Goethite formation involves nucleation and crystal growth from a solution of Fe^{3+} , $\text{Fe}(\text{OH})_2^+$, and $\text{Fe}(\text{OH})_4^-$ ions (Churchman, 2002). It has been reported that the formation of goethite is favored when carbonates or CO_2 are present in the system (Schwertmann and Taylor, 1977). The hypothesis that goethite formation is favored in calcareous system was confirmed by synthesis studies which showed that CO_3^{2-} favors the formation of goethite (Cornell and Schwertmann 1996).

The oxides formed have low solubility, reverse hydrolysis only occurs at very low pH, which is improbable in soils because the pH is seldom low enough to permit the reverse hydrolysis reaction ($\text{FeOOH} + 3\text{H}^+ \Leftrightarrow \text{Fe}^{3+} + \text{H}_2\text{O}$) to occur. However, remobilisation is more likely possible through reductive dissolution reaction: $\text{FeOOH} + \text{e}^- + 3\text{H}^+ \Leftrightarrow \text{Fe}^{2+} + 2\text{H}_2\text{O}$.

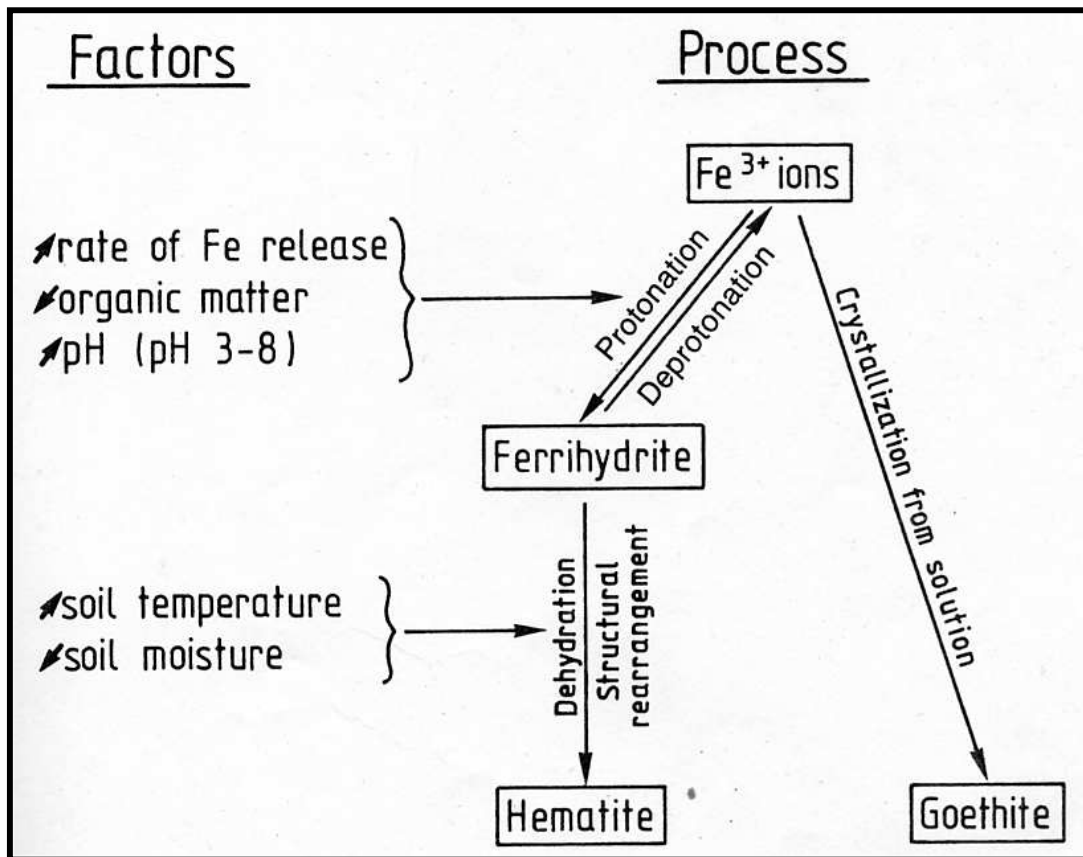


Figure 2.3: Representation of competitive process of goethite and hematite formation and factors influencing it [Schwertmann and Taylor, 1989].

2.1.4 Nature of charge

Iron oxides have variable charge with little or no permanent charge parallel to phyllosilicates. Charge of iron oxides (negative or positive) depends on adsorption of H^+ and OH^- from solution (McBride, 1994). In the presence of water, iron ions are located at the surface of an oxide completing their ligand shell with hydroxyl ions so that the surface becomes completely hydroxylated. Figure 2.4 shows the hydroxylation of the surface and adsorption of H_2O molecules through H-bonding (Breeuwsma, 1973).

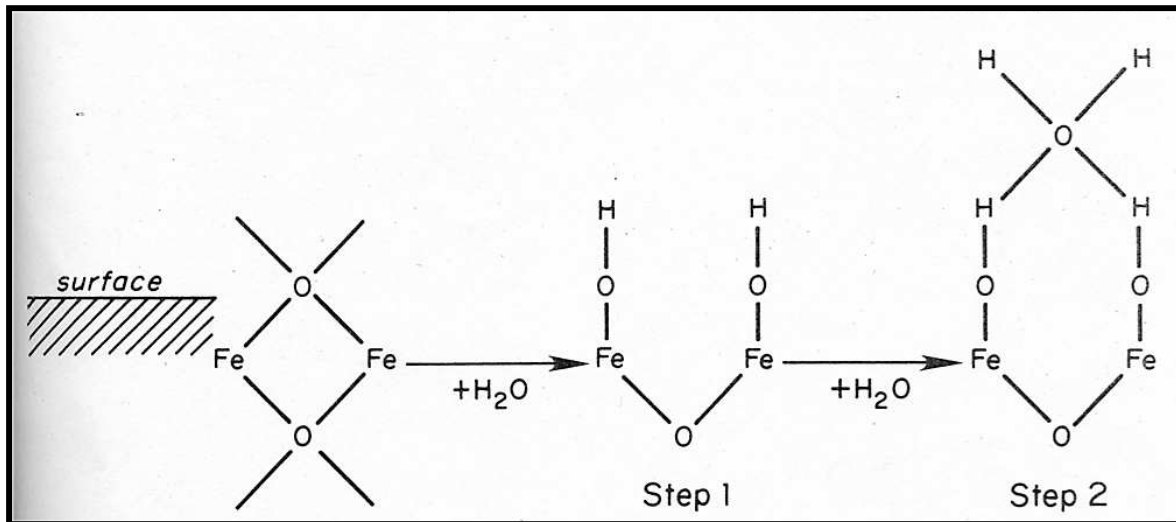


Figure 2.4: The reaction of surface groups of iron oxide particles with water [Schwertmann and Taylor, 1989].

At hydroxylated or hydrated surfaces of iron oxide, positive or negative charge is created by an adsorption or desorption of H^+ or OH^- ions, which is controlled by H^+ and OH^- ion concentration in the solution (pH dependent). One measure of the relative affinity of H^+ and OH^- for such surfaces is given by the point of zero charge (PZC). The point of zero charge of a particle is the solution pH value where total net particle charge is zero (Sposito, 1984). The total net surface charge on a particle (σ_p) is given by:

$$\sigma_p = \sigma_s + \sigma_H + \sigma_{is} = \sigma_{os} - \sigma_d$$

where σ_s is the permanent structural charge, σ_H is the proton surface charge resulting from the specific adsorption of protons and hydroxyl ions, σ_{is} is the inner-sphere complex charge resulting from specific ion adsorption, σ_{os} is the outer-sphere complex charge resulting from non-specific adsorption, and σ_d is the disassociated charge.

Apart from pH, the charge also depends on the concentration of the electrolyte and valance ions in equilibrium solution. Figure 2.5 shows that the iron ions do not participate directly in charge development. Rather the valance unsatisfied OH^- or H_2O ligands bound to surface of iron oxides that are the attracting sites.

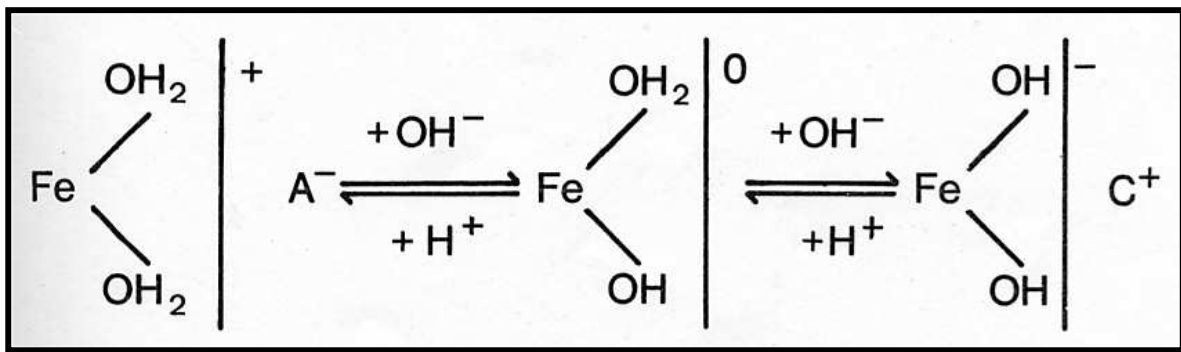


Figure 2.5: The net variable charge on the surface (point zero charge, PZC) [Schwertmann and Taylor, 1989].

Point of zero charge of goethite is 7 to 8 and that of hematite 8.0 to 8.5 (Sposito, 1998), PZC of a particular oxide may differ depending on the kind and extent of foreign ion adsorption. Specifically adsorbed anions lower the PZC and cations raise the PZC (Parks, 1967; Sposito, 1984).

2.1.5 Specific adsorption by phosphate on iron oxides

At hydroxylated surfaces, a positive or negative charge is created by the adsorption or desorption of H^+ or OH^- ions, which is balanced by an equivalent amount of anion through specific adsorption. Sorption of P occurs through ligand exchange on variable charge surfaces by the exchange of OH^- on the surface for phosphate ion. There is covalent bond between the metal ion and the phosphate ion. Phosphate is considered to sorb mainly as an inner-sphere complex, which means that the sorption takes place at specific coordination sites on the oxides or hydroxides (Fig. 2.6).

These reactions are termed as “ligand exchange reactions” because the anion displaces OH^- or H_2O from coordination positions of iron ion at the surface that are the sites of chemisorption (Hingston et al. 1968; Bowden et al. 1977).

The surface complexes have been directly confirmed by X-ray photoelectron spectroscopy (Martin and Smart, 1987). Based on experimental evidence from a variety of direct and indirect methods, a consensus exists supporting inner-sphere bidentate binuclear complexation of phosphate on various iron oxides, i.e. ferrihydrite, goethite, lepidocrocite, and hematite (Parfit et al., 1975; Yuji and Sparks, 2001). The surface complexes have been directly confirmed by X-ray photoelectron spectroscopy (Martin and Smart, 1987). Based on experimental evidence from a variety of direct and indirect methods, a

consensus exists supporting inner-sphere bidentate binuclear complexation of phosphate on various iron oxides, i.e. ferrihydrite, goethite, lepidocrocite, and hematite (Parfit et al., 1975; Yuji and Sparks, 2001).

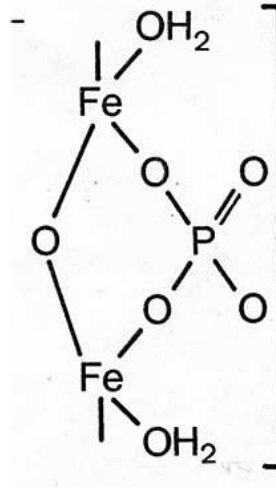


Figure 2.6: Bidentate arrangement [Schwertmann and Taylor, 1989].

Phosphorus is more strongly surface-associated through covalent bonds formed by ligand exchange with oxide surfaces' OH groups compared to SO₄, which is a non-specifically bound oxyanion and is weakly surface-associated due to electrostatic interaction (McBride, 1994; Yuji and Sparks, 2001).

The sorption reaction is strongly non-reversible and the sorbed phosphate is mostly unavailable for plant uptake. The precise nature of these reactions depends on pH, which influences the proportions of H₂O and OH⁻ groups on the solid surface, and hence its surface charge. Unlike metal cations, sorption of oxyanions decreases with increasing pH (Bigham et al., 2002). Hingston et al. (1972) showed that phosphate adsorption continually decreased with increasing pH. Phosphorus interacts more strongly with goethite, probably following an adsorption process and was observed more evenly distributed at its surface (Bertrand et al., 2001).

2.1.6 Identification and quantification of iron oxides

Crystalline and amorphous phases of iron oxides are determined by extraction with citrate bicarbonate dithionite (CBD) (Mehra and Jackson, 1960; Holmgren, 1967; Loeppert and Inskeep, 1996). The procedure is based on reductive iron dissolution with dithionite as reductant and citrate as a chelating agent to bind the dissolved iron. Bicarbonate is used to buffer the H^+ loss during the reaction.

The poorly crystalline iron oxides are separately determined by an ammonium oxalate treatment (oxalate) described by Tamm (1922) (Schwertmann, 1964; Jackson et al., 1986; Bertsch and Bloom, 1996). The method is performed in dark to avoid the solubilization of well-crystallized goethite and hematite (Campbell and Schwertmann, 1984). The ratio of Fe_o/Fe_d quantifies the more and less active fractions and has been shown to be a useful parameter for characterizing soil properties such as P sorption (McKeague and Day, 1966). Thus, Fe_d-Fe_o represents the crystalline iron oxides (Shoji et al. 1996; Kleber et al., 2005).

X-ray diffraction is the method of choice for the identification of crystalline phases. However, iron oxides often account for a small percentage of soil clay. The phase identification and quantitative determination of iron oxides by X-ray diffraction is limited by high detection limits (3 to 5% iron oxides w/w) (Bigham et al., 2002). Poor crystallinity of iron oxides increases peak widths further hampering the identification. Goethite in particular cannot be detected in low concentrations because it is frequently less crystalline than hematite and XRD peaks are broader (Schwertmann and Taylor, 1989). In the study of alkaline calcareous soil clays, hematite had a detection limit of 2% and goethite even 3% was at the edge of XRD limit (unpublished data). Therefore, it becomes necessary to include some physical enrichment in the analytical protocol.

Various methods (e.g. particle size separation, magnetic separation and 5M NaOH treatment) are used for concentrating iron oxides in clay samples (Schulze and Dixon, 1979; Norrish and Taylor, 1961).

The 5M-concentration treatment of Norrish and Taylor (1961) has been successfully reported for concentration of iron oxide in clay samples. Modifications of the original method by varying the time of extraction (Davey et al., 1975; Kämpf and Schwertmann, 1982; Bigham et al., 1978; Singh and Gilkes, 1991), the temperature of extraction (Pizarro et al., 2000; Tokashiki et al., 2003) or both (Kämpf and Schwertmann, 1982; Singh and Gilkes, 1991)

have been reported. However, results obtained by Singh and Gilkes (1991) show complete dissolution of kaolinite and removal of large amounts of precipitated sodalite.

For the quantification of various iron oxide phases, synchrotron methods (e.g. Manning et al., 1998; Waychunas et al., 1993), Mössbauer and diffuse reflectance spectroscopy (DRS) (Bigham et al., 2002), and voltammetry (Grygar et al. 2002) are being increasingly used by clay scientists.

Mössbauer spectroscopy has proven invaluable in many studies of iron oxides in soils and sediments (Murad and Johnston, 1987; Goodman, 1994). Diffuse reflectance spectroscopy, although, has lower detection limits than XRD (Grygar et al., 2002, Torrent and Barron, 2002), except of course synchrotron methods, which are highly sensitive, voltammetry with carbon paste electroactive electrode appears to be more sensitive having detection limit of 0.01% wt% in soils and sediments. Voltammetry, coupled with XRD, effectively quantified goethite, hematite or both in mixture with detection limit as low as 0.01 mg in clay sample (Memon et al, 2008).

2.2 Soil phosphorus

2.2.1 Species in soil

Dominant P species in soil solution that plants take up are H_2PO_4^- or HPO_4^{2-} in the pH range of common soils. In acidic soils H_2PO_4^- ions dominate and in alkaline soils HPO_4^{2-} ions. Figure 2.7 presents P cycle in modern eco-system where absolute quantity of soluble P is governed by input from organic and inorganic sources as well as the solid phases through precipitation and dissolution processes. Yet, at any one time absolute quantity of soluble P is low compared to the plant requirement (Delgado and Torrent, 2000) and without addition through fertilizer the natural soil P reserves are not enough to support intensive crop cultivation. For optimum crop production use of fertilizer P becomes essential to replenish soil soluble P continuously.

Soil CaCO_3 , oxides or hydroxides of metals and argillaceous clays retain P added through fertilizer or natural weathering to change it to relatively insoluble form through sorption processes and precipitation as compounds (Lindsay and Moreno, 1960; Borrero et al., 1988; Frossard et al., 1995; Castro and Torrent, 1998; Hinsinger, 2001). Sparingly soluble P minerals frequently identified in soils include apatite $[\text{Ca}_{10}(\text{F}, \text{OH}, \text{Cl})_2(\text{PO}_4)_6]$ from igneous and

sedimentary rocks. Apatite occurs in fine grains in basalt and other mafic rocks and less commonly in more siliceous rocks. In calcareous sediments, it occurs as fluorapatite $[\text{Ca}_{10}\text{F}_2(\text{PO}_4)_6]$ and hydroxyapatite $[\text{Ca}_{10}(\text{OH})_2(\text{PO}_4)_6]$, to name a few examples of P minerals. The solubility of P in apatite is low, therefore, the mineral P pool may not necessarily contribute to replenish solution P at a rate required to match crop requirement over a growing season (Lindsay et al., 1989; Syers and Curtin, 1989).

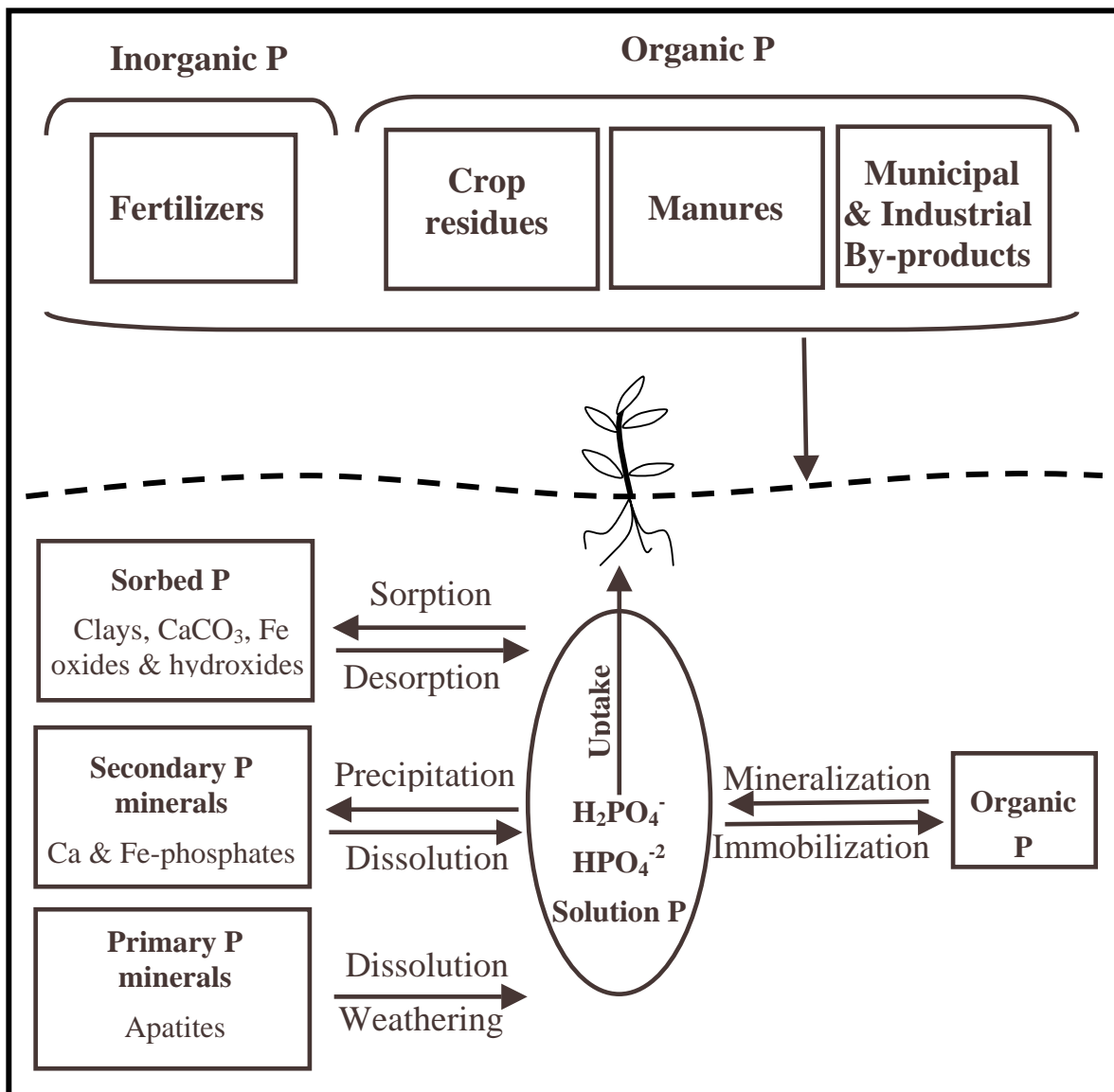


Figure 2.7: The soil P cycle in calcareous soil environment [Modified after Pierzynski et al., 1994].

2.2.2 Fertilizer P

Inorganic or organic phosphorous fertilizers are added to increase soluble P concentration. Inorganic P fertilizers include mineral rock phosphate, phosphoric acid, calcium orthophosphates, ammonium phosphates and polyphosphates, nitric phosphates and potassium phosphates. When P fertilizers are added to soils, it increases soluble P concentration and alters the equilibrium between solid P and soluble P that gets converted to solid forms by precipitation and adsorption reactions.

After initial fast adsorption the concentration in soil solution slowly decreases, indicating yet a lack of equilibrium. The fast reaction is a ligand exchange on oxide surfaces and the slow decrease in phosphate concentrations in soil solution is induced by diffusion of the adsorbed P to the interior of porous oxide material (Barrow, 1983).

The newly precipitated P material can be converted back into soluble species relatively quickly when plants take up P from soil solution, the equilibrium shifts to the other direction (i.e. soluble P concentrations are much less than the solid phase) and more P is converted from solid phase to soluble P. However, solid phase becomes more stable or more strongly adsorbed with time. When this occurs, solid phase P material cannot replenish the soil solution fast enough and P fertilizer needs to be added again. If fertilizer P is added consistently in a manner that exceeds plant needs, excess P buildup occurs.

In Pakistan natural resource phosphatic rocks are approximately 7.45 million tones and the quality is low, consequently, exploration and fertilizer production is uneconomical (Khan and Khan, 1988). In contrast, total fertilizer use is 0.400 metric ton per year at an application of 130 kg ha⁻¹. The N:P₂O₅ application ratio at farm level is wider than the recommendation (World Phosphate Institute, Annual Report, 2004) since current P fertilizer application rates approximately one-third of recommendation for optimal crop production (FAO, 2004) while 95% soils are P deficient (Memon, 1996).

2.2.3 Processes of soil P

Two reactions are controlling transformation of P from soluble to solid phase; precipitation and sorption. Precipitation involves the formation of discrete, solid phases and brings more permanent change (Campbell and Edwards, 2001). Sorption is a reversible chemical binding of P to soil particle surfaces. Both processes differ in the sense that solubility product of the least soluble P compounds in the solid phase controls dissolution and thus solution P, whereas

solution P controls the amount of P sorbed (Syers and Curtin, 1989). It is clear that these two reactions are major mechanisms of P retention in calcareous systems (von Wandruszka, 2006). Mineralization and immobilization of organic P also influence the soil soluble P (Campbell and Edwards, 2001) but we restrict our discussion to inorganic P.

2.2.3.1 Precipitation

Precipitation of P as dicalcium phosphate and surface precipitation on solid CaCO_3 are the main processes in calcareous soils (Mackay et al., 1986). High activity of calcium ions and high pH values favor the precipitation as relatively insoluble dicalcium phosphate dihydrate $[\text{Ca}_{10}(\text{PO}_4)_6(\text{OH})_2]$ and other calcium phosphates such as hydroxy-apatite and carbonate-apatite. Calcium phosphate is initially formed as mono-calcium phosphate precipitate, it is later transformed to dicalcium phosphate to octa-calcium phosphate and finally to hydroxy-apatite or carbonate-apatite, which has the least solubility (Lindsay et al., 1989; Syers and Curtin, 1989). While the intermediate precipitates are unlikely to persist in soils (Delgado et al., 2000). The amount, nature, and reactivity of carbonate minerals affect phosphate reactions only to limited extent (Matar et al., 1992). Calcium activity dominantly controls formation of Ca-P phases and free carbonate minerals are not necessary for the induction of P precipitation (Tunesi et al., 1999). XANES results showed that Ca-phosphates were present in all soils regardless of pH (Beauchemin et al., 2003). However, P sorption on carbonates strongly depends on surface area (von Wandruszka, 2006). In soils, derived from limestone parent material, weathering is decreasing total CaCO_3 content but is increasing specific surface area due to greater number of smaller CaCO_3 particles (Holford and Mattingly, 1975).

2.2.3.2 Sorption processes

“Sorption” describes two processes: (a) adsorption, which occurs when phosphate ions are adsorbed to the surface of particles and (b) absorption when adsorbed ions diffuse into the solid; and “sorption” is the general term used for these processes. Phosphate may become trapped on the surface of soil minerals under coating of iron oxide precipitates. The trapped phosphate is termed as occluded (Fig. 2.8). Phosphate ions are more strongly sorbed by iron oxide surfaces due to their large surface area (Syers and Curtin, 1989; Hinsinger, 2001). Soluble P added to soil, initially undergoes a very rapid exothermic reaction (adsorption) followed by a slow reaction (absorption) resulting in

occluded P (Barrow, 1985; Sollins, 1991). Occlusion takes place in the iron oxide structures (Galvez et al., 1999).

A rapid reaction is a ligand-exchange reaction. Phosphorus is chemisorbed on the reactive iron oxide surface groups through a binuclear bridging mechanism. An OH^- or H_2O molecule is released from the surface and phosphated bridging complexes are formed between HPO_4^{2-} ions and iron oxide surface (Parfitt et al, 1976; Goldberg and Sposito, 1985; Torrent et al, 1992; McBride, 2002). This sorption reaction is strongly non-reversible and the sorbed P is mostly unavailable for plant uptake (McBride, 2002; Bigam et al., 2002).

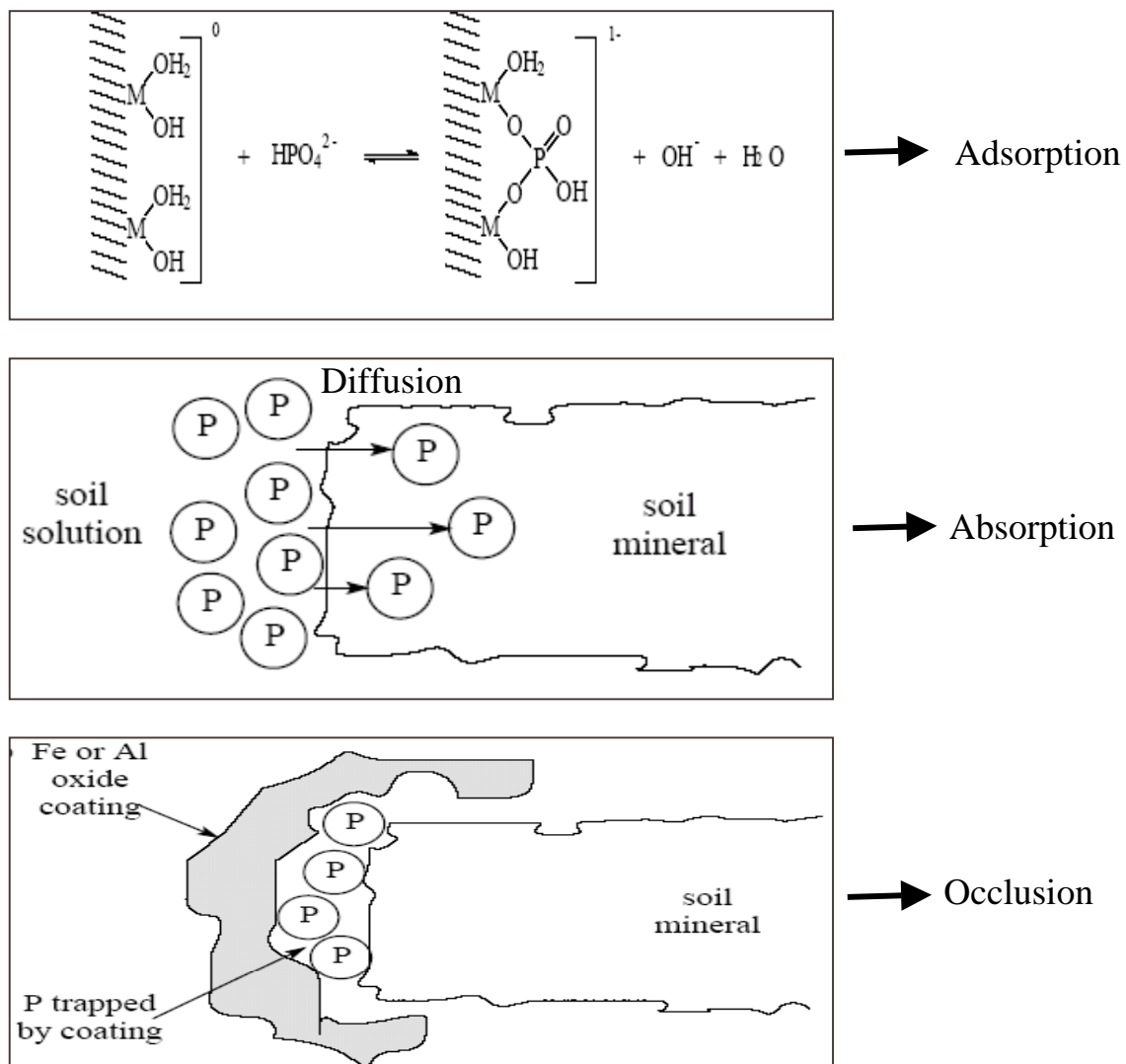


Figure 2.8: Adsorption, absorption and occlusion of P [[http://www.nzic.org.nz/ Chem-Processes/soils/2D.pdf](http://www.nzic.org.nz/Chem-Processes/soils/2D.pdf)].

Inner-sphere bidentate binuclear complexation of phosphate on iron oxides i.e. goethite, hematite and ferrihydrite was reported (Parfitt et al. 1975). Phosphorus has higher affinity to goethite surfaces (Geelhoed et al., 1997) than to hematite. Evidence of goethite retention was confirmed by transmission electron microscopy using synthetic samples. Phosphate showed strong binding in crystals of small size, consisting of thin and well developed goethite laths (Torrent et al., 1990). The average maximum quantity of sorbed phosphate reaches $2.5 \mu\text{mol P m}^{-2}$ on goethite but only $0.97 \mu\text{mol P m}^{-2}$ on hematite because of the proportion of the total surface area (Barron et al., 1988). Sorption and precipitation are controlling the solubility of P in goethite suspensions at a wide pH range and the two mechanisms are indistinguishable (Li and Stanforth, 2000). Recent work of Saavedra and Delgado (2005) also showed that in soils between pH 7.3-8.1, most of the extractable iron in soils occurred in crystalline oxide form as determined by sequential extraction. In addition, the kinetics of the slow P retention has been successively modeled by using an approach based on diffusion of P through surface coatings that are precipitated on iron oxide surface upon sorption. This approach is considered to be closer to the adsorption diffusion concept in soils.

The amorphous oxides of iron are typically found in weakly developed soils (Parfitt, 1978). They tend to dominate soil P sorption reactions when present in significant amounts because of their large surface area (Jones and Uehara, 1973; Hsu, 1989; Schwertmann and Taylor, 1989, Freese et al., 1992). Harrell and Wang (2006) observed that especially less amorphous forms play a very important role in P retention in calcareous soils where carbonate is <5%.

2.2.4 Determination of P-speciation

The identification of P compounds in soil is limited by their low concentration in soil (Hadley et al., 1982). Selective dissolution techniques help to characterize soil inorganic P and have been used extensively (Chang and Jackson, 1957; Williams et al., 1967), soil P (Bowman and Cole, 1978) or plant available P (Dalal and Hallsworth, 1976). Hadley and co-workers (1982) developed a sequential extraction procedure that served to characterize labile and more stable inorganic P and organic P (Hadley et al., 1982; Tiessen et al., 1983).

Separate sequential extraction schemes have been developed for calcareous and non-calcareous soils and are widely used to partition soil P into various fractions. The underlying assumption in fractionation schemes are based on the principle that readily available soil P is removed first with mild extractants

(e.g. NH_4Cl , NaHCO_3), and less available or plant-unavailable P is only extracted with stronger alkali and acid chemicals (e.g. NaOH , HCl , H_2SO_4). Apatite is soluble in acid solutions and iron and aluminum hydroxides in alkaline solutions. An additional procedure consisting of a citrate-bicarbonate buffered dithionite solution for removing the occluded fractions of Fe and Al is commonly applied.

Basic fractionation procedure of Chang and Jackson (1957) is used with and without some modifications (Fu, 1983; Cross and Schlesinger 1995; Solomon and Lehmann, 2000; Beauchemin et al., 2003). Formation of calcium fluoride during NH_4F extraction of calcareous soil may cause an underestimation of non-occluded Fe and Al bound P and an overestimation of acid-extractable Ca-P (Syers et al., 1972). Later, modifications made by Fife (1962), Petersen and Corey (1966), Williams et al. (1967), Smillie and Syers (1972), and important modifications by Kuo (1996) improved the extractability to be used in calcareous soils but still these methods are not particularly sensitive to the various P compounds that may exist in calcareous soils. Jiang and Gu (1989) suggested a new fractionation scheme for calcareous soils by which inorganic P could be fractionated into 6 groups, which they described as dicalcium phosphate ($\text{Ca}_2\text{-P}$), octa-calcium phosphate ($\text{Ca}_8\text{-P}$), apatite type ($\text{Ca}_{10}\text{-P}$), aluminum phosphate (Al-P), iron phosphate (Fe-P) and occluded phosphate (O-P). The method of iron phosphate (Fe-P) was also modified.

The Jiang and Gu (1989) procedure has been successfully used to investigate P fractions in alluvial soils (Tu et al., 1993); calcareous soils from North China (Chang and Yu, 1992; Shen, 1992); fertilized calcareous soils (Samadi and Gilkes, 1998); rice fertilized calcareous soils (Shen et al., 2004); and highly calcareous soils (Adhami et al., 2007).

2.2.5 Phosphorus sorption isotherms

Sorption isotherm techniques have been widely used to compare the sorption capacity of different soils. Phosphorus adsorption isotherm is constructed by equilibrating soil with graded amount of P and, then, analysing solution P remaining un-adsorbed (Barrow, 1978; Barrow and Shaw, 1975; Enfield et al., 1976; Fox and Kamprath, 1970; Larsen et al., 1965; Rajan and Fox, 1972; Shayan and Davey, 1978). Sorption isotherm is fitted to Freundlich or Langmuir equations to describe sorption in terms of quantitative parameters. Freundlich fits better to observed P isotherms (Barrow, 1978; Ratkowsky, 1986; Zhou and Li, 2001) particularly in calcareous system (Said and Dakermanji, 1993; Hassan et al., 1993; Loch and Jaszberenyi, 1995). However,

Zhang et al. (1993) reported that both Freundlich, and Langmuir equations adequately described P adsorption. Barrow (1991) modified the Freundlich equation to account for increase in P sorption with sorption time.

The Freundlich equation is often considered to be purely empirical in nature but has been used extensively to describe the sorption of P by soils (e.g. Sposito, 1980).

The Freundlich equation is given by

$$x/m = k_f C^b$$

where x/m is the amount of P sorbed by soil (mg kg^{-1}), C is the concentration in soil solution at equilibrium (mg L^{-1}), k_f and b are constants. In this case no value of maximum P sorption capacity can be derived, nevertheless “ k_f ” and “ b ” can be calculated and different soils can be compared for sorption characteristics.

The Langmuir equation can be used to calculate parameters that are indices of the capacity and the intensity of P in soil. The P buffering capacity of a soil is its ability to resist a change in the P concentration of the soluble phase (Sui and Thompson, 2000). The understanding of the P sorption capacity of a soil can help to estimate the amount of P that a soil is capable of holding (Zhang et al., 2005).

The simple Langmuir model adequately describes P sorption by soil when surfaces are covered with mono-layer of sorbate. Holford et al. (1974) used a two-surface Langmuir equation.

The simple Langmuir equation is

$$x/m = bkC/(1 + kC)$$

where x/m is the amount of P sorbed by soil (mg kg^{-1}), C is the concentration of P in soil solution at equilibrium (mg L^{-1}), parameter b is the maximum adsorption capacity, and k represents a constant related to the energy of sorption. The values of b and k are obtained from the slope ($1/b$) and intercept ($1/kb$) respectively.

The two-surface Langmuir equation is defined as

$$x/m = [b_1 k_1 C / (1 + k_1 C)] + [b_2 k_2 C / (1 + k_2 C)]$$

where x/m is the amount of P sorbed, C is the equilibrium P concentration, b_1 , b_2 are the high and low affinity maxima of P sorption, and k_1 , k_2 are related to high and low affinity binding energies of P sorption. Two straight lines can be

obtained from a plot of $(x/m)/C$ vs. x/m , if isotherm data fit the equation well and sorption parameters can be determined from the plot (Sposito, 1982; Duffera and Robarge 1999; Sui and Thompson, 2000).

The high adsorption energy determined by the two-surface Langmuir equation for a group of soils containing 8 to 244 g kg^{-1} CaCO_3 was closely associated with dithionite soluble iron (Holford and Mattingly, 1975). Wang and Tzou (1995) explained that maximum P sorption in calcareous soils could be resolved into two regions of adsorption, which might be correlated to high and low energy adsorbing surfaces. Further, complete derivation of this model was given by Sposito (1982).

3. Materials and Methods

3.1 Study area

The total of nine soil series varying in parent material and pedological development were included in this study. Seven soils namely, Shahdara, Sultanpur, Pacca, Pitafi, Murree, Peshawar and Guliana were sampled from Pakistan and two soils Parabraunerde of Osterburken and Weingarten were taken from Germany.

The Pakistani soils belonged to the following four land morphological units: (1) Indus River alluvial plain (Shahdara, Sultanpur, Pacca and Pitafi soils); (2) Loess Plain, comprising loess deposited on Tertiary Siwalik sandstone/shale bedrocks during Pleistocene period (Guliana soil); (3) Residuum/Colluvium on ridge-and-trough upland derived from Siwalik sandstone and shale interbedded (Murree soil), and (4) Piedmont alluvial plain, foothill alluvium comprising of material derived mainly from a mixture of sandstone and calcareous red shale (Peshawar soil). The four land morphological units occur between 68°24'N to 73°26'N longitude and 25°24'E to 33°56'E latitude. The map of the overall sampling area of Pakistani soils is given in figure 3.1 and the specific locations of these soils are given in figures 3.2 to 3.5.

The alluvial plains have developed on sandy base from sandy alluvium derived from the Salt Range by strong seasonal rivers running to the coast during the main part of the last glaciations. Later, the sandy base was covered by silty material mainly from loess with some sand brought during the last part of the last glaciations (Brinkman and Rafique, 1971). During early Holocene period, the present river system had cut the wide silty plains. The down cutting and the removal of the Old sediments took place along the rivers' courses. Relatively protected Old River sediments remained intact in the center between each pair of the rivers and are called Old River Terraces.

The part of the alluvial plain of the current river system, which is stable against later river erosion, is called Sub-recent flood plains and it occurs between the Old River Terraces and the present day floodplains. There are three distinct landforms in the floodplains: (a) Level Plains, (b) Basins and channel-fills, and (c) Levee remnants. Climate is semi-arid in the north and arid in the south. The erratic late monsoon showers and some winter rains constitute the precipitation. Pedogenesis in the Sub-recent floodplains is weaker than the Old River terraces mainly because of the age difference and moisture. A large-scale

decalcification, vertic characteristics, and re-distribution of plasma are absent in the soils while salinization/sodification are important pedological processes (Ahmad et al., 1986).

The Recent and Active Flood plains occur as narrow belts along the river streams where sedimentation is still going on. The soil forming processes are limited by age factor therefore the soils show limited signs of profile development. The soils of the Recent Flood plain may show homogenization in the upper 30 cm profile.

Loess has been deposited on Tertiary Siwalik sandstone/shale bedrocks during Pleistocene period. The current land morphology was created by later orogenic disturbances, erosional, and depositional cycles. The Guliana soil is developed in slightly depression position in semi-arid area. It had all the features of a well-developed profile. The Residuum/Colluvium is derived from interbedded sandstone and red shale where soils are calcareous, slightly alkaline to non-calcareous, and slightly acidic.

The Piedmont plain refers to the intermountain alluvium, which has been transported by water to a very short distance or is lying at the foothill. The material inherits minerals from the adjoining rocks and, therefore, mineralogical composition from the source rock. Locally, the plains are dissected by tributary gullies. Soils on the piedmont plains are generally very deep, well drained, homogenized to more than 150 cm depth and have weak subangular blocky structure.

The Piedmont and loess plains occur in semi-arid sub-tropical continental climate with a mean annual rainfall of 450 to 550 mm as late monsoon and some winter-rains. The part of alluvial plains where sampling was done is arid (<200 mm annual rainfall) but it irrigated from the canals diverted from the Indus.

The two German soils, Parabraunerde were from Osterburken (Prb-Ostb) and Weingarten (Prb-Wein), Baden Württemberg. Prb-Ostb occurs at longitude 9°29'37"E, latitude 49°26'38"N, and at an elevation of 1195 feet, whereas Prb-Wein occurs at longitude 8°33'34"E, latitude 49°4'25"N, and at an elevation of 810 feet (Regierungspräsidium Karlsruhe, 1999). The map showing the sampling areas are given as figure 3.6 while the maps showing specific locations for these soils are given in figures 3.7 and 3.8. The Parabraunerde at Osterburken is developed on limestone (Upper Muschelkalk) in a local colluvial position with 5% slope. The Parabraunerde at Weingarten is developed on limestone covered by glacial loess (last ice age) at the steep

transition zone from a hilly landscape (Kraichgau) to the Rhine Graben located on a historic terrace used for cultivation during the medieval period. Both German soils occur in oceanic climate and at both sites, forests dominate land use.

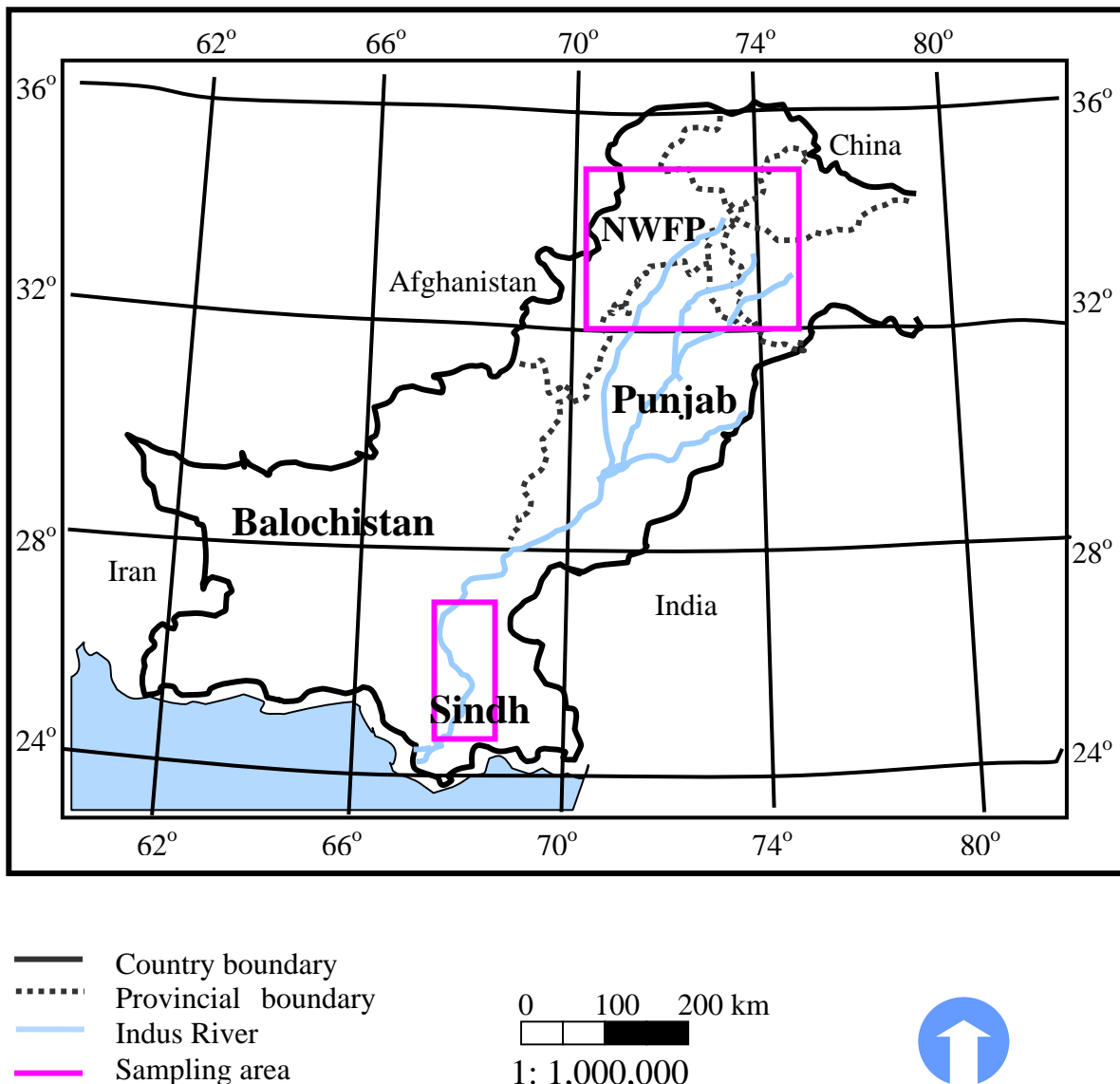


Figure 3.1: Map of Pakistan showing overall sampling areas.

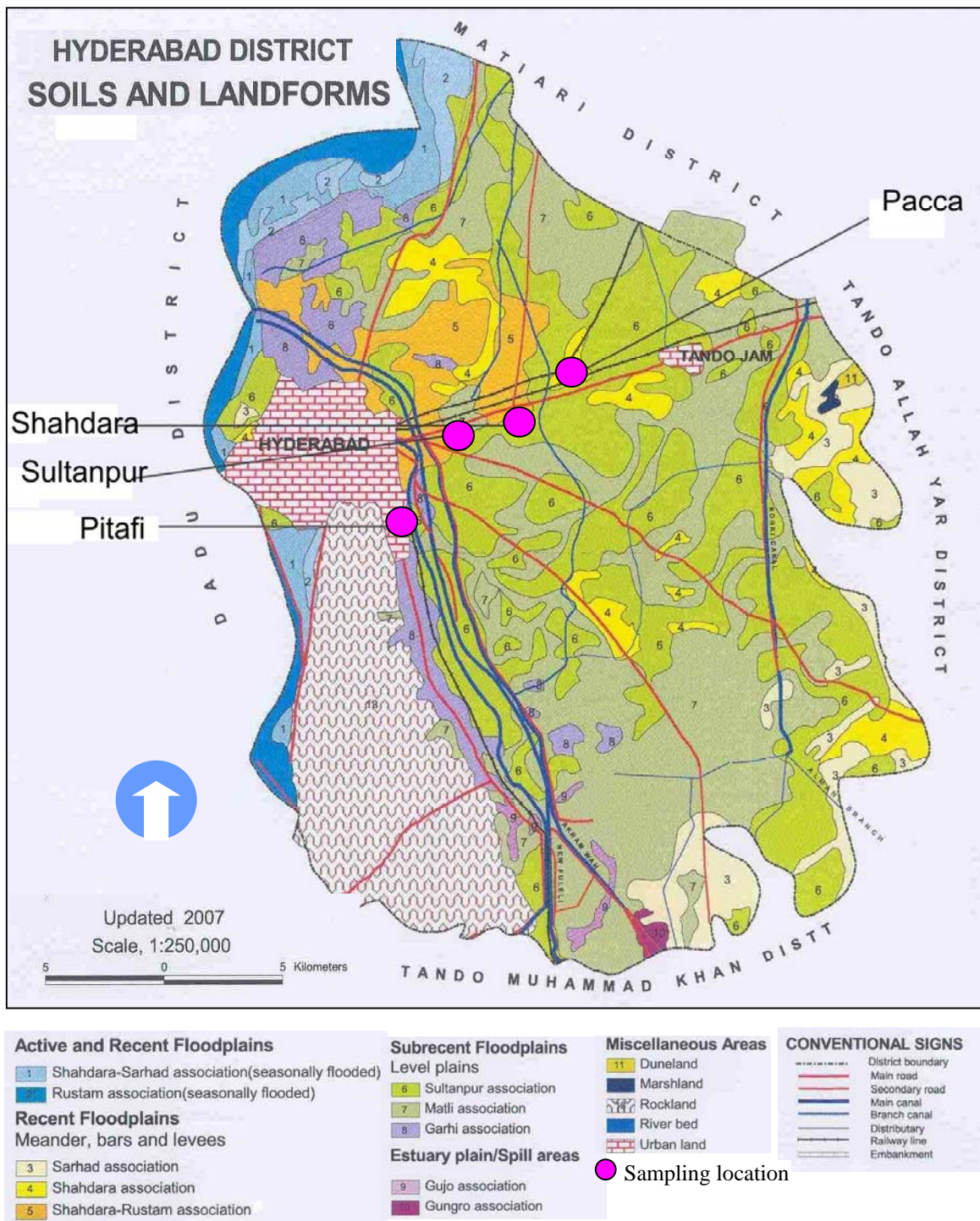
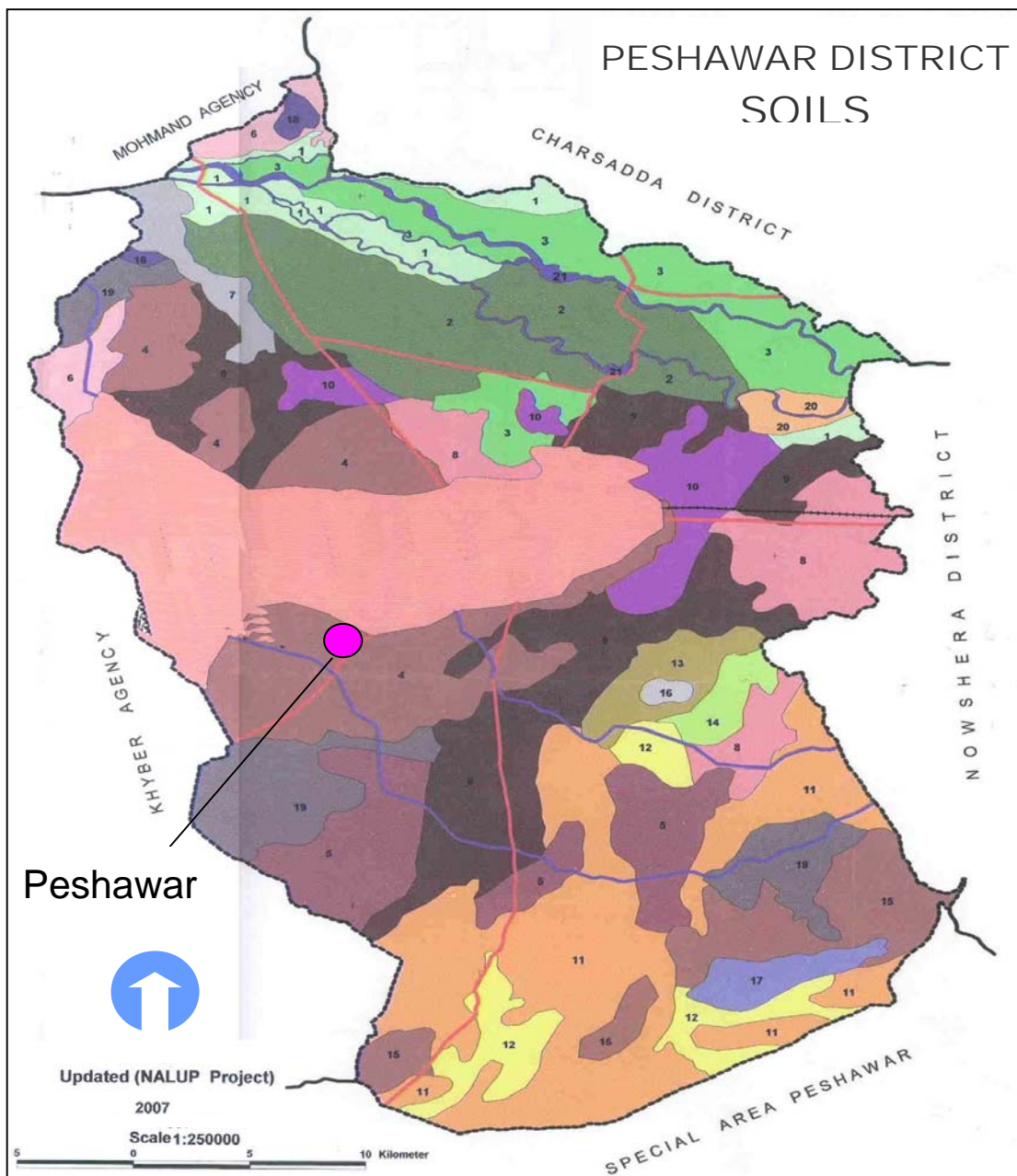


Figure 3.2: Location map of the soils Shahdara, Sultanpur, Pacca and Pitafi [Soil Survey of Pakistan, 2007].



- | | | |
|---|--|--|
| <p>ACTIVE AND RECENT KABUL RIVER PLAINS BARS AND LEVEES</p> <p>1 Babuzai - Khazana complex</p> <p>SUB - RECENT KABUL RIVER PLAINS LEVEL PLAINS</p> <p>2 Warsak association</p> <p>3 Mughulki association</p> <p>OLD PIEDMONT PLAINS</p> <p>NEARLY LEVEL PLAINS</p> <p>4 Peshawar association</p> <p>DISSECTED PLAINS</p> <p>5 Milward association</p> <p>SUB - RECENT PIEDMONT PLAINS DISSECTED PLAINS</p> <p>6 Mansooka association</p> <p>7 Chandan association</p> | <p>NEARLY LEVEL</p> <p>8 Chamkani association</p> <p>BASINS AND CHANNEL INFILLS</p> <p>9 Tarnab association</p> <p>10 Taru association</p> <p>LOESS PLAINS</p> <p>DISSECTED PLAINS</p> <p>11 Missa association</p> <p>12 Rajar Gullied land complex</p> <p>13 Shagai association</p> <p>RE - DEPOSITED LOESS PLAINS LEVEL PLAINS</p> <p>14 Pirsabak</p> | <p>MISCELLANEOUS AREAS</p> <p>15 Bad Land</p> <p>16 Dune Land</p> <p>17 Rock Outcrop</p> <p>18 Rough Mountaneous Land</p> <p>19 Gravelly and stony Land</p> <p>Marsh Land</p> <p>River</p> <p>Built up area</p> <p>CONVENTIONAL SIGNS</p> <p>— District boundary</p> <p>— Unit boundary</p> <p>— District limit</p> <p>— Main road</p> <p>— Canal</p> <p>— Railway line</p> <p>● Sampling location</p> |
|---|--|--|

Figure 3.3: Location map of Peshawar soil [Soil Survey of Pakistan, 2007].

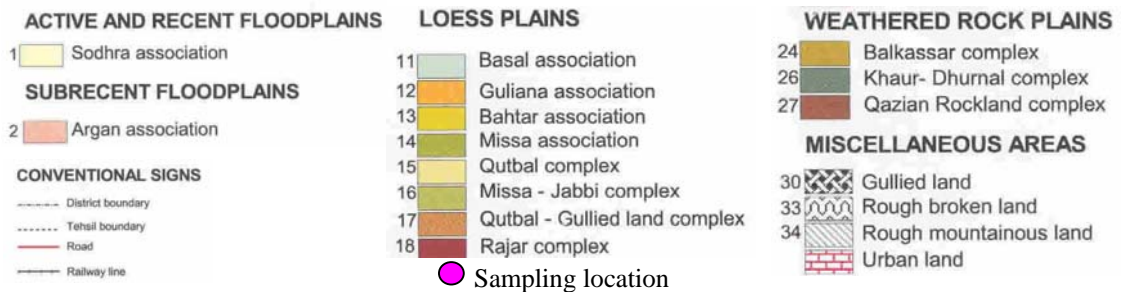
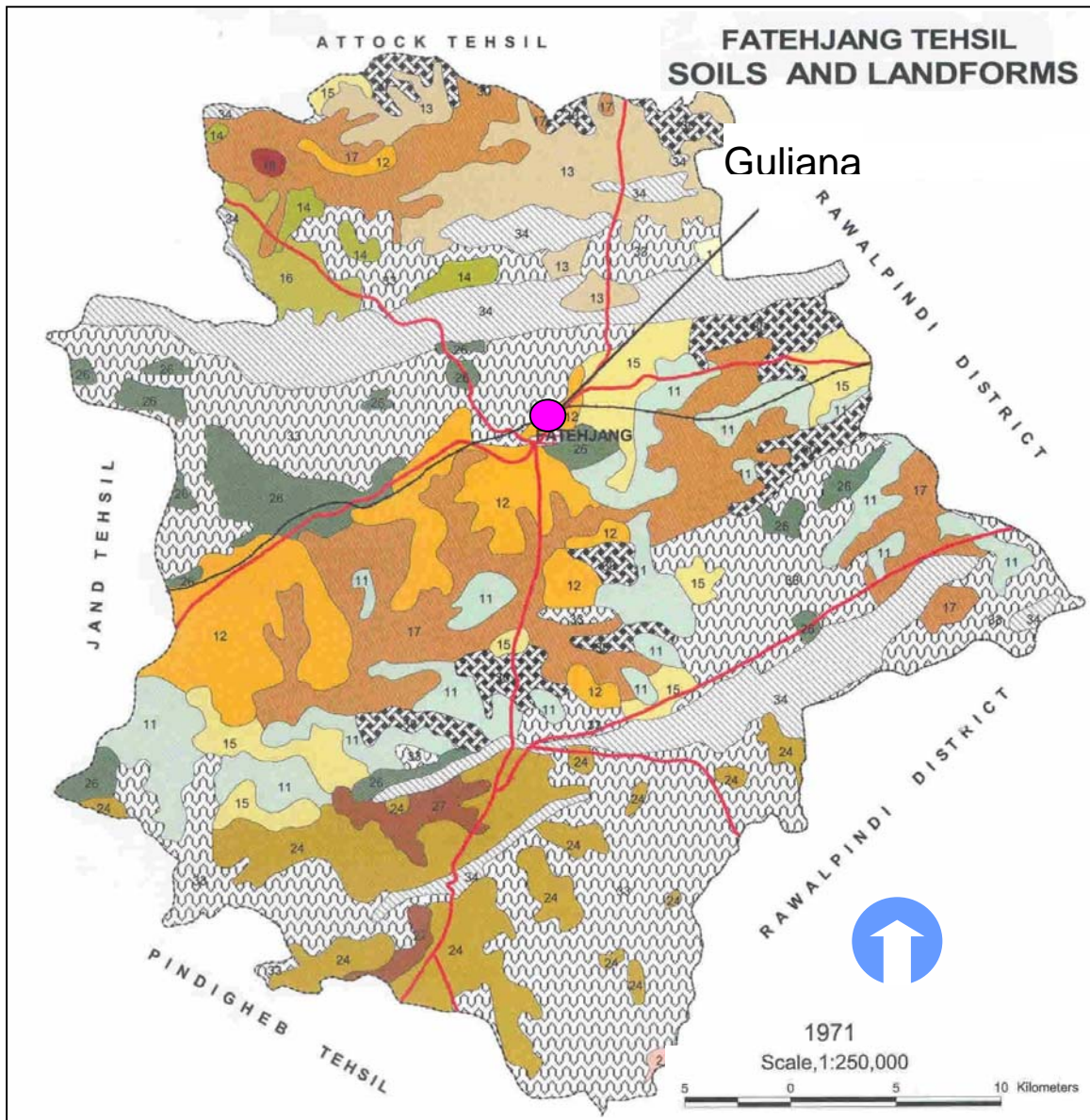


Figure 3.4: Location map of Guliana soil [Soil Survey of Pakistan, 2007].

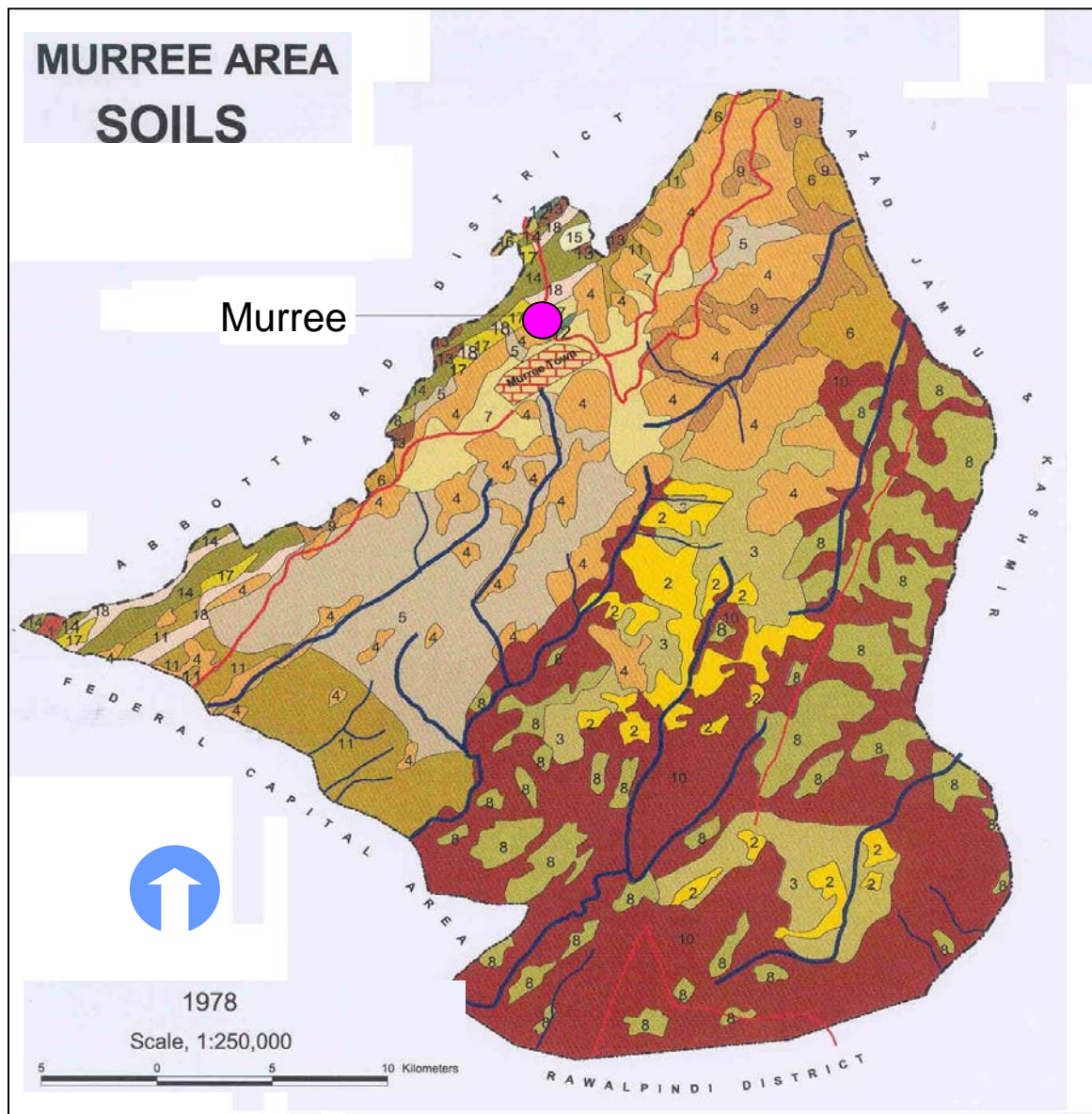


Figure 3.5: Location map of Murree soil [Soil Survey of Pakistan, 2007].

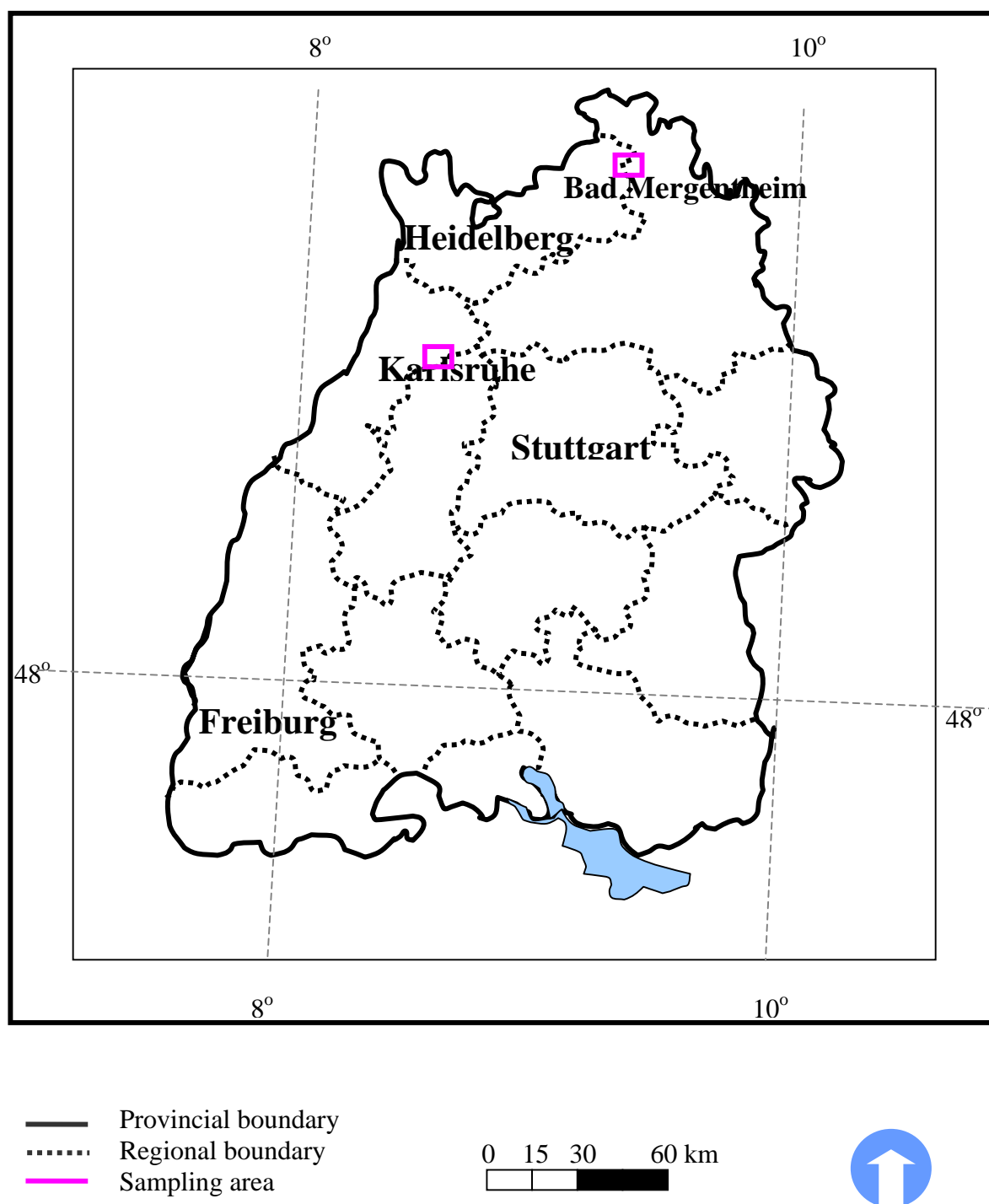


Figure 3.6: Map of Baden Württemberg, Germany showing the overall sampling sites for Prb-Ostb and Prb-Wein soils [Google Earth].

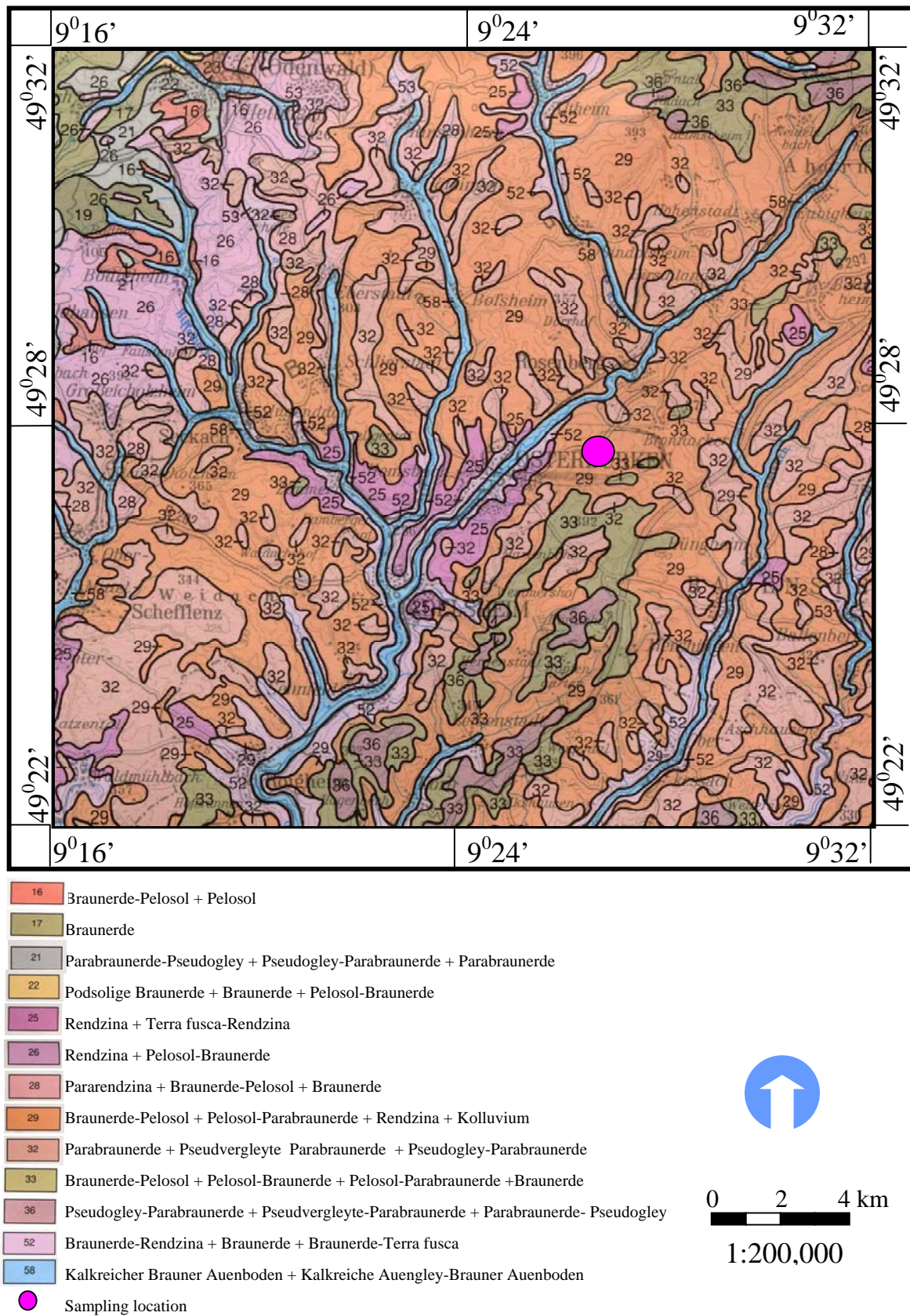
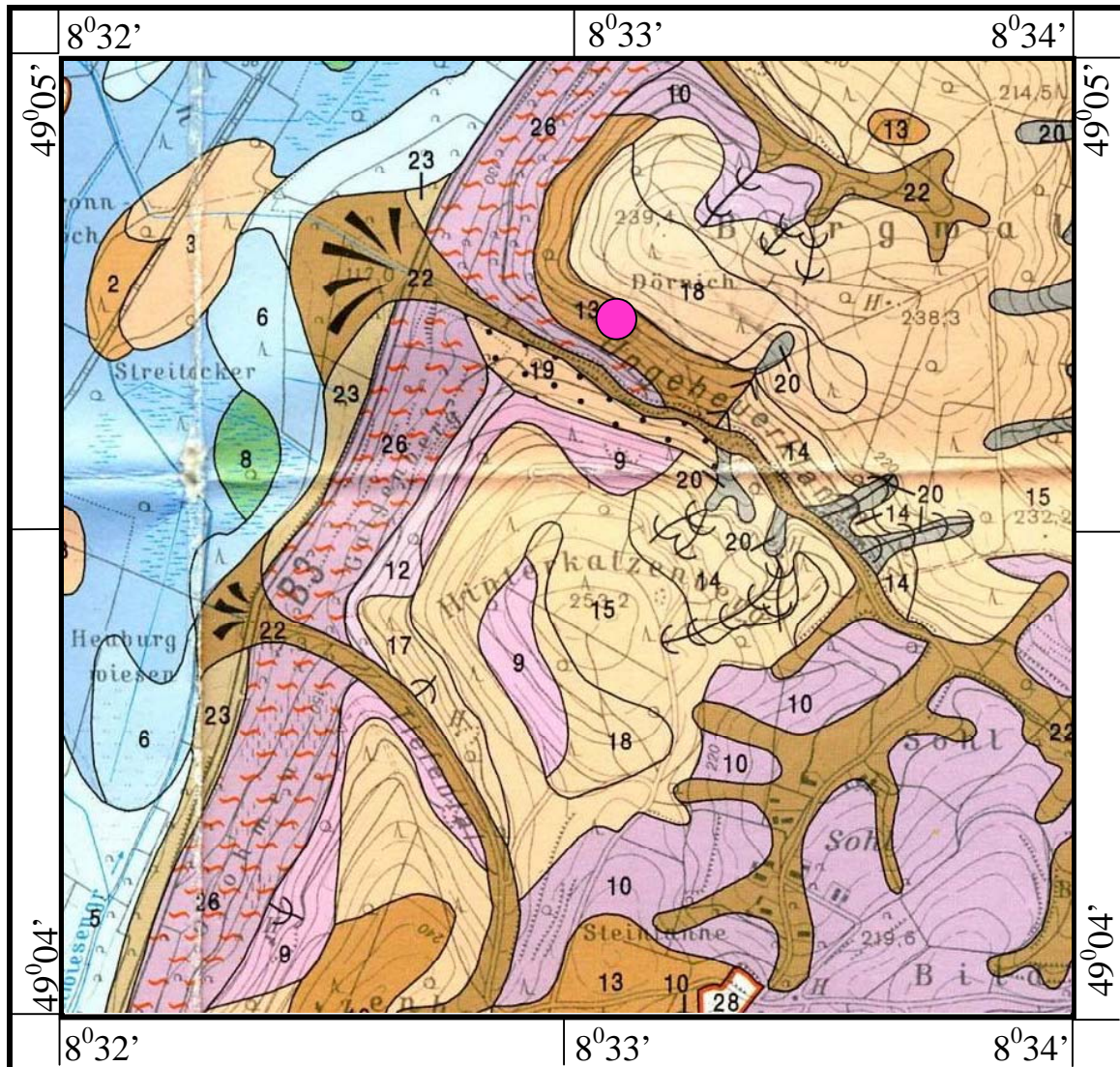

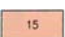


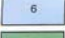
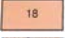
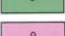
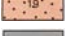
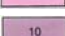
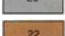
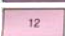
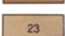


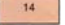

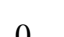



Figure 3.7: Location map of Prb-Ostb soil [Hummel et al. 1992].



- | | | | |
|--|--|--|---|
|  2 | Maßig tiefe und tiefe Pseudogley Bänderbraunerde |  15 | Maßig tiefe Parabraunerde z.T. Pseudovergleyt |
|  3 | Maßig tiefe und tiefe Parabraunerde |  17 | Maßig tiefe Parabraunerde z.T. erodiert |
|  6 | Brauner Auenboden-Auengley |  18 | Terra fusca-Parabraunerde |
|  8 | Niedermoor |  19 | Maßig tiefe und tiefe Parabraunerde |
|  9 | Braune Rendzina |  20 | Haftnässepseudogley-Braunerde |
|  10 | Tiefe Pararendzina |  22 | Tiefes kalkhaltiges Kolluvium |
|  12 | Tiefe Pararendzina aus kalksteinschuttreichem |  23 | Kalkhaltiges Pseudogley-Kolluvium |
|  13 | Mittlere Braunerde |  26 | Maßig tiefer Pararendzina-Rigosol |
|  14 | Maßig tiefe Parabraunerde |  | Sampling location |

0 500 1000 m

1:25,000



Figure 3.8: Location map of Prb-Wein soil [Krause and Fleck, 1993].

3.1.1 General profile description

The selection of the soils represented a range of clay, dithionite extractable iron, and calcite content and various iron oxide species. Soil classification and pedological environment is given in table 3.1. The soil profile was dug at each location and described with the help of pedologists. The two soils from Germany were part of another simultaneous study. Characteristics relevant to the study viz. dry and moist color, texture, structure, consistency, occurrence of clay cutan, occurrence of iron, manganese, gypsum, and CaCO₃ concretion, and field value of pH are given for each profile in the next section. Some of the descriptions viz nature abundance of pores and plant roots and nature of horizon boundary, although recorded, are not reproduced for the purposes of brevity. Bulk samples were taken from the upper four horizons of each fresh soil pit. The Prb-Ostb and Prb-Wein soils show a 0-4 cm organic/liter surface layer and the horizons deeper than 50 cm in both soils consist of gravels. Each soil sample was air-dried, crushed and passed through a 2 mm sieve. Necessary care was taken to ensure thorough mixing of each soil.

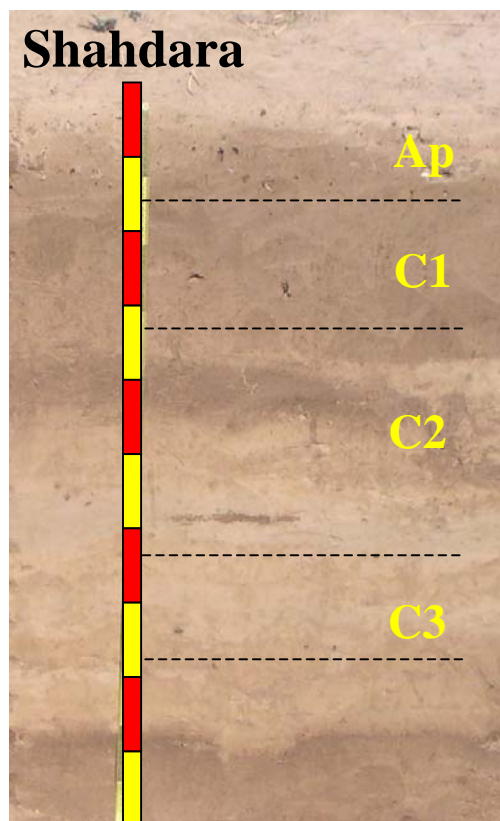
Table 3.1: Soil classification and environment (Ahmed et al., 1986; FAO, 2001).

Soil	FAO classification	Rainfall (mm)	Parent material
Shahdara	Calcaric Fluvisol	150-200	Mixed alluvium in floodplain
Sultanpur	Haplic Yermosol	150-200	Mixed alluvium in floodplain
Pacca	Haplic Yermosol	150-200	Mixed alluvium in floodplain
Pitafi	Orthic Solonchak	150-200	Mixed alluvium on river terrace
Peshawar	Haplic Yermosol	300-450	Limestone/shale piedmont alluvium
Murree	Haplic Phaeozem	1000-1200	Sandstone and shale on hill slopes
Guliana	Eutric Cambisol	550-650	Intact loess in basin
Prb-Ostb	Luvisol	800-900	Muschelkalk Colluvial
Prb-Wein	Luvisol	700-800	Limestone/glacial loess on hill side

3.1.2 Characteristics of the individual soil profiles

Shahdara profile

Shahdara is deep to very deep, a well drained, calcareous, medium textured soil, formed in Recent mixed alluvium and occupies level to nearly level Active and Recent River plains. It shows no B horizon. It shows a light grayish brown, friable, calcareous, massive silt loam topsoil and stratified layers of various silty loam and very fine sandy loam subsoil.



Ap 0-15 cm: Light grayish brown (2.5Y 5/2) moist and light brownish gray (2-5Y 6/2) dry silt loam; massive; moderately calcareous; pH 8.4.

C1 15-33 cm: Light grayish brown (2.5Y 5/2) moist and light brownish gray (2.5Y 6/2) dry; <5mm very fine faint and few distinct brown (10YR 5/6) mottles; silt loam; stratified; slightly sticky, slightly plastic, friable moist, slightly hard dry; moderately calcareous; pH 8.4.

C2 33-64 cm: Dark grayish brown (2.5Y 4/2) moist and light brownish gray (2-5Y 6/2) dry; very fine sandy loam (approaching loamy very fine sand); massive and stratified; very slightly sticky, non-plastic, very friable moist, soft dry; moderately

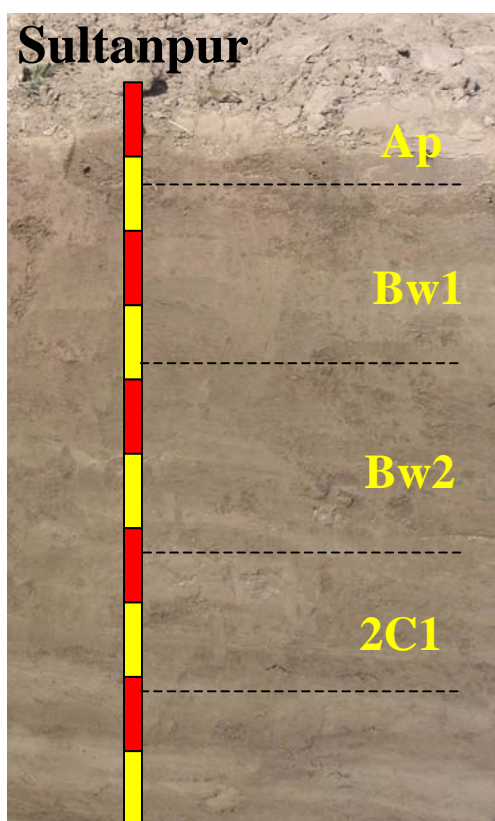
calcareous; pH 8.4.

C3 (64-78 cm) dark grayish brown (10YR 4/2) moist and light brownish gray (10YR 6/2) dry; very fine sandy loam; stratified; slightly sticky, slightly plastic, friable moist, slightly hard dry; few very fine tubular pores; moderately calcareous; pH 8.4.

C4 (78+ cm) brown/dark brown (10YR 4/3) moist and pale brown (10YR 6/3) dry; silt loam with half cm thick lens of silty clay; stratified; slightly sticky, moderately calcareous; pH 8.4.

Sultanpur profile

The Sultanpur series consists of deep, well drained, calcareous, medium textured soils developed in Subrecent period alluvium. The series occupies Subrecent level plains. It consists of a Cambic B horizon about 50 cm thick and shows a dark grayish brown, friable, calcareous massive, silty clay loam topsoil, underlain by a brown/dark brown, friable calcareous silt loam B horizon with weak coarse subangular blocky structure. The substratum may be stratified.



Ap 0-15 cm: Brown/dark (10YR 4/3) moist and light grayish brown (10YR 6/2) dry; silty loam; massive; slightly sticky, slightly plastic, very friable moist, slightly hard dry; moderately calcareous; pH 8.4.

Bw1 15-38 cm: Brown/dark brown (10YR 4/3) moist and pale brown (10YR 6/3) dry; few fine faint mottles; silt loam; weak coarse subangular blocky slightly sticky, slightly plastic, friable moist, slightly hard dry; thin patchy clay cutans; pH 8.3.

Bw2 38-62 cm: Brown (10YR 5/3) moist and light brownish gray (10YR 6/2) dry, few fine distinct yellowish brown (10YR 5/6) mottles: very fine sandy loam; massive; slightly sticky, slightly plastic, very friable moist, slightly hard dry; moderately calcareous; pH 8.3.

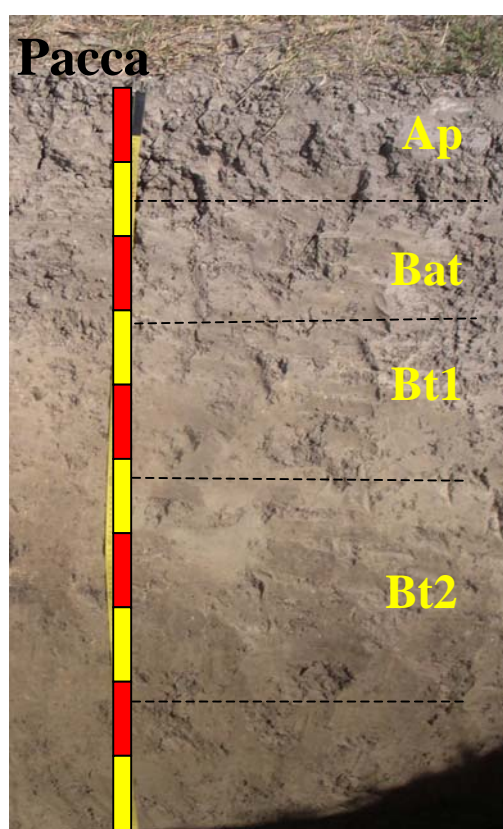
calcareous; pH 8.3.

2C1 62-82 cm: Brown/dark brown (10YR 4/3) moist and brown (10YR 5/3) dry; common fine distinct yellowish brown (10YR 5/6) mottles; silt loam; massive breaking into weak coarse sub angular blocky; slightly sticky, slightly plastic, friable moist, slightly hard dry; moderately calcareous; pH 8.3.

2C2 82-90 cm: Brown (10YR 5/3) moist and pale brown (10YR 6/3) dry; few distinct mottles; silt loam; massive; slightly sticky, slightly plastic, friable moist, hard dry; moderately calcareous; pH 8.3.

Pacca profile

The Pacca series consists of deep, imperfectly drained, fine textured, calcareous soils with a structural (Cambic) B horizon. The series occurs in level to nearly level broad in-filled basins and along drainage channels in the Subrecent sediments on Old River Terrace and in the Subrecent floodplain. It consists of a grayish brown and dark grayish brown silty clay, massive, moderately calcareous A horizon is underlain by a dark and very dark grayish, brown, silty clay, weak coarse subangular blocky, moderately to strongly calcareous B horizon usually to about 92 cm underlain by a yellowish brown silty clay, massive, strongly calcareous C_k horizon.



Ap 0-15 cm: Grayish to brown (2.5Y 5/2) moist and light brownish gray (2.5Y 6/2) dry with common very fine rusty root mottles; silty clay; massive; very sticky, very plastic, firm moist, very hard dry; pH 8.4.

Bat 15-35 cm: Dark grayish brown (10YR 4/2) moist and light gray (5Y 6/1) dry; silty clay; massive; very sticky, very plastic, firm moist, very hard, dry; very few iron and manganese concretions; moderately calcareous; pH 8.4.

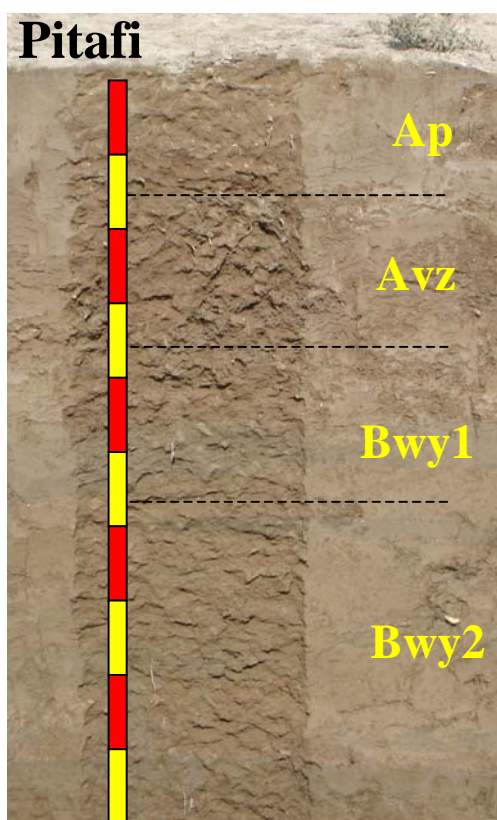
Bt1 35-66 cm; Dark grayish brown (2.5Y 4/2) moist and light gray (5Y 6/1) dry with few faint rust brown mottles (around lime specks); silty clay; weak coarse subangular blocky; very sticky, very plastic, very firm

moist, very hard dry thin patchy cutans in pores and on peds faces; common very fine lime specks and lime nodules; strongly calcareous; pH 8.4.

Bt2 66-94 cm: Very dark grayish brown (2.5Y 3/2) moist and light gray to gray (5Y 6/1) with common fine faint and distinct yellowish brown mottles; silty clay; weak coarse subangular blocky; very sticky, very plastic, firm moist, extremely hard dry; thin patchy cutans; few fine iron and manganese concretions and few fine lime concretions; strongly calcareous; pH 8.4.

Pitafi profile

The Pitafi series consists of a deep, moderately well drained, calcareous, gypsiferous, strongly saline fine textured soils formed in Subrecent mixed calcareous alluvium and occupies flat areas in the Subrecent floodplains. It shows a structural (Cambic) B horizon and a brown/dark brown, friable, calcareous, gypsiferous, strongly saline, granular clay loam topsoil underlain by a brown/dark brown, firm, calcareous, gypsiferous, strongly saline silty clay B horizon with weak coarse subangular blocky structure.



Ap 0–16 cm: Brown/dark brown (10YR 4/3) moist and light brownish gray (10YR 6/2) dry; clay loam; weak granular; sticky, plastic, friable, moist, hard dry; many soft gypsum nodules and soft salt specks; slightly calcareous; pH less than 8.0.

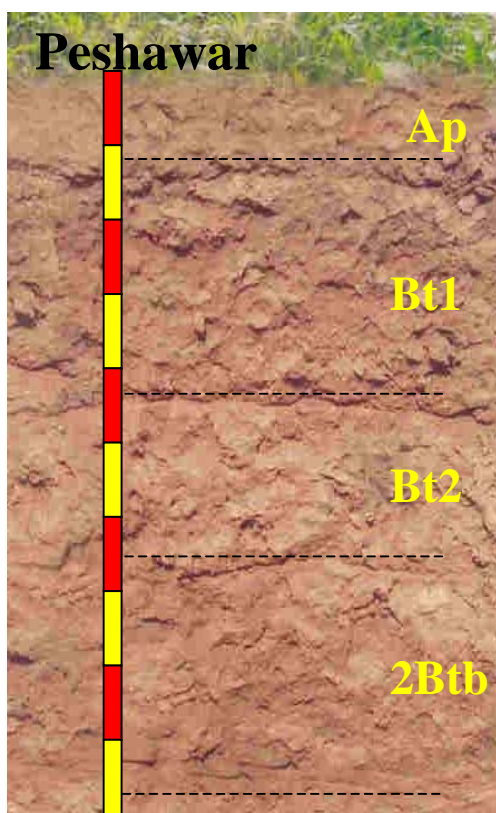
Avz 16-35 cm: Brown/dark brown (10YR 4/3) moist and pale brown (10YR 6/3) dry; silty clay; weak coarse subangular blocky; very sticky, very plastic, firm moist, very hard dry; thin broken cutans along ped faces; common pockets of fine gypsum crystals; moderately calcareous; pH 8.4.

Bwy1 35-58 cm: Brown/dark brown (10YR 4/3) moist and pale brown (10YR 6/3) dry; few fine faint yellowish brown (10YR 5/6) mottles; silty clay; very weak coarse subangular blocky; very sticky, very plastic, firm moist, very hard dry; few fine soft gypsum specks and crystals; moderately calcareous; pH 8.4.

Bwy2 58-99 cm: Brown/dark brown (10YR 4/3) moist and pale brown (10YR 6/3) dry; few fine faint yellowish brown (10YR 5/6) mottles; silty clay weak fine platy and massive; very sticky, very plastic, firm moist, very hard dry; few fine soft gypsum nodules and crystals; moderately calcareous; pH 8.4.

Peshawar profile

Peshawar soil is developed in piedmont alluvium from mixed material derived from adjacent hills.



Ap-0 to 11 cm; brown (7.5 YR 5/4) dry brown to dark brown (7.5YR 4/4) moist; silty clay loam; weak medium and coarse sub angular blocky; very hard and hard, friable, sticky, slightly plastic; strongly effervescent; moderately alkaline pH 8.2.

Bt1-11 to 43 cm; light brown (7.5 YR 6/4) brown to dark brown (7.5YR 4/4) moist; silty clay loam; weak very coarse prismatic structure parting to weak coarse sub angular blocky; very friable, sticky, slightly plastic; common continuous organic coats on peds; discontinuous faint-thin clay films in root channels and/or pores; few strongly effervescent; pH 8.2.

Bt2-43 to 66 cm; light brown (7.5 YR 6/4) dry and brown to dark brown (7.5YR 4/4)

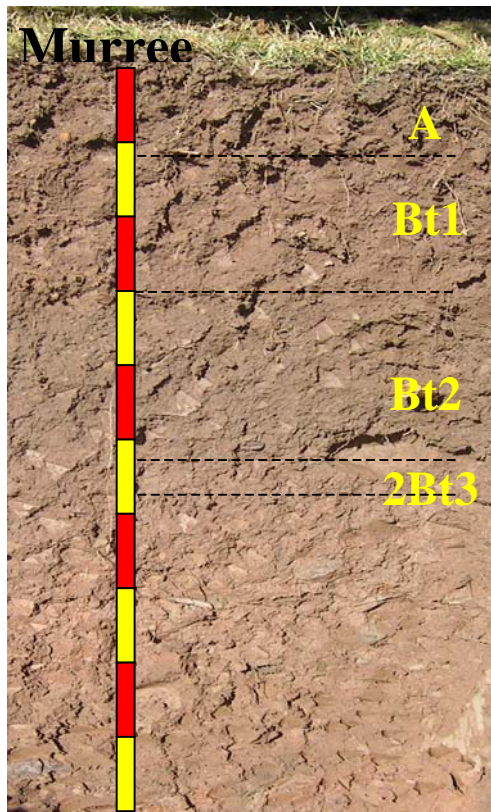
moist; silty clay loam; weak coarse prismatic structure parting to weak coarse sub angular blocky; very friable, sticky, slightly plastic; common organic coats on peds; discontinuous clay films in pores; strongly effervescent; pH 8.3.

2Btb-66 to 98 cm; brown (7.5 YR 5/4) dry and brown to dark brown (7.5YR 4/4) moist; silty clay loam; moderate coarse prismatic structure parting to weak coarse sub angular blocky; friable, sticky, plastic; continuous organic coats on peds; discontinuous clay films on peds; strongly effervescent; pH 8.4.

2Btkb-98 to 138 cm; dark brown (7.5 YR 3/4) dry and brown to dark brown (7.5YR 4/4) moist; clay loam; weak very coarse prismatic structure parting to weak medium sub angular blocky; very friable, sticky, slightly plastic; continuous organic coats on peds; continuous clay films on peds and in pores; common medium carbonate nodules; strongly effervescent; pH 8.4.

Murree profile

The Murree soil occurs in humid climate. It is slightly calcareous to non-calcareous and texture varies from gravely loam to silty clay. The loess occupies nearly level to steeply dissected plains in small patches. The climate is sub-humid in the northern part and gradually changes to semi-arid in the southeast with hot summer and cool winter.



A-0 to 11 cm; dark reddish brown (5YR 3/2) moist; silty clay loam; weak medium subangular blocky structure parting to weak fine subangular blocky; friable, slightly sticky, slightly plastic; few thin organic coats in root channels and/or pores; mildly alkaline; pH 7.6.

Bt1-11 to 30 cm; dark reddish brown (5YR 3/3) and dark reddish gray (5YR 4/2) moist; clay; moderate coarse prismatic structure parting to moderate medium prismatic; very firm, slightly sticky, very plastic; continuous distinct clay films on peds and in pores; continuous thick clay films in root channels and/or pores; shale fragments; pH 7.6.

Bt2-30 to 52 cm; dark reddish brown (5YR 3/3) interior and reddish brown (5YR 4/3) exterior moist clay; weak coarse subangular blocky structure parting to medium subangular blocky; firm, slightly sticky, very plastic; continuous clay films in pores; pH 7.7.

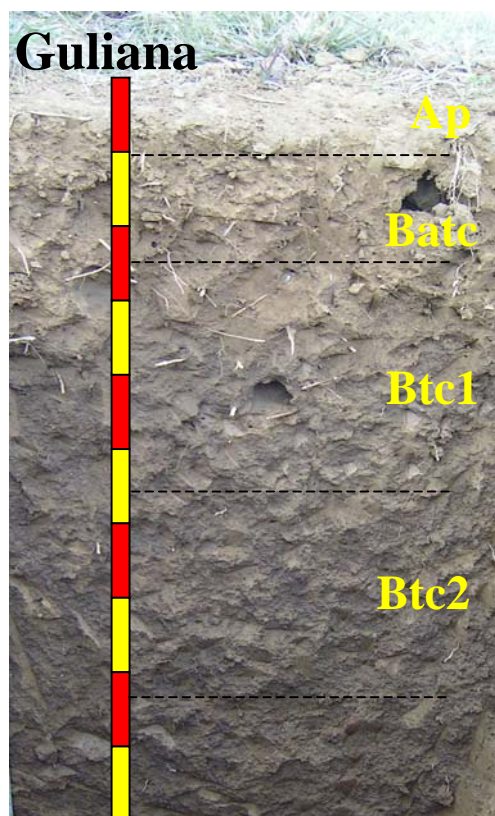
2Bt3-52 to 58 cm; dark reddish brown (5YR 3/2) moist clay loam; massive, friable, slightly sticky, slightly plastic; continuous distinct-thin clay films in pores; soft sandstone fragments within horizon; pH 7.7.

3Bt4-58 to 87 cm; dark reddish brown (5YR 3/3) moist; silty clay; moderate fine subangular blocky structure parting to moderate very fine angular blocky; friable, sticky, plastic; continuous thin cutan in pores; shale fragments; pH 7.7.

4Btk-87 to 115 cm; reddish brown (5YR 4/3) exterior, dark reddish brown (5YR 3/3) and reddish brown (2.5YR 4/4) moist; stony clay; massive; friable, sticky, plastic; continuous cutan in pores; strongly effervescent; pH 7.8.

Guliana profile

The Guliana soil occupies nearly level position in sub-humid areas and slightly depression position in semi-arid areas where runoff is collected. The soils' decalcification and elluviation processes are active.



Ap-0 to 12 cm: Yellowish brown (10YR 5/4) brown to dark brown (10YR 4/3) moist; silt loam; weak coarse subangular blocky; hard, friable, slightly sticky, slightly plastic; pH 7.8.

Bate-12 to 25 cm; brown to dark brown (10YR 5/4) silt loam; brown to dark brown (10YR 4/3) moist; weak very coarse prismatic structure parting to weak coarse prismatic; hard, friable, slightly sticky, slightly plastic; discontinuous clay films on peds and in pores; 0.5-2 mm iron-manganese concretions; very slightly effervescent; mildly alkaline; pH 7.8.

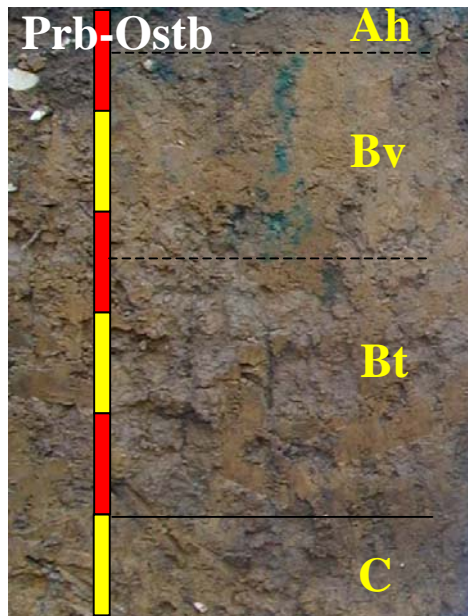
Btc1-25 to 56 cm; brown to dark brown (10YR 4/3) dark brown (10YR 3/3) moist; silty clay loam; weak fine prismatic structure parting to moderate medium subangular blocky; hard, friable, sticky, plastic; continuous distinct clay cutans; 0.5-2 mm iron-manganese shot; slightly effervescent; pH 7.8.

Btc2 56 to 83 cm: Yellowish brown (10YR 5/4) and brown to dark brown (10YR 4/3) silty clay loam; weak fine prismatic structure parting to moderate medium sub angular blocky; hard, friable, slightly sticky, slightly plastic; continuous clay cutans on peds and in pores; 0.5-2 mm iron-manganese concretions; very slightly effervescent; pH 7.8.

BCtc-83 to 117 cm; light yellowish brown (10YR 6/4) and yellowish brown (10YR 5/4) dark yellowish brown (10YR 4/4) moist; silt loam; weak medium subangular blocky structure; hard, friable, slightly sticky, slightly plastic; few discontinuous clay films on peds and in pores; 0.5-2 mm iron-manganese concretions; slightly effervescent; pH 7.8.

Prb-Ostb and Prb-Wein profiles

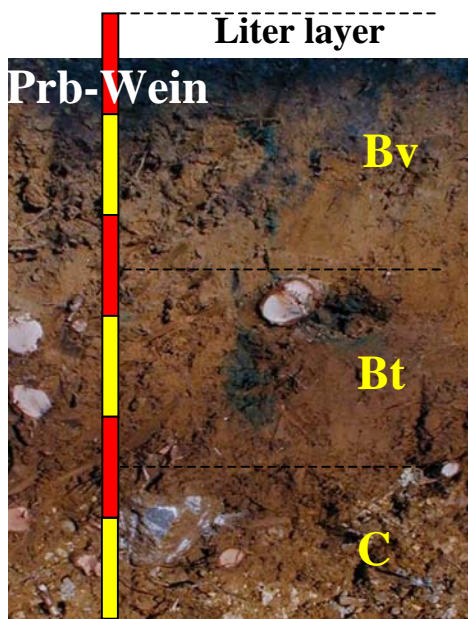
The two German soil profiles show green and blue dye patches at some places, which are due to the dye used for a separate study however the soil horizon description is the same. The color (yellow to brown) other than green and blue patches is the original color of each soil.



Ah (0-4 cm) medium granular and subangular blocky silt loam, 10YR4/2, pH 5.4, non-calcareous, soil organic matter 9.7%;

Bv (4-25 cm) moderate medium angular blocky silty clay loam, pH 4.95, non-calcareous, soil organic matter 2.4%;

Bt (25-55 cm) strong medium subangular blocky and prismatic silty clay, pH 6.2, non-calcareous, soil organic matter 2.1%.



Ah (0 – 4 cm) moderate medium granular silt loam, 10YR2/3, pH 4.66, non-calcareous, soil organic matter 7.7%.

Bv (4 – 25 cm) moderate medium and coarse angular blocky silt loam; pH 6.0; non-calcareous, soil organic matter 2.2%;

Bt (25-48 cm) moderate coarse subangular blocky silty clay loam, 10YR5/6, pH 6.5, non-calcareous, soil organic matter 1.5%.

3.2 Basic soil properties

Each sample was analyzed for pH, electrical conductivity and the contents of CaCO_3 , organic matter, Olsen P, Fe_d , Fe_o , Al_d , and Al_o and some major and trace elements. Soil pH and electrical conductivity was measured in 1:2 soil water extract using MultiLine WTW P4. Total CaCO_3 was determined by acid neutralization method. A given weight of soil was reacted with an excess of acid and the unreacted acid was back titrated with standardized NaOH solution (FAO, 1974). Organic matter content was determined by the Walkley Black method, which involved reduction of potassium dichromate ($\text{K}_2\text{Cr}_2\text{O}_7$) by organic carbon and subsequent determination of the unreduced dichromate by oxidation-reduction titration with ferrous ammonium sulfate (Walkley, 1947; FAO, 1974). Olsen P was determined by extracting the soil with 0.5M NaHCO_3 (pH 8.5). The concentration of phosphorous in the soil extract was determined by ascorbic acid method of Murphy and Riley, (1962).

3.2.1 Iron and aluminum oxide determination by CBD method

Citrate bicarbonate dithionite (CBD) method of Mehra and Jackson (1960) extracts both crystalline and poorly crystalline iron oxide phases present in a soil without any differentiation among the phases. Five g grounded, air-dried soil, passed through 250-mesh in^{-1} was placed in a 100 mL polypropylene centrifuge tube along with 40 mL of 0.3M $\text{Na}_3\text{C}_6\text{H}_5\text{O}_7 \cdot 2\text{H}_2\text{O}$ and 5 mL 1M NaHCO_3 . The material was mixed, and heated in a water bath for several minutes while stirring. When the temperature of the soil suspension had risen to 75 to 80°C, 1 g of $\text{Na}_2\text{S}_2\text{O}_4$ was added; and stirred for 1 minute then intermittently for 5 minutes. The process was repeated with a second addition of 1 g sodium dithionite. Fifteen mL of saturated NaCl was added to flocculate the contents and centrifuged for 5 minutes at 2200 rpm. The supernatant was raised to suitable volume using distilled water. Iron concentration in the extract was determined by using AAS, Perkin Elmer precisely, AAnalyst 200, with detection limit of 0.01 mg Fe L^{-1} . The values ranged between 0.36 and 2.32 mg Fe L^{-1} .

3.2.2 Iron and aluminum oxide determination by ammonium oxalate method

Poorly crystalline iron oxide was extracted with acid ammonium oxalate (McKeague and Day, 1966). The extraction procedure was carried out in dark to prevent photoreduction and retard rate of dissolution of the crystalline iron oxides. Thirty mL of 0.2M acid oxalate solutions were added into 50 mL

centrifuge tubes with a screw cap containing 0.5 g (<2 mm) air-dry soil. The tubes were wrapped with aluminum foil and shaken for 4 hours on an end-over-end shaker at 250 rpm. The tubes were left standing for 1 hour and centrifuged for 20 minutes at 2000 rpm. The clear supernatant was transferred into clean vials and was analyzed for Fe using inductively coupled plasma, optical emission spectrometer (ICP-OES), Varian 715-ES with detection limit of 25 $\mu\text{g Fe L}^{-1}$. The readings were between 215000 and 3588000 $\mu\text{g Fe L}^{-1}$.

3.2.3 Soil elemental analysis by XRF

Soil elemental analysis was carried out by wavelength dispersive X-ray fluorescence (WD-XRF) (Tertian and Claisse, 1982). Soil sample was grounded in an agate mortar. Fused glass disks were prepared by mixing 0.5 g of sample with 5 g of spectromelt from SPECTROFLUX 110 mixture of lithium tetraborate and lithium metaborate (66.5:33.5 w/w%). The mixed contents were transferred to platinum crucibles and were melted at 500°C in the first burner to about 1150°C in the last burner. Total melting time was 40 minutes, 7 minutes on each burner with swirling of the crucibles. After fusion, the melt was quenched to a flat glass tablet. The samples were measured against the BE-N standard in the SRS 303 AS instrument. Separately, loss on ignition was determined by heating the sample powders in a muffle furnace at 950°C for 4 hours.

3.3 Soil fractionation and particle size analysis

3.3.1 Pretreatments

Soil carbonates, organic matter, and free iron oxides inhibit particle dispersion. Soil carbonates and organic matter were removed by chemical treatments to improve dispersion. Sufficient quantity of 1N Na-acetate buffer (about 1 cm above the sample) was added into 250 mL polypropylene centrifuge tubes containing 45 g of soil (yielding at least 10% clay). The mixtures were heated at 95°C for 30 minutes and stirred occasionally, cooled, centrifuged at 1600 rpm for 5 minutes and the supernatant liquid was decanted. The process was repeated three times in order to achieve complete removal of soil CaCO_3 . When decanting for the third time, the centrifuge cake was kept in a hot water bath to evaporate excess water. Care was taken not to completely dry off the soil. The resulting sample material was treated to remove organic matter (Jackson, 1969; White and Dixon, 2003). The sample was transferred to a 250 mL polypropylene centrifuge tube. Then 10 mL of 30% H_2O_2 was added and kept at room temperature for 12 hours. In order to avoid sample loss by

frothing, the centrifuge tubes were placed in tall beakers covered with a watch glass. After 12 hours, the samples in which frothing had occurred, were washed back into the 250 mL centrifuge tubes with 1N Na-acetate (pH 5). Once frothing at room temperature had subsided, all samples were heated in a water bath at 90°C to ensure the complete removal of organic matter. The samples were cooled and washed with Na-acetate, centrifuged at 2000 rpm for 5 minutes and decanted. The process of centrifugation and decantation was repeated until a clear supernatant was obtained.

3.3.2 Separation into sand, silt and clay fractions

The treated soil samples were washed with 0.01 mM Na₂CO₃ (pH 10) and transferred into 500 mL beakers and dispersed by 30 s sonification with a macrotip. The separation of the sand fraction (>50 µm) was achieved by sieving through 50 µm nominal size sieve. The residue at the sieve was washed free of fine particles using pH 10 Na₂CO₃ solution, transferred to glass beaker, and oven dried at 100°C. Silt size fraction was separated on the basis of their rate of fall in liquid calculated by Stoke's law (Jackson, 1969). The suspension containing particles ≤50 µm size was transferred to a 2L cylinder, mixed by a plunger and left undisturbed. The suspension containing ≤2 µm diameter particles was siphoned out and the cylinder was filled again with Na₂CO₃ and the suspension mixed by plunging. The process was repeated until the suspension was clear. The silt fraction was transferred to glass beaker, washed with distilled water, oven dried at 100°C and weighed and the clay suspension was dialyzed to remove free salts, freeze-dried and weighed.

3.4 Soil mineralogy

3.4.1 Sand, silt and clay mineralogy by X-ray diffraction

The un-oriented powder mounts of ground sand and silt were prepared in Perspex plastic holders. X-ray scan was carried out between 15° and 50° 2θ at a scanning rate of 0.5° 2θ per minute using Siemen D500 Diffractometer with Cu target tube (Cu Kα radiation) and graphite monochromator. X-ray diffraction analysis was carried out after saturation with K and Mg ions and heat treatments and glycolation.

To saturate clays with Mg, 25 mL of 1N magnesium chloride (MgCl₂) was added into a 50 mL centrifuge tube containing 70 to 75 mg of clay fraction. The suspension was mixed, sonicated for 30 seconds to disperse and

centrifuged at 1000 rpm for 5 minutes and clear liquid was decanted. The process was repeated and then the clay was washed with distilled water until dispersion had started (maximum 4 washings). After dispersion, the clay material was centrifuged at higher speed such as 2000 rpm for 5 minutes (longer if required). Slowly and carefully the supernatant was discarded, leaving about 3-4 mL amount of water, hand mixed and sonicated for 30 seconds. The spectrographic clean microscopic slides were labeled, placed on smooth and undisturbed surface and the prepared sample was dispersed onto the slides using disposable bulb pipette (using same bulb pipette, the sample was mixed several times by sucking liquid up into the pipette and then discharging it with force upon the un-dispersed material at the bottom of the tube). The slides were left for about 24 hours to dry up. Use of lamp was avoided because it resulted in curling up of slides. The clay was K-saturated using 1N KCl using the same steps.

The Mg- and K-saturated air-dry clay was determined by X-ray diffraction. The glycol treatment was applied to the Mg-saturated clay. The slides were kept on wire gauze in a covered rectangular container having glycol beneath, at 40°C. After 24 hours of glycol treatment in oven the Mg-saturated glycol solvated slides were ready for XRD measurement. In order to avoid the drying of glycol, 3 slides at a time were run on XRD. The K-saturated clay was heat treated first at 350°C for 2 hours and then at 550°C for 2 hours in a furnace. After each treatment, the clay was X-rayed.

3.4.2 Smectite and vermiculite quantification by CEC

Vermiculite and smectite were determined from the Ca/Mg and K/NH₄ CEC. Vermiculite in clays was determined by measuring the loss of CEC when a K-saturated clay was heated at 110°C. First, Ca/Mg CEC was determined by washing the clay with 1N CaCl₂ solution and replacing the Ca by washing with 1N MgCl₂. Then, K/NH₄ was determined by washing with 1N KCl and heating the K-saturated clay and then replacing the K with 1N NH₄Cl. The Ca/Mg CEC was attributed to both vermiculite and smectite and K/NH₄ to smectite only. Vermiculite was assumed to have CEC of 160 cmol_c kg⁻¹ than smectite 110 cmol_c kg⁻¹ (Marshall, 1935; Alexiades and Jackson, 1965). The following steps describe the procedure in detail:

1. One hundred mg of clay was weighed into the pre-weighed 50 mL plastic centrifuge tubes, which were resistant to heating at 110°C temperature.

2. Twenty mL of 1N CaCl₂ solution was added to the tubes, shaken for 10 minutes on an end-over-end shaker at 300 rpm, centrifuged for 5 minutes at 2000 rpm and the supernatant was carefully discarded avoiding any clay loss. The process was repeated two more times.
3. The same clay was washed with 0.01N CaCl₂ by hand mixing and centrifugation and the supernatant was discarded. This process was repeated 3 times. The amount of interstitial solution was recorded by weight difference of dry-tube +clay – wet-tube+clay.
4. The Ca-saturated clay was washed 4 times with 1N MgCl₂ each time decanting the supernatant into a 100 mL flask. The final volume was raised to 100 mL. Calcium content in the extract was determined using atomic absorption spectrophotometry.
5. Next, the clay was saturated with K by four washings of 1N KCl and then with four washings of 0.01N KCl. After the final wash the interstitial solution was recorded by weighing the tubes.
6. The clay was oven dried overnight at 105°C.
7. The dried clay was first soaked with few drops of distilled water and then with addition of 20 mL 1N NH₄Cl, then was thoroughly dispersed using 30 seconds sonification and was centrifuged. Washing with 1N NH₄Cl, dispersion and centrifugation was repeated 4 times saving the supernatant each time into 100 mL flask and volume was raised by additional 1N NH₄Cl.
8. Potassium content in the extract was determined using atomic absorption spectrophotometry.

Calcium and K contents were analyzed using Perkin Elmer precisely, AAnalyst 200, Atomic Absorption Spectrometer with detection limits of 0.001 and 0.085 mg L⁻¹ for Ca and K respectively. Vermiculite and smectite were calculated from the exchangeable Ca and K content.

3.4.3 Kaolinite quantification by STA

Kaolinite in clay fraction was quantified by simultaneous thermal analysis (STA). The measurements were performed on a STA 449 C Jupiter from NETZSCH-Gerätebau GmbH with a Thermogravimetry/Differential Scanning Calorimetry (TG/DSC) sample holder. The STA is connected with a quadruple mass spectrometer 403 C Aëolos from IPI/InProcess Instruments/NETZSCH-Gerätebau GmbH. All samples were measured after

storage in closed containers at laboratory conditions (T about 20-25°C and relative humidity of 45-65%). The conditions for the STA measurements are reported in table 3.2. Since the dehydroxylation from smectite, vermiculite, and mica also occurs between 450°C and 590°C, necessary correction was made using the smectite and vermiculite content calculated from the Ca/Mg and K/NH₄ CEC values. Further, the molecular weight of kaolinite was taken as 258 g mol⁻¹, and due to dehydroxylation, 2 moles of H₂O equal to 36 g mol⁻¹ were taken as removed with each mole of kaolinite. Hence, the change in mass amounted to 14% ((36/258)*100) and change in mass due to smectite/vermiculite was assumed to be 10% ((36/360)*100), where one mole of smectite amounted to 360 g.

Table 3.2. Simultaneous thermal analysis measurement conditions.

Parameters	TG/DSC/MS
Sample amount	100 mg
Grain size	Powder
Packing density	Loosely packed, no pressing
Reference material	Empty crucible with lid
Furnace atmosphere	50 mL min ⁻¹ air + 20 mL min ⁻¹ N ₂
Crucibles	Pt/Rh with lid
Thermocouples	Pt/Pt ₉₀ Rh ₁₀
Heating rate	10 K min ⁻¹
Temperature range	35-1000 °C

3.5 Iron oxide determination

3.5.1 Pre-concentration and phase identification by XRD

Iron oxides often account for a small percentage of the soil clay fraction and phase analysis is limited by relatively high detection limit especially in case of goethite, which is less crystalline than hematite. Clays were concentrated before XRD analysis to help identifying the minor concentrations of iron oxide.

One hundred mL of 5M NaOH was added into a covered 150 mL Teflon beaker containing 1 g clay (<2 µm) and 0.2M Si. The mixture was boiled for 2 hours on a sand bath and transferred to centrifuge tubes after cooling. The sample was then washed once with 5M NaOH and two times with 0.5M HCl to

dissolve sodalite, twice with 1N ammonium carbonate $(\text{NH}_4)_2\text{CO}_3$ to remove NaCl and twice with distilled water to remove excess NH_4^+ and CO_3^{2-} . Finally, the clay was dried overnight at 110°C to volatilize the remaining $(\text{NH}_4)_2\text{CO}_3$ and X-ray analysis of the concentrated iron oxides was carried out.

3.5.2 Iron oxide determination by cyclic voltammetry

Goethite and hematite in mixture or as separate phases were determined using cyclic voltammetry with a carbon paste electroactive electrode (CPEE). Current change against Ag/AgCl reference electrode during re-oxidation of Fe^{2+} released from reductive dissolution of iron oxide was measured (Grygar et al., 2002). The working electrode was CPEE consisting of a 60 mm long and 4 mm diameter graphite rod. The graphite rod was impregnated with boiling paraffin under vacuum and both the ends were polished to make them conductive before use. One end attached to the voltammeter circuit and the other was coated with the weighed (40 mg) clay-powdered graphite paste, covered with a piece of porous paper secured with a rubber band. The clay-graphite paste had butter like consistency prepared by mixing of 20 mg clay, 100 mg laboratory grade graphite powder and 0.1 mL acetate buffer (acetic acid to Na-acetate 1:1; total acetate 1M) in an agate mortar. Acetate buffer (1:1, total acetate 0.2M) was used as supporting electrolyte. The working electrode was placed in 50 mL cup containing supporting electrolyte solution under Metrohm VA Stand 694 and measurements were made on a computer-controlled voltammeter (Metrohm VA Processor 693).

Cyclic voltammetry uses the recording of current change as potential (E) progressed from -1000 mV to +1000 mV and, in reverse cycle, +1000 mV to -1000 mV at a scanning rate of 10 mV sec^{-1} after 3 min purging with N_2 . The N_2 purging continued during the scan. The peak area (W) was calculated from the plot of potential (V) vs. current (A) by integrating (within the limits of reaction) the polynomial regression equations fitted on both sides of the curve implemented in a spreadsheet. Standard calibration graphs were developed using reference goethite and hematite material. Memon et al. (2008) presented the detection limit of the technique. Quantity of goethite and hematite in the soil clay was read from calibration graphs.

3.6 Phosphorus determination

3.6.1 Total phosphorus

Total P was digested using the HClO_4 method of Olsen and Sommers (1982). Thirty mL of 60% HClO_4 was placed in 250-mL calibrated digestion tube containing 2 g air-dry soil (0.15 mm) along with few pumice-boiling granules. The tubes were placed in a block-digester, first heated to 100°C , slowly the temperature was raised to 180°C and the samples were digested till the material was like white sand. The mixture was cooled, raised to suitable volume and filtered through ashless filter paper (Schleichel & Schuell 589³, Germany). The P in the filtrate was determined by the molybdenum blue color method (Murphy and Riley, 1962) using Perkin Elmer UV/Vis Spectrometer Lambda 2S with detection limit of $0.015 \text{ mg P L}^{-1}$. The values ranged between 0.13 and $0.856 \text{ mg P L}^{-1}$.

3.6.2 Sequential extraction of inorganic phosphorus

Sequential extraction procedure of P was carried out according to the method of Jiang and Gu (1989) for calcareous soils, and was further carried out in accordance with Samadi and Gilkes (1998). A brief methodology is given below:

NaHCO_3 -extractable P (Ca_2 -P): Phosphorus related to di-calcium phosphate. One g soil along with 50 mL of 0.25 M NaHCO_3 (pH 7.5) was shaken in an orbital shaker for 1 hour, centrifuged, decanted and the supernatant was analyzed for P.

NH_4 -Ac-extractable P (Ca_8 -P): Phosphorus related to octa-calcium phosphate. The soil residue was washed twice with 95% alcohol and kept for 4 hours after adding 50 mL of 0.5 M $\text{CH}_3\text{COONH}_4$ (pH 4.2), shaken for 1 hour, centrifuged, decanted and the supernatant was analyzed for P.

NH_4 -F-extractable P (Al-P): Phosphorus adsorbed by Al oxides. The soil residue was washed twice with saturated NaCl solution, shaken for 1 hour after adding 50 mL 0.5 M NH_4F (pH 8.2), centrifuged, decanted and the supernatant was analyzed for P.

$\text{NaOH-Na}_2\text{CO}_3$ -extractable P (Fe-P): Phosphorus adsorbed by Fe oxides. The soil residue was washed twice with saturated NaCl solution, shaken for 2 hours after adding 50 mL mixture in 1:1 ratio 0.1M NaOH -0.1M Na_2CO_3 , left unshaken for 16 hours, shaken again for 2 hours, centrifuged, decanted and the supernatant was analyzed for P.

Occluded P (Occluded-P): Phosphorus incorporated or trapped in Fe oxide coatings. The soil residue was washed twice with saturated NaCl, kept in hot water bath after adding 40 mL 0.3M sodium citrate solution. When the temperature reached 80°C, 1 g of sodium dithionite was added and the suspension was stirred continuously for 15 minutes, centrifuged and decanted. The supernatant was digested with 3 acid solutions (1 H₂SO₄ : 2 HClO₄ : 7 HNO₃) and raised to suitable volume for P determination.

H₂SO₄-extractable-P (Ca₁₀-P): Phosphorus present as apatite. Fifty mL of 0.5M H₂SO₄ were added to the remaining soil residue, shaken for 1 hour, centrifuged, and the supernatant analyzed for P. The residue was discarded.

In all steps, shaking of soil was carried out on an orbital shaker at 150 rpm. Temperature throughout the experiment was between 20-25°C (April 2007). The centrifugation of supernatant, followed after shaking was done on 2000 rpm for 10 minutes for all the steps. Centrifugation for washing was done at 2000 rpm for 5 minutes for all the steps. Washing of soil was done by mixing with hand, till all the residue (soil sample at the bottom) was mixed and then centrifuged.

The amount of P in each fraction was determined using inductively coupled plasma, optical emission spectrometer (ICP-OES), Varian 715-ES having detection limit of 0.1 mg P L⁻¹. The majority of the samples lied in the range of the detection limit. Those lying below the detection limit of 0.1 mg were considered having <0.1 mg P L⁻¹. All the standards were prepared using the same matrix as that of each fraction.

3.6.3 Phosphorus sorption isotherms

Phosphorus sorption experiments were carried out according to the method of Fox and Kamprath (1970). Two g air-dried, <2 mm sized soil was placed in a 50 mL centrifuge tube with a screw cap and was equilibrated with 20 mL of 1 of 13 P solutions: 0, 1, 5, 10, 15, 20, 50, 100, 150 and 250 μ P mL⁻¹ (equal to additions of 0, 10, 50, 100, 150, 200, 500, 1000, 1500 and 2500 mg P kg⁻¹ soil). The P solutions were prepared by dissolving monobasic potassium phosphate (KH₂PO₄) in 0.01M CaCl₂. Three drops of chloroform were added to each tube to inhibit microbial activity. The tubes were shaken for 24 hours on an end-over-end shaker at 150 rpm. After equilibration, the tubes were centrifuged at 2000 rpm at 25°C for 15 minutes. The supernatant was then passed through ashless filter paper (Schleicher & Schuell 589³, Germany) and the P in solution was measured by the molybdenum blue color method

(Murphy and Riley, 1962) using Perkin Elmer UV/Vis Spectrometer Lambda 2S with detection limit $0.015 \text{ mg P L}^{-1}$. The amount of P adsorbed was determined by the difference between the initial and final amounts of P in solution. The sorption isotherm of P was modeled using Freundlich and two surface Langmuir equations.

3.7 Transmission electron microscopy (TEM)

Identification of iron particles goethite and hematite was carried out by TEM. Dilute suspension of the clay was prepared in water and a fine mist of the clay suspension was sputtered on a 200-mesh grid with Formvar (sp.) film on it. The sample was viewed on Zeiss EM 912 ω transmission electron microscope operated at 120 kV, which gave a resolution of 0.33 nm.

The association of P with iron oxide was tested by saturating the iron oxides with phosphorus and analyzing on TEM equipped with microanalysis probe. One g of clay was washed with 25 mL of 1M KH_2PO_4 solutions in 50 mL centrifuge tubes. The suspension was shaken for 30 minutes on an orbital shaker at 150 rpm. After equilibration the suspension was centrifuged at 4000 rpm for 10 minutes and the supernatant was discarded. The clay residue was suspended in distilled water and centrifuged and the supernatant discarded. This washing was repeated for three times. After the final washing the clay was dried in oven at 50°C . The P-saturated dried clay was further processed for TEM in the similar manner mentioned above.

3.8 Statistics

Statistical analyses were performed using SAS version 9.0 (SAS institute, 2003) for analysis of variance and multiple regression analysis. Data for most parameters was transformed using standard Box and Cox generalized power transformation (Joseph and Bhaumik, 1997). Soil means (mean of horizons) were compared using Duncan Multiple range test. Stepwise regression analysis maximizing r^2 was undertaken to generate empirical model for predicting P sorption based on the available basic properties. In the regression analysis “soil” was taken as a variable and the simple multiple regression models generated different intercepts where soil was a significant variable. The empirical models was selected when C_p value was close to the number parameter in the equation and each estimate included had $p < 0.05$. Further specific details are given with the results.

4. Results

4.1 Basic soil properties

The basic soil properties include texture, pH, electrical conductivity and the contents of CaCO_3 , organic matter, and citrate bicarbonate dithionite (CBD) extractable iron and aluminum (Fe_d , Al_d) and oxalate extractable iron fraction (Fe_o , Al_o). Also, in this section parent material homogeneity as determined by the Zr/Ti and sand/silt ratio is presented. These parameters varied with the parent material and the climatic conditions, which had caused multiple variations in soil forming processes. Complete data are given in Appendix I.

Most soils in the study were dominantly silty. Particle size distribution on soil CaCO_3 /organic matter-free basis is presented in figure 4.1. The young alluvial soils vis. Shahdara, Sultanpur and Pitafi consisted of silty loam to very fine sandy loam. Shahdara C2 horizon showed loamy sand. The textures seemed inherited from the parent sediments, as homogenization was limited. As it occurred in broad basins in the fluvial plain, the Pacca soil showed silty clay due to accumulation of fine sediments. The Peshawar soil was derived from limestone and shale admixture, therefore, consisted of silty clay loam with a minor proportion of sand was mixed from the sandstone. The Murree soil consisted of silty loam as it was derived from shale interbedded with sandstone. Although the Guliana soil was derived from loess which is a strongly sorted material having most particles between 5 to 20 μm size diameter (Brinkman and Rafique, 1971) it occurred in basin position and due to collection of runoff weathering had resulted in the change of texture to silty clay loam and silty clay. The Prb-Ostb consisted of silty clay as it was developed in the parent derived from Muschelkalk. The Prb-Wein soil consisted of silty clay loam due to its source of parent material.

The soils from arid and semi-arid climate vis. Shahdara, Sultanpur, Pacca and Pitafi showed pH values in the range of 7.9 to 8.8. The Murree, Peshawar and Guliana soils showed slightly lower pH values (7.2 to 7.8) probably due to leaching of the bases under sub-humid and humid climate. The pH value of Prb-Ostb and Prb-Wein soils was acidic in the upper parts of the soil profile and >7 in the deeper profiles. Decalcification and leaching of the bases and illuviation at lower depths in humid environment resulted in free lime of the soil matrix and it may be responsible for the change in soil pH values.

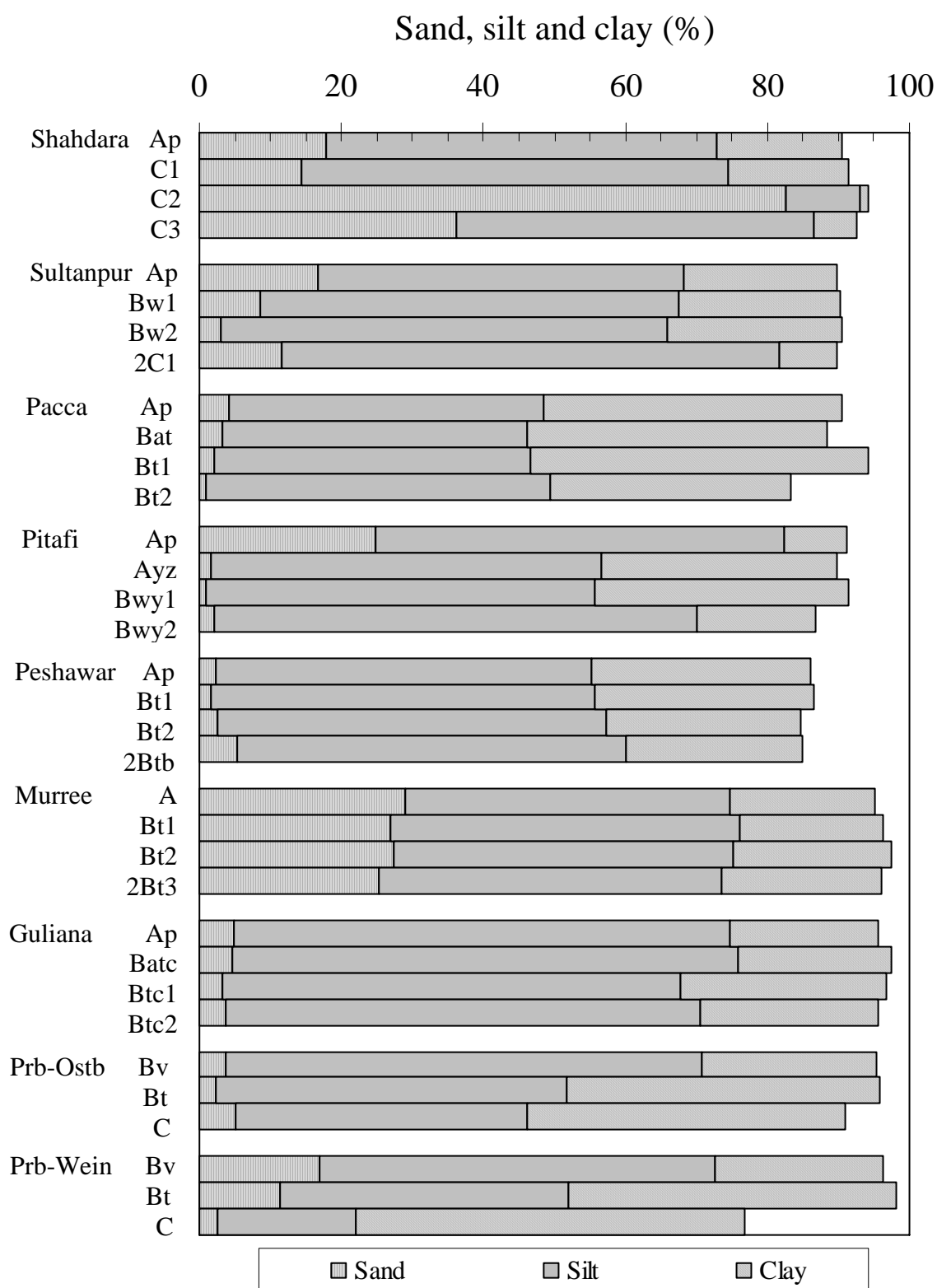


Figure 4.1: Sand, silt and clay distribution of CaCO_3 and organic matter free basis for the soil samples investigated.

As presented in figure 4.2 most soils from Pakistan contain free CaCO_3 due to the calcareous parent material and the limited decalcification.

The Shahdara, Sultanpur, Pacca and Pitafi soils contain CaCO_3 content as high as 250 g kg^{-1} where decalcification was minimal due to dry climate and limited profile development time. Guliana soil was observed to contain only 10 to 20 g kg^{-1} free soil CaCO_3 with profile depth. Collection of runoff due to its basin position in sub-humid condition appeared to have resulted in the decalcification of the surface horizons and accumulation at $> 90 \text{ cm}$ depth. The Peshawar soil was derived from limestone and shale admixture deposited as alluvium at the foothill. Decalcification was limited by low frequency of rainfall therefore, uniform CaCO_3 content throughout the profile was observed.

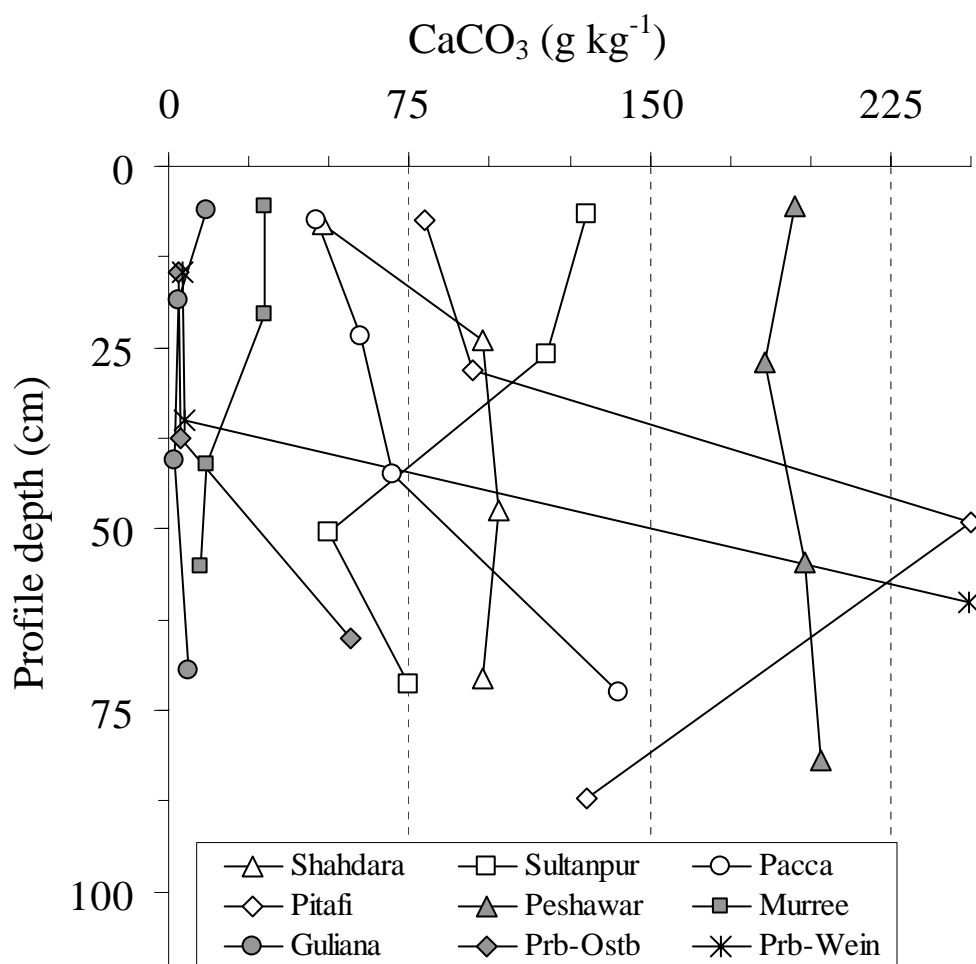


Figure 4.2: Soil CaCO_3 distribution in the profiles investigated.

Prb-Ostb and Prb-Wein soils show translocation of CaCO_3 due to leaching and accumulation in high soil moisture condition. Both the soils show free CaCO_3 in the matrix below the surface layer and the CaCO_3 content increased with depth.

The organic matter content of the soils ranged between 2 and 25 g kg^{-1} , which decreased with profile depth in all the soils as given in figure 4.3. Shahdara and Pitafi soils were observed for significantly ($p < 0.01$) lower organic matter content than the other soils. Hot and dry climatic conditions cause rapid oxidation especially in light texture soils. Murree, Peshawar and Guliana soils and also the two Parabraunerde soils, showed significantly higher organic matter content (10 to 24 g kg^{-1}), due to higher clay content and humid/sub-humid climate, at least in the surface horizons. The subsurface (Bv) of the Prb-Ostb and Prb-Wein profiles showed organic matter content in the range of 5 to 12 g kg^{-1} . The organic matter rich surface layer from both soils was excluded from this study.

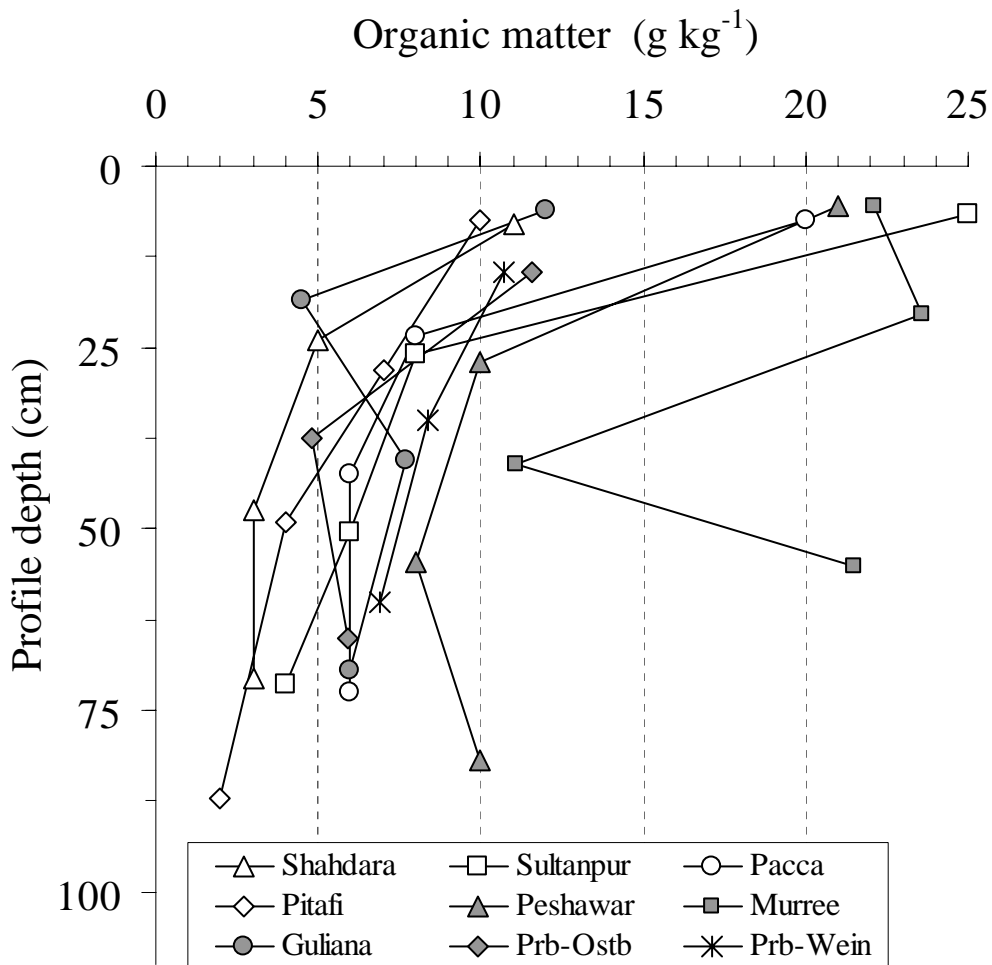


Figure 4.3: Distribution of soil organic matter in the profiles investigated.

The electrical conductivity (EC) as a measure of soluble salts was $<2 \text{ dS m}^{-1}$ ('normal' in terms of salinity level for crop production) for all soils investigated except for the Pitafi soil (Appendix I). Extract of saturated paste of Pitafi soil showed EC 59, 11.5, 5.6, 3.9 dS m^{-1} in Ap (0-15 cm), Ayz (15-41 cm), Bwy1 (41-57 cm), and Bwy2 (63-111 cm) horizons, respectively. Shahdara, Sultanpur, and Pacca soils were observed for EC between 0.2 to 2.6 dS m^{-1} . These soils occurring in active floodplain and occasional river outflow showed removed surface salts. The irrigated alluvial soils contained surface horizons of several times greater Olsen P content due to accumulation of fertilizer application.

The CBD extractable iron (Fe_d) content was mostly 6 to 9 g kg^{-1} in the alluvial soils and slightly higher in the Peshawar soil (9 to 11 g kg^{-1}). The CBD extractable iron content was the highest in the two Parabraunerde soils from Germany. The shale derived Murree soil and the weathered loess soils showed higher Fe_d content than the alluvial soils but less than that of both Parabraunerde soils. Oxalate extractable (Fe_o) iron content was generally a small fraction (0.30 to 1.40 g kg^{-1}) in all soils. The alluvial soils including the Peshawar soil and the loess derived Guliana soil showed generally low Fe_o content than the Prb-Ostb and Prb-Wein soils. Acidic conditions appeared to favor formation of poorly crystalline iron oxides. The figure 4.4 presents Fe_o and Fe_d distribution in all the soils.

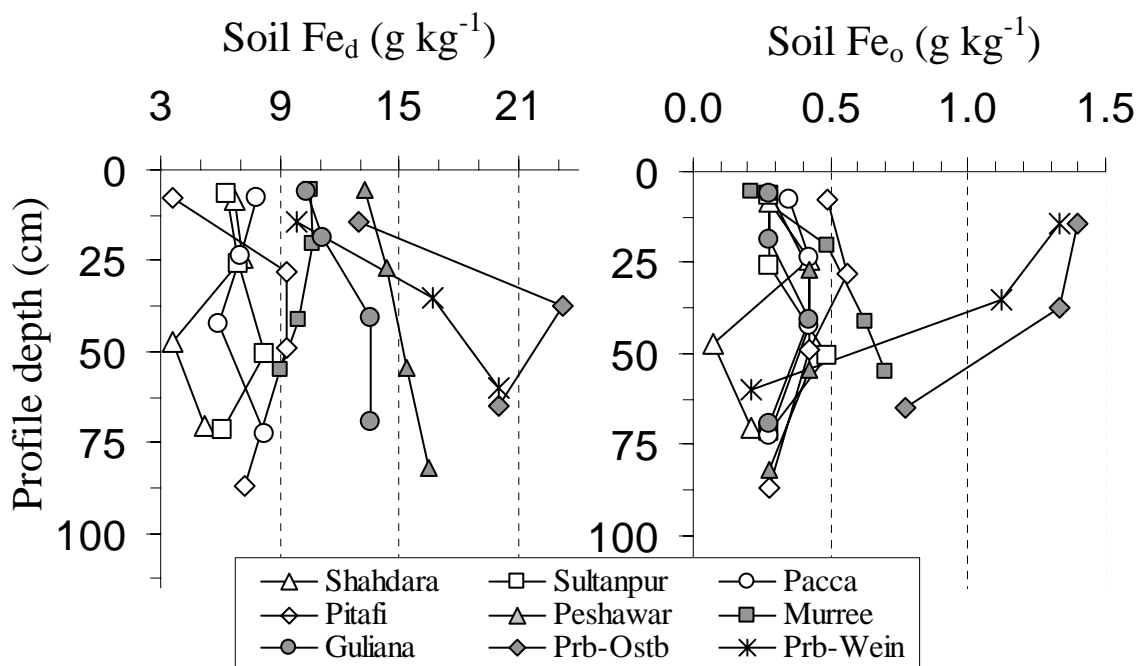


Figure 4.4: Citrate bicarbonate dithionite extractable iron (Fe_d) and ammonium oxalate extractable iron (Fe_o) distribution in the soil profiles.

In the more weathered soils Prb-Ostb, Prb-Wein, and Guliana Fe_d values in the range of 14 to 23.2 $g\ kg^{-1}$ were determined which are higher than the alluvial soils (Shahdara, Sultanpur, Pacca and Pitafi). In the less weathered soils, Fe_d content spread around 10 $g\ kg^{-1}$ line.

The Prb-Ostb soil contained 22 $g\ kg^{-1}$ mean Fe_d content in the profile. This value was higher than that of Murree, Prb-Wein and Guliana soils. Fe_d mean content of Peshawar soil profile was statistically similar to that of Prb-Wein and Guliana soils but was lower than that for Murree and Prb-Ostb soils. The Prb-Ostb, Prb-Wein, Murree and Guliana soils showed an increase in Fe_d content with depth while Shahdara, Sultanpur, Pacca and Pitafi soils showed an irregular distribution throughout the profile (Fig. 4.4).

Citrate bicarbonate extractable aluminum (Al_d) content was higher in weathered soils (Prb-Ostb and Prb-Wein and Guliana) compared to alluvial and the shale-derived soils (Fig. 4.5). It increased in the second horizon in case of Prb-Ostb and Prb-Wein soils and throughout Guliana soil. The alluvial soils (Sultanpur, Pacca, Pitafi including Peshawar soil) showed uniform distributions in the Al_d content of the profile whereas in Shahdara soil it increased towards the surface.

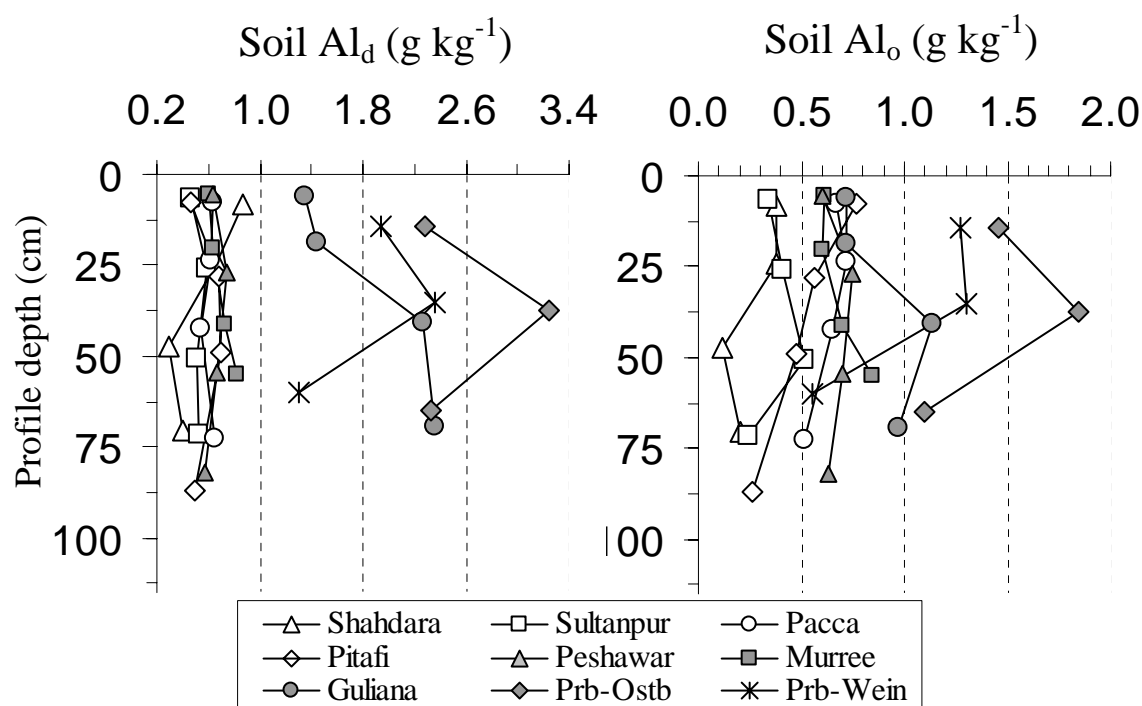


Figure: 4.5: Citrate bicarbonate dithionite extractable aluminum (Al_d) and ammonium oxalate extractable aluminum (Al_o) distribution in the soil profiles investigated.

In the shale derived Murree soil Al_d content increased with the depth of profile. The oxalate extractable aluminum (Al_o) content was lower than the Al_d content and both followed the same distribution trend.

Dithionate extractable iron and aluminum contents were highly correlated (r^2 0.71, < 0.0001) suggesting that the aluminum content dissolved by CBD may be substituted for iron in soil iron oxide. Similarly, oxalate extractable iron and aluminum were highly correlated (r^2 0.85, < 0.0001) suggesting a common source. Oxalate extractable aluminum is present as amorphous or Al-OM (organic matter complex) rather than as free oxides.

Bulk soil analysis by X-ray fluorescence (XRF) indicated a SiO_2 content of 600 to 700 $g\ kg^{-1}$ in alluvial soils, which is equivalent to 50 to 60 % quartz (Appendix II). The Peshawar soil was observed to contain 500 $g\ SiO_2\ kg^{-1}$ soil and the Murree soil 700 $g\ SiO_2\ kg^{-1}$. Due to calcareous parent material, CaO content reached up to 37 to 111 $g\ kg^{-1}$ in alluvial soils including Peshawar soil. Low SiO_2 content in soil samples corresponded to high CaO (and MgO) content indicating dilution of quartz with $CaCO_3$. Calcium oxide and $CaCO_3$ content corresponded well in all soils except for Shahdara soil, which showed higher CaO content than possibly determined by the soil $CaCO_3$. Silicate oxide and Al_2O_3 were the major oxides because of the presence of detrital quartz and layered alumino-silicates in various fractions. Similarly, the calcareous soils show higher MgO content than the decalcified soils. Calcium is a constituent of primary minerals (feldspars) and carbonate minerals (dolomite and Ca-Mg calcite). An increase in alkaline earth metal (CaO, MgO) content with depth in soils where decalcification had occurred was noted.

Prb-Ostb, Prb-Wein, Guliana and Murree soils contained only small fraction (5 to 16.8 $g\ kg^{-1}$) of Ca either due to high leaching of soil $CaCO_3$ or due to non-calcareous soil parent material. Total soil iron oxide content ranged from 31.9 to 71 $g\ kg^{-1}$ in the alluvial soils and in the Murree and Peshawar soils. Contribution of iron from various sources resulted in no depth trend of iron oxide distribution.

Lithological discontinuity in the profiles was assessed on the basis of Zr/Ti ratio and sand/silt ratio as presented in figure 4.6. Zirconium/titanium ratio suggested lithological breaks in the Shahdara profile at 32 cm depth and another at 63 cm depth. The sand/silt ratio also changed at the same depths suggesting that the horizons C2 (32-63 cm) and C3 (63-78 cm) are containing different parent material of different sources than the upper two horizons.

The alluvial soils, Sultanpur and Pacca were developed of parent material derived from uniform lithology. The surface layer of Pitafi soil showed Zr/Ti and sand/silt ratios different than the underlain sections of the profile and, therefore, suggesting that the Ap (0-15 cm) horizon is lithologically different from the lower horizons. A lithological break at 63 cm depth in Peshawar pedon was identified by field pedologist as suggested by the horizon name “2Btb”, however, Zr/Ti and sand/silt ratios do not support this field observation. Among the residual soils, the shale derived Murree soil and loess derived Guliana soil showed parent material homogeneity up to the profile depth studied. Similarly, Prb-Ostb soil was also found to be lithologically uniform. But both Zr/Ti and sand/silt ratios suggested a lithological break at 45 cm depth in the Prb-Wein soil profile (Fig. 4.6) but both Bv (4-25 cm) and Bt (25-45) horizons appeared to be developed from uniform lithological parent material.

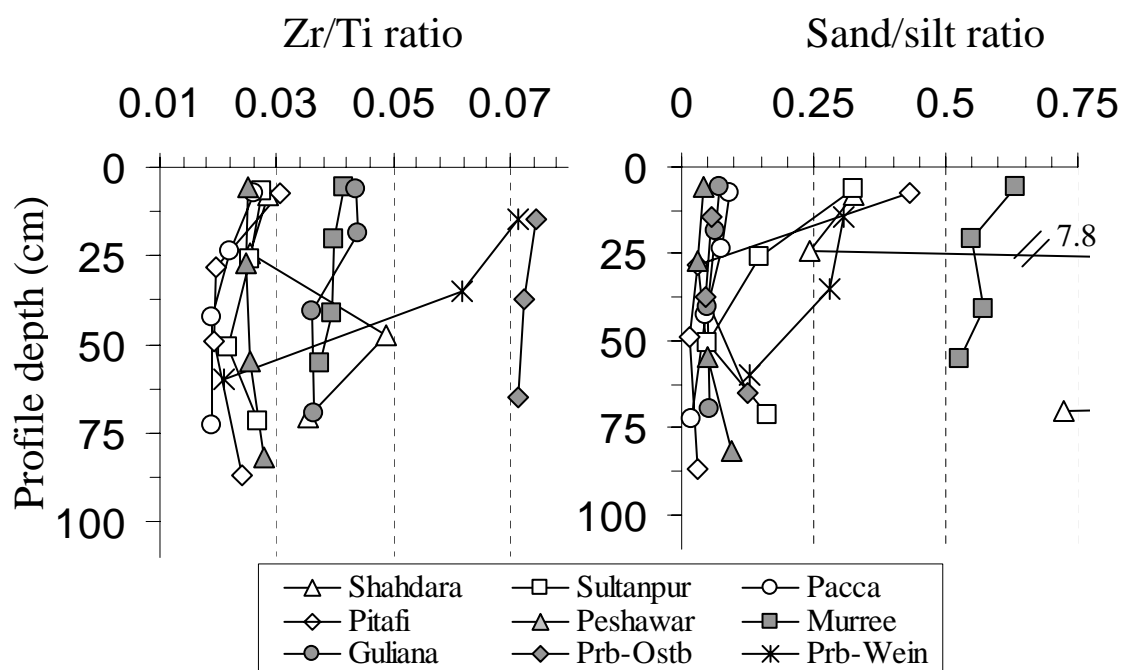


Figure 4.6: Zirconium/titanium (Zr/Ti) and sand/silt ratio in the soil profiles investigated.

4.2 Soil mineralogy

Soil mineralogical composition as determined by X-ray diffraction of randomly oriented powder mounts of the sand and silt and by preferentially oriented mounts of the clay are presented in this section. The quantitative distribution of

kaolinite by DSC/TG and vermiculite as well as smectite determined by Ca/Mg and K/NH₄ CEC are also covered in this section.

4.2.1 Sand and silt mineral composition by XRD

The sand was mainly composed of quartz, feldspars and mica. The silt fraction was composed of quartz, feldspars, mica and kaolinite. The X-ray diffraction patterns of the sand and silt fractions for all soils are presented in Appendix III, whereas representative data (Sultanpur soil) are presented in figure 4.7. Quartz was recognized by XRD lines 4.26 and 3.34 Å from the 100 and 101 hkl respectively. Mica was recognized at 10, 5, 3.33, 2.0, and 1.51 Å peaks from 002, 004, 024, 10 and 060 diffraction lines, respectively. Since the other quartz peaks at 3.34 and 1.54 Å overlap with that of mica peaks, the 4.26 Å peak was used for the identification of quartz.

The 4.03, 3.20, 3.18 and 3.26 Å peaks characterize the feldspar mineral group. A peak at 7.16 Å representing 001 diffraction line in the absence of chlorite 14.2 Å peak (001 hkl) was ascribed to kaolinite as in case of silt.

Quartz was a ubiquitous and dominant mineral in all sand fractions while feldspars and mica varied with parent material. The alluvial soils, Shahdara, Sultanpur (Fig. 4.7), Pacca and Pitafi soils were abundant in mica and feldspars. The Guliana sand was composed of quartz with relatively low intensity peaks for feldspars and traces of mica, which increased with depth. The shale derived Murree and Peshawar soils contained mainly quartz with yet low intensity peaks for feldspar. The Prb-Ostb and Prb-Wein showed mainly quartz and small peaks of feldspar. All alluvial soils were abundant in mica compared to the residual soils but with no clear depth trend. The alluvial soils also appeared to show more feldspar as indicated by the intensity of the 3.18 and 3.20 Å peaks.

The silt fraction was also composed of mainly quartz, feldspar, and mica with small amounts of chlorite and in some soils kaolinite (Fig. 4.7). The alluvial soils showed stronger mica peaks, compared to the residual soils and Murree and Peshawar soils. In Guliana soil, the peak intensity for mica increased with depth. In Prb-Ostb and Prb-Wein soils the silt fractions were mainly composed of quartz and small amounts of feldspar while mica and kaolinite appeared only in traces. The alluvial soils showed traces of chlorite, which increased with the depth of profile.

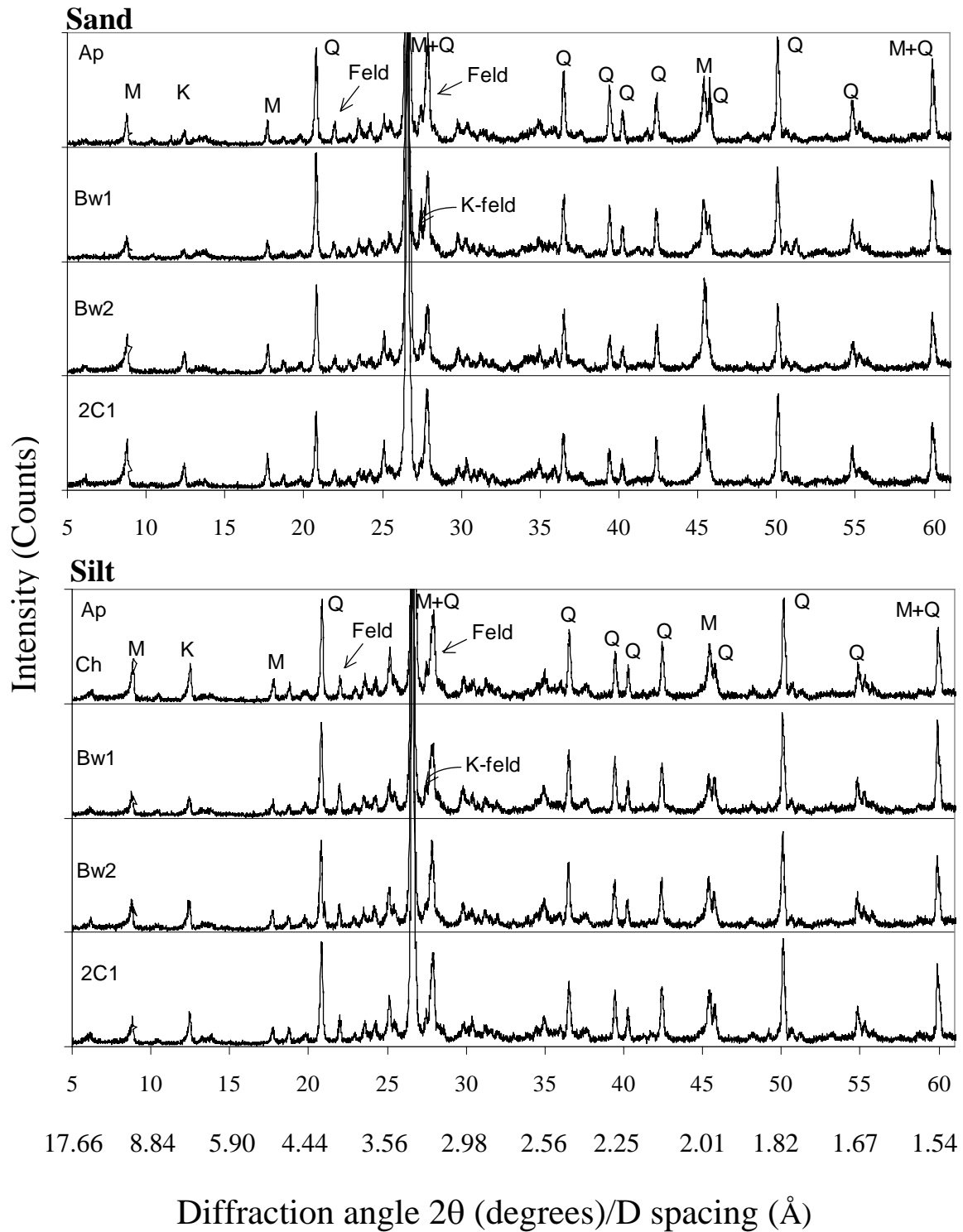


Figure 4.7: Sand and silt mineralogy of Sultanpur soil: Q, quartz; M, mica; Ch., chlorite, K-feld., K-feldspar.

4.2.2 Clay (<2 μm) mineral composition by XRD

The soil clays were composed of dominantly kaolinite, mica, smectite and vermiculite and smaller proportion of hydroxyinterlayer smectite/vermiculite

(HIS/HIV) and chlorite as determined by X-ray diffraction. The relative proportion of clay minerals varied with parent material and the soil development stage. Complete X-ray diffraction data for all soil clays are given in Appendix IV. Only representative data depicting the variability in clay mineral composition are shown in figure 4.8.

Mica was recognized by X-ray diffraction peaks at 10, 5, and 3.33 Å in Mg-saturated air-dried clays. Kaolinite was recognized by 7.2, and 3.6 Å X-ray diffraction lines in K-saturated and air-dried clays and the same diffraction lines disappeared due to decomposition of kaolinite structure when K-saturated clays were heat-treated for two hours at 550°C. Vermiculite and smectite both give peaks at 14.2 Å when Mg-saturated air-dried clay is X-rayed.

Smectite was recognized by the 17 Å peak in Mg-saturated glycolated clay. Also, the 10 Å peak enhanced due to collapse of vermiculite and smectite structure with K-saturation and the heat treatment. The second order peak (5 Å) of mica was as intense as the first order (10 Å), which may reflect the presence of dioctahedral crystallite. Chlorite was recognized by 14.2 Å peak in K-saturated clays treated at 350 °C and by further enhancement in intensity of the same peak upon heating at 550 °C.

The alluvial soil clays from the Shahdara and Sultanpur, exhibited complete expansion of Mg-saturated clay from 14.2 Å peak to 17 Å upon glycolation indicating the presence of smectite. The smectite peak in different alluvial soil clays was sharp, indicating the presence of well crystalline smectite (Fig. 4.8a). Smectite in these soils is most probably inherited from the alluvium. The Pacca and Pitafi soils also showed well-defined 17 Å peak representative of smectite but with recognizable unexpanded portion indicating the occurrence of both smectite and vermiculite. The surface horizons of both the soils showed vermiculite and HIS/HIV indicated by partial expansion of the 14.2 Å peak in the Mg-saturated glycolated clay between 14.2 and 17 Å and an additional shoulder on the lower angle side of the peak indicating only partial expansion (Fig. 4.8a). X-ray diffraction also showed presence of chlorite and/or HIS/HIV in the alluvial soil clays as indicated by the peak at 14.2 Å position in K-saturated clays when heated to 550 °C and a broad shoulder on the lower angle side of 10 Å peak which was due to partial collapse of the 2:1 type layered structure.

The loess derived clay from Guliana soil showed both smectite and vermiculite indicated by broad peak covering 14.2 Å and 17 Å with glycolation of Mg-saturated clay (Fig. 4.8b).

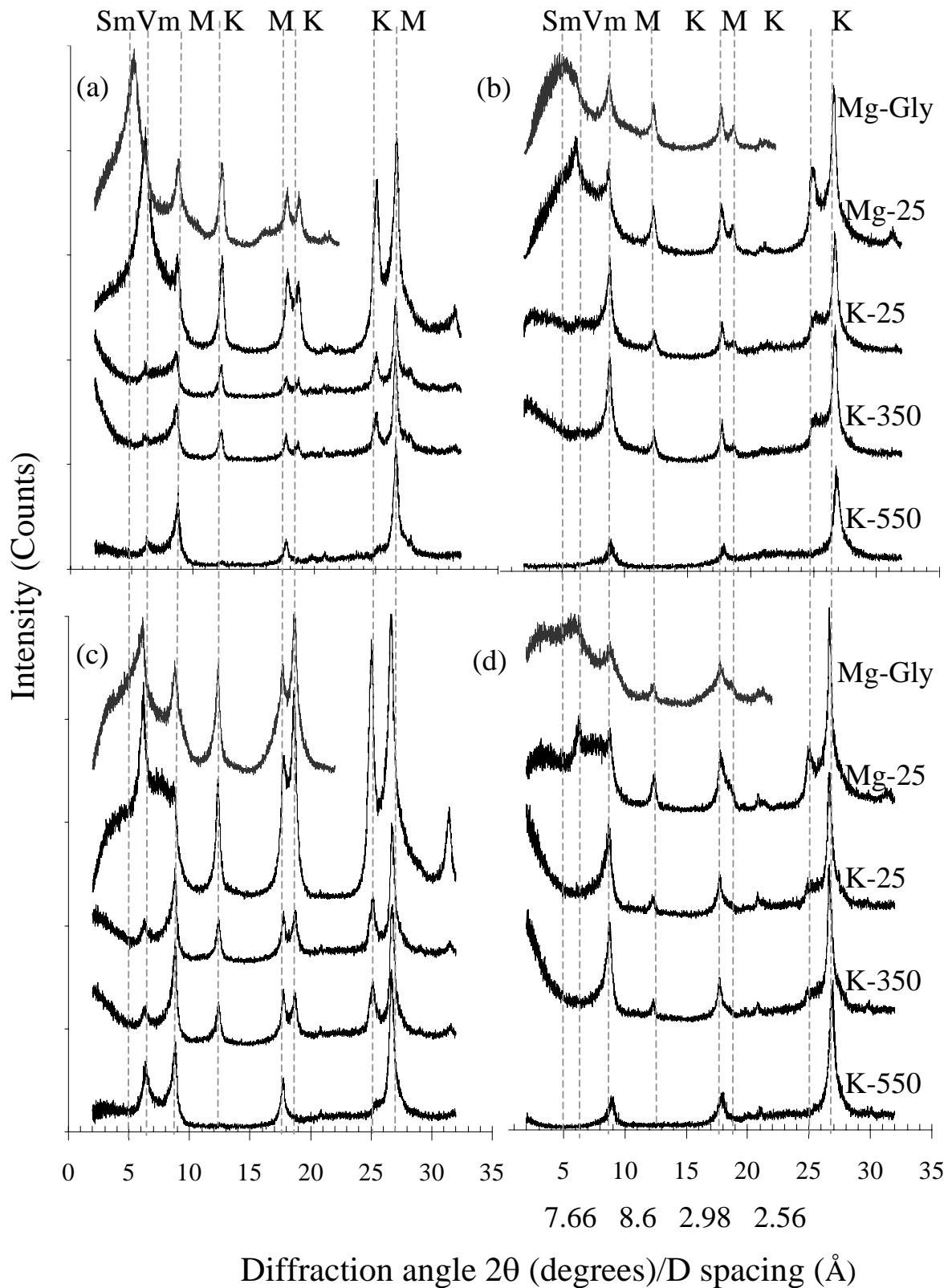


Figure 4.8: X-ray diffraction pattern for clay (<math><2\mu\text{m}</math>) (a) Shahdara C1 soil, (b) Guliana Ap soil, (c) Murree soil from Ap horizon and (d) Prb-Ostb Bv soil: Mg-Gly., Mg saturated and glycolated; Mg-25, Mg saturated and air dried; K-25, K saturated and air dried; K-350, K saturated and heated at 350°C ; and K-550, K saturated and heated at 550°C .

Chlorite and HIS/HIV were also present in the upper three surface horizons (Ap, BA_{tc}, B_{tc}1) as indicated by 14.2 Å peak and a broad shoulder on lower angle side of 10 Å peak in K-saturated clay heated to 550 °C.

The Murree soil was composed of mostly vermiculite, mica, and kaolinite with small amount of chlorite. The 14.2 Å peak in Mg-saturated clay expanded (Fig. 4.8c). Mineralogical composition of Peshawar soil was similar to Murree soil but it contained high smectite content compared to Murree soil as shown by, at least, the expansion of 14.2 Å peak upon glycolation. The Murree and Peshawar soil clays showed both chlorite and HIS/HIV. Chlorite peak intensity increased with depth in the Pitafi soil; it increased towards the surface in Shahdara, Sultanpur, Murree, and Pacca soils. The alluvial soils showed relatively sharp mica peaks compared to broad peaks of the shale or the loess derived soils. The Prb-Ostb soil clay showed 14.2 Å peak upon Mg saturation, which expanded to various degrees, leaving only a small intensity 14 Å peak depictive of vermiculite but there was no clear peak at 17 Å position (Fig. 4.8d).

The mass loss due to dehydroxylation between 450 °C and 590 °C determined by TG-DSC was used for the estimation of kaolinite content. The mass loss due to dehydration of free water (around 110 °C) and dehydroxylation of goethite/gibbsite between 270 to 380 °C, was excluded. Typical TG-DSC graph covering the range of variability for the clay selected soils Murree, Guliana and Prb-Wein is depicted in figure 4.9. DSC showed a stronger endothermic peak at higher temperature in Murree than in Guliana and Prb-Wein soils. Also, TG and DSC measurements indicated sharp endothermic peaks in Murree soil and relatively broad in Guliana and Prb-Wein soils. Overall smaller and broad peaks of DSC measurements corroborated with less intense X-ray diffraction peaks. Complete data set is given in (Appendix V).

The Murree soil clay contained higher amounts of kaolinite up to 25% and the Guliana clay contained 27.4 to 32.4 % of kaolinite as determined from the dehydroxylation measured by TG (Fig. 4.9). Both soils were observed for detectable kaolinite contents also in the silt fraction as indicated by XRD (Fig. 4.7). Kaolinite in the clay fraction increases toward surface soil of Guliana profile due to greater weathering and appeared to be pedogenic. The alluvial soils developed in arid and semi-arid climate contained 17 to 19 % kaolinite lacking any distribution trend in the profiles. Kaolinite content in these alluvial soils appeared to be inherited from parent sediments rather than being pedogenic. Both the Prb-Ostb and Prb-Wein soils were observed for low (13 to 17 %) kaolinite content in the clay fraction, which may be due to high leaching

of silica under humid climate. Peshawar soil clay also contained 19 to 20.5% kaolinite, which was similar in all horizons. Appendix VI presents quantitative mineral composition of the clay fraction.

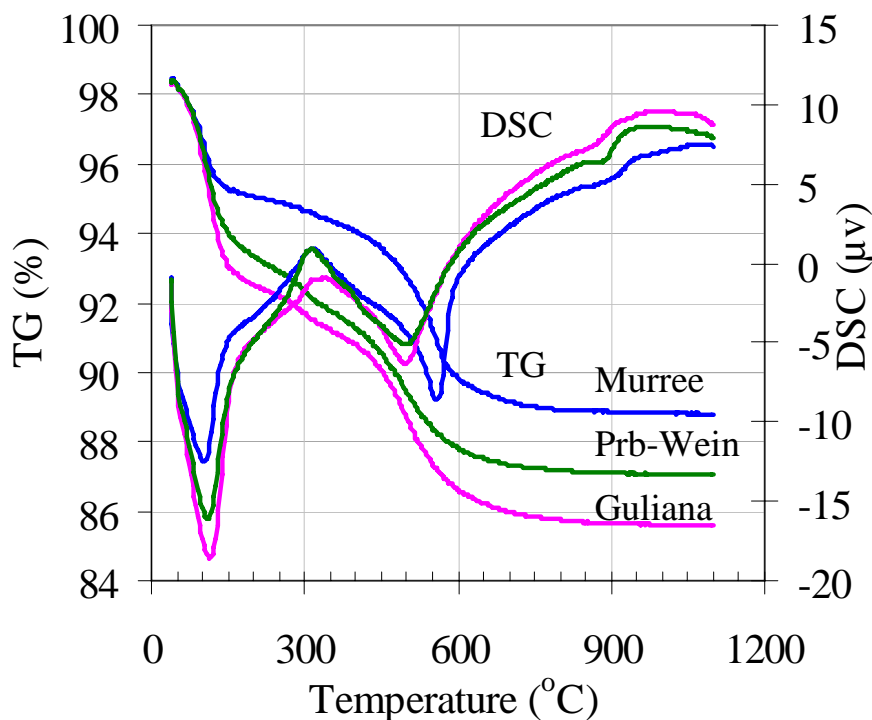


Figure 4.9: TG and DSC curves for Murree (Bt1), Guliana (Btc) and Prb-Wein (Bv) soil clays.

Smectite and vermiculite distribution in clays determined quantitatively by Ca/Mg and K/NH₄ CEC generally corroborated well with the X-ray diffraction data. The alluvial soils contained 17 to 22 % smectite and were distributed uniformly among horizons (Fig. 4.10). The shale derived Murree and Peshawar soils showed 11 to 18% smectite content in the clay. The highest smectite content was detected in the Guliana soil clay from Btc2 (56-83 cm) horizon and in this soil smectite showed an increasing trend with depth probably due to higher *in situ* weathering and translocation of argillaceous clay.

The Prb-Ostb soil profile derived from Muschelkalk contained 18 to 23% smectite in the clay fraction and the Prb-Wein soil clay derived from limestone of glacial loess contained 14 to 17% smectite. Vermiculite in the clay had large variability where the content ranged from 0 to 15% and no depth related distribution trend in the alluvial soils was given. The Murree and Peshawar soil

clays showed 4 to 13% vermiculite content while the X-ray diffraction showed presence of large amount of vermiculite. The Guliana soil contained the highest vermiculite content and it increased with depth. Similarly, the clays from Parabraunerde contained 1 to 14% vermiculite (Appendix VI).

Overall the clays were composed of layered silicates with minor proportion of tectosilicates and iron oxides (Fig. 4.10). Most of the clays contained detectable amounts of quartz and some clays contained feldspars (both not labeled). Assuming quartz and feldspars amounting to 10% of clays, which is the detection limit of XRD for minerals, mica accounts for 45 to 50%. Previous studies have reported the presence of mica broadly in this range in Pakistani soils (Akhtar, 1989; Ahmad et al. 1986).

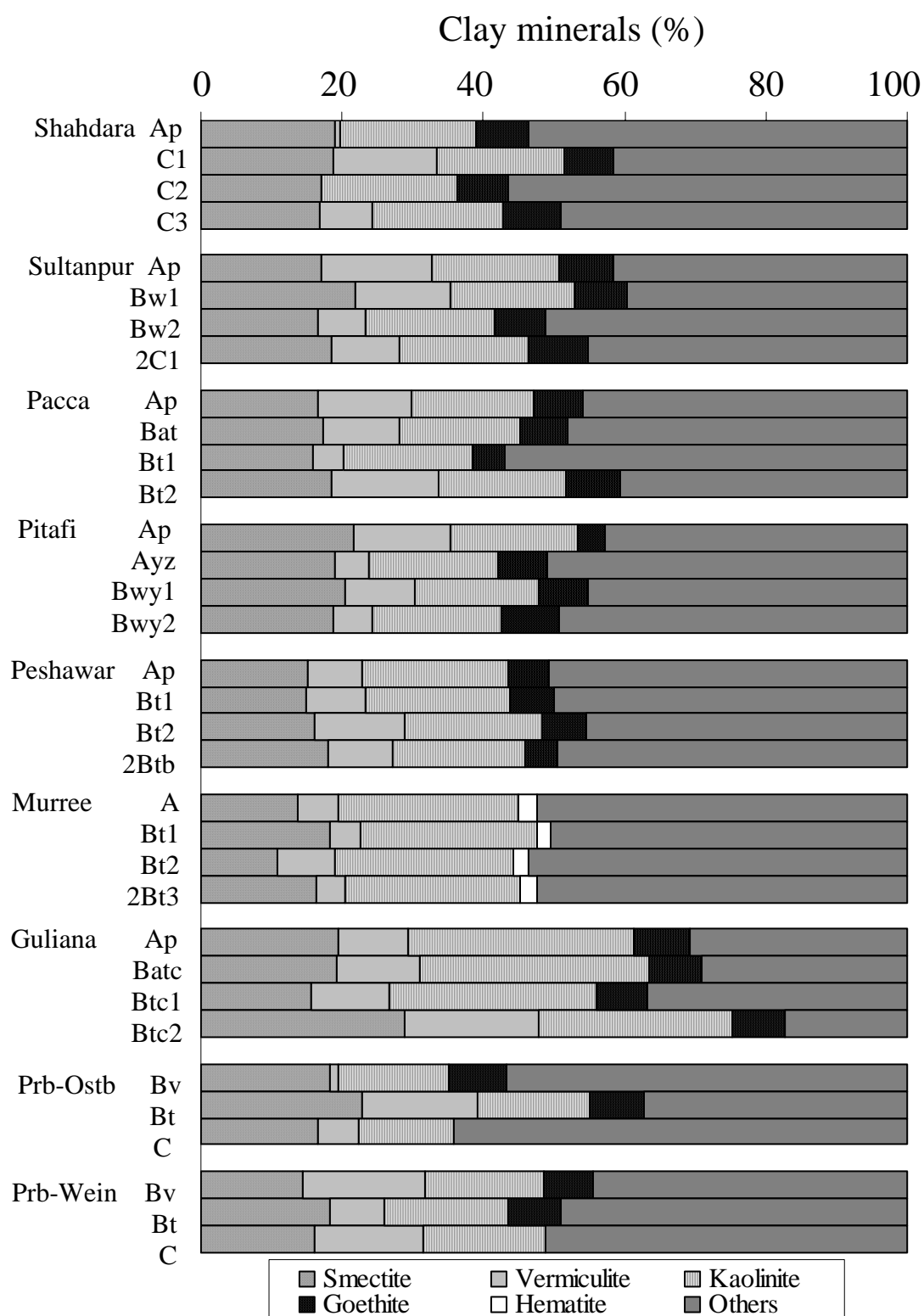


Figure 4.10: Clay mineral composition of the soils investigated.

4.3 Iron Oxide

This section presents the iron oxide mineral composition in the clays. X-ray diffraction data before and after concentration is presented in Appendix VII. Quantitative distribution assessed by voltammetry is included in Appendix VI. Quantitative distribution of poorly crystalline iron oxides determined by oxalate extraction was presented in section 4.1.

4.3.1 Iron oxide phase identification by XRD

The alluvial soils along with Guliana, Prb-Ostb and Prb-Wein contained goethite; the Murree soil contained hematite and poorly formed goethite; and the Peshawar soil contained goethite and traces of hematite as the phases of crystalline iron oxides in the clay fraction. Selected data are depicted in figure 4.11. Since the clay fraction contained low concentrations of iron oxides thus, were treated with 5M NaOH to remove kaolin type minerals. X-ray diffraction analysis before and after concentration treatment with 5M NaOH is included for all soils. The X-ray diffraction peaks at 4.18, 2.69, 2.45 Å from 110, 130, 111 hkl plains were ascribed to goethite; 2.70 and 2.52 Å from 104 and 110 hkl plains to hematite (Schwertmann and Taylor, 1989), respectively.

X-ray diffraction showed sparse lines for goethite and hematite in the clay patterns before the chemical treatment (Fig. 4.11a). Though the most intense hematite peak at 2.70 Å in the Murree and Peshawar (Fig. 4.11c,d) soils derived from parent material with shale mixture and goethite peak at 2.45 Å in relatively more ferruginous soils such as Prb-Ostb and Prb-Wein were observed before concentration treatment. The Murree sample consisting of higher shale mixture, also showed hematite peaks at 2.52 Å and 2.21 Å before concentration treatment. The Prb-Ostb soil samples, which contained the highest iron oxide content measured by CBD extraction, showed goethite peaks at 4.18 Å and 2.69 Å before concentration treatment. The iron oxide content in most other soils was too low for phase identification by X-ray diffraction without chemical treatment.

Using X-ray diffraction after the concentration treatment, goethite in most soils including Prb-Ostb, Prb-Wein and Guliana (the weathered soils) as well as in Shahdara, Sultanpur, Pacca and Pitafi (the alluvial soils) could be identified. The goethite peaks at 4.18 Å and 2.69 Å were visible only after the chemical treatment while the 2.45 Å peak enhanced considerably. Overall, peak intensity increased by two to five folds. The alluvial soils, Shahdara, Sultanpur,

Pacca and Pitafi showed relatively sharp goethite peaks compared to the more weathered soils such as Prb-Ostb, Prb-Wein and Guliana (Fig.4.11a,b).

The Murree and Peshawar soils showed hematite and peak intensity increased two-fold after concentration. Hematite peaks were sharp even before concentration treatment. This showed the clear advantage of the concentration treatment.

Prb-Ostb, Prb-Wein and Guliana soils also contained goethite as indicated by X-ray diffraction but showed broader peaks compared to the young alluvial soils (Shahdara, Sultanpur, Pacca and Pitafi). Goethite appeared to be pedogenic at least in the more weathered soils. Hematite was dominant in Murree soil. In Peshawar soil both goethite and hematite were observed. Both these soils contain admixture of red shale in their parent material. Therefore, hematite in these soils appeared to be lithogenic and the weathering conditions also preclude pedogenesis of hematite.

Transmission electron microscope showed that the morphology of iron oxides varied with soil type: The alluvial soils were observed for well-crystallized goethite, the weathered soils for relatively less crystalline, and the shale mixed soils for hematite and very poorly crystalline goethite associated with ferrihydrite. The figure. 4.12 depict morphologies of soil clay iron oxides in the alluvial soils, the weathered soils, and the shale mixed soils, respectively. The TEM figures show a range of particle morphology for each soil. Small and the least crystalline particles found in respective clays are shown on the left and the well crystalline particles on the right side. The Pitafi soil consisted of particles ranging from 0.1 to 0.4 μm in the shape of thick twined laths and structurally controlled terminations with v-shaped grooves. In Shahdara soil goethite particles ranged from about 0.2 to 0.5 μm scale, and were of larger size than that of goethite in Pitafi soil with undefined terminations to well defined twined shape (Fig. 4.12).

Sultanpur soil containing mostly large particles ranging from 0.2 to 0.3 μm size, mono-domainic thick particles showing lattice fringes and sharp edges, some with frayed edges and low electron density areas within particle (Fig. 4.12). Among alluvial soils, the Pacca soil was observed for comparatively smaller, less crystalline particles of about 0.1 μm size. Few particles showed less developed lattice fringe but many other goethite particles were multi-domainic sharp edged and were well crystalline.

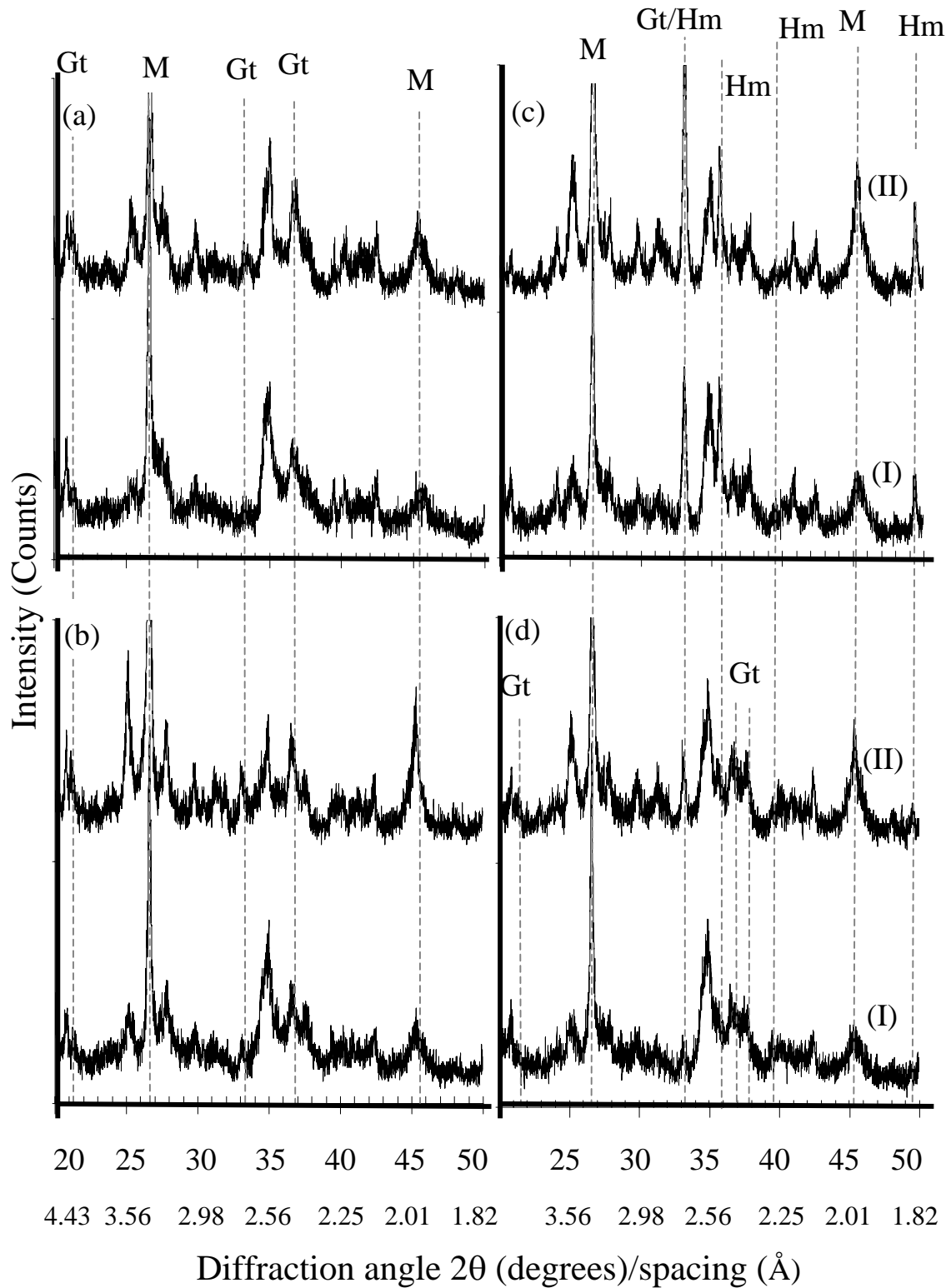


Figure 4.11: X-ray diffraction patterns of clay ($<2\mu\text{m}$) before (I) and after (II) pre-concentration treatment: (a) Shahdara C2 (32-63 cm), and (b) Prb-Wein Bv (4-25 cm) showing goethite, (c) Murree Bt1 (11-43 cm) showing hematite and (d) Peshawar Bt1 (11-43 cm) showing both goethite and hematite.

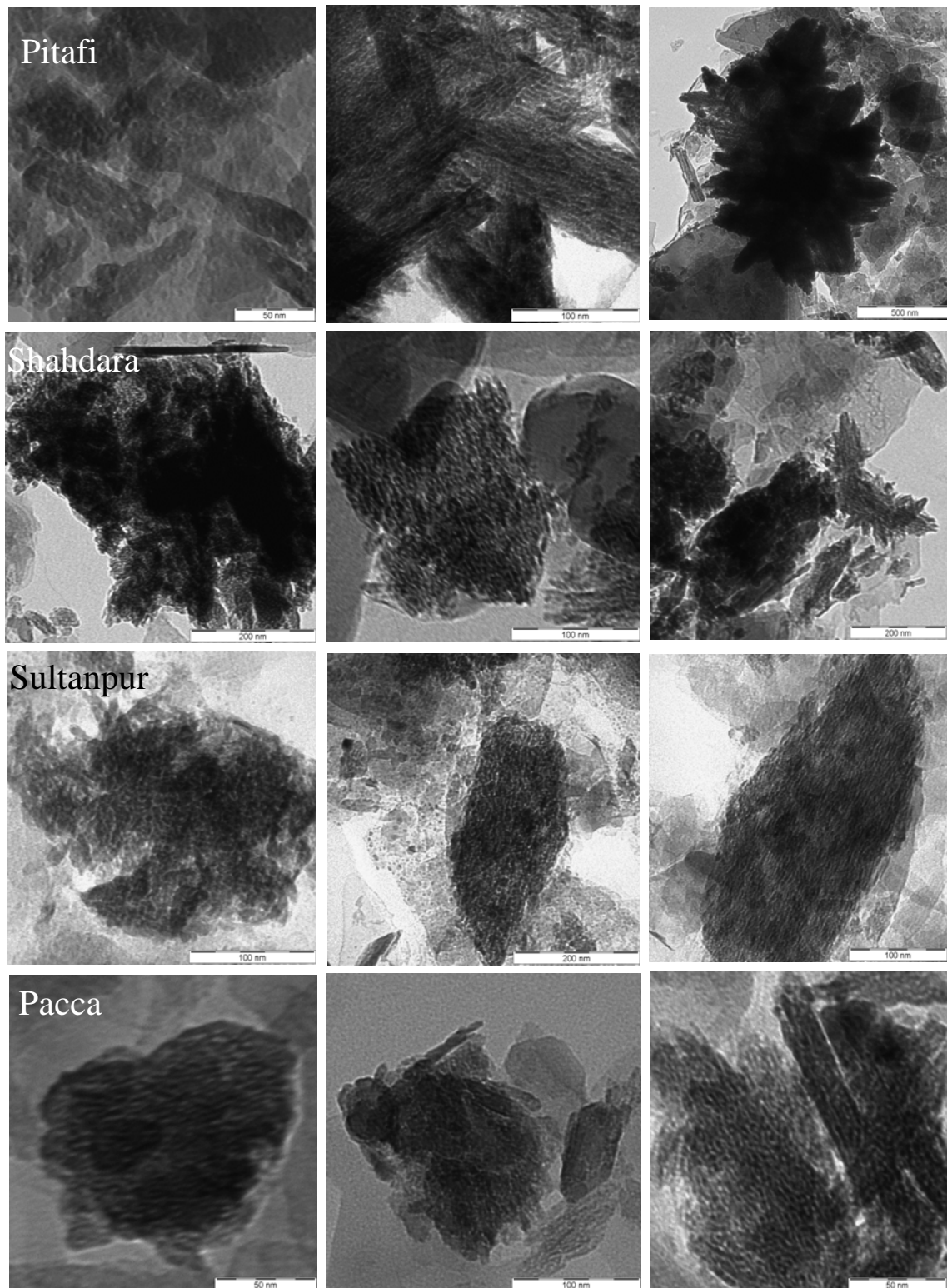


Figure 4.12: Transmission electron micrographs of alluvial soils showing well crystalline goethite particles.

In Guliana soil smaller, less crystalline goethite particles of 0.1 μm size were encountered frequently while few were mono-domainic-serrated laths showing well-developed lattice fringes. Particles of similar size (0.1 μm) were found in Prb-Wein soil showing large number of individual goethite laths with lattice fringes and serrated edges. Many goethite particles did not show lattice fringes (Fig. 4.13). In Prb-Ostb soil there were many thick laths often lacking lattice fringes.

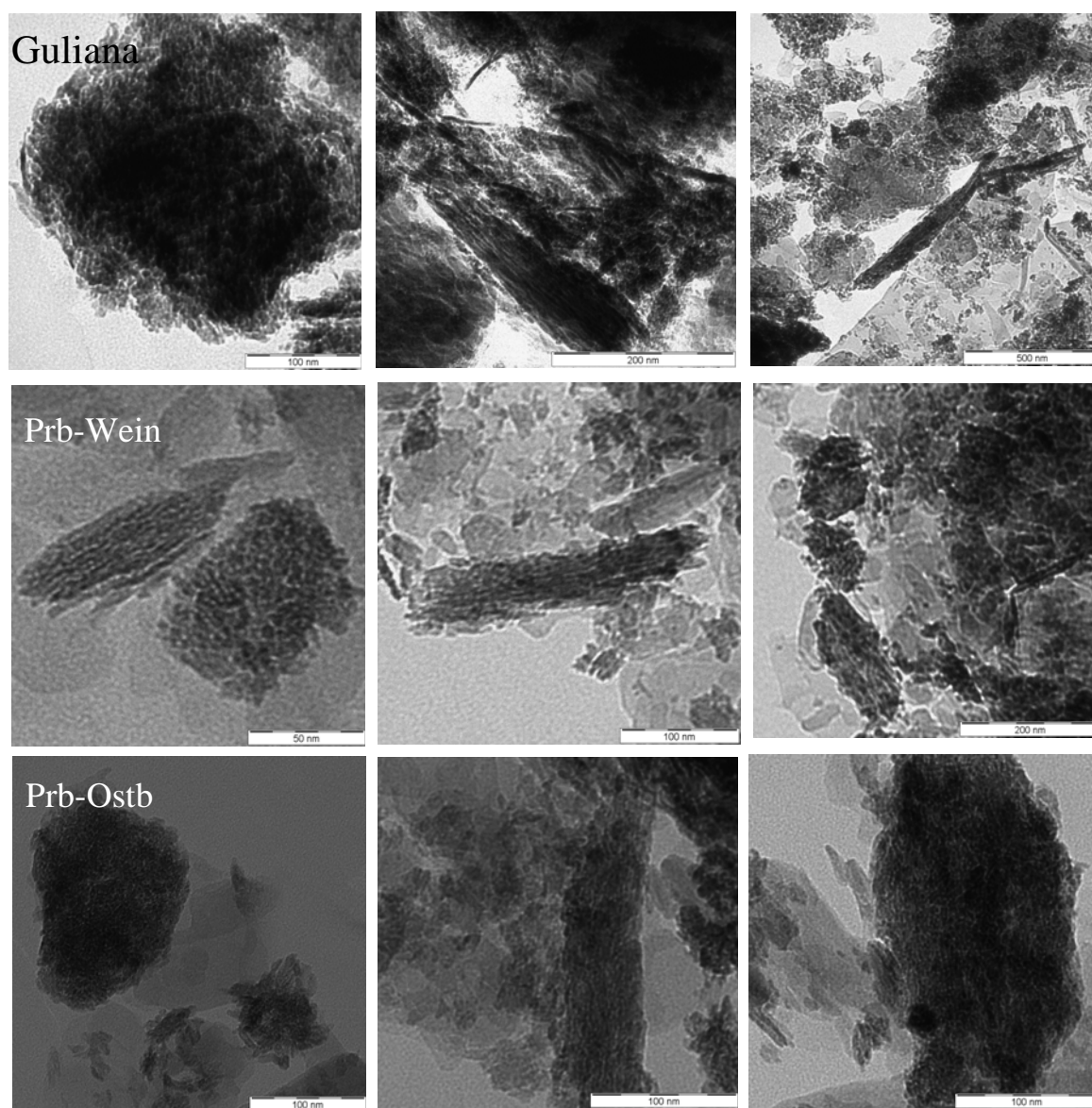


Figure 4.13: Transmission electron micrographs of weathered residual soils showing less crystalline goethite particles.

The Peshawar soil clay showed goethite particles with different stages of crystallinity. Some seen as aggregates without any lattice fringes, appearing to be composed of smaller particles; several goethite particles looked as laths with

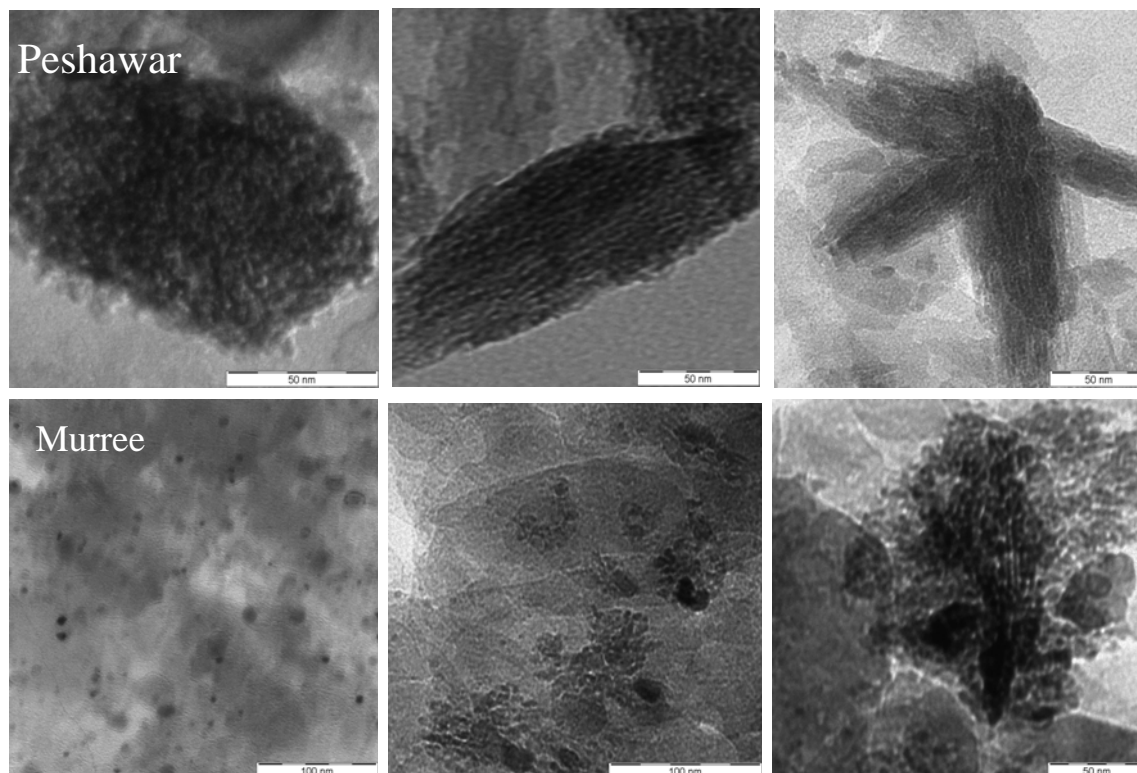


Figure 4.14: Transmission electron micrographs of shale derived soils showing well to poorly crystalline goethite and hematite particles.

sharp edges and lattice fringes; and few multi-domainic goethite appearing as star-shaped particles. Several individual hexagonal plates of hematite were seen in the Murree soil clay. The second TEM micrograph of Murree soil clay shows several irregular aggregates with diffused edges in association with hematite hexagonal plates. Hematite crystallite appeared to be sintered as aggregate of few tens to several hundred-nanometer sizes with matrix of low-density material. Some aggregates showed goethite lattice fringes in the centre (Fig. 4.14).

Overall TEM showed that the alluvial soils contained large well-crystallized goethite, which appeared to be multi-domainic and of v-shaped grooved edges. The weathered soils showed relatively less crystalline (serrated laths) mainly acicular goethite. Finally, the shale mixed soils contained hematite and very poorly crystalline goethite associated with ferrihydrite. Often a feature of

goethite in highly weathered soils occurs as subrounded crystals with no acicular morphology. Goethite was observed for acicular morphology with rough surfaces and apparent structurally controlled terminations, sometimes, arranged into stars and is characteristic of well-oxidized environment while hematite has hexagonal plates (Schwertmann and Taylor, 1989).

4.3.2 Quantification of iron oxide in clay by voltammetry

The voltammetric analysis showed that most of the clays contained 6 to 8% goethite content and the shale derived Murree clay contained 2.0 to 2.75 % hematite content. Voltammetric response was assigned to goethite or hematite based on XRD and TEM observations. X-ray diffraction and TEM helped to identify hematite and poorly crystalline goethite in Murree soil, poorly crystalline goethite and traces of hematite in Peshawar soil, and poorly crystallized to strongly crystalline goethite particles in the other soils.

Mean iron oxide content in soil clays and iron oxide calculated on soil basis is presented in table 6.1. The Prb-Ostb soil was observed for the highest mean clay goethite content in the profile, which was statistically same as compared to Shahdara, Sultanpur, Guliana, Pacca, Pitafi, and Prb-Wein soils. The Peshawar soil profile contained statistically the same level of clay size goethite as that of Pacca and Pitafi soil but lower than the Shahdara, Sultanpur, Guliana, and Prb-Wein (Table 4.1) soils. Goethite determined by voltammetry and the peak intensities by XRD of goethite corroborated well. As the X-Ray diffraction detection limit is approximately 5% for any mineral, goethite concentrations ranging from 6.5 to 8 % were just above the detection limit to generate recognizable diffraction lines.

Goethite and hematite concentrations of soils were calculated taking into account the clay content in respective soils and assuming that most iron oxides occur in the clay fraction. Goethite content in the soils ranged from 7.8 to 34.0 g kg⁻¹. The Prb-Ostb and Prb-Wein soils showed the highest goethite content in the profiles followed by Pacca (Table 4.1) soil.

These soils showed high goethite containing clays and the clay content of these soils was high as well. Statistically, Prb-Ostb and Pacca soils were similar. Guliana, Peshawar Pitafi and Prb-Wein soils contained similar but lower goethite content than Prb-Ostb and Pacca soils, while lower goethite content was observed in Shahdara.

Table 4.1: Mean goethite calculated on clay content and soil bases in the profiles investigated.

Soil	Goethite	Hematite	Goethite [§]	Hematite
	-----g 100 ⁻¹ g clay-----		-----g kg ⁻¹ soil-----	
Shahdara	7.55a	-	7.8c	-
Sultanpur	7.72a	-	14.6bc	-
Pacca	6.45ab	-	26.2a	-
Pitafi	6.56ab	-	16.5abc	-
Peshawar	5.72b	-	16.4abc	-
Murree	-	2.40	-	4.8
Guliana	7.47a	-	18.0abc	-
Prb-Ostb	8.00a	-	27.2a	-
Prb-Wein	7.20ab	-	25.2ab	-

§, Clay goethite content calculated on soil bases = Goethite % in clay x % clay.

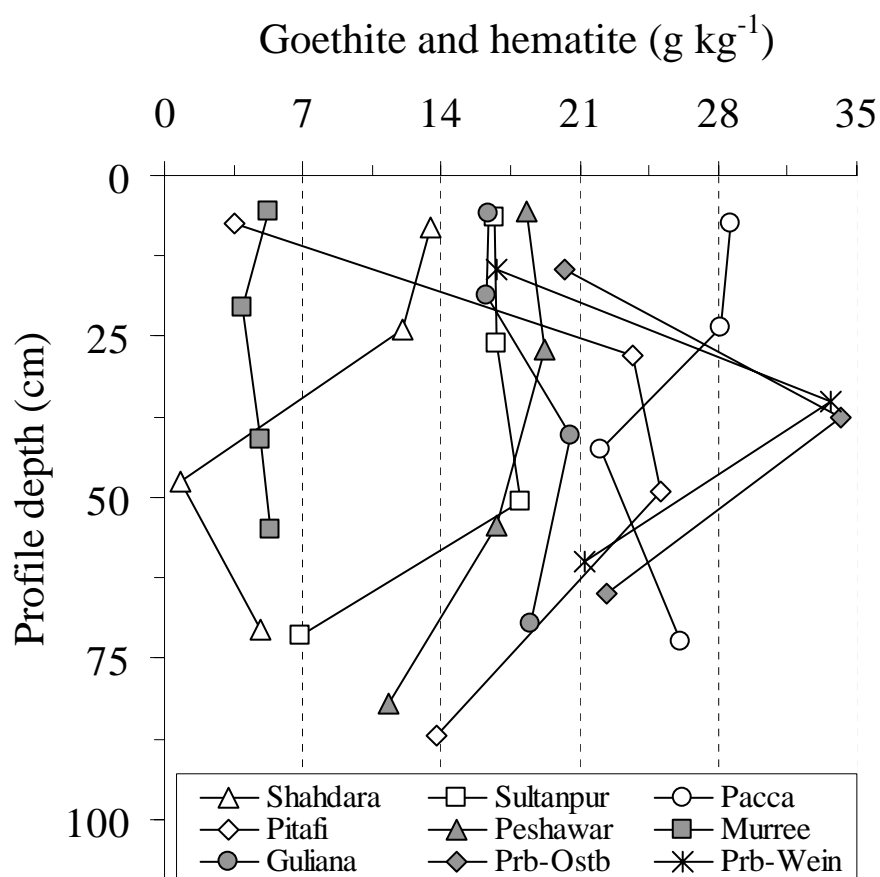


Figure 4.15: Goethite distribution in the soil profiles (hematite in case of Murree profile).

The goethite distribution in the profiles (and hematite in case of Murree soil) is presented in figure 4.15. The goethite content was higher below the two surface horizons in the Prb-Ostb, Prb-Wein soils. Lowest goethite content was given in the Shahdara soil of C2 and C3 horizons, which also were lithologically different in material than the surface soils. The Pacca soil contained approximately 20 g kg^{-1} goethite at 20 to 50 cm profile depth and was higher at the surface layer and the fourth horizon but not as high as in case of Prb-Ostb, Prb-Wein soils. A slight increase in goethite content with profile depth and then decrease at fourth horizon level was noted in Pitafi, Sultanpur, and Peshawar soils.

4.4 Phosphorus sorption

Phosphorus adsorption isotherms developed for each soil sample are presented in Appendix VIII. Adsorption parameters obtained by fitting the adsorption data to Freundlich equation ($\log C$ vs. $\log x/m$) and to the two-surface Langmuir equation ($C/(x/m)$ vs. C) are presented here. Figure 4.16 shows complete P sorption isotherms for three soil samples.

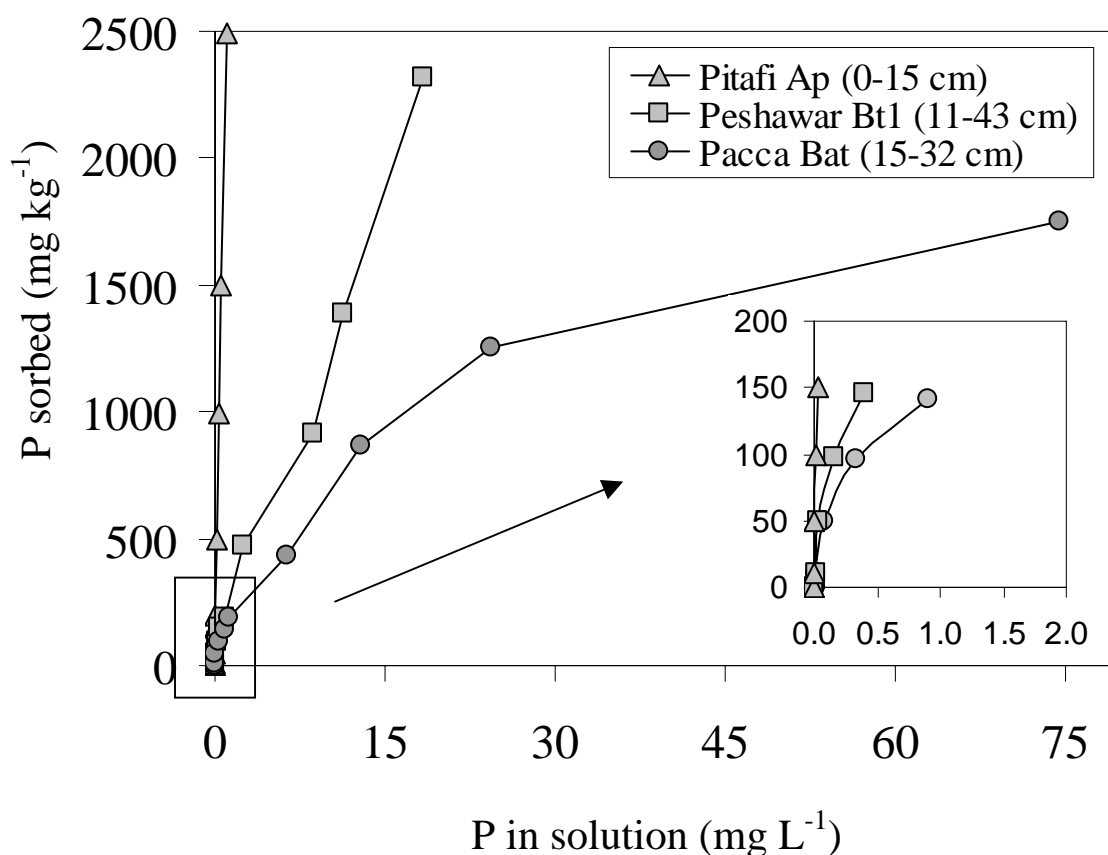


Figure 4.16: Phosphorus sorption isotherms for Pitafi Ap, Peshawar Bt1 and Pacca Bat soils.

The Pitafi soil shows the steepest slope, highest increase in adsorbed P along the ordinate with smallest increase in soluble P along the abscissa. It attained a meagre soluble P concentration of 0.1 mg L^{-1} with as adsorbed P content as high as 2500 mg kg^{-1} soil. In Pacca soil after initial high P sorption, the soluble P concentration increased with application rate and the maximum sorption was 1400 mg kg^{-1} soil. The third isotherm is given for Bt1 horizon of Peshawar soil, it also showed high initial P concentration but P sorption was lower than for Pitafi soil and higher than for Pacca soil.

The order in which the soils adsorbed P to achieve 2 mg L^{-1} solution P (mean) is given as Pitafi>Prb-Wein>Prb-Ostb>Guliana>Peshawar>Pacca>Sultanpur>Murree>Shahdara. Soluble P concentration at the same level then P applied was generally higher in the surface horizons compared to the sub-surface horizons in most soils. All isotherms showed initial high slopes, followed by a region of low slope after in most cases 100 mg P kg^{-1} soil had been adsorbed. The slope of the second region varied from soil to soil. The low P adsorbing samples of Murree, Shahdara, Sultanpur soils, Ap horizon of Peshawar and Ap and Batc horizons of Guliana soil achieved a constant slope (uniform rise in P sorbed with increase in solution P) while the high adsorbing samples showed, for most part, curvilinear isotherms or just continuous rise within the applied P, as in case of Pitafi soil. While the initial high slope region represents adsorption on high-affinity sites and the later part the low affinity sites, the intercept of the linear line on the y-axis would be the amount of P sorbed on high-affinity sites.

4.4.1 Freundlich sorption parameters

All P adsorption isotherms fitted to Freundlich equation, regression equations of each is presented in Appendix IX. Representative plots of Freundlich equation for the same three soil samples given is depicted in figure 4.17. The Freundlich parameters calculated from the regression equations for other soils are presented in Appendix X.

Freundlich equation is

$$x/m = k_f C^{1/b}$$

where x/m is the amount of P sorbed in mg kg^{-1} soil, C the solution P concentration mg L^{-1} , and k_f and b are the constants.

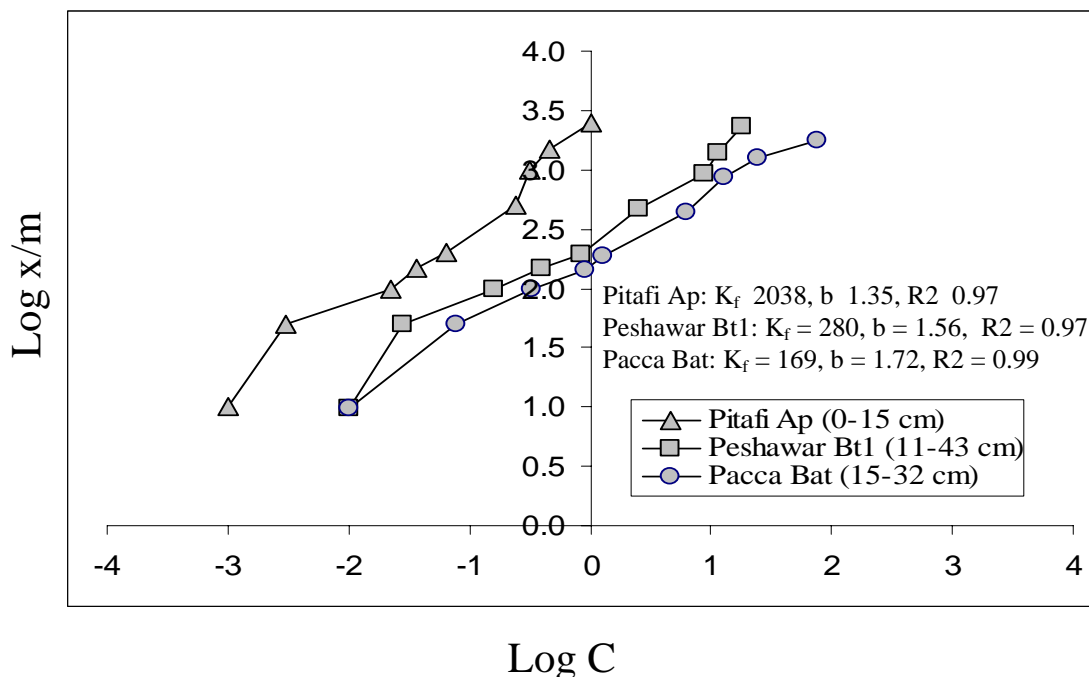


Figure 4.17: Freundlich sorption parameters Pitafi Ap, Peshawar Bt1 and Pacca Bat soils.

The linear form of the Freundlich equation is

$$\log x/m = \log k_f + 1/b \log C$$

A plot of $\log(x/m)$ vs. $\log(C)$ yields an intercept $\log(k_f)$ and a slope $1/b$. Freundlich equation fitted well with a given r^2 of 0.97 or even higher for the three cases depicted which covers the variability in the data set (discussed later).

The Freundlich parameter k_f was higher in Pitafi soil (2040) followed by Prb-Wein (466), Prb-Ostb (427), Guliana (293), Peshawar (280), Shahdara soil, Sultanpur and Pacca (111 to 247) soil, and the parameter “b” was higher in Prb-Wein and Prb-Ostb soil but similar in all other soils. The k_f and b are in fact just empirical parameters and lack any physical or stoichiometric interpretation. k_f , the intercept of the linear form of Freundlich equation was the slope of original P adsorption isotherm and b, the slope of the linear form, was actually a measure of curvilinearity of the original isotherm. The Pitafi soil showed straight rise along the ordinate within the range observed. However, with application of P at higher rate, the line will ultimately move parallel to the abscissa when the adsorbing sites are satisfied. Then “b” parameter might have different value than currently calculated, since it will have covered the complete curvilinear range then.

Nevertheless, the Freundlich parameters given in table 4.2 presented as soil means differed significantly except for the correlation coefficient, r^2 . The statistical analysis indicated that the Freundlich equation fitted well to all the different data sets. Among all the soils, the lowest “ r^2 ” was 0.93 and there was no statistically significant variability in the fit of the equation due to soil.

The Freundlich coefficient k_f was statistically similar in Pitafi, Prb-Ostb and Prb-Wein soils and significantly higher than all the other soils ($P \geq 0.05$). The lowest k_f mean was calculated for Shahdara soil. The “ k_f ” coefficient in Freundlich equation was related to the sorption affinity as the “ k ” coefficient in the Langmuir equation (discussed later) whereas “ b ” is considered as the sorption intensity (Wallace, et al., 2003).

The parameter “ b ” was significantly higher in Prb-Ostb and Prb-Wein soils than in Murree and Guliana soils. The parameter “ b ” was significantly higher in Murree and Guliana soils than the Shahdara, Sultanpur, Pacca and Peshawar soils. The Pitafi soil was observed for the lowest “ b ” which differed significantly from all other soils.

Table 4.2: Mean values of Freundlich parameters calculated for the different soils.

Soil	k_f	b	r^2
	mg kg ⁻¹	kg L ⁻¹	
Shahdara	139b	1.634cd	0.97a
Sultanpur	164b	1.550d	0.98a
Pacca	173b	1.563d	0.99a
Pitafi	790a	1.322e	0.97a
Peshawar	230b	1.475d	0.97a
Murree	190b	1.8301b	0.97a
Guliana	214b	1.720cb	0.97a
Prb-Ostb	425a	2.196a	0.96a
Prb-Wein	438a	2.251a	0.96a

*Mean of two horizons for Prb-Ostb and Prb-Wein soil and as four horizons for other soils; the numbers sharing the same alphabets do not differ significantly at p 0.05.

The Freundlich parameters k_f and b are plotted against the soil depth for each soil in figure 4.18. Exceptionally high k_f values (2040 mg kg^{-1}) were observed in the surface horizon of Pitafi soil and plotted out-side the plot area.

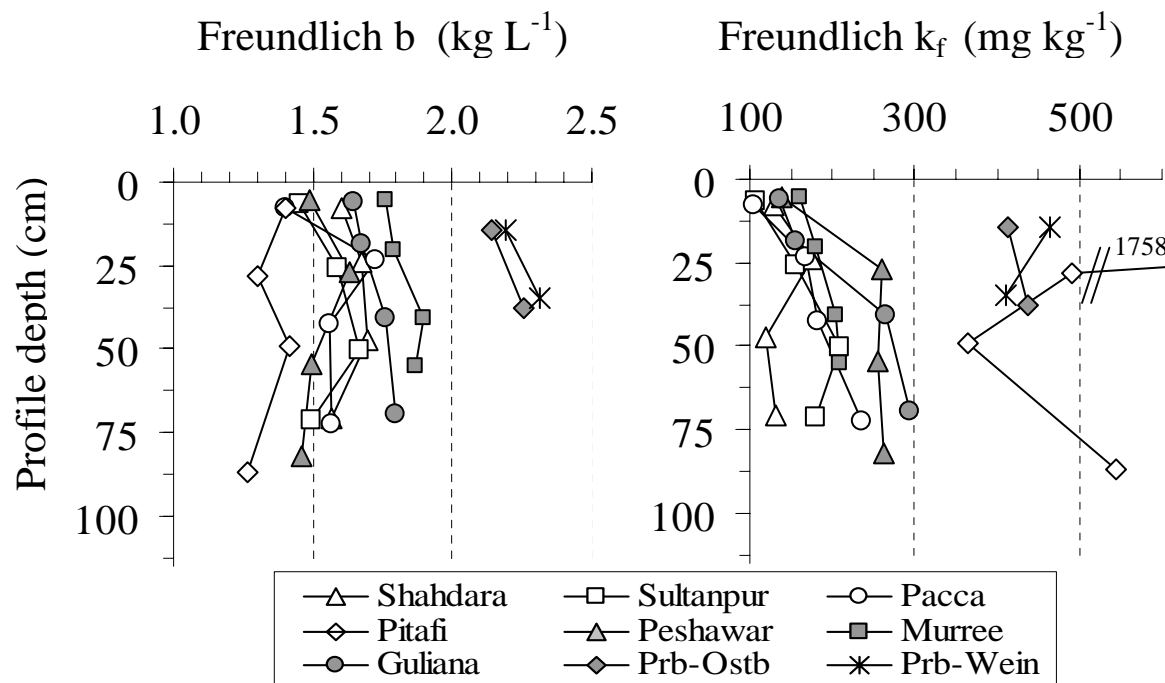


Figure 4.18: Distribution of the Freundlich parameters b and k_f calculated for the different soils.

The other horizons of the Pitafi soil and all the samples of Prb-Ostb and Prb-Wein soils showed k_f ranging from 400 to 500 mg kg^{-1} . k_f values for all other soils, Shahdara, Pitafi, Sultanpur and Murree (ranging from 100 to 150 mg kg^{-1}) and Guliana and Peshawar (ranging from 100 to 300 mg kg^{-1}) soils showed an increase with profile depth. Similarly, the Freundlich parameter “ b ” showed an increase with soil depth in all the soils and the surface soils showed slightly lower “ b ” values. Unlike the Pitafi soil, which showed the highest k_f and the lowest b values, Prb-Ostb and Prb-Wein soils showed high values for both “ k_f ” and “ b ”.

4.4.2 Langmuir sorption parameters

The simple Langmuir equation is

$$x/m = bkC/(1 + kC)$$

or

$$C/(x/m) = 1/kb + 1/b C$$

where x/m is P sorbed given in mg kg^{-1} soil, C is equilibrium soluble P concentration mg L^{-1} , “ b ” is the maximum adsorption capacity, and “ k ” represents a constant related to sorption affinity. The linear plot of $C/(x/m)$ vs. C yields a “ b ” (inverse of slope) and a “ $1/kb$ ” value (intercept) on the ordinate. The parameter “ k ” was obtained, dividing the intercept by slope. Further, the two-surface Langmuir equation is defined as

$$x/m = [b_1k_1C/(1 + k_1C)] + [b_2k_2C/(1 + k_2C)]$$

where b_1 and b_2 represent maximum P sorption at high and low affinity sites, respectively. Similarly, k_1 and k_2 are binding energies of high and low affinity sites, respectively. These parameters can be determined from the plot only when adsorption isotherm data fit the two equations well (Duffera and Robarge 1999; Sui and Thompson, 2000). Since in case of Pitafi soil the adsorption process had not been completed within the application rate as shown by straight rise of the line along y-axis in the simple adsorption isotherm, fitting of the Pitafi soil data to two-surface Langmuir equation would yield erroneous values on the parameter.

Except for Pitafi soil, the P adsorption isotherms were plotted as $C/(x/m)$ vs. C partitioned into two linear segments. Fitted to Langmuir equation, the three selected cases (Pitafi Ap, Peshawar Bt1, and Pacca Bat soils, the same as depicted in figure 4.16) are shown in figure 4.19. Phosphorus sorption isotherm data fitted the two-surface Langmuir equation equally well as that of Freundlich equation with r^2 of 95 or above in most of the cases. Fitting of the two-surface Langmuir equation did not differ among the soils indicated by non-significant differences in the coefficient of correlation for both the lines. The calculated parameters for all the soils are given in Appendix X.

The graph show that initially there was minimal increase in soluble P in both soils with increase in $C/(x/m)$ due to sorption on high-affinity sites given by the first part of the graph, however, the slope and intercept of the lines differed with soil type. Maximum sorption and binding strength were taken as inverse of slope and intercept, respectively. The second part of the graph also depicted different intercept for each sample. The high intercept translated into the lowest binding strength. The slope lines of Langmuir isotherm for Pacca and Peshawar soils were parallel in the second region. Langmuir soil mean parameters given in table 4.3 differed significantly with the soil type. The results are described in more detail in the following section.

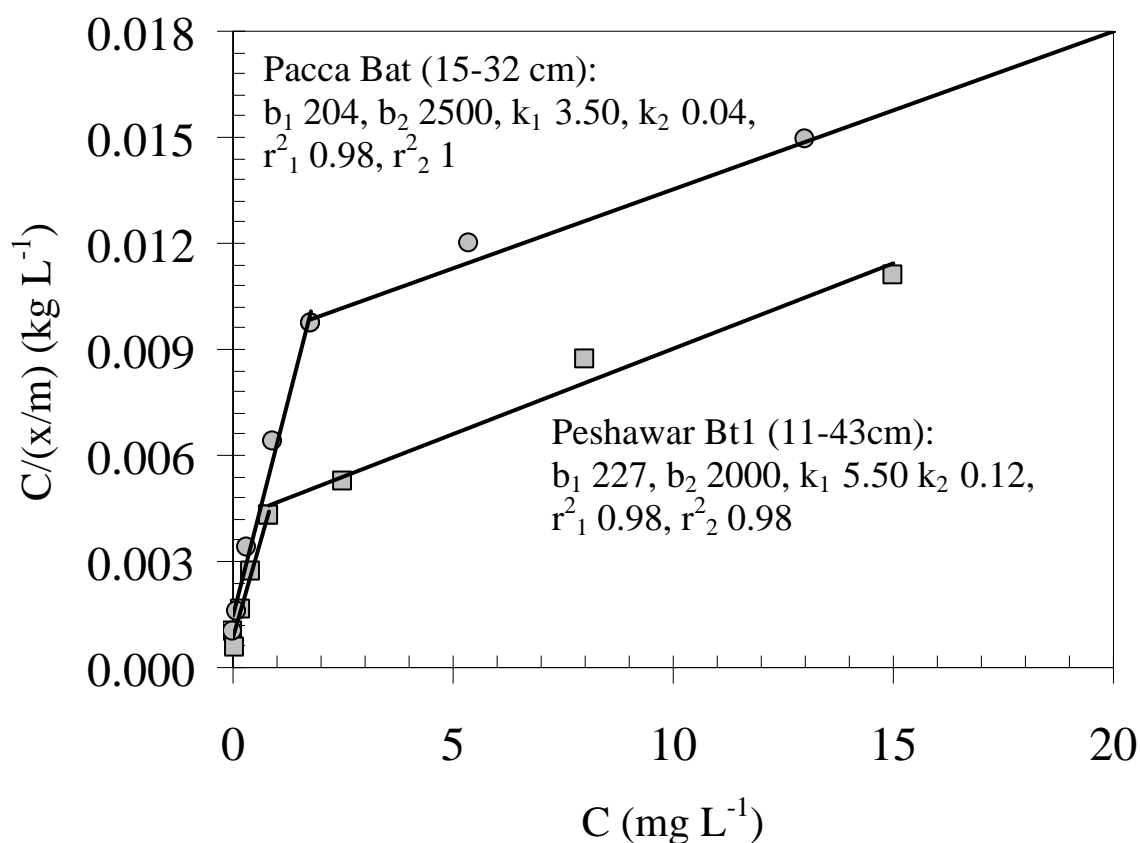


Figure 4.19: Langmuir sorption parameters of Pacca Bat and Peshawar Bt1 soils..

4.4.2.1 Maximum sorption by Langmuir

Maximum sorption on high-affinity sites “ b_1 ” in soils was observed to be higher in Guliana, Prb-Wein, Prb-Ostb, and Peshawar soils and also was statistically similar to Murree and Shahdara soils. Sultanpur was observed to be the lowest (Table 4.3). Maximum sorption on low-affinity sites “ b_2 ” in soils also differed with the soil type significantly (p 0.05). Sultanpur soil was observed for significantly greater P sorption related to low-affinity sites, although it was statistically similar to Shahdara, Pacca, Murree, Peshawar and Prb-Wein soils. The Guliana and Prb-Ostb soils showed the lowest P sorption related to low-affinity sites but they were also statistically similar to Murree, Peshawar, and Prb-Wein soils.

Table 4.3: Mean values of two-surface Langmuir parameters calculated for the different soils*.

Soil	b_1	b_2	k_1	k_2	$(r^2)_1$	$(r^2)_2$
	-----mg kg ⁻¹ -----		----- (L mg ⁻¹) -----			
Shahdara	200a	3357abc	2.19c	0.025c	0.94	0.93
Sultanpur	197a	4501a	3.64c	0.025c	0.93	0.95
Pacca	224a	3169abc	3.04c	0.038c	0.97	0.91
Pitafi	194a	3801ab	20.80b	0.168a	0.88	0.88
Peshawar	234a	2708bc	3.82c	0.076bc	0.98	0.92
Murree	217a	2876bc	4.75c	0.031c	0.98	0.86
Guliana	239a	2483bc	3.96c	0.064c	0.94	0.89
Prb-Ostb	231a	2341c	37.20a	0.131ab	0.96	0.97
Prb-Wein	238a	2272c	44.51a	0.158a	0.96	0.89

*Mean of two horizons for Prb-Ostb and Prb-Wein soils and as four horizons for other soils; the numbers sharing the same alphabets do not differ significantly at p 0.05.

The major part of P sorption was related to low-affinity sites in soils. High-affinity sites P ranged between 120 and 280 mg kg⁻¹ compared to the maximum sorption on low-affinity sites of 1200 to 5000 mg kg⁻¹. The maximum sorption values related to high-affinity sites are similar to the one reported by Sui and Thompson (2000) but this study suggests greater maximum sorption capacity values related to low-affinity sites compared to their reported values. Figure 4.20 depicts profile distribution of maximum sorption capacity related to high- and low-affinity adsorbing sites, respectively. Maximum adsorption on high-affinity site increased with profile depth in the Guliana, Prb-Ostb and Prb-Wein soils and the shale derived Murree and Peshawar soils while in the alluvial soils there was generally no depth trend. The high-affinity P sorption sites followed no particular depth trend except that it decreased in Peshawar and Shahdara soils.

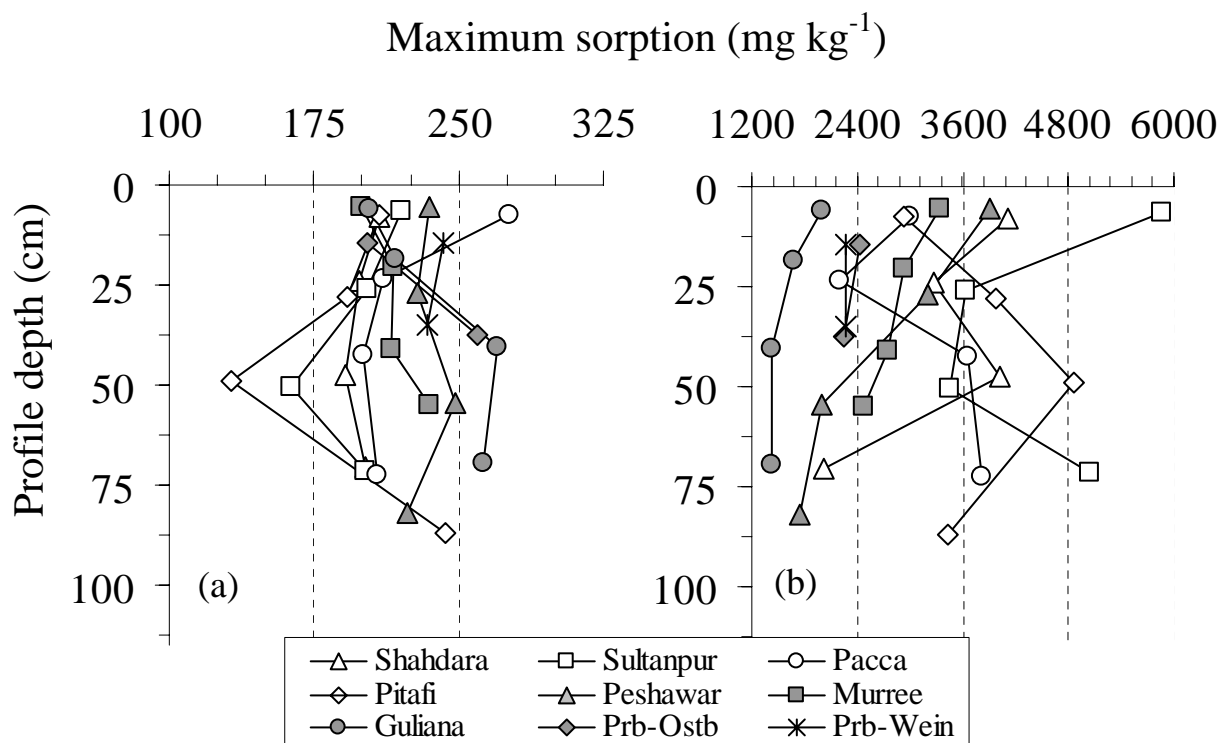


Figure 4.20: Maximum P sorption distribution in the soil profiles as determined by Langmuir equation: (a) related to high-affinity sorption sites b_1 and (b) related to low-affinity sites b_2 .

4.4.2.2 Binding strength by Langmuir

Table 4.3 presents mean binding strength of soils. The profile distribution of binding strength related to high- (k_1) and low-affinity adsorbing sites (k_2) is depicted in figure 4.21a & b, respectively. Both the Prb-Ostb and Prb-Wein soils showed statistically greater mean binding strength related to high-affinity sites than all other soils (Table 4.3). Binding strength related to the low-affinity sites was greatest in both horizons of the Prb-Ostb and the Prb-Wein soils and both the values were very similar to Pakistan soils (Table 4.3). Lower binding strength means greater intercept of the second segment on y-axes and low sorption. The highest values of k_1 (38 to 48 L mg⁻¹) were observed in Prb-Ostb (higher in Bv horizon) and Prb-Wein (higher in Bt horizon) soils. Among all the other soils, the values were within a narrow range and there was no clear depth trend.

The P binding strength on high-affinity sites was more (0.75 to 48 L mg^{-1}) than on low affinity sites (0.01 to 0.467 L mg^{-1}). Although the maximum P sorption capacity at high P sorption sites was low but required high binding affinity as compared to the maximum sorption capacity at low P sorption sites which required negligible binding affinity.

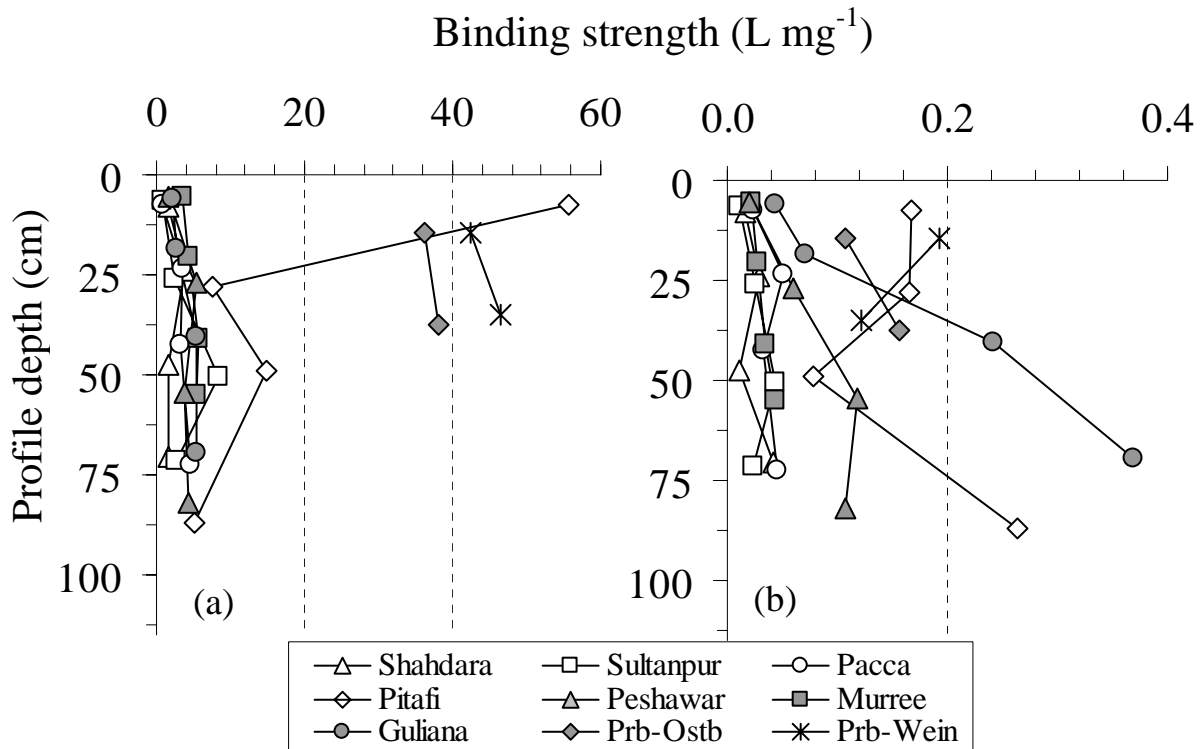


Figure 4.21: Phosphorus binding affinity distribution in the soil profiles as determined by Langmuir equation: (a) related to high-affinity sorption sites k_1 and (b) related to low-affinity sites k_2 .

This suggests that in these soils less binding affinity (k_2) was required where maximum sorption (b_1) has taken place. In other words, in these soils P is easily sorbed and can be attributed to a quick surface reaction (adsorption), whereas, the b_2 , which requires more binding affinity, can be a slow and long-term reaction.

The P binding affinity related to high sorption sites (k_1) increased with soil depth in Guliana and Pacca soils, but was in reverse order in Peshawar soil, whereas it was more or less consistent in Sultanpur soil except in its Bw2 horizon but Shahdara soil followed an irregular trend. The P binding energy

related to low-affinity sorption sites (k_2) increased with soil depth in Guliana, Pitafi, and Peshawar pedons. In Murree, Prb-Wein, Shahdara, and Pacca soil profiles P binding energy related to low-affinity sorption sites was less and there was no change with depth of profile.

4.5 Phosphorous fractions

Total P determined by HClO_4 acid digestion, organic P (total P minus the sum of inorganic P fractions), and the sum of inorganic P fractions are presented first in this section. Sequentially extracted inorganic P fractions vis. apatite P (Ca_{10}P) and other P fractions are presented later in the section. Complete data are presented as Appendix XI. The readings marked as $<0.1 \text{ mg kg}^{-1}$ in Appendix X were lower than the detection limit of the instrument and mostly these values belong to the subsurface of alluvial soils.

4.5.1 Total phosphorus

Total P content ranged from 163 to 1050 mg kg^{-1} in the soil investigated, the highest is given in the Peshawar 2Btb horizon and the lowest in Prb-Wein Bv horizon. Total P content (mean of the profile) was also higher in Peshawar and Prb-Ostb soils but was statistically similar to Shahdara, Sultanpur, Pacca and Pitafi soil and was significantly lower in the Guliana and Prb-Wein soils (Table 4.4). In Prb-Ostb and Prb-Wein soils, total P increased with depth while in less weathered Sultanpur, Pacca and Peshawar soils it increased towards the surface whereas the soils Guliana, Murree and Pitafi showed uniform total P distribution in the profile (Fig. 4.22).

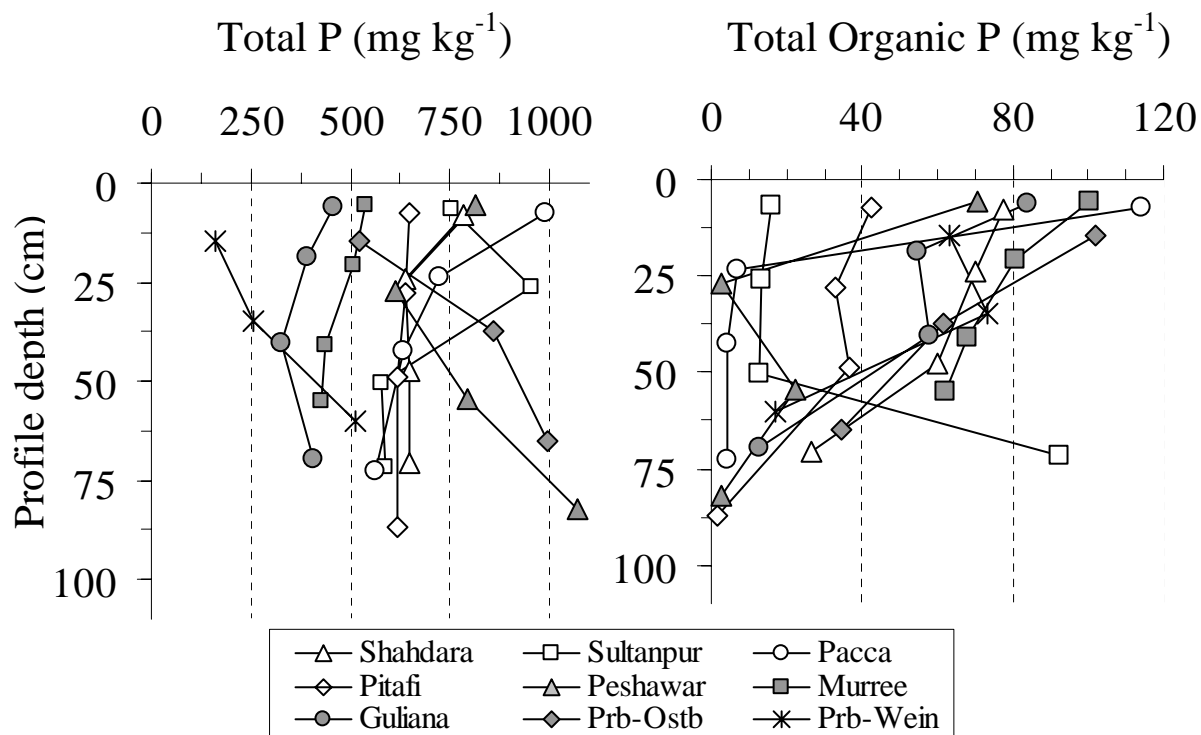


Figure 4.22: Distribution of total P content determined by HClO_4 acid digestion and total organic P by difference of the total P and sum of inorganic fractions of the soils.

4.5.2 Total organic P

Phosphorus associated with soil organic matter is presented in Appendix X indicating that the Ap horizon of Pacca soil contained the highest organic P (114 mg kg^{-1}) and the Bwy2 horizon of Pitafi soil contained the lowest (1.50 mg kg^{-1}). Statistically all the soil were similar in organic P content (Table 4.4). The surface horizons of Prb-Ostb and Prb-Wein soils, containing high organic matter, were not included in the means of the profiles; the remaining portion of the two profiles was statistically similar in organic P compared to that of the arid soils of the region from Pakistan. Organic P increased toward the surface in all soils except for Sultanpur 2C1 horizon showing several times higher values (Fig. 4.22). The Sultanpur soil profile contained stratified layers and this sudden increase in organic P well below 75 cm may indeed be related to buried high organic matter rather than to a pedological phenomena.

Table 4.4: Total soil P (extracted by H₂SO₄ digestion method), total inorganic P (sum of inorganic P fractions) and organic P content (the difference between total P and inorganic P) of the soils.

Soil	Total P	Organic-P	Total inorganic P
Shahdara	679ab	58.6a	621ab
Sultanpur	718ab	33.6a	685a
Pacca	727ab	32.4a	695a
Pitafi	631ab	28.5a	602ab
Peshawar	821a	24.5a	797a
Murree	476bc	77.8a	398bc
Guliana	395cd	52.3a	343c
Prb-Ostb	792a	66.1a	726a
Prb-Wein	309d	51.1a	258d

Mean of two horizons of Prb-Ostb and Prb-Wein soils and mean of four horizons in all other soils.

4.5.3 Total sum of the sequentially extracted inorganic fractions

Inorganic fractions include sequentially extracted P bound as Ca₂-P, Ca₈-P, Al-P, P adsorbed onto iron oxides, P released by dissolution of iron oxides, and the apatite-P. The sum of inorganic P is presented first in this section and, due to its relation with parent material, apatite P is discussed before the other more soluble P fractions.

The alluvial soils from Pakistan showed significantly greater means of sequentially extracted inorganic P fractions than the residual soils vis. Murree and Guliana soils. The Prb-Ostb soil was observed for the highest mean total inorganic P content (statistically also similar to the alluvial soils) and the Prb-Wein soil showed the lowest, significantly lower than all the soils under study. The figure 4.23 presents distribution of the sum of inorganic P fractions in the different profiles. The surface of the Prb-Wein and the Prb-Ostb soil contained approximately 150 mg kg⁻¹ and 500 mg kg⁻¹ soil, sum of inorganic P fractions, and it increased with depth to 500 mg kg⁻¹ and 1000 mg kg⁻¹ soil, respectively. The total inorganic P of Guliana soil was between 300 and 400 mg kg⁻¹ and that of Murree soil was around 400 mg kg⁻¹ soil throughout the profile depth. The Pitafi and Shahdara soils contained approximately 600 mg kg⁻¹ soil total

inorganic P fractions and overall there was no change in the total inorganic P content fraction with soil depth. The Sultanpur soil contained the highest (925 mg kg⁻¹) total inorganic P fractions. It was 700 mg kg⁻¹ at the surface and less than 500 mg kg⁻¹ the lower two horizons. The Peshawar soil surface layer contained 775 mg kg⁻¹ soil total inorganic P fractions which first decreased to 625 mg kg⁻¹ soil at 25 cm depth and again increased to about 1070 mg kg⁻¹ soil with depth.

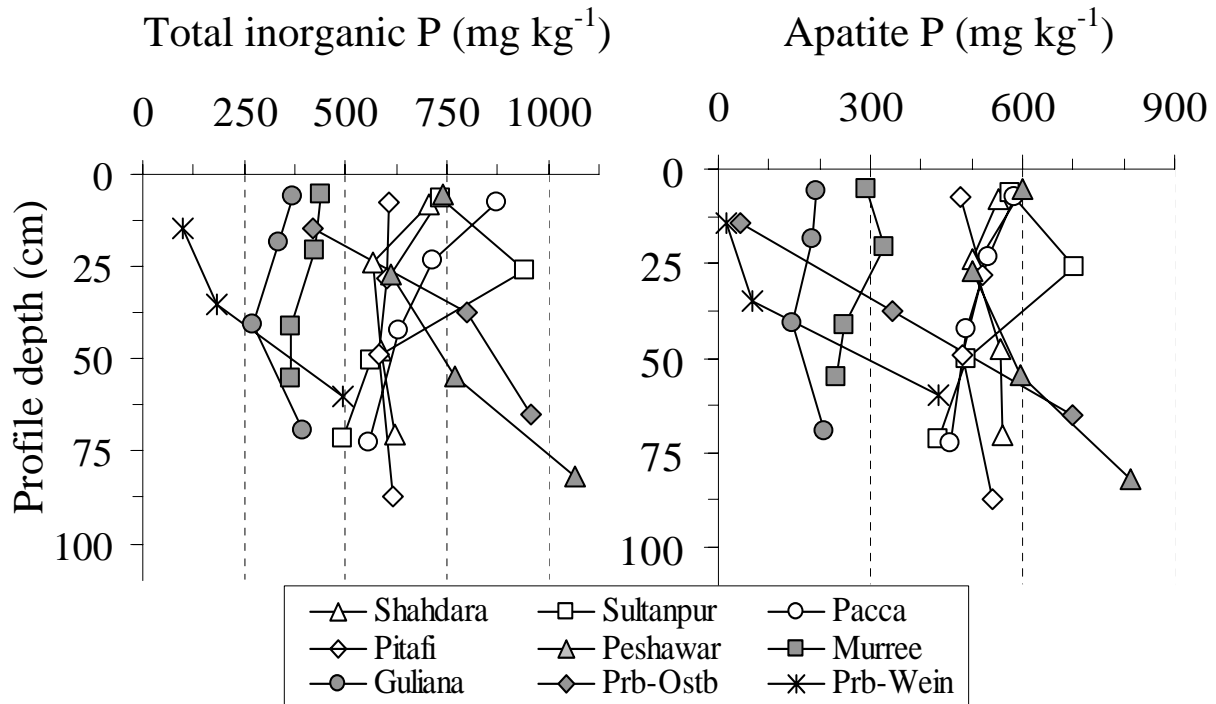


Figure 4.23: Distribution of total inorganic P content (calculated from sum of inorganic P fractions), and the apatite P (extracted by H₂SO₄ digestion) fraction of the soils.

In the two German soils the total inorganic P fractions increased with profile depth, while in the alluvial soils the total inorganic P fractions either slightly increased at the surface or stayed constant and, secondly, the residual soils contained less total inorganic P fractions than the alluvial soils. The component fractions are presented next in this section starting with apatite-P. Change in apatite P occurs only on geological time scale as apposed to more labile P fractions associated with iron oxide and CaCO₃. The labile fractions are more strongly influenced by interaction of biotic factors and anthropogenic inputs.

4.5.3.1 Apatite-P (Ca_{10} -P)

The H_2SO_4 -extracted P assumed to be apatite derived was the largest fraction of total inorganic P. The content ranged from 43 to 1070 mg kg^{-1} soil and was lowest in Prb-Ostb Bv horizons and the highest in Peshawar 2Btb horizon. Mean apatite P content was higher and statistically significant in Peshawar, Sultanpur, Shahdara, Pacca, and Pitafi soils than that of Murree and Prb-Ostb soils and was significantly lower in Prb-Wein and Guliana soils (Table 4.5).

The apatite-P content increased towards soil surface in Prb-Ostb, Prb-Wein and Peshawar profiles and to some extent in Pitafi profile while Shahdara and Pacca soils showed uniform distribution pattern over the profile. The Murree, Guliana and Sultanpur soils followed an irregular depth trend (Fig. 4.23).

Table 4.5: Soil P fractions extracted by NaOH- Na_2CO_3 (Fe-P), by sodium dithionite (occluded P) and by NH_4 -F (Al-P).

Soil	Apatite P	Fe-P	Occluded-P
-----mg kg^{-1} soil-----			
Shahdara	543a	4.2d	48.7c
Sultanpur	551a	5.5d	88.4bc
Pacca	516a	8.0d	98.4b
Pitafi	506a	0.5d	74.4bc
Peshawar	629a	6.6d	106.2b
Murree	275ab	79.5ab	18.2d
Guliana	185bc	54.8b	61.2bc
Prb-Ostb	362ab	139.8a	181.2a
Prb-Wein	172c	27.2c	45.6c

Mean of two horizons in Prb-Ostb and Prb-Wein soils and mean of four horizons in all other soils.

The apatite fraction accounted for 10 to 95% of total inorganic P. The alluvial soils and the soil as the shale mixed Peshawar soil contained the highest apatite content (500 to 600 mg kg^{-1} soil) due to unweathered mineral material while the soil of the shale derived Murree profile and the soil of the loess derived Guliana showed apatite fraction between 200 to 300 mg kg^{-1} soil. The Prb-Ostb and Prb-Wein soils showed an increase in apatite P with the depth from few tens of mg at the surface to 700 mg kg^{-1} soil at lower depth. The loss of apatite P fraction at the surface may be related to intensive weathering under the pluvial conditions.

Wang and Tzou (1995) reported calcium bound P in calcareous Nan-Wan and Hou-Liao soils in the range of the tested soils. Beauchemin et al., (2003) also found 70% and 50% P as apatite from calcareous and non-calcareous parent material respectively stating that hydroxyapatite occurred in all soils, but comparatively lower concentrations are found in acidic soils than in neutral to slightly alkaline soils.

4.5.3.2 Phosphorus desorbed from Iron Oxides

The NaOH-Na₂CO₃ extractable P fraction referred as P-desorbed content ranged from 0.3 to 193 mg kg⁻¹ soil in the data set: the lowest content was observed in Pitafi Bwy2 horizon and the highest in Prb-Ostb Bv horizon. The Prb-Ostb soil also showed the highest mean P desorbed from iron oxides (Table 4.5). The alluvial soils including Peshawar contained 10 to 17 mg kg⁻¹ soil P desorbed at the surface and the subsurface horizons contained P desorbed below the detection limit, and therefore, soils had statistically similar but significantly low values than the more ferruginous soils. Phosphorus desorbed from iron oxides increased towards surface in Prb-Ostb, and Prb-Wein soils (Fig. 4.24). The alluvial soils including Peshawar soil also showed that the P fraction increased towards the surface within the 2 to 20 mg P kg⁻¹ soil values.

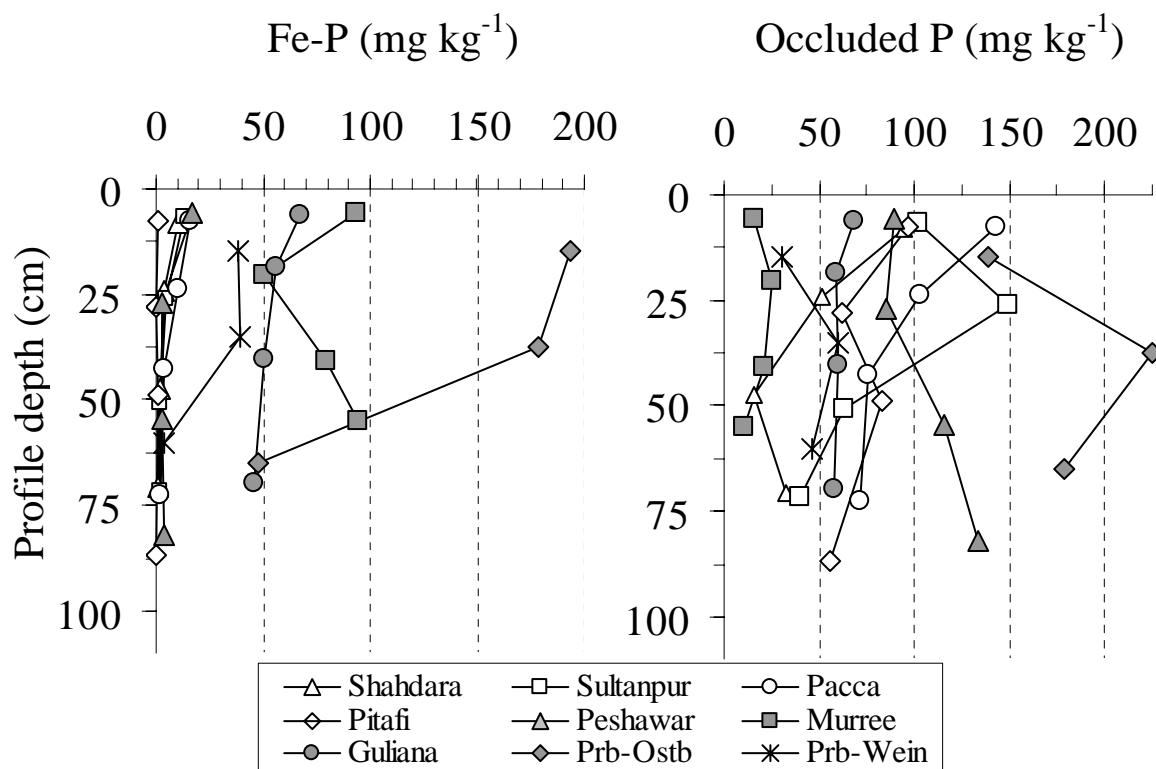


Figure 4.24: Distribution of Fe-P fraction extracted by NaOH-Na₂CO₃ and occluded-P extracted by Na- dithionite in soils.

Phosphorus desorbed from iron oxides of Murree soil lay in the range of 50 to 95 mg kg⁻¹ soil, which was higher than the 46 to 67 mg kg⁻¹ of Guliana soil. Phosphorus desorption of Murree soil followed no depth trend in values while the Guliana soil showed an increase towards the surface.

The Pacca, Sultanpur, Peshawar, Pitafi, and Guliana soils contained statistically similar desorbed P content but these contents were significantly lower than that of Prb-Ostb soil and higher than that of Murree profile. Phosphorus desorbed from iron oxides in alluvial soils including Peshawar soil ranged from below the detection limit to 18 mg kg⁻¹ soil. But the P contents occluded in iron oxide coatings were several times higher. In Murree soil more P was desorbed from the iron oxide (Fe-P) (mean ca 80 mg kg⁻¹) fraction than that released by dissolution of iron oxide (occluded-P) (mean ca 18 mg kg⁻¹) fraction. However, Guliana and Prb-Ostb soils contained higher P contents in both fractions (Fe-P and occluded-P). Also, the P fraction increased with depth in Peshawar soil and towards the surface in Shahdara, Sultanpur and Pacca soils and was uniform in all other soils (Fig. 4.24).

4.5.3.3 Phosphorus dissolved from iron oxides (Occluded P)

The iron oxides occurring as coatings on soil particles or as aggregates are dissolved by sodium dithionite and release the occluded P fraction. In the data set this fraction of P ranged from 11 to 225 mg kg⁻¹ soil. The highest value was recorded in Prb-Ostb Bt horizon and lowest in Murree 2Bt3 horizon. The mean occluded P was also significantly high in Prb-Ostb soil and low in the Murree soil compared to all other soils (Table 4.5)

The sodium dithionate extractable P (occluded-P) was a dominant fraction of the total inorganic P. The highest, 14 to 33% occluded P contributed to total inorganic P was in case of weathered Prb-Ostb, Prb-Wein and Guliana soils and lowest in case of alluvial soils. Dithionite extractable P in Murree soil contributed 3 to 6% in the total inorganic P. Samadi and Gilkes (1998) reported similar occluded P contents of young alluvial soils and of Peshawar soil in the fractionation study of fertilized calcareous soils.

4.5.3.4 Aluminum P

The P fraction extracted by NH₄-F referred as soil Al-P fraction ranged from 2.3 to 80.2 mg kg⁻¹ where the highest value in the samples investigated was in Peshawar 2Btb horizon and lowest in Shahdara C3 horizon. The mean soil Al-P fraction was high in the samples of Pacca soil but was statistically similar to that of Peshawar, Prb-Ostb and Sultanpur soils and significantly low in Prb-

Wein soil which was also similar to that of Shahdara, Pitafi, Guliana and Murree soil (Table 4.6). The means of Al-P fraction in Pacca, Peshawar and Sultanpur soils appeared to be affected by few exceptionally low or high values in the profiles. The Pacca soil profile showed an increase in Al-P fraction towards the surface while in Peshawar soil it increased with depth of profile (data not presented).

4.5.3.5 Phosphorus bound to di- and octa-calcium phosphate:

The P fraction extracted by NaOH-NaHCO₃ referred as soil Ca₂-P fraction ranged from 0.6 to 70 mg kg⁻¹ soil. The highest Ca₂-P fraction was given in Btc2 horizon of Guliana soil and lowest in Ap horizon of Shahdara soil. The mean soil profile Ca₂-P fraction varied from 5 to 20 mg kg⁻¹ soil and did not vary statistically in the different soils (Table 4.6) partly because distribution of Ca₂-P in the profiles had non-uniform trend. The P bound to di- and octa-calcium distribution is presented in figure 4.25.

Table 4.6: Soil phosphorus fractions extracted by NaHCO₃ (Ca₂-P) and by NH₄-acetate (Ca₈-P).

Soil	Ca ₂ -P	Ca ₈ -P	Al-P
-----mg kg ⁻¹ soil-----			
Shahdara	7.7a	6.3a	10.7bc
Sultanpur	5.8a	7.2a	26.8abc
Pacca	5.9a	7.9a	58.8a
Pitafi	9.4a	5.2a	7.5bc
Peshawar	10.3a	7.1a	37.7ab
Murree	7.8a	6.4a	11.5bc
Guliana	20.6a	5.4a	15.8bc
Prb-Ostb	16.7a	5.5a	20.4abc
Prb-Wein	5.2a	5.9a	1.9c

Mean of two horizons in Prb-Ostb and Prb-Wein soil and mean of four horizons in all other soils.

Except for the Prb-Ostb and Prb-Wein soils, most other soils contained higher Ca₂-P fraction at the surface, which were reduced at the second and third level horizon and, then, increased to more than that of surface horizons (Fig. 4.25). The Guliana Btc2 soil contained exceptionally high dicalcium phosphate bound P fraction, 70 mg kg⁻¹ per kg soil. The data plotted outside the plot area. The P fraction extracted by NH₄-acetate referred as Ca₈-P fraction ranged from 3.7 to

13.3 mg kg⁻¹ where the lowest value was in the Shahdara C1 horizon and the highest in the Sultanpur Ap horizon. The soils showed statistically similar means for Ca₈-P fraction. Proportionately, in the surface layer Ca₈-P fraction was more compared to the Ca₂-P fraction especially in the alluvial soils (Fig. 4.25). In Prb-Ostb and Prb-Wein soils Ca₈-P fraction was uniformly distributed in the profiles and in some soils it increased towards the surface as well as increased with the depth of profile. The surface horizons contained lower Ca₂-P fraction compared to Ca₈-P fraction.

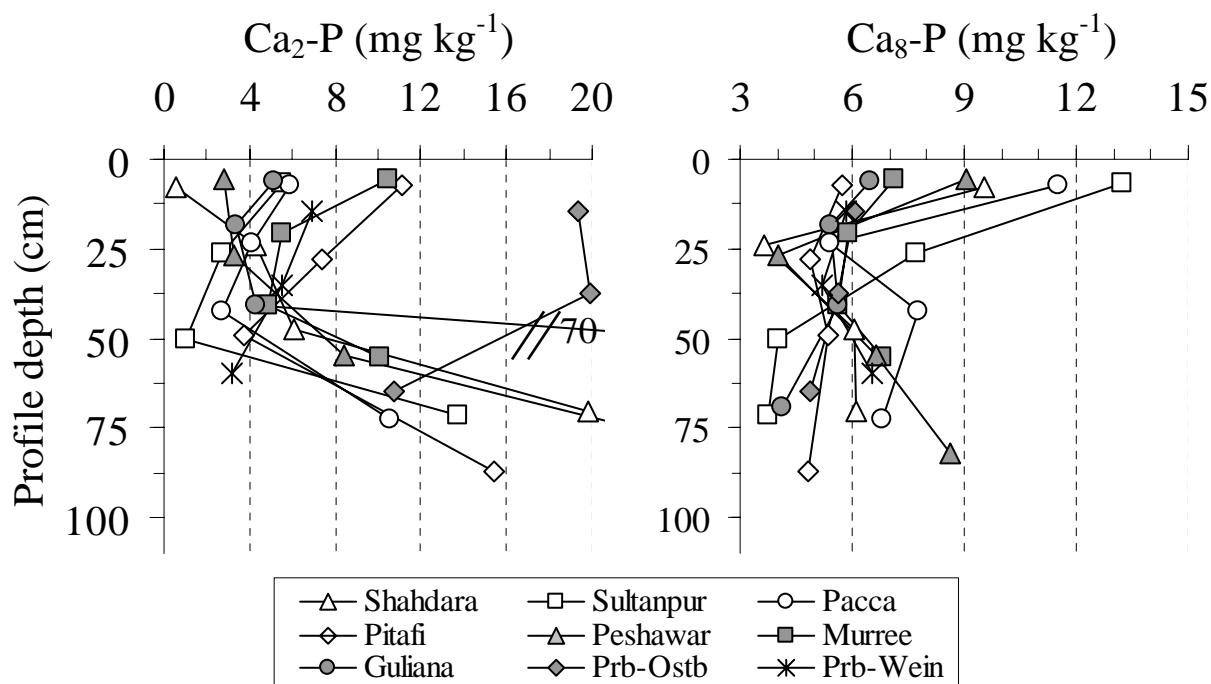


Figure 4.25: Distribution of Ca₂-P extracted by NaHCO₃ and Ca₈-P extracted by NH₄-acetate in the soils.

4.5.3.6 Iron co-extracted with P in NaOH-Na₂CO₃ and Na-dithionite

Iron co-extracted with P by NaOH-Na₂CO₃ and by Na-dithionite extractions was analysed by ICP. Its distribution in the soil profiles is presented in figure 4.26. The NaOH-Na₂CO₃ extracted samples from Guliana, Murree, and Prb-Wein soils released 500 to 1000 mg Fe kg⁻¹ soil, several times higher than the other soils. It was noted that in Prb-Ostb soil at 4-25 cm horizon iron release was measurable to be 425 mg and only few mg at the 25-50 and >50 cm profile depth. Shahdara soil also released more iron than the remaining alluvial soils by NaOH-Na₂CO₃ extraction. Due to the stronger dithionite treatment not only the overall release of iron was higher in all soils but also the more ferruginous soils

(Prb-Ostb, Prb-Wein, Murree and Guliana) released more iron than the less ferruginous soils (Shahdara, Sultanpur). The iron distribution by Na-dithionite in the profiles followed the same trend as that of total iron extracted by CBD (presented earlier, Fig. 4.4).

Overall, there was no significant relation between Fe and P released by these two extractions, neither there was any relation between the Fe extracted by the two extractants (data not presented). However, the ratio (Fe:P in NaOH-Na₂CO₃: Fe:P in Na₂-dithionate) varied with soil type (Fig. 4.27). In Guliana soil desorbed-P and dissolved-P was approximately 50 mg kg⁻¹ soil.

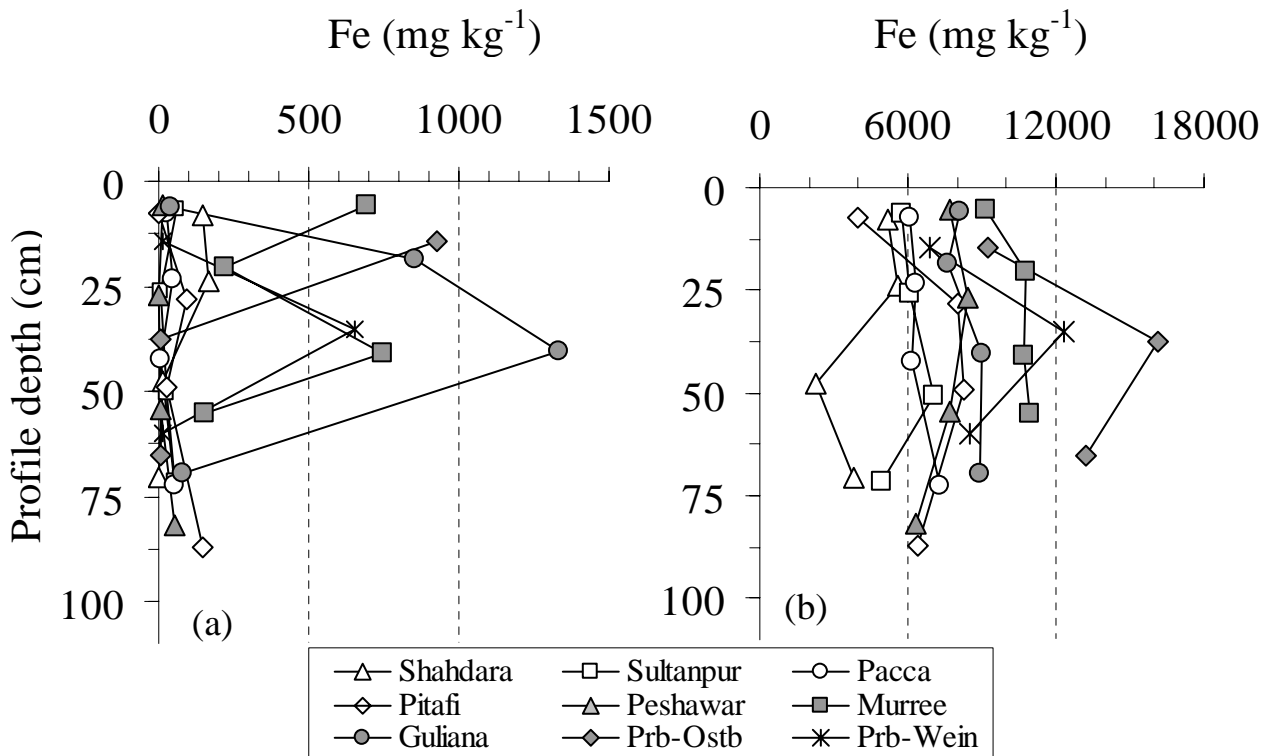


Figure 4.26: Distribution of the Fe co-extracted with P (a) in NaOH-Na₂CO₃ and (b) Na-dithionite in the soils.

Na-dithionite dissolved-Fe ranged from 8000 to 9000 mg kg⁻¹ compared to a lower amount of 60 to 70 mg kg⁻¹ soil extracted by NaOH-Na₂CO₃, (Fig. 4.27a). In the alluvial soils, Pacca soil is an example, Fe distribution in both the extracted fractions was approximately similar in Guliana soil (6000 - 7300 mg kg⁻¹ in Na-dithionate and 10 and 50 mg kg⁻¹ in NaOH-Na₂CO₃) but P in dithionite was 70 to 145 and only 2 to 16 mg kg⁻¹ in NaOH-Na₂CO₃ (Fig. 4.27b). Almost an opposite trend was noted in the shale derived Murree soil with approximately the same Fe distribution by Na-dithionite and by NaOH-

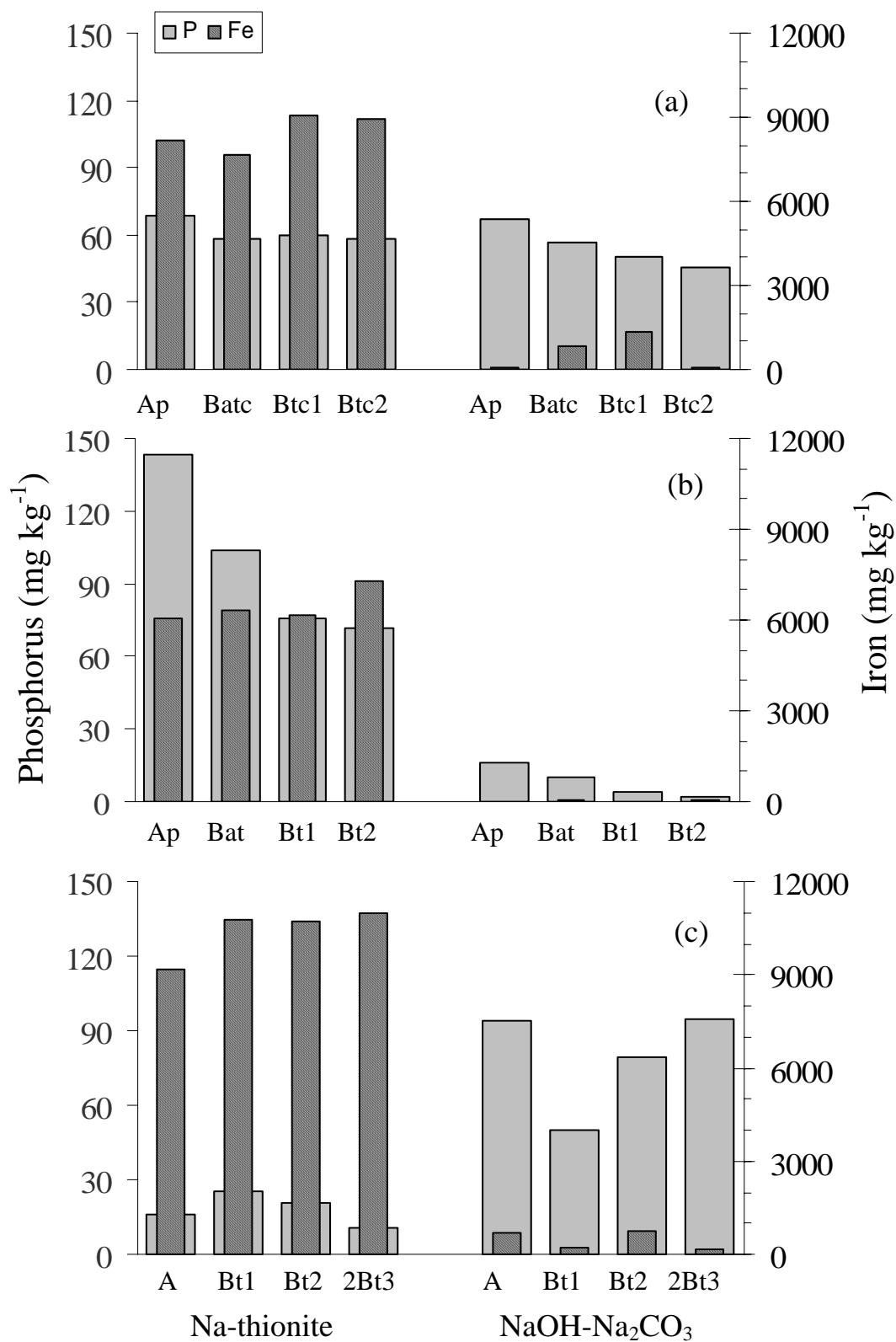


Figure 4.27: Comparative distribution of P and the co-extracted Fe in Na-dithionite and NaOH- Na_2CO_3 in the (a) Guliana soil, (b) Pacca soil, and (c) Murree soil.

Na_2CO_3 (as in Guliana and the Pacca soils) but Murree soil had three to four times more P by Na-dithionite extraction than by $\text{NaOH-Na}_2\text{CO}_3$ (Fig. 4.27c)

4.5.4 Overall distribution of sequentially extracted P fractions

Figure 4.28 shows the various P fractions as percent of the sum of six inorganic P fractions vis. Apatite-P, P released by decomposition of iron oxides (occluded-P), P displaced from iron oxides (Fe-P), P released by decomposition of Al oxides (Al-P), P released by decomposition of octa-calcium phosphate ($\text{Ca}_8\text{-P}$), and the P released by decomposition of dicalcium phosphate ($\text{Ca}_2\text{-P}$).

The dominant inorganic P fraction in the alluvial soils including Peshawar soil was apatite-P, proportionate contribution of Ca bound P ($\text{Ca}_2\text{-P}$, $\text{Ca}_8\text{-P}$ and $\text{Ca}_{10}\text{-P}$ fractions) iron bound P varied with the different soils.

The $\text{Ca}_{10}\text{-P}$ fraction was the major contributor to Ca-associated P fractions and the $\text{Ca}_2\text{-P}$ and $\text{Ca}_8\text{-P}$ fractions were only minor fractions. Shen et al. (2004) also observed similar results in rice calcareous soils. The $\text{Ca}_2\text{-P}$ and $\text{Ca}_8\text{-P}$ fractions ranged from 0.2 to 7% and 0.70 to 5.9%, respectively for all soils except for the Btc2 horizon of Guliana soil, which contained 17.7% $\text{Ca}_2\text{-P}$ due to its loess parent material. There was no relationship between the total inorganic P and the $\text{Ca}_2\text{-P}$ fraction. In contrast the $\text{Ca}_8\text{-P}$ fraction was higher in surface soils and there was some relationship between the total inorganic P and $\text{Ca}_8\text{-P}$ (r^2 0.40).

4.6 Microanalysis of P saturated clay

Energy dispersive X-ray (EDX) analysis of the soil clay fraction pre-treated with P solution showed variable P and Fe ratios, which appeared to be related to particle morphology. The morphology of these iron oxide particles was similar to that discussed under section 4.3.1. EDX spectra and TEM image of the specific particles are depicted together in these figures for comparison. Phosphorus peak occurred at 2 keV and that of Fe at 6.4 keV. The other measurable peaks were for Si and Al, which might have been originated from neighbouring and/or underlain phyllosilicates. Aluminum may also be substituted in the iron oxide particles. A large number of particles were analysed from each clay sample from second horizon in each soil. The EDX spectra with K, Mg, Si, Al and proportionally small peak of Fe were not included due to possibility of these particles being phyllosilicates. However, the EDX spectra with strongest Fe peak and with or without traces of Al/Si and showing one of goethite morphologies were counted.

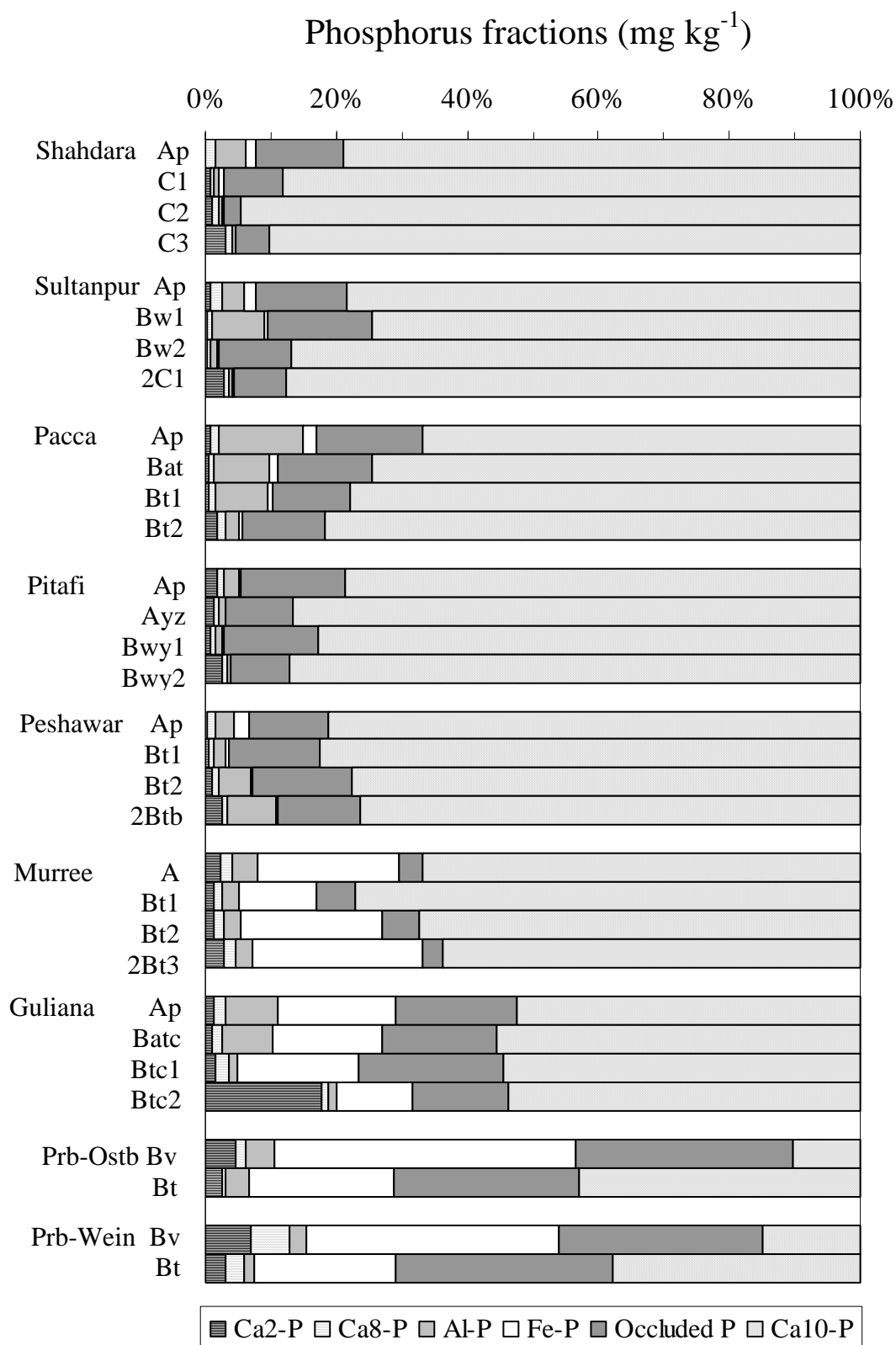


Figure 4.28. Distribution of proportion of various inorganic P fractions in the soils.

Phosphorus and Fe ratios were calculated for approximately 10 particles in each soil clay sample. The representative TEM images with EDX spectra are presented in figures 4.29, 4.30, and 4.31 for different soils.

The iron oxide particles in alluvial soil clays contained P:Fe ratio between 0.20 and 0.30 and mean of 10 particles showed the following order of P:Fe ratio Pitafi>Pacca>Shahdara>Sultanpur. Although iron peak of Pitafi clay was the lowest (16 counts) and the highest of Pacca clay (104 counts), the P to Fe ratio was similar in both samples vis., 0.31 and 0.29, respectively.

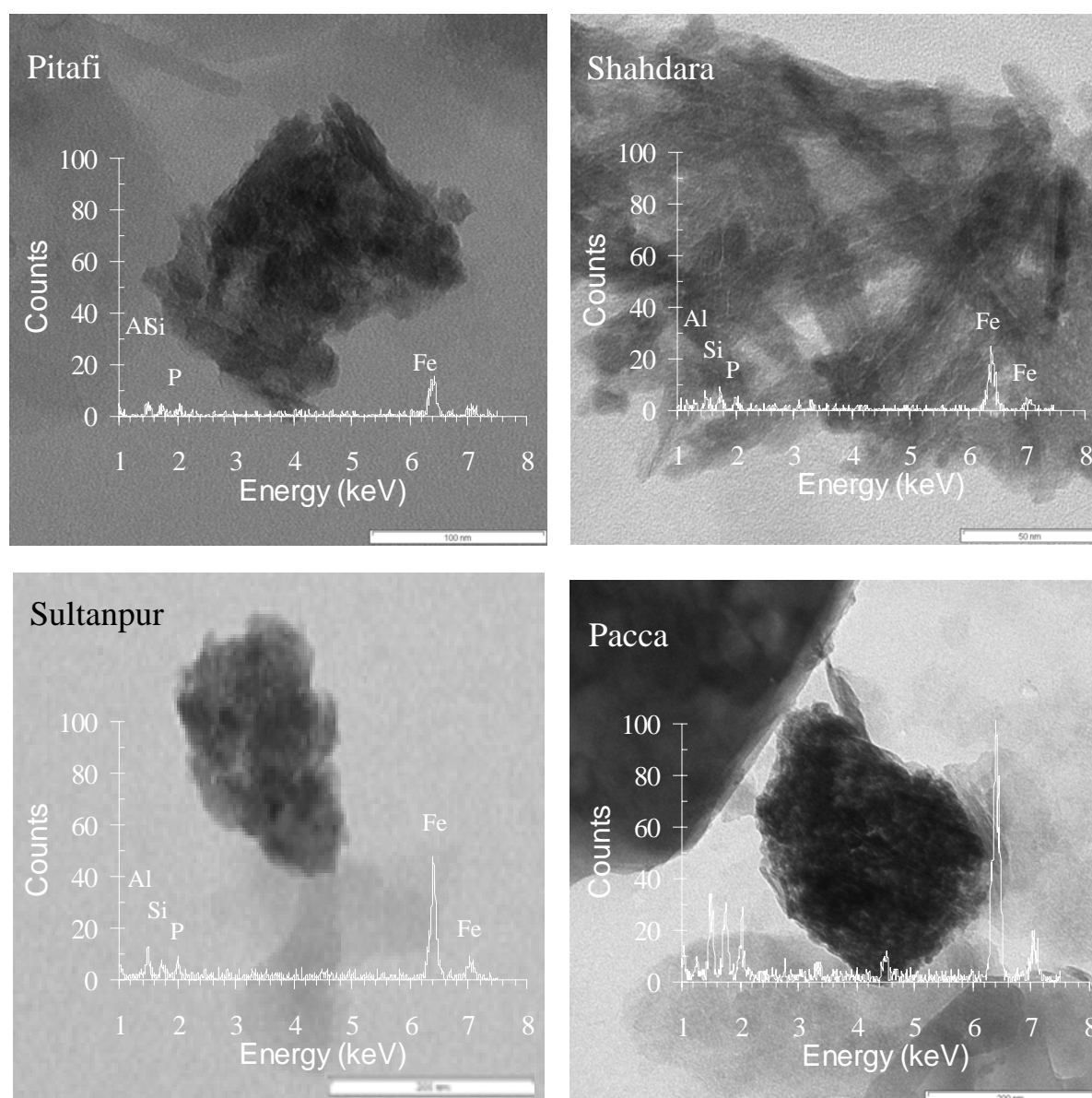


Figure 4.29: TEM images with relevant EDX spectra of P saturated goethite particles from alluvial soil clays.

These clays showed well crystalline goethite with several multidomainic particles with v-shaped grooved edges and thick twinned laths. Figure 4.29 depicts morphology of the goethite particles from the alluvial soils. The goethite particles of Peshawar soil clay contained P:Fe ratio of 0.2 as that of goethite from alluvial soils, and showed morphology including laths with sharp edges and lattice fringes and few multidomainic particles.

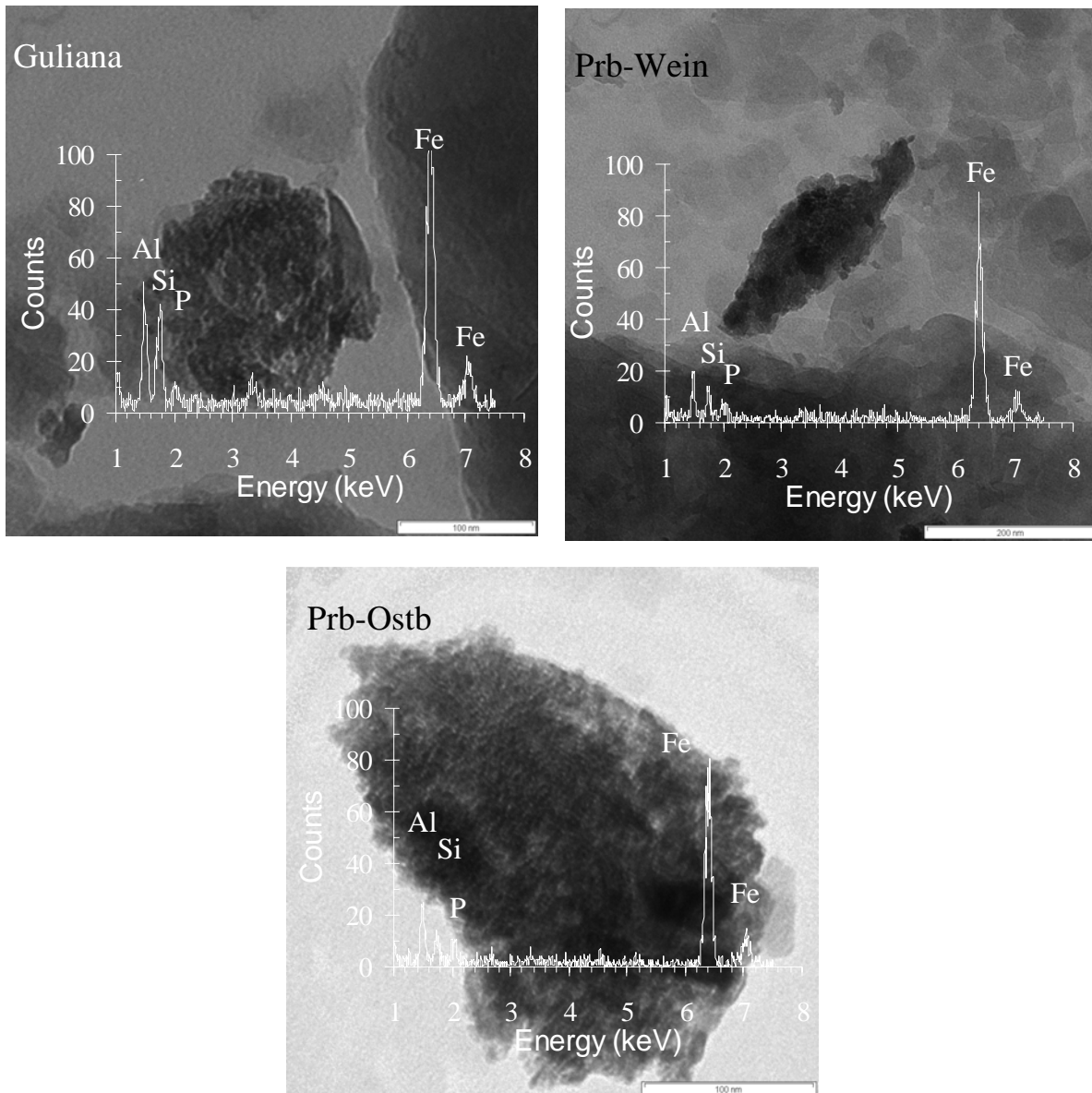


Figure 4.30: TEM images with relevant EDX spectra of P saturated goethite particles from weathered soil clays.

The Guliana, Prb-Wein and Prb-Ostb soil clays contained goethite P:Fe ratio in the range of 0.09 to 0.15, the lowest in Guliana soil clay and the highest in Prb-Wein soil clay. The weathered soil clays showed intense iron peaks compared to alluvial soil clay peaks but contained low P content. The goethite particles of Guliana soil clay of 0.2μ size contained P:Fe ratio of 0.09 and Prb-Ostb and Prb-Wein soil clays of 0.3μ size contained P:Fe ratio of 0.14 and 0.15 respectively. The goethite particles were less crystalline, mostly monodomainic-serrated laths with well-developed lattice fringes as the morphology has been described in detail in section 4.3.1 (Fig. 4.30).

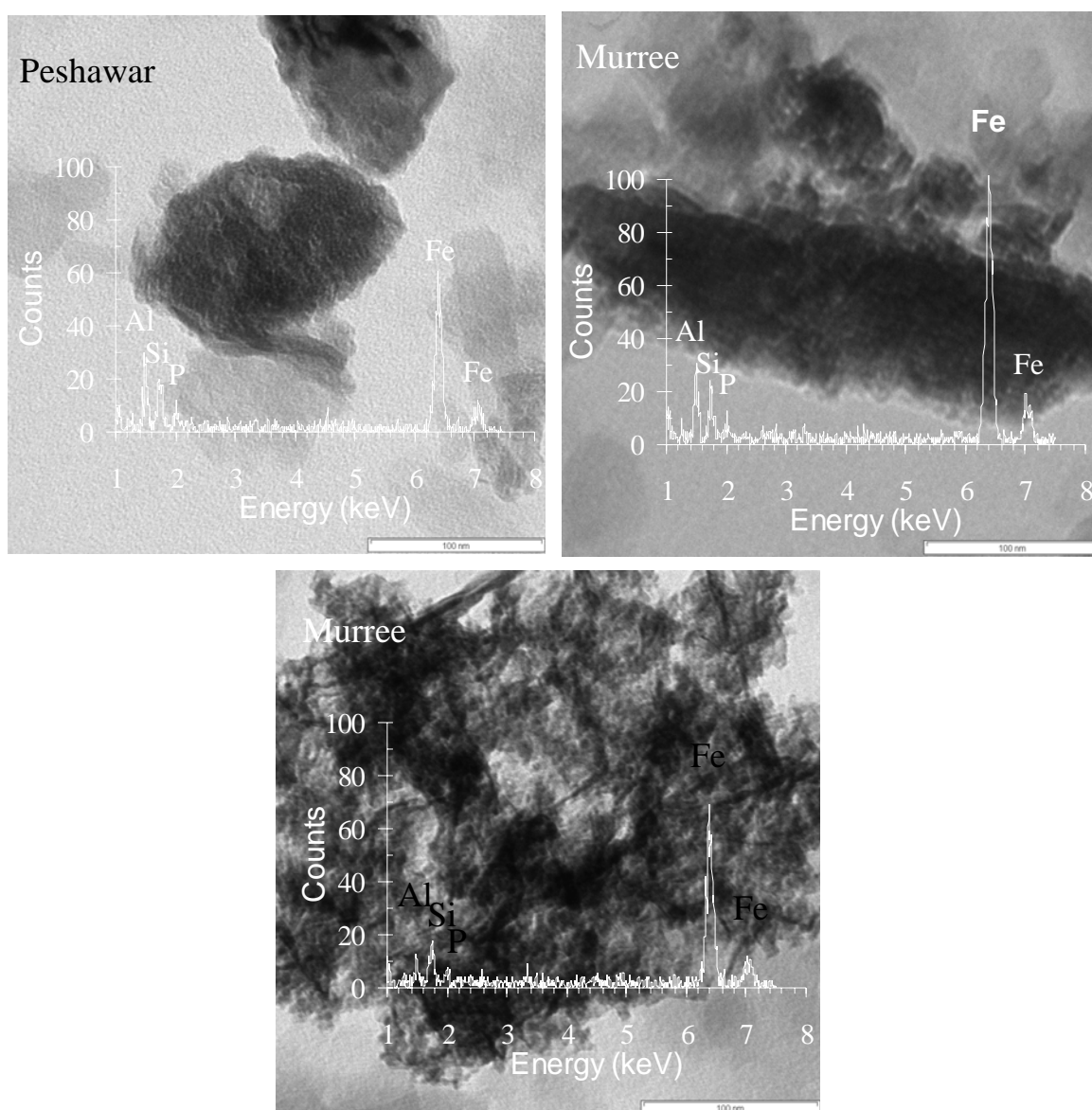


Figure 4.31: TEM images with relevant EDX spectra of P saturated goethite particles from shale derived soil clays.

The goethite particles of Murree soil clay contained P:Fe ratio of 0.12, similar to that of Guliana, Prb-Wein and Prb-Ostb soil clays. Many individual hematite particles were too small to be analytically resolved by TEM. However, the hematite particles sintered as irregular aggregates with diffused edges were analysed (Fig. 4.31). In Murree soil clays TEM also indicated the integrated single-mineral particles of iron containing P:Fe ratio of 0.12 and morphology similar reported for red soils (Nornberg et al., 2003). Colours of materials as red as 5YR (Nornberg et al., 1991) indicate the presence of hematite (Scheinost and Schwertmann, 1999). In summary, the alluvial soils (Shahdara, Sultanpur, Pacca and Pitafi) show high P:Fe ratio compared to ratio in the weathered soils including Guliana, Prb-Ostb and Prb-Wein. Therefore, it appeared that as the crystallinity seen by TEM increased the P:Fe ratio also increased.

5. Discussion

Soil P chemistry has been investigated in developed countries mostly on highly weathered and acidic soils (Frossard et al., 1995; Sinaj et al., 1992; Said and Dakermanji, 1993) and parallel studies have not been conducted in developing countries where the P deficiency in soils is even wide spread and, while cost of inorganic fertilizers is high, its use efficiency is low. This research is one of a few studies carried out on Pakistani soils. It focuses on the P chemistry and on iron oxide phases in calcareous soils sampled from different land morphological units and of different climatic regimes. The role of soil matrix components in regard to P sorption is discussed later after viewing the nature of the soils.

5.1 The soils and their mineral composition

Component minerals of soil matrix and its soluble species are controlling phosphorus retention. It is necessary to understand distribution of minerals or solution species in the prospects of pedogenic processes before their relation with P sorption can be developed. The alluvial soils are relatively light textured and the particle size distribution seems to be inherited from the parent sediments. Profile development (homogenization, weathering, and translocation of plasmic material) is limited not only by the scarcity of water but also due to the fact that the soils are young and are developed from Sub-recent sediments laid between 10000 and 5000 years in arid and semi-arid climate. The Pacca soil occurring in broad basins in the fluvial plain consists of silty clay due to accumulation of fine sediments. The pH value of the soils is high. Irregular distribution of free CaCO_3 in the soil matrix, low organic matter content and citrate bicarbonate dithionite (CBD) extractable iron were the main features. The Peshawar soil was developed in intermountain alluvium referred as Piedmont alluvial-plain, derived mainly from limestone and a mixture of sandstone and calcareous red shale and laid after the main part of glaciations period in semi-arid climate (450 to 550 mm mean annual precipitation). An important characteristic of this soil was the occurrence of litho-relicts from the adjoining hills as been previously reported (Akhtar et al., 1989).

Texture of the Guliana soil consists of silty clay loam and silty clay. It is decalcified leaving only 10 to 20 mg kg^{-1} free soil CaCO_3 in the profile through 90 cm depth. CaCO_3 accumulation at lower depths and weathering occurred due to the collection of runoff, which also resulted in the change in texture

from original loess to silt clay (Brinkman and Rafique, 1971). CBD extractable iron oxide also increased in Guliana soil with depth suggesting intense *in situ* weathering. The Murree soil occurred in humid climate and contained greater CBD extractable iron oxide ascribed mainly to its shale derived parent material rather than *in situ* weathering. The climatic conditions although favor hematite formation but accelerated runoff due to the trough and ridge land morphology had altered the effect of rainfall. The soil texture of the Murree soil is characterized by silt loam, organic matter (10 to 24 mg kg⁻¹) accumulated under forest, matrix slightly alkaline to non-calcareous, and lower pH (7.2 to 7.8).

The Parabraunerde of Osterburken (Prb-Ostb) and of Weingarten (Prb-Wein) consisted of decalcified silty clay loam with acidic pH as they occurred under forest cover in oceanic climate with mean annual precipitation of 700 to 900 mm. Decalcification and leaching of the basis in humid environment and illuviation at lower depths resulting in free lime in the soil matrix may be responsible for the increase in soil pH at lower depths.

Phosphorus adsorption on argillaceous minerals is characterized as an electrostatic adsorption on low affinity sites; therefore, it is to be recognized that clay minerals are sorbing less P ions than oxides. Clay mineral composition, especially the dominance of kaolinite may influence P sorption in soil. At low P levels kaolinite dominant soils are sorbing higher P fractions than illite dominant soils (Tomar et al. 1995). The clay mineral composition of these soils will be related to P sorption capacity. Clay minerals of these soil clays are discussed in terms of soil genesis and parent material. The soil clays were composed of dominantly kaolinite, mica, smectite and vermiculite and smaller proportion of hydroxyinterlayer smectite/vermiculite (HIS/HIV), chlorite and tectosilicates with minor proportion of iron oxides (goethite and hematite). Relative proportion of these minerals varied with parent material and the soil development stage. Assuming quartz and feldspars amounting to 10% of clays, which was the detection limit for XRD for minerals, mica accounts for 45 to 50%. This range of mica corroborates with previous studies undertaken in these soils (Ahmad et al. 1986; Akhtar, 1989; Akhtar and Dixon, 1993).

The alluvial soil clays contained smectite from 7 to 22 %, vermiculite from 0 to 15%, and kaolinite from 17 to 19 %. These minerals were uniformly distributed among horizons (no depth trend). Relatively sharp mica peaks were observed in the alluvial soils compared to the broad peaks in the shale derived

or the loess soils. As weathering of primary minerals in these soils is only limited, the clay minerals appeared to be inherited from the parent sediments. Shahdara and Sultanpur soil clays showed only smectite whereas Pacca and Pitafi soil clays, in addition to smectite showed vermiculite; and the surface horizons of Pacca and Pitafi soils were observed for containing HIS/HIV and chlorite fraction. The Murree and Peshawar soil clay was composed of mostly vermiculite, mica, and kaolinite with small amounts of chlorite. Smectite content in these soils was less than that of alluvial soils and kaolinite content was higher.

The loess derived Guliana soil showed kaolinite, smectite, mica, vermiculite, chlorite and a HIS/HIV fraction of the clay fraction. Amount of kaolinite and smectite was the highest, smectite showed an increasing trend with depth probably due to greater *in situ* weathering rate and translocation of argillaceous clay. The Prb-Ostb soil was observed for clay mineral composition exhibiting 14.2 Å peak upon Mg saturation, which expanded to various degrees leaving only a small intensity of 14.2 Å peak, depictive of vermiculite, but, there was no clear peak at 17 Å position. Both the Prb-Ostb and Prb-Wein soils showed low kaolinite contents in the clay fraction probably due to high leaching of silica under humid climate.

5.2 Soil iron oxides

Whether iron oxides are affecting P sorption in calcareous soils is the main thrust of the study. Iron oxides in the study were characterized as extractable fraction with dithionite and ammonium oxalate and the crystalline phase determined by XRD, TEM and quantitative reductable iron oxides by cyclic voltammetry. Variation in iron oxide composition and their characteristics are related to the pedogenesis. This discussion focuses on the distribution of various phases of iron oxides and provides explanations in terms of pedogenesis.

Oxalate extractable iron (amorphous) was generally a small fraction of the total extractable iron oxide fraction in all the soils. Since, it has high surface area, the impact of amorphous iron on P sorption is very high (discussed later). Our results showing that amorphous iron is a minor fraction of total extractable iron oxide are in agreement with the statement that crystalline iron oxides (goethite and hematite) are usually the dominant iron oxides in soils (Saavedra and Delgado, 2005). Yet, the lowest ratio of oxalate to dithionite extractable iron was given in the alluvial soils and highest in Parabraunerde soils, which

concurrent with their weathering rates. X-ray diffraction results (Fig. 4.11) showed that crystalline Al hydroxides such as gibbsite and boehmite do not occur in these soils but substantial amounts of Al were extracted with oxalate. The amount of oxalate extractable Al of most soils was higher than that of iron of the same extract. Further, the content of oxalate extractable iron and aluminum were highly correlated (r^2 0.84, < 0.0001 , based on the data given in Appendix XII) suggesting a common source. Oxalate extractable aluminum is also present as amorphous or Al-OM (aluminum organic matter complex) species rather than free oxides. The contents of dithionate extractable iron and aluminum were also highly correlated (r^2 0.74, < 0.0001 , based on data given in Appendix XII) suggesting that the aluminum fraction dissolved by CBD may be substituted for iron as was reported for Australian calcareous soils (Samadi and Gilkes, 1998). The substitution of Al in goethite has been correlated with P sorption of different mineral phases (Agbenin, 2003; Harrel and Wang, 2006).

Iron oxides and organic matter are soils' pigmenting agents and, therefore, color is one of the obvious attributes for rating the differences. Goethite is responsible for the yellowish and brownish colours and hematite imparts the red color to soils. Good relationship between the Brazilian soils and the nature of iron oxides has been reported (Bigham et al., 1978; Kämpf & Schwertmann, 1983; Fontes, 1988). Hematite has a high pigmenting power and is very effective in masking the yellow color of goethite (Resende, 1976). The color of the soil as of Murree soil was dark brown and that of Peshawar soil light brown to dark brown but showed only a few percent to only traces of hematite, as presented later. The alluvial soils were lighter in color, since, majority of the soils contained low organic matter content.

The trend in extractable iron oxide content with depth was related to either possibility of translocation as in case of the highly developed profiles of Prb-Ostb, Prb-Wein and Guliana soils or to the presence of the shale derived horizon as in case of Murree soil. Since there was minimum translocation of plasma in Shahdara, Pitafi and Peshawar soils, they showed no trend or an irregular trend of iron oxide content in these profiles.

Iron oxide phases differ in their capacity of P sorption. X-ray diffraction and TEM analysis found goethite content in all the soils, the Murree and Peshawar, in addition, these soils contained hematite (less in Peshawar). Quantitative distribution of iron oxides in the soil clays determined by reductive dissolution technique using cyclic voltammetry (and that calculated on soil bases), as well

as the morphology and crystallinity of goethite particles varied among the soils. The total goethite content in Shahdara and Sultanpur soils was the lowest though goethite content in clay fraction was as high as of the Prb-Ostb soil. This was because of the low clay content in the soils. On the other hand, goethite content of Pacca on the soil bases was as high as in Prb-Ostb soil but was low within the clay fraction, which was due to high total clay content. Goethite content did not follow any depth trend in the young alluvial profiles but more goethite was accumulated in the lower part of the weathered profiles.

Goethite of the alluvial soils was well crystallized, multi-domainic with v-shape grooved edges as seen by TEM and the sharp goethite peaks depicted by XRD. Comparatively smaller, less crystalline goethite particles with less developed lattice fringes were found in the Pacca soil but some goethite particles were multi-domainic, sharp edged and well crystalline.

In the Peshawar soil goethite particles were seen as aggregates without any lattice fringes, appearing to be composed of smaller particles; several goethite particles viewed as laths with sharp edges and lattice fringes; and few multidomainic goethites appearing as star-shaped particles. Star-shaped crystals and also some very narrow and long single crystals associated with stars as in case of Peshawar soil were observed. The star-shaped crystals have a core with a higher electron density than that of its arms. The core yields the electron diffraction pattern of hematite (Barron et al., 1997). The hematite traces were also observed along with goethite in this sample by XRD, but the hematite peaks were minor. This might be due to the fact that in randomly oriented powder samples the star core is hidden from the X-ray beam in many of the possible star orientations (Barron et al., 1997).

Hematite was the major iron oxide of the Murree soil as it was developed from shale mixed material. Sharp and relatively intense hematite peaks were observed in XRD patterns even before concentration treatment. There were fewer mobilizations of hematite particles to lower horizons because of limited profile development. Rainfall had only little control over hematite distribution mainly due to topographic position of the soil. High-sloped hillside causes faster erosion than the soil formation. Hematite of Murree soil appears to be lithogenic. The weathering conditions also preclude pedogenesis of hematite. Very poorly crystalline goethite associated with ferrihydrite was also seen in Murree soil samples. Several individual hexagonal plates confirmed occurrence of hematite in the Murree clay fraction although it was missed in the Peshawar clays.

Mean goethite content of the loess derived Guliana soil clay was the same as in Prb-Ostb and Prb-Wein soils. In all the three soils smaller and less crystalline goethite particles were encountered frequently. Few particles were mono-domainic-serrated laths showing well-developed lattice fringes. In situ weathering is causing goethite formation in the profiles reflected by the increase in concentration with the depth as apposed to the alluvial soils. The Parabraunerde being relatively more weathered than all the other soils contained the highest goethite content. Goethite appeared to be pedogenic at least in the more weathered soils. Although goethite exhibit acicular morphology with rough surfaces and apparent structurally controlled terminations, sometimes, arranged in stars and hematite particles hexagonal plates (Schwertmann and Taylor, 1989). In highly weathered soils often a feature of goethite shows subrounded crystal morphology.

Phosphate sorption by goethite is high in thin, ragged, multi-domainic crystals and low in mono-domainic crystals (Torrent et al., 1990). Further on they explained that multi-domainic crystals are binding phosphate stronger due to the v-shaped grooves (determined by the 110 or the 110 and 100 faces between contiguous domains) or due to the slit shaped micropores, which exist between the domains. This structure might have sites to retain P stronger or might have the accessibility of lower amounts of hydroxyl or hydronium ions. Schulze and Schwertmann (1984) also reported strong binding of P favored in crystals of small size, consisting of thin laths with high domainicity (several coherently diffracting domains) and jagged ends. Findings in this study are in line of previous work as shown by energy dispersive X-ray analysis (EDX) of the soil clay fraction pre-treated with P solution.

Phosphorus to Fe ratios varied with goethite particle morphology (Fig. 4.29 to 4.31). Phosphorus to iron ratio between 0.20 and 0.30 was noted to relate to well crystalline, multi-domainic goethite particles with v-shape grooved edges or thick laths as seen in case of alluvial soil clays. The goethite particles of Peshawar soil were observed to contain P:Fe ratio of 0.2. Goethites of alluvial soils were laths with sharp edges and lattice fringes and few multi-domainic particles. P:Fe ratio of 0.09 to 0.15 was observed for the less crystalline mono-domainic-serrated goethite laths of Guliana, Prb-Wein, and Prb-Ostb soil clays. Individual hematite particles were too small to be analytically resolved by TEM. However, the hematite particles sintering as irregular aggregates with diffused edges were analyzed and showed a P:Fe ratio of 0.1. Therefore, as crystallinity increased determined by TEM, the P:Fe ratio also increased. Scanning force and transmission electron microscopic study of synthesis of

goethite on hematite in phosphate media showed that when only small amounts of phosphate were present, goethite crystals were lath-shaped and elongated (Barron et al., 1988) as in case of alluvial soils in this study.

5.3 Phosphorus sorption and its relation with soil matrix components

Phosphorus sorption is governed by proportionate distribution and characteristics of various crystalline phases in soil as adsorbent, beside co-precipitation with soil solution species (e.g., Ca^{2+}). Freundlich or Langmuir equation parameters help to explain sorption processes. Comparative fits of the models, the range of parameters of different soils, and the relation of matrix's mineral components are discussed here.

Freundlich equation fits well to the different data sets irrespective of type of soil. Freundlich k_f parameter seemed to relate with weathering with one exception (Pitafi soil), which will be discussed separately. Freundlich k_f value was high for weathered soils. The lowest k_f value is given in the Shahdara soil of C2 and C3 horizons, which contained the least clay content. Freundlich k_f value is positively correlated with exchangeable calcium content (r^2 0.63, $p < 0.006$, Appendix XII) but is not related to the CaCO_3 content or clay content. Freundlich parameter k_f is related to the sorption affinity as the k coefficient in the Langmuir equation (discussed later). The parameter "b" was significantly higher in Prb-Ostb and Prb-Wein soils than in Murree and Guliana soils. Significantly higher "b" values were observed in the Murree and Guliana soils compared to that for alluvial soils. The Pitafi soil contained the lowest "b" values and the highest k_f parameters differing significantly from that of all the other soils. The b value of Pitafi soil may not be unique partly because the isotherm was not complete within the P application experiment as discussed in the result section 4.4.

Higher Olsen P values given at the surface of the alluvial soils (Appendix I) seem to have affected adsorption parameters reflected by both values Freundlich k_f and b values that were low at the surface layer. However Olsen P value and the adsorption parameters were not statistically correlated (Appendix XII). Overall, the b parameter was positively correlated with the oxalate extractable iron fraction (r^2 0.78, $p < 0.001$), the dithionate extractable iron fraction (r^2 0.70) and crystalline iron oxide fraction (the difference of both fractions) (the; r^2 0.67). It was also positively correlated with the dithionate extractable aluminum fraction (r^2 0.76) and the oxalate extractable aluminum

fraction (r^2 0.77). The negatively correlated properties were pH (r^2 -0.78) and CaCO_3 (r^2 -0.65). Freundlich “b” value is considered to be an indicator for the sorption intensity (Wallace, et al., 2003). The negative relation between pH and b value indicated competition between phosphate and hydroxyl ions as reported by Wang and Tzou (1995). The study also supports the hypothesis that sorption intensity is not necessarily related to the abundance of CaCO_3 but rather to the abundance of reactive forms of aluminum and iron competing with P at the adsorption sites of CaCO_3 . Wang and Tzou (1995) have shown that only 8 to 25% of the calcite surfaces are covered by phosphate anion and that higher coverage is given by the metal oxide particles.

Freundlich b values can be predicted using the soil properties based on stepwise selection. The parameter’s selection was based on maximizing r^2 selected from the determined properties except for soil type which itself is not included as variable. Two equations appeared promising: (1) $Y = 2.584 + 0.018\text{Fe}_d - 0.132\text{pH} - 0.013\text{CaCO}_3$ (r^2 0.80, $p < 0.0001$) and (2) $Y = 2.685 + 0.159 \text{Fe}_{\text{crs}} - 0.012 \text{Kl} - 0.115 \text{pH} - 0.0016 \text{CaCO}_3$ (r^2 0.82, $p < 0.0001$) where Fe_d , value indicates the CBD extractable iron fraction (mg kg^{-1} soil) and CaCO_3 content is given as g kg^{-1} in soil, Fe_{crs} oxide content is given as CBD Fe oxide minus oxalate Fe oxide fraction expressed in g kg^{-1} soil, Kl is kaolinite percentage in clay fraction. Similarly for Freundlich k_f value for the following multiple regression relation yield independent, significant parameter estimates: $Y = -296.53 - 322.48\text{Fe}_{\text{crs}} + 424.12\text{Fe}_d + 1.63\text{CaCO}_3 - 17.85\text{clay} + 513.16\text{Al}_o + 409.16\text{Ca}_{\text{ex}}$ (r^2 0.90, $p < 0.0001$) where Fe_{crs} is the crystalline iron oxide fraction in g kg^{-1} of soil, Fe_d CBD extractable iron fraction in g kg^{-1} of soil, CaCO_3 content in g kg^{-1} of soil, clay percentage in soil, Al_o oxalate extractable aluminum fraction, and Ca_{ex} exchangeable calcium content in g kg^{-1} of soil).

The precision of the predicted values of Freundlich k_f and b improved considerably when the soil types were incorporated as character variable. Each of the soils, for which equation is given, was observed for significantly different intercept (Table 5.1). Strong relationships between b and dithionite extractable iron/soil pH values are noticeable, based on very common tests performed in most laboratories. Similarly, exchangeable Ca and CaCO_3 contents are routinely determined and can be used to predict these sorption parameters. Our data showed that although small in total quantity, Al_{ox} content of calcareous soils plays a very important role in P sorption. Besides, non-crystalline Al oxides, some of aluminum in calcareous soils could be originated from edges of clay mineral (Pena and Torrent, 1984; Jackson et al., 1986; Harrell and Wang, 2006). In addition, the positive relationship of Freundlich

parameter with Fe_d in our study also corroborated with the results by Beaucheman et al. (2003).

Table 5.1: Stepwise multiple regression equations between soil properties and Freundlich parameters.

Type	Soil	Equation	Fit
k_f	All soils*	$Y = -326.24 - 18.62\text{clay} + 184.98Ca_{ex} + 489.85Al_o + 0.49Al_o/Al_d$	
	Shahdara	$Y = 231.50 - 18.62\text{clay} + 184.98Ca_{ex} + 489.85Al_o + 0.49Al_o/Al_d$	$p < 0.001$
	Pitafi	$Y = 149.96 - 18.62\text{clay} + 184.98Ca_{ex} + 489.85Al_o + 0.49Al_o/Al_d$	$r^2 0.96$
	Murree	$Y = -588.57 - 18.62\text{clay} + 184.98Ca_{ex} + 489.85Al_o + 0.49Al_o/Al_d$	
	Prb-Wein	$Y = -84.89 - 18.62\text{clay} + 184.98Ca_{ex} + 489.85Al_o + 0.49Al_o/Al_d$	
b	All soils*	$Y = 2.523 + 0.025Fe_d - 0.166pH - 0.001CaCO_3 + 0.076Ca_{ex}$	
	Shahdara	$Y = 2.672 + 0.025Fe_d - 0.166pH - 0.001CaCO_3 + 0.076Ca_{ex}$	$r^2 0.95$
	Pitafi	$Y = 2.162 + 0.025Fe_d - 0.166pH - 0.001CaCO_3 + 0.076Ca_{ex}$	$p < 0.001$
	Prb-Wein	$Y = 2.674 + 0.025Fe_d - 0.166pH - 0.001CaCO_3 + 0.076Ca_{ex}$	

*All the soils other than listed.

Ca_{ex} , exchangeable calcium ($g\ kg^{-1}$); Fe_d , CBD extractable iron ($g\ kg^{-1}\ soil$); Al_d , CBD extractable aluminum; ($g\ kg^{-1}\ soil$); Al_o , oxalate extractable aluminum ($g\ kg^{-1}\ soil$); OM , organic matter ($g\ kg^{-1}$)

Langmuir parameters are also relating to the soil properties and predictive equations have been developed for different soils except for Pitafi soil. The b_1 value showing maximum P sorption capacity at high-affinity sites (inverse of the slope of the first segment) was high in the more weathered soils compared to the less weathered soils. The correlation of parameter b_1 with Fe_d showed significant ($p < 0.001$) correlations ($r^2 0.53$), with crystalline iron oxide ($r^2 0.53$), with Al_d ($r^2 0.55$) and with Al_o ($r^2 0.56$). Maximum sorption on low-affinity sites also differed with the soil type significantly ($p < 0.05$) and was less strongly and negatively correlated with Fe_d , values, crystalline iron content, Al_d , and Al_o values (r^2 below 0.50) and there was no significant relation with $CaCO_3$ or clay content. The major part of soil P sorption capacity was due to the low-affinity sites (b_2) e.g. 1200 to 6000 $mg\ kg^{-1}$ compared to 120 and 280 $mg\ kg^{-1}$ of high-affinity sites. Sui and Thompson (2000) reported a ratio of 1:3 for $b_1:b_2$ in the case of biosolids. The ratio of $b_1:b_2$ showed positive correlation with Al_d ($r^2 0.71$), Al_o ($r^2 0.65$) and Fe_d ($r^2 0.58$) fractions. This means, an increase in these oxides is favoring maximum sorption on high-affinity sites compared to that of low-affinity sites.

Binding strength of high-affinity sites for P (k_1) was 0.75 to 48 $L\ mg^{-1}$ compared to binding strength of low-affinity (k_2) of 0.01 to 0.467 $L\ mg^{-1}$. The parameter k_1 showed strong correlation with ammonium oxalate extractable

iron fraction, Fe_o (r^2 0.93) and aluminum, Al_o (r^2 0.79) and CBD extractable iron, Fe_d (r^2 0.51) and aluminum, Al_d (r^2 0.73) fraction. It also showed significant but negative correlation with $CaCO_3$ content (r^2 0.41) and pH value (r^2 0.87). The parameter k_2 showed significant positive correlation with Al_o (r^2 0.55) and Al_d (r^2 0.56) fractions, and also significant and positive correlation with Fe_d (r^2 0.59) and Fe_o (r^2 0.53) fractions beside a positive correlation with crystalline iron oxide contents in soils (r^2 0.57). The parameter k_2 also showed negative correlation with pH values (r^2 0.53) but the correlation with $CaCO_3$ content was non-significant.

Mean binding strength related to high-affinity (k_1) sites was higher in the weathered soils than in all other soils. Binding strength related to the low-affinity (k_2) sites was the highest in Prb-Ostb and the Prb-Wein soils, both showed values which were very similar to that of Pakistan soils. Lower binding strength means greater intercept of the second segment on y-axes and low sorption capacity. The highest values of k_1 (38 to 48 L mg⁻¹) were given for Prb-Ostb soil data (higher in Bv horizon) and for Prb-Wein soil data (higher in Bt horizon). The maximum P sorption capacity (b_1) at high P sorption sites was low and required high binding affinity. On the other hand, the maximum sorption capacity at low affinity sites required negligible binding affinity (k_2). This suggests that less binding affinity was required where maximum sorption is taking place.

Multiple regression analysis was carried out using stepwise procedure adopted for selection of parameters maximizing r square to predict Langmuir parameters b_1 , b_2 , k_1 and k_2 from the basic soil properties. Independent of soil type, the following regression was selected as best model (r^2 0.67), $p < 0.0001$) to predict Langmuir parameter b_1 : $Y = 231.6 - 72.0Fe_o + 39.82Fe_d = 5.9clay - 53.82Ca_{ex} - 3.95Gt_s$. The properties were defined earlier. The parameter b_2 could not be predicted from the given properties. This could be due to the fact that the original P adsorption isotherm had achieved the plateau in many samples and that maximum sorption on low affinity site could have been satisfied. Adding P ions at greater rate can help to predict maximum sorption. Binding strength for P ions due to high-affinity sites can be predicted independently of soil type using the following regression equation: $Y = 73.15 + 10.384Fe_o - 7.150pH - 0.040CaCO_3 - 0.735k_1 + 0.217Gt_s$ (r^2 0.94, $p < 0.001$) where Fe_o is the oxalate extractable iron fraction (g kg⁻¹ soil), soil $CaCO_3$ content (g kg⁻¹), Kl the kaolinite percentage in clay, and Gt_s the goethite content in soil (g kg⁻¹). Binding strength low-affinity sites for P can also be predicted independent of soil using the following regression equation:

$Y = -0.686 + 0.461Al_o + 0.048pH + 0.0005CaCO_3 + 0.011Sm - 0.006clay$ (r^2 0.81, $p < 0.001$) with definition of the parameters given above. The parameter estimate in all the cases showed probabilities of $p > F < 0.0001$. The regression analyses indicated that Fe_o , Fe_{crs} , Al_d , kaolinite, $CaCO_3$, Ca_{ex} and pH in various combinations were the dominant properties explaining 75 to 95% of the variation.

Multiple regression analysis using stepwise procedure based on the soil properties including soil type as a predictive parameter is given for some of the Langmuir parameters (Table 5.2). The values of these equations are given to understand sorption rather than the prediction of the effect of the included parameters. The Fe_o value seemed to reflect the dominant oxide followed by Fe_{crs} and Al_o values. The parameter estimates for Fe_o , kaolinite and $CaCO_3$ showed negative signs indicating the reducing effect on b_1 value. The Al_d and the organic matter content showed positive sign with parameter estimates indicating their enhancing effect on b_1 parameter. In case of k_1 the parameters Fe_o , Al_d , $CaCO_3$ and Ca_{ox} were positive and kaolinite and pH were negative. In case of k_2 , Fe_o , kaolinite and pH were negative and Fe_{crs} was positive. It may be recalled that the CBD iron fraction was observed to be an indicator of increased and crystalline iron and decreasing values are showing good relations with a decrease in weathering. Previous studies of P sorption capacity and, consequently, of soluble P concentration are depending on many soil properties such as clay content (Olsen and Watanabe, 1963; Yost et al., 1992; Said and Dakermanji, 1993; Zhang et al., 1993; Cox, 1994; Castro and Torrent, 1994; Tomar et al., 1995), $CaCO_3$ content (Tiessen et al., 1984) and extractable iron content (Sharpley et al., 1989). Phosphorus sorption studies of calcareous systems (Said and Dakermanji, 1993; Hassan et al., 1993; Adhami et al., 2006, and 2007) are relevant here in this study.

Phosphorus adsorption maxima (given by Langmuir and Freundlich equation) was found to be positively correlated with the clay content (Zhang et al., 1993; Harrell and Wang, 2006) especially with the clay fraction of $< 0.01\mu m$ size (Moughli et al., 1991). It should be noted that amorphous iron and aluminum oxides are also occurring in this size fraction.

This study conformed recent findings that not only the clay content but also the clay mineral composition is controlling P sorption. Kaolinite was selected as significant contributor to sorption determined by Langmuir k coefficient (Table 5.2). At low P content, kaolinite dominant soils are sorbing highest amounts of P ions followed by illite dominant soils and 2:1 expanding layered

mineral dominated soils. But the sequence of P adsorption rate may change with P rates (Tomar et al., 1995). Phosphorus adsorption on argillaceous material is characterized by an electrostatic adsorption on low affinity sites, which are abundant in 2:1 layered silicates. Yet, it is to be recognized that clay minerals are sorbing less P than metal oxides.

Table 5.2: Stepwise multiple regression equations between soil properties and the Langmuir parameters.

Type	Soil	Equation	Fit
b ₁	All soils*	$Y = 160.46 + 95.89Fe_d - 77.00Al_o + 2.41Gt_s + 1.95OM$	p<0.0001 r ² 0.75
	Pacca	$Y = 248.40 + 95.89Fe_d - 77.00Al_o + 2.41Gt_s + 1.95OM$	
	Peshawar	$Y = 236.8 + 95.89Fe_d - 77.00Al_o + 2.41Gt_s + 1.95OM$	
k ₁	All soils*	$Y = 45.67 + 20.19Fe_o - 7.27 pH - 0.60Kl + 0.06CaCO_3 + 4.27Ca_{ex}$	p<0.0001 r ² 0.95
	Peshawar	$Y = 32.36 + 20.19Fe_o - 7.27 pH - 0.60Kl + 0.06CaCO_3 + 4.27Ca_{ex}$	
	Murree	$Y = 40.25 + 20.19Fe_o - 7.27 pH - 0.60Kl + 0.06CaCO_3 + 4.27Ca_{ex}$	
	Prb-Wein	$Y = 51.75 + 20.19Fe_o - 7.27 pH - 0.60Kl + 0.06CaCO_3 + 4.27Ca_{ex}$	
k ₂	All soils*	$Y = 1.50 - 1.05Fe_o + 0.13Fe_{crs} - 0.04Kl - 0.09pH$	p<0.0001 r ² 0.91
	Pitafi	$Y = 1.60 - 1.05Fe_o + 0.13Fe_{crs} - 0.04Kl - 0.09pH$	
	Guliana	$Y = 2.02 - 1.05Fe_o + 0.13Fe_{crs} - 0.04Kl - 0.09pH$	
	Murree	$Y = 1.63 - 1.05Fe_o + 0.13Fe_{crs} - 0.04Kl - 0.09pH$	
	Prb-Wein	$Y = 1.25 - 1.05Fe_o + 0.13Fe_{crs} - 0.04Kl - 0.09pH$	

**All the soils other than listed.

Fe_d, CBD extractable iron (g kg⁻¹ soil); **Fe_o**, oxalate extractable iron (g kg⁻¹ soil); **Al_o**, oxalate extractable aluminum (g kg⁻¹ soil); (**Gt_s**, soil goethite (g kg⁻¹); **OM**, organic matter (g kg⁻¹), **Ca_{ex}**, exchangeable calcium (g kg⁻¹); **Fe_{crs}**, crystalline (Fe_d - Fe_o) (g kg⁻¹ soil)

Iron oxides influence P sorption by far more than any other soil constituent (Tomar et al., 1995), except exchangeable Al. Many studies reported increased P sorption rate with increasing extractable iron oxide values (Zhang et al., 1993; Moughli et al., 1991). Phosphorus adsorption maxima were found to be positively correlated with extractable iron oxide fractions (Zhang et al., 1993; Zhou and Li, 2001). Bruland and Richardson (2004) used soils with similar vegetation and hydrology and found out that the soils contain substantially different mean P sorption capacities due to differences in clay and amorphous iron oxide fractions. Olsen P fraction decreases sharply with the increase in the ratio of clay (or iron oxides) to total (or active) calcium carbonate content equivalent (Moughli et al., 1991). Although clay minerals (argillaceous) are sorbing less P ions than oxides (Frossard et al., 1995), the recovery of applied P ions from soils containing more clay has been reported to be lower than 100%.

Iron oxides vary in their P adsorption capacity - hematite adsorbs $34 \mu\text{mole g}^{-1}$ and goethite $80 \mu\text{mole g}^{-1}$ (Schwertmann and Taylor, 1989) - therefore, the total quantity of iron oxide in soil and the oxide phase determine the P sorption capacity (Frossard et al., 1995). The higher sorption rate of P on goethite ($\alpha\text{-FeOOH}$) than on hematite ($\alpha\text{-Fe}_2\text{O}_3$) surfaces can be explained by a greater accessibility to phosphate of singly coordinated OH surface groups on {110} plans (Torrent et al., 1990). Due to lower accessibility of sorption site on hematite (Parfitt et al., 1975; Torrent et al., 1990; Colombo et al., 1991), the soils with large amounts of hematite (rich red colored soil) are sorbing less P ions than soils rich in goethite (Colombo et al., 1991). Hence, one or a combination of these properties is influencing P sorption characteristics (Zhang et al., 2005).

5.4 Soil phosphorus fractions

Phosphorus fractionation has been widely used to interpret native inorganic P status and the fate of the applied P in soils (Adhami et al., 2007). Generally, variability in soil P-forms can be explained in terms of type of parent material and weathering. Apatite is derived from parent material; therefore, a difference in lithology creates inherent levels of apatite P in soil. Then, surface weathering creates a specific distribution trend within that level of apatite P. Pedo-functions explaining distribution of various P forms are discussed here.

In these soil studies apatite is forming the major portion of the total P fraction and of the total sum of inorganic fractions. Apatite P fraction being the dominant P fraction was also supported by other studies (Harrell and Wang, 2006). Using same fractionation scheme Shen et al. (2004) reported that 90% of the total P fraction is occurring as apatite P fraction in long-term fertilized rice monoculture system on calcareous soils. Wang and Tzou (1995) and Carreira et al. (2006) found out that the Ca bound P fraction could also be the dominant P fraction in calcareous soils.

The content of total P, inorganic P, and apatite P fractions in the alluvial soils including Peshawar soil was similar and significantly higher than the loess derived Guliana soil and the shale derived Murree soil. It was also apparent that total P, inorganic P, and apatite P fractions were also high in the Prb-Ostb and Prb-Wein soils and that weathering is resulting in loss of apatite at the surface layer. The alluvial soils P content increased towards surface layer indicating addition of fresh mineral matter. In the semi-arid tropics where organic matter production is limited due to climate conditions, the organic

forms of P comprise smaller portion of total P (Agbenin and Tiessen, 1995; Buresh et al., 1997). The results are similar to those reported by Udo and Ogunwale (1977), and Solomon and Lehmann (2000) reported for Alfisols in the savannah zone of Nigeria and for semi-arid soil from North Tanzania respectively.

Using stepwise regression procedure the total P, inorganic P, and apatite P forms were related to some of the soil properties. The variable selection was based on maximizing the “ r^2 ” value and soil type was included as character variable. When the soil type was significant, it generated different intercept for one soil or for a group of soils. The regression analyses indicated that CBD, crystalline iron oxide (Fe_d - Fe_o), kaolinite, and pH values in various combinations were the dominant properties explaining 85 to 92% of the variation (Table 5.3). The parameter estimate in all these cases showed probabilities of $p > F < 0.02$. The CBD and crystalline iron oxide fraction appeared to be the proxy indicators for the rate of weathering. The parameter estimates for CBD and kaolinite fractions showed negative signs indicating their reducing effect. The crystalline iron oxides and pH values showed positive signs with parameter estimates indicating their enhancing effect on total P, total inorganic, or apatite P fraction. It may be recalled that Fe_d values were observed to indicate increasing fractions of iron and of their crystallinity, which was decreasing during weathering. The predicted parameters (total P, total inorganic P and apatite P) are decreasing with weathering rate as mentioned above. For all three independent parameters (total P, total inorganic P and apatite P) the intercept differed significantly in the order of: Peshawar > (Shahdara, Sultanpur, Pacca, Pitafi, Murree, Guliana, Prb-Ostb) > Prb-Wein (Table 5.3).

The organic P was a small fraction and it did not differ statistically among the soils investigated however the content increased toward the surface layer in most soils, which may be due to the accumulation of organic matter at the surface layer. All the basic soil properties including the iron oxide fraction and the mineral composition, when regressed/selected stepwise explained not more than 54% of the variation in the organic P pool. However, exchangeable Ca and soil $CaCO_3$ showed negative signs on the parameter estimate and soil organic matter showed greater parameter estimates with positive sign. Since the intercept was non-significant, the model was dropped and it was assumed that yet some other properties, not determined, could be responsible for the variation of the organic pool.

Table 5.3: Stepwise multiple regression equations between soil properties and total P, total inorganic P and apatite P.

P fraction	Soil	Equation	Fit
Total P	All soils*	$Y = 8.77 - 45.81LFe_d + 47.71LFe_{crs} - 2.00LKl$	$p < 0.001$ $r^2 = 0.86$
	Peshawar	$Y = 8.97 - 45.81LFe_d + 47.71LFe_{crs} - 2.00LKl$	
	Prb-Wein	$Y = 7.84 - 45.81LFe_d + 47.71LFe_{crs} - 2.00LKl$	
Total P _{in}	All soils*	$Y = 5.86 - 1.67LKl + 2.12LpH$	$p < 0.001$ $r^2 = 0.87$
	Peshawar	$Y = 6.24 - 1.67LKl + 2.12LpH$	
	Prb-Wein	$Y = 4.66 - 1.67LKl + 2.12LpH$	
Apatite P	All soils*	$Y = -16.50 - 1.71LKl + 9.66LpH$	$p < 0.001$ $r^2 = 0.91$
	Peshawar	$Y = -16.92 - 1.71LKl + 9.66LpH$	
	Prb-Wein	$Y = -17.37 - 1.71LKl + 9.66LpH$	

*All the soils other than listed.

Fe_d , CBD extractable iron ($g\ kg^{-1}$ soil); Fe_o , oxalate extractable iron ($g\ kg^{-1}$ soil); Fe_{crs} , crystalline ($Fe_d - Fe_o$) ($g\ kg^{-1}$ soil), Kl , kaolinite (% clay);

L is the transformation of the data

$$LCBD = (((CBD+11)^{0.00015}-1)/0.00015)$$

Phosphorus content desorbed from iron oxides in the alluvial soils was lower compared to that in the highly weathered Prb-Ostb soil or even Guliana and Murree soil. On the other hand, the P fraction released by decomposition of iron oxides even in alluvial soils was comparable to that of Murree and Guliana soil although less than that of in the Prb-Ostb. This observation may imply that NaOH-Na₂CO₃ solutions were not effective in displacing P from the well crystalline goethite particles found in the alluvial soil. Goethite particles in the alluvial soils are shown to be multi-domainic with v-shape grooved edges, which may have protected P ions to be released during NaOH-Na₂CO₃ treatment and the trapped P ions were released only by stronger CBD-treatment, which is dissolving goethite particles completely. Phosphorus desorbed by iron oxides particles contributed to 0.13 to 46% of the total inorganic P (higher contribution in highly weathered Prb-Ostb soil). Samadi and Gilkes (1998) showed that in the fractionation study of fertilized calcareous soils similar contents of occluded P have been detected compared to that of young alluvial and Peshawar soils in this study.

Phosphorus desorbed from iron oxides is correlating positively with various fractions of iron and organic matter. Exchangeable Ca and CaCO₃ contents are negatively correlated with this P fraction as indicated by parameter estimates selected stepwise from soil properties regressing Fe-P fractions and from occluded P fraction (Table 5.4). The selected soil properties jointly explain the

92% of the variation of the P fraction desorbed from iron oxides and 79% of the variation of the fraction released by iron decomposition. Since the Prb-Wein soil was observed to reflect lowest mean values of occluded P, it showed more negative intercept. Each of the parameter estimates showed significance of $p < 0.002$. It is obvious that the crystalline iron oxide fraction determined by the difference of CBD and oxalate extractable iron or directly by voltammetry of the clay portion is a positive determinant of iron related P fraction. Soil carbonate contents, as an indirect proxy parameter for the rate of weathering, showed a reducing effect on P ion release, but the rate was not a significant factor of the occluded P fraction.

Often contradicting evidences are given in the literature whether Fe or Ca is the predominant cation associated with soluble P in calcareous soils. Results of this study suggest that P retention is likely governed by iron oxides through the formation of Fe-P minerals even in calcareous soils. Phosphorus bound minerals iron oxides could be released to replenish the depleted P (Saavedra and Delgado, 2005). Goethite, smectite kaolinite and oxalate extractable Al can jointly explain 0.79% of the variability of the occluded P fraction (P trapped in iron oxide coatings) with a significance of $p < 0.001$. Kaolinite parameter estimate carried negative signs. The intercept of the data of Prb-Wein, Peshawar, and of all other soils differed significantly when soil type was used additionally as character variable (Table 5.4).

The $\text{Ca}_2\text{-P}$ fraction extracted by NaOH-NaHCO_3 was higher at the surface in alluvial soils, the shale derived Murree and the Peshawar and the loess derived Guliana soil. $\text{Ca}_8\text{-P}$ fraction extracted by $\text{NH}_4\text{-acetate}$ was higher only in alluvial soils including the Peshawar soil as compared to all other soils. This might be related to land use. Due to availability of irrigation, intensive agriculture is practiced with extensive fertilizer use. The soils of Prb-Ostb and Prb-Wein that were under permanent forest, showed an increase in Ca bound P with depth. The Guliana Btc2 soil horizon was exceptionally high in $\text{Ca}_2\text{-P}$ (70 mg kg^{-1} soil), which may suggest leaching of P through the moderate medium prismatic soil structural peds and later on accumulation at lower depth.

The $\text{Ca}_2\text{-P}$ and $\text{Ca}_8\text{-P}$ are the intermediate fractions formed during precipitation before the apatite compounds can be formed (Jiang and Gu, 1989). The $\text{Ca}_2\text{-P}$ fraction is water soluble P and partially adsorbed P, and can be readily taken up by plants, (Shen et al., 2004). A positive relationship between Olsen P and $\text{Ca}_2\text{-P}$ fractions has been reported because the forms are determined by NaHCO_3 (Zhang et al., 2004). Instead, this study indicated a non-significant

Pearson correlation coefficient for the two parameters. Contrary, Ca₈-P and Olsen P fractions showed a significant correlation factor of r² of 0.61. No relationship between Ca₂-P and Ca₈-P with CaCO₃ fraction could be found indicating that formation of Ca₂-P and Ca₈-P may not be related to the abundance of CaCO₃ in soil. Octa-calcium phosphate is a product of the gradual transformation of Ca₂-P when P fertilizer is applied to soils (Syers and Curtin, 1988). It is sparingly soluble and only partly used by plants. The hydroxyapatite (Ca₁₀-P) is the least soluble soil inorganic P fraction, which transforms very slowly.

Table 5.4: Stepwise multiple regression equations between soil properties and Fe-P and occluded P fractions.

P fraction	Soil	Equation	Fit
Fe-P	All soils*	LY= -25.62 + 10.42LFe _{crs} - 0.45LCa _{ex} + 3.98LOM - 1.31LCaCO ₃	p<0.001 r ² 0.92
	Prb-Wein	LY= -26.15 + 10.42LFe _{crs} - 0.45LCa _{ex} + 3.98LOM - 1.31LCaCO ₃	
Occluded P	All soils*	LY= -5.96 + 1.28LSm - 1.35LKI + 3.80LGt _s +0.24LAl _o	p<0.001 r ² 0.79
	Peshawar	LY= -5.25 + 1.28LSm - 1.35LKI + 3.80LGt _s +0.24LAl _o	
	Prb-Wein	LY= -6.77+ 1.28LSm - 1.35LKI + 3.80LGt _s +0.24LAl _o	

*, All the other soils except the two listed;

Fe_{crs}, crystalline (Fe_d - Fe_o) (g kg⁻¹) **Fe_d**, CBD extractable iron (g kg⁻¹ soil); **Fe_o**, oxalate extractable iron (g kg⁻¹ soil); **Al_o**, oxalate extractable aluminum; **Gt_s**, soil goethite (g kg⁻¹); **Sm**, smectite (% clay); **KI**, kaolinite (% clay); **OM**, organic matter (g kg⁻¹), **Ca_{ex}**, exchangeable calcium (g kg⁻¹); ,

L is the transformation of the data = (((X+11)^{0.00015})-1)/0.00015

Octa-calcium phosphate and Olsen P fractions showed significant (r² 0.68, p < 0.001) correlation but at the same time Olsen P and Ca₂-P correlation was non-significant. Contrary, Samadi and Gilkes (1999) reported significant correlation coefficients (r²) of Olsen P and Ca₂-P fractions (0.63 p < 0.05) and non-significant relation of Olsen P and Ca₈-P fraction. In this study the content of Olsen P fraction was higher than that of both other fractions Ca₂-P and Ca₈-P. The relationship between Olsen P and Ca₂-P fraction is expected as both forms of P are determined by NaHCO₃ extraction then it is an analytical artifact. The concentration of NaHCO₃ in Olsen P determination was 0.5M and pH was 8.5 whereas for Ca₂-P fraction NaHCO₃ content was 0.25M and pH was 7.5. The explanation lies in the fact that the solubility of Ca₂-P increases with increasing concentration of NaHCO₃ when of the extracting medium is pH 8.5 (Baifan and Yichu, 1989). The Ca₂-P and Ca₈-P were the main source of available soil P, as Ca₈-P fraction could be transformed to Ca₂-P under P

depletion being consistent with the literature (Jiang and Gu, 1989; Liu et al., 1999; Sharpley, 2000). Phosphorus recovering in Ca₂-P fraction does exist as discrete dicalcium phosphate crystals (Samadi and Gilkes 1998). As generally believed, CaCO₃ content remained a non-significant factor even in control of Ca related P fractions. This is due to either the effect of solid phase CaCO₃ being masked by dominant effect-of iron oxides or by P ions recovered of the Ca₂-P/Ca₈-P fractions existing as discrete phases.

Table 5.5: Stepwise multiple regression equations between soil properties and Ca₂-P and Ca₈-P fractions.

P fraction	Soil	Equation	Fit
Ca ₂ -P	All soils*	$Y = 198 - 232Fe_o + 1.78Sm - 7.83Kl - 8.17pH - 3.58OM$	p<0.0003 r ² 0.81
	Peshawar	$Y = 213 - 232Fe_o + 1.78Sm - 7.83Kl - 8.17pH - 3.58OM$	
	Guliana	$Y = 296 - 232Fe_o + 1.78Sm - 7.83Kl - 8.17pH - 3.58OM$	
	Murree	$Y = 264 - 232Fe_o + 1.78Sm - 7.83Kl - 8.17pH - 3.58OM$	
Ca ₈ -P	All soils*	$Y = 4.88 - 21.86Fe_o + 1.83Fe_{crs} - 2.81Gt_s + 0.18clay + 3.41OM$	p<0.0002 r ² 0.73
	Peshawar	$Y = 1.99 - 21.86Fe_o + 1.83Fe_{crs} - 2.81Gt_s + 0.18clay + 3.41OM$	
	Guliana	$Y = 2.67 - 21.86Fe_o + 1.83Fe_{crs} - 2.81Gt_s + 0.18clay + 3.41OM$	
	Murree	$Y = -5.02 - 21.86Fe_o + 1.83Fe_{crs} - 2.81Gt_s + 0.18clay + 3.41OM$	

*, All the other soils except the two listed;

Fe_{crs}, crystalline (Fe_d - Fe_o) (g kg⁻¹) **Fe_d**, CBD extractable iron (g kg⁻¹ soil); **Fe_o**, oxalate extractable iron (g kg⁻¹ soil); **Gt_s**, soil goethite (g kg⁻¹); **Sm**, smectite (% clay); **Kl**, kaolinite (% clay); **OM**, organic matter (g kg⁻¹),

L is the transformation of the data e.g. $LCBD = (((CBD+11)^{0.00015}-1)/0.00015)$

Phosphorus associated to soil iron oxides (adsorbed or occluded) was a dominant fraction compared to P bound to di- and octa-calcium phosphate. Oxalate extractable iron showed negative signs of the parameter estimates in the regression of the prediction of the P fraction bound to calcium (expressed as Ca₂-P or Ca₈-P). Similarly, soil goethite and kaolinite parameters showed negative signs during regression analyses while kaolinite, pH and organic matter fractions showing positive signs (Table 5.5). The best selected models were highly significant with coefficients of r² 0.81 in case of Ca₂-P and 0.73 in case of Ca₈-P. Although the ratio of oxalate extractable iron to CBD extractable iron in soil is low, small quantities of amorphous iron oxide with a large surface area may have a great effect on initial P retention (Ryan et al., 1985; Samadi and Gilkes, 1999). Iron and Al oxides and the edge surfaces of kaolinite crystals provided adsorption sites of higher affinity than the surfaces of calcite (Penna and Torrent, 1990; Afif et al., 1993; Samadi and Gilkes, 1999).

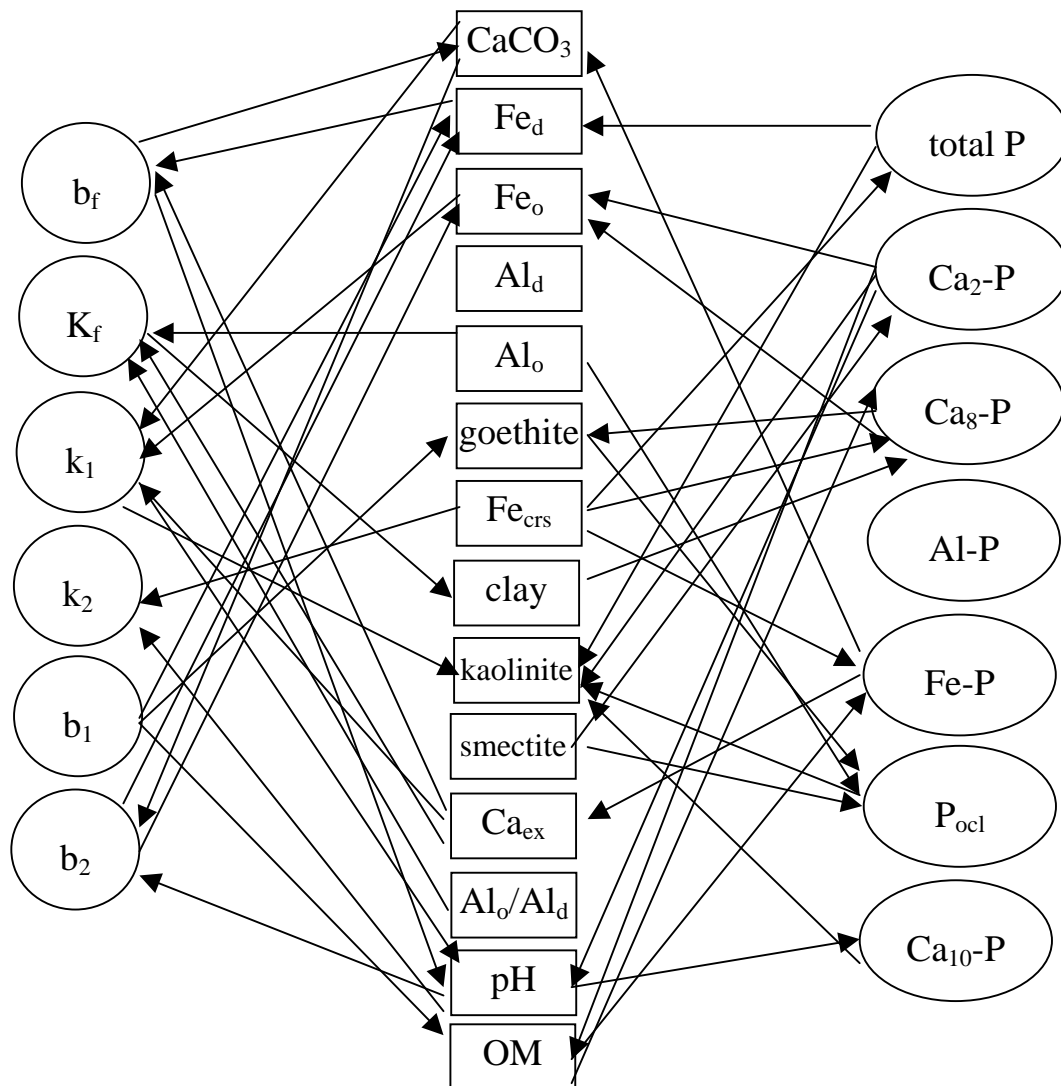


Figure 5.1: Schematic diagram depicting relationship between P sorption parameters and P fractions with soil properties: The inward arrows on both sides indicate negative relationship and the outward arrows on both sides indicate positive relationship.

It is apparent that P retention in soils is a consequence of cumulative effects of several soil properties (Fig. 5.1). Finally, the release of P ions to soil solution or to extracting solution (Olsen P) is governed by several factors (Table 5.6): As an indicator of P saturation, $\text{Ca}_8\text{-P}$ fraction can explain only 45% of the variability of Olsen P fraction, $\text{Ca}_8\text{-P}$ with P fraction occluded in iron oxides can explained 57%, and with addition of organic matter the model explained 70% of the variation. Occluded P in addition with $\text{Ca}_2\text{-P}$, $\text{Ca}_8\text{-P}$, and organic matter explained 76%, with addition of vermiculite explained 78%. The

occluded P together with Ca₂-P, Ca₈-P, organic matter, vermiculite and organic P explained 80% of the variation. In the same combination when organic P was replaced with total P the variation improved to only 81%. In the same combination when Ca₈-P replaced with clay variation improved to 82%. Adding smectite to this combination variation improved to 83% but smectite showed negative effect on Olsen P, clay replaced by soil goethite improved to 84% with negative smectite effect, adding kaolinite improved explained variation to 86%. Historically negative relationship between plant available P and soil CaCO₃ has been reported (Afif et al., 1993). Our results imply that CBD extractable and oxalate extractable iron play an important role in governing the plant available P. The results corroborate well with recent studies done in calcareous soils by Harrell and Wang (2006).

Table 5.6: Stepwise multiple regression equations between Olsen P and soil properties.

Soil	Selected model	r ²
All soils	$-5.34+2.15Ca_8P$	0.45
All soils	$-6.83+1.80Ca_8P+0.05P_{oc1}$	0.57
All soils	$-6.53+1.08Ca_8P +3.26OM +0.06P_{oc1}$	0.62
All soils	$-2.41+0.05P_{oc1} +8.15OM$	0.67
Murree	$-11.82+0.05P_{oc1} +8.15OM$	
All soils	$-3.37+0.05P_{oc1} +8.57OM$	0.70
Murree	$-12.68+0.05P_{oc1} +8.57OM$	
Pitafi	$0.15+0.05P_{oc1} +8.57OM$	
All soils	$-4.57+0.10Ca_2P +9.02OM +0.05P_{oc1}$	0.73
Murree	$-14.25+0.10Ca_2P +9.02OM +0.05P_{oc1}$	
Pitafi	$-0.82+0.10Ca_2P +9.02OM +0.05P_{oc1}$	
All soils	$-7.35+0.79Ca_2P +0.11Ca_8P +0.04P_{oc1} + 6.883OM$	0.76
Murree	$-15.07+0.79Ca_2P +0.11Ca_8P +0.04P_{oc1} + 6.883OM$	
Pitafi	$-3.30+0.79Ca_2P +0.11Ca_8P +0.04P_{oc1} + 6.883OM$	
All soils	$-9.31+0.90Ca_8P+0.09Ca_2P +0.04P_{oc1} +0.22Vm +6.41OM$	0.78
Murree	$-15.81+0.90Ca_8P+0.09Ca_2P +0.04P_{oc1} +0.22Vm +6.41OM$	
Pitafi	$-4.92+0.90Ca_8P+0.09Ca_2P +0.04P_{oc1} +0.22Vm +6.41OM$	
All soils	$-11.25+0.03P_O+1.04Ca_8P +0.04P_{oc1} +0.25Vm +0.10Ca_2P +5.60OM$	0.80
Murree	$-17.74+0.03P_O +1.04Ca_8P +0.04P_{oc1} +0.25Vm +0.10Ca_2P +5.60OM$	
Pitafi	$-6.35+0.03P_O+1.04Ca_8P +0.04P_{oc1} +0.25Vm +0.10Ca_2P +5.60OM$	
All soils	$-14.29+0.01P_T+0.04P_O +0.71Ca_8P +0.10Ca_2P +0.37Vm +6.13OM$	0.81
Murree	$-22.16+0.01P_T+0.04P_O +0.71Ca_8P +0.10Ca_2P +0.37Vm +6.13OM$	
Pitafi	$-9.66+0.01P_T +0.04P_O +0.71Ca_8P +0.10Ca_2P +0.37Vm +6.13OM$	
All soils	$-14.63+0.01P_T +0.04P_O +0.10Ca_2P +0.30Vm +0.10clay +7.69OM$	0.82
Murree	$-23.78+0.01P_T +0.04P_O +0.10Ca_2P +0.30Vm +0.10clay +7.69OM$	
Pitafi	$-10.28+0.01P_T +0.04P_O +0.10Ca_2P +0.30Vm +0.10clay +7.69OM$	
All soils	$-8.16+0.01P_T +0.05P_O +0.12Ca_2P+0.35Vm-0.47Sm +0.09clay+7.48OM$	0.83
Murree	$-18.22+0.01P_T +0.05P_O +0.12Ca_2P+0.35Vm-0.47Sm +0.09clay+7.48OM$	
Pitafi	$-2.75+0.01P_T +0.05P_O +0.12Ca_2P+0.35Vm-0.47Sm +0.09clay+7.48OM$	
All soils	$-7.39+0.01P_T +0.05P_O +0.18Ca_2P+0.34Vm -0.52Sm +1.48Gt_{s+}+7.52OM$	0.84
Murree	$-15.30+0.01P_T +0.05P_O +0.18Ca_2P+0.34Vm-0.52Sm +1.48Gt_{s+}+7.52OM$	
Pitafi	$-1.95+0.01P_T +0.05P_O +0.18Ca_2P+0.34Vm -0.52Sm +1.48Gt_{s+}+7.52OM$	
All soils	$-12.67+0.02P_T +0.05P_O +0.19Ca_2P+0.34Vm-0.67Sm+0.28Kl +1.76Gt_s +7.33OM$	0.86
Murree	$-21.30+0.02P_T +0.05P_O +0.19Ca_2P+0.34Vm-0.67Sm+0.28Kl +1.76Gt_s +7.33OM$	
Pitafi	$-6.34+0.02P_T +0.05P_O +0.19Ca_2P+0.34Vm-0.67Sm+0.28Kl + 1.76Gt_s +7.33OM$	

6. Summary

Soil P deficiency is widespread in agricultural soils and limits crop production. Therefore, fertilizer application is necessary in many agro-ecological systems but at the same time P enrichment by manure and inorganic applications causes eutrophication of freshwater bodies under pluvial conditions. High P retention in soils which is believed to be due to strong binding to metal oxide surfaces in acidic soils and due to precipitation of P species and surface sorption on CaCO_3 particles in neutral to basic soils, causes low fertilizer P efficiency and, hence, economic loss. More recent work has highlighted the role of iron oxides in regard to P availability in even calcareous soils. Further work is needed to illustrate P retention processes in different lithologies and under pedological conditions to provide a good basis for agronomic recommendations and environmentally best management practices. This study hypothesizes that prediction of P sorption in calcareous soils can be improved by incorporating concentration and quantity of iron oxide phases in predictive scheme. The objectives of the study were to identify soil iron oxides and other clay minerals and to investigate the role of clay particles, especially iron oxides in regard to P sorption.

To test the hypothesis, soil samples were collected from the upper four horizons of different soils covering a range of various lithological and pedological conditions: five calcareous alluvial soils developed from Subrecent sediments in arid and semi-arid environment; and two residual soils, one developed from shale and the other one developed from loess in sub-humid and humid climate Pakistan. These data were compared to data of two soil profiles sampled in Germany, one developed on top of the residuum of Muschelkalk and the other on top of glacial loess under sub-humid continental climate. The soil samples were separated into sand, silt, and clay fractions and each fraction was analyzed by X-Ray diffraction. In addition vermiculite, smectite (Ca/Mg and K/NH₄ CEC) and kaolinite (TG/DSC) in the clay fraction were determined. The clays were also examined by X-ray diffraction to identify mineral phases of iron oxides before and after chemical concentration treatment. Confirmation of iron oxides in clays by their morphology was achieved by TEM, and quantitatively measurements were done by voltammetry. Phosphorus and the soil clay iron oxide association were also measured by microanalysis of P-loaded soil clay. Soil mean values of various parameters were compared by using Duncan Multiple Range tests and multiple regression equations to develop a prediction model of P adsorption and P

fractions using common soil properties with or without soil types as an independent parameter.

The alluvial soil types showed a dominant silty and light texture with pH values above 8.0, high CaCO₃ content, low organic matter content and CBD/oxalate extractable Fe and Al content demonstrating an irregular soil profile distribution with soil depth. The shale and loess derived soil types are consisting of silty clay/clay loam, show pH values of 7 to 8, lower CaCO₃ contents with CBD/oxalate extractable Fe and Al values, higher compared to the data of the alluvial soils. CBD extractable Fe and Al fractions increased with depth in the loess derived soils and the organic matter content increased in the shale-derived soils. The two residual soils from Germany consisted of silty clay showing decalcification are characterized by low pH value at the surface layer, and high pH value below 25 cm depth and an accumulation of CaCO₃ in the subsurface where CBD and oxalate extractable Fe and Al fractions were highest and the Fe_d value increased with depth.

The soil clays were composed of mostly layered silicates, minor proportion of tectosilicates and iron oxides: In the alluvial soils smectite content ranged around 15 to 30% and kaolinite from 14 to 32%. The composition seemed to be inherited from the parent material of the soil. *In situ* weathering of Guliana soil had resulted in relatively higher amounts of smectite and kaolinite compared to that of the other soils. Smectite content increased and mica content decreased from surface to soil depth. Although goethite content ranged from 0.81 to 28.63 g kg⁻¹ in the alluvial soils, the goethite particles were well-crystallized compared to the one found in the residual soils which contained goethite values of 16.5 to 34.2 g kg⁻¹ but with often poor crystallinity and with an association of ferrihydrite. The goethite particles of shale derived Murree and Peshawar soil were also poorly crystalline and associated with hematite particles especially in case of Murree soil.

Phosphorus sorption was initially high in all the soils investigated and P sorption occurred to be low after adsorption rate of 100 mg P kg⁻¹ of soil. The order of P sorption of different soils to achieve two mg L⁻¹ P of the solution was Pitafi>Prb-Wein=Prb-Ostb≥Peshawar>GulianaPacca=Sultanpur=Murree=Shahdara. The fitting of P sorption isotherms to Freundlich equation indicated the same order of sorption affinity (k_f) of different soils as given above. Maximum sorption on high affinity sites was greater in the weathered soils, which was associated with greater content of crystalline and amorphous Fe and Al phases compared to that of the less weathered alluvial soils. Interestingly, P

sorbed on high affinity sites in some alluvial soils was the same as that of weathered soils which may be due to high crystallinity of goethite as shown by TEM microanalysis. The microanalysis showed well crystalline goethite in the alluvial soils with greater P:Fe ratios. Poorly crystalline goethite in the weathered residual soils (Parabraunerde, Murree and Guliana soils) with low P:F ratios. Phosphorus sorption was not necessarily related to only the abundance of CaCO_3 content. Regression equation for all Freundlich and Langmuir parameters was significant only when various fractions of soil iron and aluminum were included. Reliability on prediction of adsorption parameters further increased considerably when soil type was incorporated as independent character variable suggesting there are some other hidden factors, which have not been accounted yet.

Total P content was higher in the less weathered alluvial soils compared to the weathered soils except for Prb-Ostb soil. Organic P fraction was only a small fraction of total P in all soils. The apatite P fraction, although a dominant P form, was highest in alluvial soils especially in Peshawar soil. The Ca_2 -P and Ca_8 -P fractions had accumulated at the surface layers especially in the alluvial soils where fertilizer application was intense or leaching has taken place below 50 cm soil depth in the well structured soil (Guliana). The P fraction desorbed from iron oxide surfaces (Fe-P) was higher in weathered soils and lower in alluvial soils, which correlated well with the distribution of iron oxide content in these soils. The occluded P fraction (released by dissolution of iron oxide) in some of the alluvial soils was as high as the P fraction of the more ferruginous soils although the highest amount was given again of the samples of Prb-Ostb soil. The occluded P fraction was lowest in Murree and Prb-Wein soils probably due to the lack of fertilizer application. Both the soils are under permanent forestry.

In conclusion, well crystalline goethite was found in the alluvial soils, relatively less crystalline goethite but in larger quantity in the residual soils, and poorly crystalline goethite and hematite in the shale derived Murree soils. Well-crystallized goethite particles were able to retain more phosphate than poorly crystalline phases. Nevertheless P sorption capacity strongly depends on both amorphous and crystalline iron and aluminium oxide phases especially on goethite. Among the layered silicate kaolinite appeared to be the most significant parameter in regard to phosphorus binding capacity calculated by Langmuir equation. The decrease in soil kaolinite content was also related to the decrease in total P content, total inorganic P content, apatite P content, and occluded P content. Finally, it is apparent that P retention is a consequence of

cumulative effects of several soil properties. The P enrichment indicators (Ca₂-P, Ca₈-P, and apatite) play a less important role in explaining P release to soil solution (Olsen P). The P enrichment indicators and the clay minerals (smectite, kaolinite, and goethite) are explaining up to 86% variation with significantly different intercepts of the soil type. To give proper prediction data further investigations have to be undertaken on soil organic matter and manganese fractions.

References

- Adhami, E., H.R. Memarian, F. Rassaei, E. Mahdavi, M. Maftoun, A.M. Ronaghi, and R.G. Fasaie. 2007. Relationship between phosphorus fractions and properties of highly calcareous soils. *Australian J. Soil Res.* 45:255-261.
- Adhami, E., M. Maftoun, A. Ronaghi, N. Karimian, J. Yasrebi, and M.T. Assad. 2006. Inorganic phosphorus fractionation of highly calcareous soils of Iran. *Commun. Soil Sci. Plant Anal. J.* 37:1877-1888.
- Afif, E., A. Matar, and J. Torrent. 1993. Availability of phosphate applied to calcareous soils of West Asia and North Africa. *Soil Sci. Soc. Am. J.* 57:756-760.
- Agbenin, J.O., and H. Tiessen. 1995. Phosphorus forms in particle-size fractions of a toposequence from northeast Brazil. *Soil Sci. Soc. Am. J.* 59:1687-1693.
- Ahmad, M., M. Akram, M.S. Baig, M.Y. Javad, and Raiz-ul-Amin. 1986. Proc. XII Intl. Forum Soil Taxonomy Agro-Technology Transfer. Oct. 1985. 2nd Vol. Field Excursions. Soil survey of Pakistan and soil management support services USA. Soil Survey of Pakistan, Multan Road Lahore.
- Akhtar, M.S. 1989. Mineralogy and potassium quantity/intensity relation in three alluvial soils of Pakistan. PhD Thesis Department of Soil and Crop Sciences, Texas A&M University, College Station, Texas. 1989.
- Akhtar, M.S., and J.B. Dixon 1993. Mineralogy and mineral properties of surface soils from the Indus plain of Pakistan. *Clay Res.* 12: 22-32.
- Akhtar, M.S., J. B. Dixon, and L.P. Wilding. 1989. Pedogenic changes and mineral weathering in three soils from the Indus river plain of Pakistan. Proc. VIIIth Intl. Working Group of Soil Micromorphology, San Antonio, 1988, L. A. Douglas (ed.) *Soil Micromorphology: A Basic and Applied Science. Development in Soil Science 19*, Elsevier Amsterdam. p.161-168.
- Alexiades, C.A. and M.L. Jackson. 1965. Quantitative determination of vermiculite in soils: *Soil Sci. Soc. Am. Proc.* 29:522-527.
- Allen, B.L., B.F. Hajek. 1989. Mineral occurrence in soil environments. In: *Minerals in soil environments*, 2nd edition. J.B., Dixon, S.B. Weed (Eds.). SSSA, Madison, WI. 199-278.
- Baifan J. and G. Yichu, 1989. A suggested fractionation scheme of inorganic phosphorus in calcareous soils. *Fert. Res.* 20:159-165.

- Barrón, V., M. Heruzo, and J. Torrent. 1988. Phosphate adsorption by aluminous hematites of different shapes. *Soil Sci. Soc. Am. J.* 52:647-651.
- Barron, V., N. Galvez, M.F. Hochella, and J. Torrent. 1997. Epitaxial overgrowth of goethite on hematite synthesized in phosphate media: A scanning force and transmission electron microscopy study. *Am. Mineral.* 82:1091-1100.
- Barrow, N.J. 1978. The description of phosphate adsorption curves. *J. Soil Sci.* 29:447-462.
- Barrow, N.J. 1983. On the reversibility of phosphate sorption by soils. *J. Soil Sci.* 34:751-758.
- Barrow, N.J. 1985. Reactions of anions and cations with variable-charge soils. *Adv. Agron.* 38:183-230.
- Barrow, N.J. 1991. Testing a mechanistic model. XI. The effect of time and level of application on isotopically exchangeable phosphate. *J. Soil Sci.* 42:277-288.
- Barrow, N.J., and T.C. Shaw, 1975. The slow reactions between soil and anions. 2. Effect of time and temperature on the decrease in phosphate concentration in the soil solution. *J. Soil. Sci.* 119:167-177.
- Beauchemin, S., D. Hesterberg, J. Chou, M. Beauchemin, R.R. Simrad, and D.E. Sayers. 2003. Speciation of phosphorus in phosphorus enriched agricultural soils using X-ray absorption near-edge structure spectroscopy and chemical fractionation. *J. Environ. Qual.* 32:1809-1819.
- Bertrand, I., N. Grignon, P. Hinsinger, G. Souche, and B. Jaillard. 2001. The use of secondary ion mass spectroscopy coupled with image analysis to identify and locate chemical element in soil minerals: The example of phosphorus. *Scanning.* 23:279-291.
- Bertsch, P.M., and P.R. Bloom. 1996. Aluminium. *In: Methods of soil analysis: Part 3. Chemical methods* D.L. Sparks (eds.), ASA and SSSA, Madison, WI. 517-550.
- Bigham, J.M., D.C. Golden, L.H. Bowen, S.W. Buol, and S.B. Weed. 1978. Iron oxide mineralogy of well drained Ultisols and Oxisols: II. Influence on colour, surface area and phosphate retention. *Soil Sci. Soc. Am. J.* 42:816-825.
- Bigham, J.M., R.W. Fitzpatrick, and D.G. Schulze. 2002. Iron oxides. *In: Soil mineralogy with environmental applications.* J.B. Dixon and D.G. Schulze (eds.). SSSA Book Ser. 7, SSSA, Madison, WI. 323-366.

- Borggaard, O.K. 1983. Effect of surface area and mineralogy of iron oxides on their surface charge and anion adsorption properties. *Clays Clay Miner.* 31:230-232.
- Borrero, C., F. Pena, and J. Torrent. 1988. Phosphate sorption by calcium carbonate in some soils of the Mediterranean part of Spain. *Geoderma.* 42:261-269.
- Bowden, J.W., A.M. Posner, and J.P. Quirk. 1977. Ionic adsorption on variable charge mineral surfaces. Theoretical charge development and titration curves. *Aust. J. Soil Res.* 15:121-136.
- Bowman, J.R., and C.V. Cole. 1978. Transformations of organic phosphorus substrates in soils evaluated by NaHCO₃ extraction. *J. Soil Sci.* 125:49-54.
- Breeuwsma, A. 1973. Adsorption of ions on hematite (α -Fe₂O₃). Med. Landbouwhoghe School, Wageningen 73-1.
- Bresson, L.M. 1974. A study of integrated microscopy: rubefaction under wet temperate climate in comparison with Mediterranean rubefaction. *In: Soil microscopy.* G.K. Rutherford (eds.) Limestone Press, Kingston, Canada. 526-541.
- Brinkman, R. and Ch. M. Rafiq. 1971. Landforms and soil parent material in West Pakistan. *Pakistan Soils Bull no. 2.* Central Soil Research Institute. Lahore – Dacca. (presently Soil Survey of Pakistan, Multan road Lahore Pakistan.)
- Bruland, G.L., and C.J. Richardson. 2004. A spatially explicit investigation of phosphorus sorption and related soil properties in two riparian wetlands. *J. Environ. Qual.* 33:785–794.
- Buresh, R.J., P.C. Smithson, and D.T. Hellums. 1997. Phosphorus capital in Africa. *In: Replenishing soil fertility in Africa* (eds. R.J. Buresh, P.A. Sanchez and F. Callhoun), 111-149. Special publication No. 51, Soil Sci. Soc. Am. Madison, WI.
- Bürkert, A., M. Bagayoko, S. Alvey, and A. Bationo. 2001. Causes of legume-rotation effects in increasing cereal yields across the Sudanian, Sahelian and Guinean zone of West Africa. *In: Plant nutrition. Food security and sustainability of agro-ecosystem through basic and applied research.* W. Horst. et al., (eds.). *Developm. Plant and Soil Sci.* Kluwer Academic Publishers, Dordrecht, Netherlands: 972-973.
- Campbell, A.S., and U. Schwertmann. 1984. Iron oxide mineralogy of placic horizons. *J. Soil Sci.* 35:569-582.

- Campbell, K.L., and D.R. Edwards. 2001. Phosphorus and water quality. *In: Agricultural nonpoint source pollution: Watershed management and hydrology.* W.F. Ritter and A. Shirmonhamadi (eds.). Lewis publisher, Boca Raton, London, NY. 91-107.
- Carreira, J.A., B. Vinegla, and K. Lajtha. 2006. Secondary CaCO_3 and precipitation of P-Ca compounds control the retention of soil P in arid ecosystems. *J. Arid Env.* 64:460-473.
- Castro, B. and J. Torrent. 1994. Phosphate availability in calcareous Vertisols and Inceptisols in relation to fertilizer type and soil properties. *Fert. Res.* 40:109-119.
- Castro, B., and J. Torrent. 1998. Phosphate sorption by calcareous Vertisols and Inceptisols as evaluated from extended P-sorption curves. *Eur. J. Soil Sci.* 49:661-667.
- Chang, S.C., and S.F. Yu. 1992. Study on the fractions and availability of inorganic P in calcareous soils. *Soil and Fert.* (in Chinese) 3:1-4.
- Chang, S.C., and M.L. Jackson. 1957. Fractionation of soil phosphorus. *J. Soil Sci.* 84:133-144.
- Chukhrov, F.V., B.B. Zvyagin, A.I. Gorshkov, L.P. Ermilova, and V.V. Balashova. 1973. Ferrihydrite. *Izv. Adak. Nauk. SSSR, Ser. Geol.* 4:23-33.
- Churchman, G.J. 2002. The alteration and formation of soil minerals by weathering. *In: Handbook of soil science.* M. E. Sumner. CRC Press, London, NY. F3-F76.
- Colombo, C., A. Boundonno, A. Violante, and J. Torrent. 1991. The contrasting effect of goethite and hematite on phosphate sorption and desorption by Terre Rossse. *Z. Pflanzenernahr Bodenk* 154:301-305.
- Cornell, R.M., and U. Schwertmann. 1996. *The iron oxides.* VCH Publ., Weinheim, Germany.
- Cox, F. R. 1994. Predicting increase in extractable phosphorus from fertilizing soils of varying clay content. *Soil Sci. Soc. Am. J.* 58:1249-1253.
- Cross A.F, W.H Schlesinger. 1995. A literature review and evaluation of the Hedley fractionation: applications to the biogeochemical cycle of soil phosphorus in natural ecosystems. *Geoderma.* 64:197-214.
- Dalal, R.C., and E.G. Hallsworth. 1976. Evaluation of the parameters of soil phosphorus availability factors in predicting yield response and phosphorus uptake. *Soil Sci. Soc. Am. J.* 40:541-546.

- Davey, B.G., J.D. Russel, and M.J. Wilson. 1975. Iron oxide and clay minerals and their relation to colours of red and yellow podzolic soils near Sydney, Australia. *Geoderma* 14:125-138.
- Delgado, A., and J. Torrent. 2000. Phosphorus forms and desorption patterns in heavily fertilized calcareous and limed acid soils. *Soil Sci. Soc. Am. J.* 64:2031-2037.
- Delgado, A., J.R. Ruiz, M.C. del Campillo, S. Kassem, and L. Andreu. 2000. Calcium and iron related phosphorus in calcareous and calcareous marsh soils: sequential chemical fractionation and ^{31}P NMR study. *Commun. Soil Sci. Plant Anal.* 31:2483-2499.
- Domínguez, R., M.C. del Campillo, F. Peña, and A. Delgado. 2001. Effect of soil properties and reclamation practices on phosphorus dynamics in reclaimed calcareous marsh soils from the Guadalquivir Valley, SW Spain. *Arid Land Res. Manage.* 15:203-221.
- Duffera, M., and W.P. Robarge. 1999. Effect of soil management practices on phosphorus sorption characteristics of the highland plateau soils of Ethiopia. *Soil Sci. Soc. Am. J.* 63(5):1455-1462.
- Enfield, C.G., C.C. Harline, and B.E. Bledsoe. 1976. Comparison of five kinetic models for orthophosphate reactions in mineral soils. *Soil Sci. Soc. Am. J.* 40:243-248.
- FAO, 2004. Fertilizer use by crop in Pakistan. Food and Agriculture Organization of the United Nations, Rome, Italy.
- FAO. 1974. The Euphrates pilot irrigation project. Methods of soil analysis, Gadeb soil laboratory (A laboratory manual). Food and Agriculture Organization, Rome, Italy.
- FAO. 2001. Lecture notes on the major soils of the world. of the United Nations, Rome, Italy.
- Feitknecht, W., and W. Michaelis. 1962. Über die hydrolyse von Eisen-(III)-perchloratlösungen. *Helv. Chim. Acta.* 45:212-224.
- Fife, C.V. 1962. An evaluation of ammonium fluoride as a selective extractant for aluminium-bound soil phosphate: III. Detailed studies on selected soils (1). *J. Soil Sci.* 93:133-123.
- Fontes, M.P.F. 1988. Iron oxide mineralogy in some Brazilian Oxisols. Ph.D. thesis. North Carolina State Univ., Raleigh.
- Fox, L.E. 1989. A model for inorganic control of phosphate concentrations in river waters. *Geochim. Cosmochim. Acta* 53:417-428.

- Fox, R.L. and E. J. Kamprath. 1970. Phosphate sorption isotherms for evaluating the phosphate requirements of soils. *Soil Sci. Soc. Am. Proc.* 34:902-907.
- Freese, D., S.E.A.T.M. van der Zee, and W.H. van Riemsdijk. 1992. Comparison of different models for phosphate sorption as a function of the iron and aluminium oxides of soils. *J. Soil Sci.* 43:729-738.
- Frossard, E., M. Brossard, M. J. Hedley, and A. Metherell. 1995. Reactions controlling the cycling of P in soils. *In: Phosphorus in the global environment.* H. Tiessen (eds.). John Wiley & Sons, NY. 107-138.
- Fu, J..P. 1983. Fractionation of soil combined humus, *Chinese J. Soil Sci.* 2: 36-37.
- Galvez, N., V. Barron, and J. Torrent.1999. Preparation and properties of hematite with structural phosphorus. *Clays Clay Miner.* 47:375-385.
- Geelhoed, J.S., T. Hiemstra, W.H.V. Riemsdijk.1997. Phosphate and sulfate adsorption on goethite: Single anion and competitive adsorption. *Geoch. Cosmochi. Acta.* 61:2389-2396.
- Goldberg, S., and G. Sposito. 1985. On the mechanism of phosphate adsorption by hydroxylated mineral surfaces: A review. *Commun. Soil Sci. Plant Anal. J.* 16:801-821.
- Goodman, B.A. 1994. Mössbauer spectroscopy. *In: Clay mineralogy: spectroscopic and chemical determinative methods.* M.J. Wilson (eds.) Chapman & Hall, London, UK. 68-119.
- Grygar, T., J. Dedecek, and D. Hradil. 2002. Analysis of low concentration of free ferric oxides in clays by vis. diffuse reflectance spectroscopy and voltammetry. *Geologica Carpathica, Bratislava.* 53:1-7.
- Hadley, M.J., W.B. Stewart, and B.S. Chauhan. 1982. Changes in inorganic and organic soil phosphorus fractions induced by cultivation practices and by laboratory incubations. *Soil Sci. Soc. Am. J.* 46:970-976.
- Hamad, M.E., D.L. Rimmer, and J.K. Syers. 1992. Effect of iron oxides on phosphate sorption by calcite and calcareous soils. *J. Soil Sci.* 43:273-281.
- Harrell, D.L., and J.J. Wang. 2006. Fractionation and sorption of inorganic phosphorus in Louisiana calcareous soils. *Soil Science.* 171(1):39-51.
- Hassan, M.M., A. Rashid, and M.S. Akhtar. 1993. Phosphorus requirement of corn and sunflower grown on calcareous soils of Pakistan. *Commun. Soil Sci. Plant Anal. J.* 24:1529-1541.

- Haygarth, P.M., A.L. Heathwaite, S.C. Jarvis, and T.R. Harrod. 2000. Hydrological factors for phosphorus transfer from agricultural soils. *Adv. Agron.* 69:153-178.
- Hedley, M.J. and Sharpley, A.N. 1998. Strategies for global nutrient cycling. *In: Long-term nutrient needs for New Zealand's primary industries: Global supply, production requirements and environmental constraints.* L Currie (eds.). Fert. & Lime Res. Cent., Massey Univ., Palmerston North, NZ. 70-95.
- Hingston, F.J., A.M. Posner, and J.P. Quirk. 1972. Anion adsorption by goethite and gibbsite. I. *J. Soil Sci.* 23:177.
- Hingston, F.J., R.J. Atkinson, A.M. Posner, and J.P. Quirk. 1968. Specific adsorption of anions on goethite. *Int. Congr. Soil Sci. Trans.* 9th (Adelaide) 1:669.
- Hinsinger, P. 2001. Bioavailability of soil inorganic P in the rhizosphere as affected by root-induced chemical changes: a review. *Plant and Soil.* 237:173-195.
- Holford, I.C.R. and G.E.G. Mattingly. 1975. The high and low-energy phosphate adsorbing surface in calcareous soils. *J. Soil Sci.* 26:407-417.
- Holford, I.C.R., R.W.M. Wedderburn, and G.E.G. Mattingly. 1974. A Langmuir two-surface equation as a model for phosphate adsorption by soils. *J. Soil Sci.* 25:242-255.
- Holmgren, G.G.S. 1967. A rapid citrate-dithionite extractable iron procedure. *Soil Sci. Soc. Am. Proc.* 31:210-211.
- Hsu, P.H. 1989. Aluminium hydroxides and oxyhydroxides. *In: Minerals in soil environments*, 2nd edition. J.B. Dixon, S.B. Weed, (Eds.). SSSA, Madison, WI. 331-378.
- Hummel, P., K. Rilling, and F. Waldmann. 1992. *Bodenübersichtskarte von Baden-Württemberg 1:200000: CC 7118 Stuttgart-Nord.* Geologisches Landesamt Baden-Württemberg Freiburg i. Br.
- Jackson, M.L. 1965. Free oxides, hydroxides, and amorphous aluminosilicates. *In: Methods of soil analysis, Part 1.* C.A. Black (eds.). ASA, Ser. 9. ASA, Madison, WI. 578-603.
- Jackson, M.L. 1969. Mineral fractionation for soils. *In: Soil chemical analyses: Advanced course.* M.L. Jackson (eds.). Univ. Wisconsin, Madison, WI. 100-168.
- Jackson, M.L., C.H. Lim, and L.W. Zelazny. 1986. Oxides, hydroxides and aluminosilicates. *In: Methods of soil analysis: Physical and mineralogical methods, Part 1.* 2nd edition. A. Klute (eds.). ASA and SSSA, Madison, WI. 101-150.

- Jiang, B., and Y. Gu. 1989. A suggested fractionation scheme for inorganic phosphorus in calcareous soils. *Fert. Res.* 20:159-165.
- Jones, R.C, and G. Uehara. 1973. Amorphous coatings on mineral surfaces, *Proc. Soil Sci. Soc. Am.* 37:792-798.
- Joseph, L., and B.K. Bhaumik. 1997. Improved estimation of the Box-Cox transform parameter and its application to hydrogeochemical data. *Mathematical geology* 29:963-976.
- Kämpf, N., A. C. Scheinost and D. G. Schulze. 2002. Oxide minerals. *In: Handbook of soil science.* M. E. Sumner. CRC Press, London, NY. F125-F168.
- Kämpf, N., and U. Schwertmann. 1982. The 5-M-NaOH concentration treatment for iron oxides in soils. *Clays Clay Miner.* 30:401-408.
- Kämpf, N., and U. Schwertmann. 1983. Relations between iron oxides and soil colour in kaolinitic soils of Southern Brazil. (In Portuguese with English summary.) *Rev. Bras. Cienc. Solo* 7:27-31.
- Karageorgiou, K., Paschalis M., and G.N. Anastassakis. 2007. Removal of phosphate species from solution by adsorption onto calcite used as natural adsorbent. *J. Hazardous Mater.* 139:447-452.
- Karim, M.I., and W.A. Adams. 1984. Relationships between sesquioxides, kaolinite, and phosphate sorption in a Catena of oxisols in Malawi. *Soil Sci. Soc. Am. J.* 48:406-409.
- Kazemi, M. 1983. Interrelationship among biosequences, available phosphorus distribution, and other soil variables in Eastern Iowa. Unpublished M.S. thesis. Library. Iowa State University, Ames. Iowa.
- Khan, Z.A, and S.A. Khan. 1988. Utilization of Pakistan phosphates and its future, UNIDO Proc. First African Regional Consultation on the Fertilizer and Pesticide Industry, Lahore, October 17-20. 31-49.
- Kleber, M., R. Mikutta, M. S. Torn, and R. Jahn. 2005. Poorly crystalline mineral phases protect organic matter in acid subsoil horizons. *Eur. J. Soil Sci.* 56:717-725.
- Krause, W., and W. Fleck. 1993. *Bodenkarte von Baden-Württemberg 1:25000: Blatt 6917 Weingarten (Baden).* Geologisches Landesamt Baden-Wurttemberg Freiburg i. Br.
- Kuo, S., 1996. Phosphorous. *In: Methods of soil analysis: Part 3, Chemical methods.* D.L. Sparks, (eds.). SSSA Book Ser., No. 5. SSSA, Madison, WI. 869-919.

- Lajtha, K. and S.H. and Bloomer. 1988. Factors affecting phosphorus adsorption and phosphorus retention in an arid ecosystem. *Soil Sci.* 146:160-167.
- Larsen, S., D. Gunnary, and C.D. Sutton. 1965. The rate of immobilization of applied phosphate in relation to soil properties. *J. Soil Sci.* 16:141-148.
- Li, L. and R. Stanforth. 2000. Distinguishing adsorption and surface precipitation of phosphate on goethite (α -FeOOH), *Journal of Colloid and Interface Science* 230:12-21.
- Lindsay, W.L., and E.C. Moreno. 1960. Phosphate phase equilibria in soils, *Soil Sci Am. Proc.* 24:177-182.
- Lindsay, W.L., P.L.G. Vlek, and S.H. Chien. 1989. Phosphate minerals. *In: Minerals in soil environment*, 2nd edition. J.B. Dixon and S.B. Weed (eds.). SSSA, Madison, WI. 1089-1130.
- Liu, F., J. He, C. Colombo, and A.J. Violante. 1999. Competitive adsorption of sulfate and oxalate on goethite in the absence or presence of phosphate. *Soil Sci.* 164:180-189.
- Loch, J., and I. Jaszberenyi. 1995. The examination of the phosphate adsorption and desorption in long-term fertilizer application experiments. *Agribiol. Res.* 48:53-62.
- Loeppert, R.H., and W.P. Inskeep. 1996. Iron. *In: Methods of soil analysis: Chemical methods, Part 3.* D.L. Sparks (eds.). ASA and SSSA, Madison, WI. 639-664.
- Mackay, A.D., J.K. Syers, R.W. Tillman, and P.E.H. Gregg. 1986. A simple model to describe the dissolution of phosphate rock in soil. *Soil Sci. Soc. Am. J.* 50:291-296.
- Manning, B.A., S.E. Fendorf, and S. Goldberg. 1998. Surface structures and stability of arsenic (III) on goethite: Spectroscopic evidence for inner-sphere complexes. *Environ. Sci. Tech.* 32:2383-2388.
- Manojlovic, D., M. Todorovic, J. Jovicic, V.D. Krsmanovic, P.A. Pfenndt, and R. Golubovic. 2007. Preservation of water quality in accumulation Lake Rovni: The estimate of the emission of phosphorus from inundation area. *Desalination*, 213:104-109.
- Marshall, C.E. 1935. Layer lattices and base-exchange clays: *Z. Kristallogr.* 91:433-449.
- Martin, R.R., and R.S.C. Smart. 1987. X-ray photoelectron studies of anion adsorption on goethite, *Soil Sci. Soc. Am. J.* 53:54-56.

- Matar, A., J. Torrent, and J. Yayn. 1992. Soil and fertilizer phosphorus and crop response in the dryland mediterranean zone. *Adv. Soil Sci.* 18:81-146.
- McBride, M.B. 1994. *Environmental chemistry of soils*. Oxford Univ. Press. NY. 121-168.
- McBride, M.B. 2002. Chemisorption and precipitation reactions. *In: Handbook of soil science*. M. E. Sumner. CRC Press, London, NY. B265-B299.
- McKeague, J.A., and J.H. Day. 1966. Dithionite and oxalate extractable Fe and Al as aids in differentiating various classes of soils. *Cand. J. Soil Sci.* 46:13-22.
- Mehra, O.P., and M.L. Jackson. 1960. Iron oxide removal from soils and clays by dithionite-citrate system buffered with sodium bicarbonate. *In: Clays and Clay Miner. Proc. 7th Natl. Congr.* Pergamon, London. 317-327.
- Melo, V.F., B. Singh, C.E.G.R. Schaefer, R.F. Novais, and M.P.F. Fontes. 2001. Chemical and mineralogical properties of kaolinite-rich Brazilian soils. *Soil Sci. Soc. Am. J.* 65:1324-1333.
- Memon, K.S., and R.L. Fox. 1983. Utility of phosphate sorption curves in estimating P requirements of cereal crops: Wheat (*Triticum aestivum*). *Proc. Third Int. Cong. on phosphorus compounds*. Brussels. Belgium Oct 4-6.
- Memon, K.S., H.K. Puno, and R.L. Fox. 1991. Phosphate sorption approach for determining phosphorus requirements of wheat in calcareous soils. *Fert. Res.* 28:67-72.
- Memon, K.S. 1996. Soil fertilizer phosphorus. *In: Soil science*. A. Rashid, and K.S. Memon. National Book Found., Islamabad, Pakistan. 291-316.
- Memon, M., K.S. Memon, M.S. Akhtar, D. Stueben. 2008. Iron oxides characterization and quantification in low concentration in soils. *Comm. Soil. Sci. Pl. Anal.* (accepted).
- Moughli, L., D.G. Westfall, A. Boukhal, J. Ryan, and A. Matar. 1991. A Soil phosphorus adsorption, and evaluation of soil phosphorus buffering capacity indices. Fertilizer use efficiency under rain-fed agriculture in West Asia and North Africa: *In: proceedings of the 4th regional workshop*, 5-10 May, 1991, Agadir, Morocco. 28-38.
- Murad, E., and J.H. Johnston. 1987. Iron oxides and oxyhydroxides. *In: Mössbauer spectroscopy applied to inorganic chemistry*. G.J. Long (eds.) Plenum, NY. 507-582.
- Murphy, J., and J.P. Riley. 1962. A modified single solution method for determination of phosphate in natural waters. *Anal. Chim. Acta.* 27:31-36.

- Nornberg, P., J. Wulf Petersen, and C.B. Koch. 1991. Present day formation of hematite in Danish soils. Proceedings of the 7th Euroclay Conference, Dresden. 801-804.
- Nornberg, P., U. Schwertmann, H. Stanjek, T. Andersen, and H.P. Gunnlaugsson. 2003. Mineralogy of a burned soil compared with four anomalously red quaternary deposits in Denmark. *Clay Minerals*, 39: 85-98.
- Norrish, K., and R.M. Taylor. 1961. The isomorphous replacement of iron by aluminium in soil goethites. *J. Soil Sci.* 12:294-306.
- Olsen, S.R., and F.S. Watanabe. 1963. Diffusion of phosphorous as related to soil texture and plant uptake, *Soil Sci. Soc. Am. Proc.* 27:648-652.
- Olsen, S.R., and Sommers. 1982. Phosphorus. In: Methods of soil analysis. Part 2. 2nd edition. 9. A.L. Page et al. (eds.). Agron. Monogr. ASA and SSSA, Madison, WI. 403-430.
- Parfitt, R.L. 1978. Anion adsorption by soils and soil material. *Adv. Agron.* 30:1-50.
- Parfitt, R.L., J.D. Russell, and V.C. Farmer. 1976. Confirmation of the surface structures of goethite (α -FeOOH) and phosphated goethite by infrared spectroscopy. *J. Chem. Soc., Faraday Trans. I.* 72:1082-1087.
- Parfitt, R.L., R.J. Atkinson, and R.St.C. Smart. 1975. The mechanism of phosphate fixation by iron oxides. *Soil Sci. Soc. Am. Proc.* 39:837-842.
- Parks, G.A. 1967. Aqueous surface chemistry of oxides and complex oxide minerals. Isoelectric point and zero point of charge. In: Equilibrium concepts in natural water systems. R.F Gould (eds.). *Adv. Chem. Ser.* 67:121-160.
- Pena, F. J. Torrent. 1990. Predicting phosphate sorption in soils of Mediterranean regions. *Fertilizer Res.* 23:173-179.
- Pena, F., J. Torrent, 1984. Relationships between phosphate sorption and iron oxides in alfisols from a river terrace sequence of Mediterranean Spain. *Geoderma*, 33:283-296.
- Petersen, G.W., and R.B. Corey. (1966). A modified Chang and Jackson procedure for routine fractionation of inorganic soil phosphates. *Soil Sci. Soc. Am. Proc.* 30:563-565.
- Pierzynski, G.M., J.T. Sims, and G.F. Vance. 1994. *Soils and environmental quality*. Lewis/CRC Press, Boca Raton, FL.
- Pizarro, C., N. Furet, R. Venegas, J.D. Fabris, and M. Escudey. 2000. Some cautions on the interpretation of Mössbauer spectra in mineralogical studies of volcanic soils. *Bol. Soc. Chi. Guim.* 45.

- Rajan, S.S.S. 1975. Adsorption of divalent phosphate on hydrous aluminum oxide. *Nature (London)*. 253:434-436.
- Rajan, S.S.S., and R.L. Fox. 1972. Phosphate adsorption by soils. 1. Influence of time and ionic environment on phosphate adsorption. *Commun. Soil Sci. Plant Anal. J.* 3:493-504.
- Ratkowsky, D.A. 1986. A statistical study of seven curves for describing the sorption of phosphate by soil. *J. Soil Sci.* 37:183-189.
- Regierungspräsidium Karlsruhe, 1999. *Landschaften und Böden im Regierungsbezirk Karlsruhe, BadenWürttemberg*. E. Schweizerbart'sche Verlagsbuchhandlung (Nägele u. Obermiller), Stuttgart.
- Resende, M. 1976. Mineralogy, chemistry, morphology and geomorphology of some soils of Central Plateau of Brazil. Ph.D. thesis. Purdue Univ., West Lafayette, IN.
- Ryan, J.C., D. Curtin, and M.A. Cheema. 1984. Significance of iron oxides and calcium carbonate particle size in phosphate sorption by calcareous soils. *Soil Sci. Soc. Am. J.* 48:74-76.
- Ryan, J., D. Curtin, and M.A. Cheema. 1985. Significance of iron oxides and calcium carbonate particle size in phosphate sorption by calcareous soils. *Soil Sci. Soc. Am. J.* 49:74-76.
- Saavedra, C., and A. Delgado. 2005. Phosphorus fractions and release patterns in typical mediterranean soils. *Soil Sci. Soc. Am. J.* 69:607-615.
- Said, M.B., and A. Dakermanji. 1993. Phosphate adsorption and desorption by calcareous soils of Syria. *Commun. Soil Sci. Plant Anal. J.* 24:197-210.
- Samadi, A., and R.J. Gilkes. 1998. Forms of phosphorus in virgin and fertilized calcareous soils of Western Australia. *Aust. J. Soil Res.* 36:585-601.
- Samadi, A., and R.J. Gilkes. 1999. Phosphorus transformations and their relationships with calcareous soil properties of south western Australia. *Soil Sci. Soc. Am. J.* 63:809-805.
- SAS Institute, 1999. *SAS for Windows. Version 8.02*. SAS Institute, Cary, NC.
- Scheinost, A.C., and U. Schwertmann. 1999. Color identification of iron oxides and hydroxysulfates: Use and limitations. *Soil Sci. Soc. Am. J.* 63:1463-1471.
- Schroeder, D. 1988. Zur Geschichte des Mineralnamens „Goethit“. *Z. Pflanzenernähr. Bodenkd.* 151:137-139.

- Schulze, D.G., and J.B. Dixon. 1979. High gradient magnetic separation of iron oxides and magnetic minerals from soil clays. *Soil Sci. Soc. Am. J.* 43:793-799.
- Schulze, D.G., and U. Schwertmann. 1984. The influence of aluminum on iron oxides. X. Properties of Al substituted goethites. *Clay Miner.*, 19:521-539.
- Schulze, D.G., and U. Schwertmann. 1987. The influence of aluminum on iron oxides. XII. Properties of goethites synthesized in 0.3M KOH at 25°C, *Clay Miner.*, 22:83-92.
- Schwertmann, U. 1964. Differenzierung der Eisenoxide des Bodens durch photochemische Extraktion mit saurer Ammoniumoxalat-lösung. *Z. Pflanzenernähr. Bodenkd.* 105:194-202.
- Schwertmann, U. 1985. The effect of pedogenic environments on iron oxide minerals. *In: Advances in soil science.* B.A. Stewart (eds.). I. Springer-Verlag, New York, NY. 171-200.
- Schwertmann, U. and R.M. Taylor. 1977. Iron oxides. *In: Minerals in soil environments.* J.B Dixon. and S.B Weed. (Eds.). SSSA Madison, WI. 145-180.
- Schwertmann, U. and R.M. Taylor. 1989. Iron oxides. *In: Minerals in soil environment.* J.B. Dixon and S.B. Weed (eds.). SSSA Book Ser.1. SSSA, Madison, WI. 379-438.
- Schwertmann, U., and W.R. Fischer. 1966. Zur Bildung von α -FeOOH und α -Fe₂O₃ aus amorphem Eisen (III)-hydroxid. III. *Z. Anorg. Allg. Chem.* 346:137-142.
- Schwertmann, U., E. Murad, and D.G. Schulze. 1982. Is there holocene reddening (hematite formation) in soils of axeric temperate areas? *Geoderma.* 27:209-223.
- Sharpley, A.N. 2000. Bioavailable phosphorus in soil. pp. 38-43. In G.M. Pierzynski (ed.), *Methods for phosphorus analysis for soils, sediments, residuals, and waters.* Southern Cooperative Series Bull. XXX.
- Sharpley, A.N., T.C. Daniel, B. Wright, P. Kleinman, T. Sobecki, R. Parry, and B. Joern. 1999. National research project to identify sources of agricultural phosphorus loss. *Better Crops* 83:12-15.
- Sharpley, A.N., U. Singh, G. Uehara, and J. Kimble. 1989. Modeling soil and plant phosphorus dynamics in calcareous and highly weathered soils. *Soil Sci. Soc. Am. J.* 53:153-158.
- Shayan, A., B.G. Davey. 1978. A universal dimensionless phosphate adsorption isotherm for soils. *Soil Sci. Soc. Am. J.* 42:878-882.

- Shen, J., R. Li, F. Zhang, J. Fan, C. Tang, and Z. Rengel. 2004. Crop yields, soil fertility and phosphorus fractions in response to long-term fertilization under the rice monoculture system on a calcareous soil. *Field Crops Res.* 86:225-238.
- Shen, R.F. 1992. Studies on the fractions, transformation and availability of phosphorus in calcareous Fluvisol of Jinghan Plain (in Chinese). M.Sc. Thesis, Huazhong Agriculture University.
- Shoji, S., M. Nanzyo, R.A., Dahlgren, and P. Quantin. 1996. Evaluation and proposed revisions of criteria for Andosols in the world reference base for soil resources. *Soil Science.* 161:604-615.
- Simard, R.R., D. Cluis, G. Gangbazo and A.R. Pesant. 1994. Phosphorus sorption and desorption indices in soil. *Commun. Soil Sci. Plant Anal. J.* 25:1483-1494.
- Sims, J.T., A.C. Edwards, O.F. Schoumans, and R.R. Simard. 2000. Integrating soil phosphorus testing into environmentally based agricultural management practices. *J. Environ. Qual.* 29:60–71.
- Sinaj, S., E. Frossard, and J.L. Morel. 1992. Phosphate availability in Albanian soils. *In: Proceedings of second european society of agronomy congress.* A. Scaife (eds.). Warwick, UK. 23–28 Aug. 1992. ESA, HRI, Wellesbourne, UK. 306-307.
- Singh, B., and R.J. Gilkes. 1991. Concentration of iron oxides from soil clays by 5M NaOH treatment: the complete removal of sodalite and kaolin. *Clay Miner.* 26:463-472.
- Singh, B., and R.J. Gilkes. 1992. Properties of soil kaolinites from southwestern Australia. *J. Soil Sci.* 43:645–667.
- Smadi, A., R.J. Gilkes. 1998. Forms of phosphorus in virgin and fertilised calcareous soils of Western Australia. *Aust. J. soil Res.* 36:586-601.
- Smillie, G.W., and J.K. Syers. 1972. Calcium fluoride formation during extraction of calcareous soils with fluoride. II. Implications to the Bray P-1 Test. *Soil Sci Soc. Am. Proc.* 36:25-30.
- Smykatz-Kloss, W. 1975. The DTA determination of the degree of (dis-) order of kaolinites: Method and application to some kaolin deposits of Germany. p. 429–438. *In Proc. Int. Clay Conf.* Wilmette, IL.
- Soil Survey of Pakistan. 2007. Unpublished data.
- Solis, P., and J. Torrent 1989. Phosphate by calcareous Vertisols and Inceptisols of Spain. *Soil Sci. Soc. Am. J.* 53:456-459.

- Sollins, P. 1991. Effects of soil microstructure on phosphorus sorption in soils of the humid tropics, *In*: Phosphorus cycles in terrestrial and aquatic ecosystem. Regional workshop 3: H. Tiessen, D. Lopez-Hernandez, and I.H. Salcedo (eds.), South and Central America, Saskatchewan Institute of Pedology, Univ. Saskatchewan, Saskatoon. 168-175.
- Solomon, D., and J. Lehmann. 2000. Loss of phosphorus from soil in semiarid northern Tanzania as a result of cropping: evidence from sequential extraction and ³¹P NMR spectroscopy. *Eur. J. Soil Sci.* 51:699-708.
- Speter, M. 1935. Final summary of the research into the origin of superphosphate. *Superphosphate* 8:141-151.
- Sposito, G. 1984. *The surface chemistry of soils*. Oxford Univ. Press, New York, NY.
- Sposito, G. 1998. On points of zero charge. *Env. Sci. Tech.* 32:2815-2819.
- Sposito, G., 1980. General criteria for the validity of the Buckingham-Darcy Flow Law. *Soil Sci. Soc. Am. J.* 44:1159-1168.
- Sposito, G. 1982. On the use of Langmuir equation in the interpretation of "adsorption" phenomena II: The "Two surface" Langmuir equation. *Soil Sci. Soc. Am. J.* 46:1147-1152.
- Sui, Y., and M.L. Thompson. 2000. Phosphorus sorption, desorption, and buffering capacity in biosolids-amended mollisol. *Soil Sci. Soc. Am. J.* 64:164-169.
- Syers, J.K. and P.E.H. Curtin .1988. Inorganic reactions controlling phosphate cycling. *In*: Phosphate cycles in terrestrial and aquatic ecosystems. H. Tiessen (eds.) Regional workshop 1: Europe. SCOPE/UNEP Proc., Univ. Saskatchewan, Saskatoon, Canada. 17-29.
- Syers, J.K., G.W. Smillie, and J.D.H. Williams. 1972. Calcium fluoride formation during extraction of calcareous soils with fluoride: I. Implication to inorganic phosphorus fractionation schemes. *Soil Sci. Soc. Am. J.* 36:20-24.
- Tamm, O. 1922. Eine methode zur bestimmung der anorganischen komponenten des gelkomplexes in boden. *Meddel. Statens Skogsförsöksanst (Sweden)*. 19:385-404.
- Tertian, R., and F. Claisse. 1982. *Principles of quantitative X-ray fluorescence analysis*. Heyden, London Philadelphia-Rheine.
- Tiessen, H., J.W.B. Stewart, C.V. Cole. 1984. Pathways of phosphorus transformation in soils of differing pedogenesis. *Soil Sci. Soc. Am. J.* 48:853-858.

- Tiessen, H., J.W.B. Stewart, and J.O. Moir. 1983. Changes in organic and inorganic phosphorus in particle size fractions of two soils during 60 to 90 years of cultivation. *J. Soil Sci.* 34:815–823.
- Tokashiki, Y., T., Hentona, M. Shimo, and A.L.P. Vidhana. 2003. Improvement of the successive selective dissolution procedure for the separation of birnessite, lithiophorite, and goethite in soil manganese nodules. *Soil Sci. Soc. Am. J.* 67(3):837-843.
- Tomar, K.P., A. Ramesh, and A.K. Biswas. 1995. Phosphorus sorption as influenced by soil clay minerals in major soil groups of India. *J. Indian Soc. Soil Sci.* 43:577-582.
- Torrent, J., and V. Barron. 2002. Diffuse reflectance spectroscopy of iron oxides. *In: Encyclopedia of surface and colloid science.* Marcel Dekker, Inc. CL. 1438-1446.
- Torrent, J., U. Schwertmann, and V. Barron. 1992. Fast and slow phosphate sorption by goethite-rich natural minerals. *Clays Clay Miner.*, 40:14-21.
- Torrent, J., V. Barron, and U. Schwertmann. 1990. Phosphate adsorption and desorption by goethites differing in crystal morphology. *Soil Sci. Soc. Am. J.* 54:1007-1012.
- Tu, S.X., Z.F. Guo, and S.S. Chen. 1993. Transformation of applied phosphorus in a calcareous Fluvisol. *Pedosphere.* 3:277-283.
- Tunesi, S., V. Poggie, and C. Gessa. 1999. Phosphate adsorption and precipitation in calcareous soils: The role of calcium ions in solution and carbonate minerals. *Nutr. Cycling Agroecosyst.* 53:219–227
- Udo, E.J., and J.A. Ogunwale. 1977. Phosphorus fraction in selected Nigerian soils. *Soil Sci. Soc. Am. J.* 41:1141-1146.
- Walkley, A. 1947. A critical examination of a rapid method for determining soil organic carbon in soils. Effect of variations in digestion conditions and inorganic soil constituents. *J. Soil Sci.* 63:251-263.
- Wallace, M., S. Aderval, A. Cristiane, and C. Antonio. 2003. An evaluation of copper biosorption by brown seaweed under optimized conditions. *Electronic Journal of Biotechnology.* ISSN: 0717-3458.
- Wandruszka, R. von. 2006. Phosphorus retention in calcareous soils and the effect of organic matter on its mobility. *Geochemical Transactions* 7:6, doi:10.1186/1467-4866-7-6.
- Wang, M.K., and Y.M. Tzou. 1995. Phosphate sorption by calcite, and iron-rich calcareous soils. *Geoderma* 65:249-261.

- Waychunas, G.A., B.A. Rea, C.C. Fuller, and J.A. Davis. 1993. Surface chemistry of ferrihydrite: Part 1. EXAFS studies of the geometry of co-precipitated and adsorbed arsenate. *Geochim. Cosmochim. Acta* 57:2251-2269.
- White, G.N., and J.B. Dixon. 2003. *Soil mineralogy laboratory Manual*. 9th Edition. Dep. Soil Crop Sci. Texas A&M Univ. Coll. Station, Texas.
- Williams, J.D.H., J.K. Syers, R.F. Harris, and T.E. Walker. 1967. Fractionation of soil inorganic phosphate by a modification of Chang and Jackson procedure. *Soil Sci. Soc. Am. Proc.* 31:736-739.
- World Phosphate Institute. 2004. *Annual Report*. IMPHOS member companies.
- Yost, R., A.B. Onken, F. Cox, and S. Rcid. 1992. The diagnosis of phosphorus deficiency and predicting phosphorus requirements *In: Proc. Trop Soils Bull. No.92-03, phosphorus decision support system workshop, College, Station Texas, March 11-12, 1992. University of Hawaii, Honolulu, HI, USA.*1-20.
- Yuji, A. and D.L. Sparks. 2001. ATR-FTIR Spectroscopic investigation on phosphate adsorption mechanism at the ferrihydrite-water interface. *J. Colloid and Interface Sci.* 241:317-326.
- Zhang, F., S. Kang, J. Zhang, R. Zhang and F. Li. 2004. Nitrogen fertilization on ptake of soil inorganic phosphorus fractions n the wheat root zone. *Soil Sci. Soc. Am. J.* 68:1890-1895.
- Zhang, H., J.L. Schroder, J.K. Fuhrman, N.T. Basta, D.E. Storm, and M.E. Payton. 2005. Path and multiple regression analysis of phosphorus sorption capacity. *Soil Sci. Soc. Am. J.* 69:96-106.
- Zhang, Y.M. D. X. Luo, S. R. He, Y. R. Ma, J. W. Miao. 1993. A preliminary study of phosphorus adsorption and desorption in the soils of Yinbei. *Ningxia J. Agro-Forestry Sci. Tech.* 4:17-21.
- Zhou, M., and Y. Li. 2001. Phosphorus sorption characteristics of calcareous soils and limestone from the southern Everglades and adjacent farmlands. *Soil Sci. Soc. Am. J.* 65:1404-1412.

Appendix I. Selected properties of the soils studied.

Soil	Horizon	Depth cm	pH	CaCO ₃ Ca _{ex}		OM	EC	Olsen P	Fe _d	Fe _o	Al _d	Al _o
				-----g kg ⁻¹ -----								
Shahdara	Ap	0-16	8.3	48	1.42	11.0	0.4	8.5	6.7	0.28	0.88	0.38
	C1	16-32	8.4	98	1.54	5.0	0.3	2.4	7.1	0.42	0.67	0.38
	C2	32-63	8.0	103	0.50	3.0	0.2	1.7	3.6	0.07	0.30	0.11
	C3	63-78	8.3	98	0.97	3.0	0.2	2.3	5.2	0.21	0.41	0.20
Sultanpur	Ap	0-13	8.3	130	1.82	25.0	0.9	27.4	6.3	0.28	0.47	0.34
	Bw1	13-39	8.2	118	1.71	8.0	1.6	3.0	6.9	0.28	0.58	0.41
	Bw2	39-62	8.1	50	2.20	6.0	2.6	1.4	8.2	0.49	0.52	0.52
	2C1	62-81	8.2	75	1.12	4.0	1.9	6.2	6.1	0.28	0.53	0.25
Pacca	Ap	0-15	8.6	46	1.93	20.0	0.6	30.8	7.8	0.35	0.63	0.60
	Bat	15-32	8.3	60	2.11	8.0	1.0	6.7	7.0	0.42	0.62	0.74
	Bt1	32-53	8.2	70	2.49	6.0	1.5	4.3	5.9	0.42	0.55	0.70
	Bt2	53-92	8.8	140	1.63	6.0	0.9	4.2	8.2	0.28	0.65	0.63
Pitafi	Ap	0-15	7.9	80	4.30	10.0	59.0	11.9	3.6	0.49	0.47	0.77
	Ayz	15-41	8.0	95	1.84	7.0	11.5	10.8	9.3	0.56	0.68	0.56
	Bwy1	41-57	8.3	250	1.56	4.0	5.6	8.4	9.3	0.42	0.70	0.47
	Bwy2	63-111	8.1	130	2.22	2.0	3.9	4.5	7.2	0.28	0.50	0.27
Peshawar	Ap	0-11	7.5	195	1.53	21.0	0.6	16.1	10.5	0.28	0.64	0.60
	Bt1	11-43	7.3	186	1.61	10.0	0.3	11.2	10.6	0.42	0.75	0.74
	Bt2	43-66	7.4	198	1.52	8.0	0.3	10.1	9.9	0.42	0.67	0.70
	2Btb	66-98	7.4	203	1.35	10.0	0.3	13.5	9.0	0.28	0.58	0.63
Murree	A	0-11	7.5	30	2.18	22.1	0.2	8.4	13.2	0.21	0.61	0.62
	Bt1	11-30	7.8	30	1.82	23.6	0.2	4.5	14.4	0.49	0.63	0.60
	Bt2	30-52	7.4	12	1.85	11.1	0.1	3.4	15.4	0.63	0.74	0.70
	2Bt3	52-58	7.7	10	1.93	21.5	0.1	3.9	16.5	0.70	0.83	0.84
Guliana	Ap	0-12	7.6	12	1.59	12.0	2.4	11.5	10.3	0.28	1.35	0.71
	Batc	12-25	7.2	3	1.63	4.5	0.2	5.6	11.1	0.28	1.45	0.72
	Btc1	25-56	7.8	2	2.08	7.7	0.2	2.9	13.5	0.42	2.28	1.13
	Btc2	56-83	7.5	6	1.93	6.0	0.3	10.6	13.6	0.28	2.37	0.98
Prb-Ostb	Ah	0-4	5.2	15	0.06	57.8	0.2	17.0	15.0	1.26	2.17	1.30
	Bv	4-25	4.7	3	0.66	11.6	0.1	6.7	12.9	1.40	2.30	1.46
	Bt	25-50	6.0	4	2.21	4.8	0.1	16.0	23.2	1.33	3.27	1.84
	C	>50	7.7	57	0.05	5.9	0.3	7.5	20.0	0.77	2.34	1.10
Prb-Wein	Bv	4-25	4.5	5	0.48	10.7	0.1	5.0	9.8	1.33	1.95	1.28
	Bt	25-45	5.9	5	2.21	8.4	0.2	5.5	16.7	1.12	2.37	1.31
	C	>45	7.1	250	0.07	6.9	3.2	5.5	20.0	0.21	1.31	0.55

Ca_{ex}, exchangeable calcium; **OM**, organic matter; **EC**, electrical conductivity; **Fe_d**, citrate bicarbonate dithionite extractable iron; **Fe_o**, oxalate extractable iron; **Al_d**, citrate bicarbonate dithionite extractable aluminium; **Al_o**, oxalate extractable aluminium.

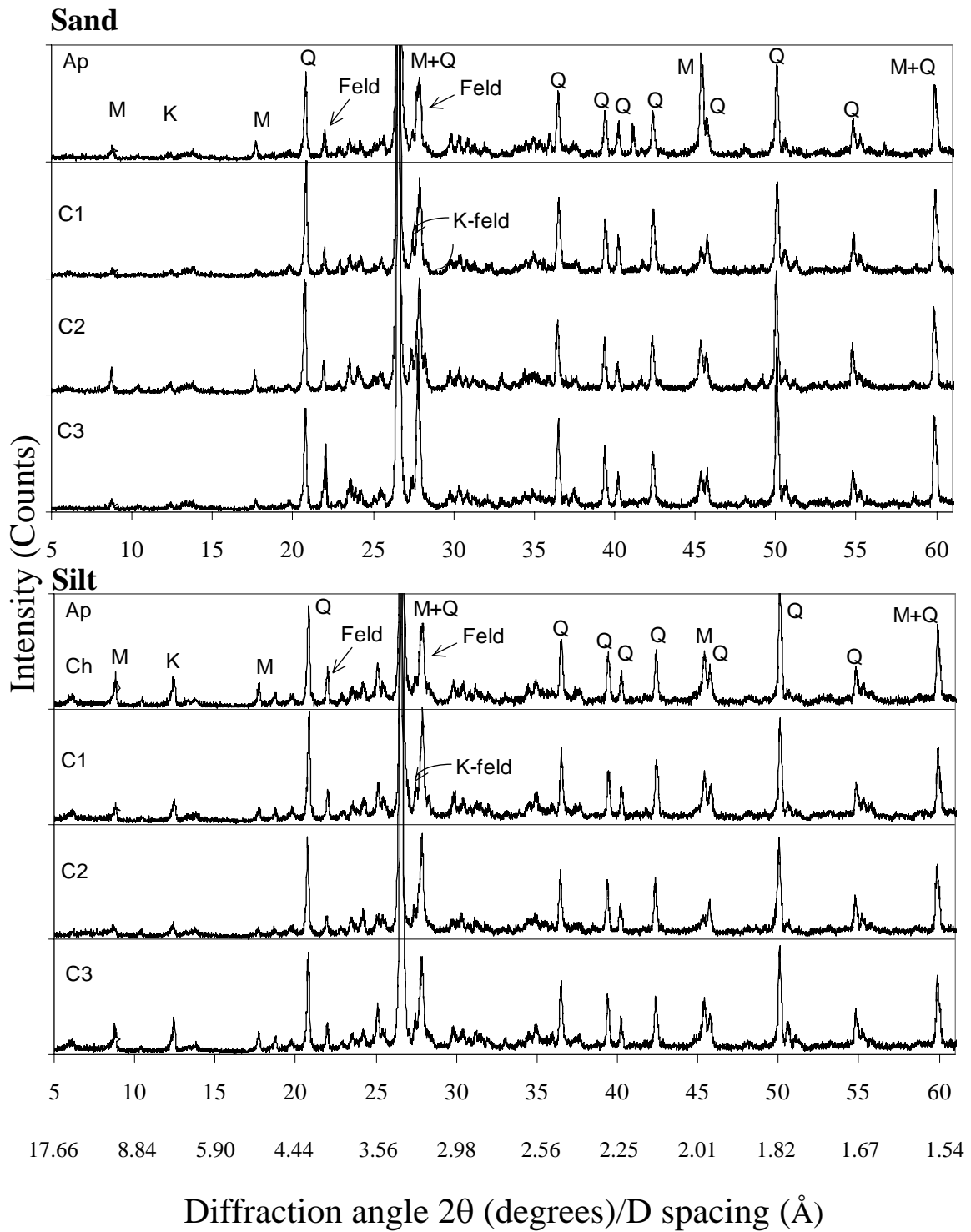
Appendix II. Major and trace elemental analysis of the soils studied as determined by XRF.

Soil	Horizon	Depth cm	Al ₂ O ₃	SiO ₂	Fe ₂ O ₃	CaO	MgO	K ₂ O	P ₂ O ₅	TiO ₂	Zr
			g kg ⁻¹						mg kg ⁻¹		
Shahdara	Ap	0-16	133	569	52.1	72.7	28.50	25.29	1799	6780	194
	C1	16-32	137	563	53.8	73.5	29.54	25.38	1340	7200	183
	C2	32-63	108	685	35.2	61.8	19.62	20.42	1356	6100	298
	C3	63-78	122	624	44.8	69.0	24.78	23.35	1416	6560	233
Sultanpur	Ap	0-13	132	557	53.0	71.7	29.15	26.10	1715	6850	188
	Bw1	13-39	140	557	55.5	71.9	30.22	27.33	1555	7280	186
	Bw2	39-62	148	529	61.3	74.5	32.60	28.40	1314	7230	156
	2C1	62-81	134	575	51.8	73.9	29.41	25.79	1332	6880	185
Pacca	Ap	0-15	157	545	65.9	42.4	33.09	30.96	2224	7700	201
	Bat	15-32	168	538	71.0	37.2	33.85	32.83	1632	7830	172
	Bt1	32-53	165	523	69.6	50.3	34.79	32.28	1493	7940	150
	Bt2	53-92	157	501	66.5	70.5	32.89	30.28	1219	7700	145
Pitafi	Ap	0-15	95	434	40.4	93.1	53.00	19.78	1323	5260	161
	Ayz	15-41	155	497	66.5	71.3	35.97	30.31	1324	7860	155
	Bwy1	41-57	158	505	67.4	66.7	36.63	30.63	1282	7880	152
	Bwy2	63-111	151	598	59.2	83.0	35.04	29.19	1419	7280	176
Peshawar	Ap	0-11	127	497	55.8	98.8	32.36	23.57	1701	7430	187
	Bt1	11-43	127	499	55.9	101.9	30.16	23.04	1391	7360	183
	Bt2	43-66	125	506	54.2	105.6	29.64	22.90	1716	7310	187
	2Btb	66-98	117	508	51.7	111.3	29.34	22.08	2142	7170	199
Murree	A	0-11	108	690	46.0	8.0	17.92	17.60	1177	7580	315
	Bt1	11-30	115	695	48.0	16.6	19.23	18.77	1102	7720	308
	Bt2	30-52	119	704	51.4	8.4	19.62	19.16	979	8040	317
	2Bt3	52-58	122	693	52.0	8.3	19.81	19.55	963	8010	300
Guliana	Ap	0-12	134	666	52.5	16.8	18.27	23.91	994	7980	348
	Batc	12-25	136	673	53.2	15.3	18.47	23.90	854	8020	353
	Btc1	25-56	151	638	62.4	15.4	20.56	25.06	782	8370	301
	Btc2	56-83	151	633	63.8	14.6	21.50	25.52	883	8200	298
Prb-Ostb	Ah	0-4	96	665	35.5	7.6	9.62	26.41	1856	7690	588
	Bv	4-25	110	729	40.6	5.0	10.62	28.91	1057	8140	607
	Bt	25-50	153	621	68.2	9.4	17.60	30.48	1799	7120	515
	C	>50	133	600	57.6	46.0	17.24	29.35	2033	7330	523
Prb-Wein	Bv	4-25	98	766	31.9	5.5	7.45	24.63	291	7310	522
	Bt	25-45	133	668	51.3	9.1	13.93	28.45	494	6690	413
	C	>45	104	321	38.3	249.2	13.59	27.06	1131	4730	99

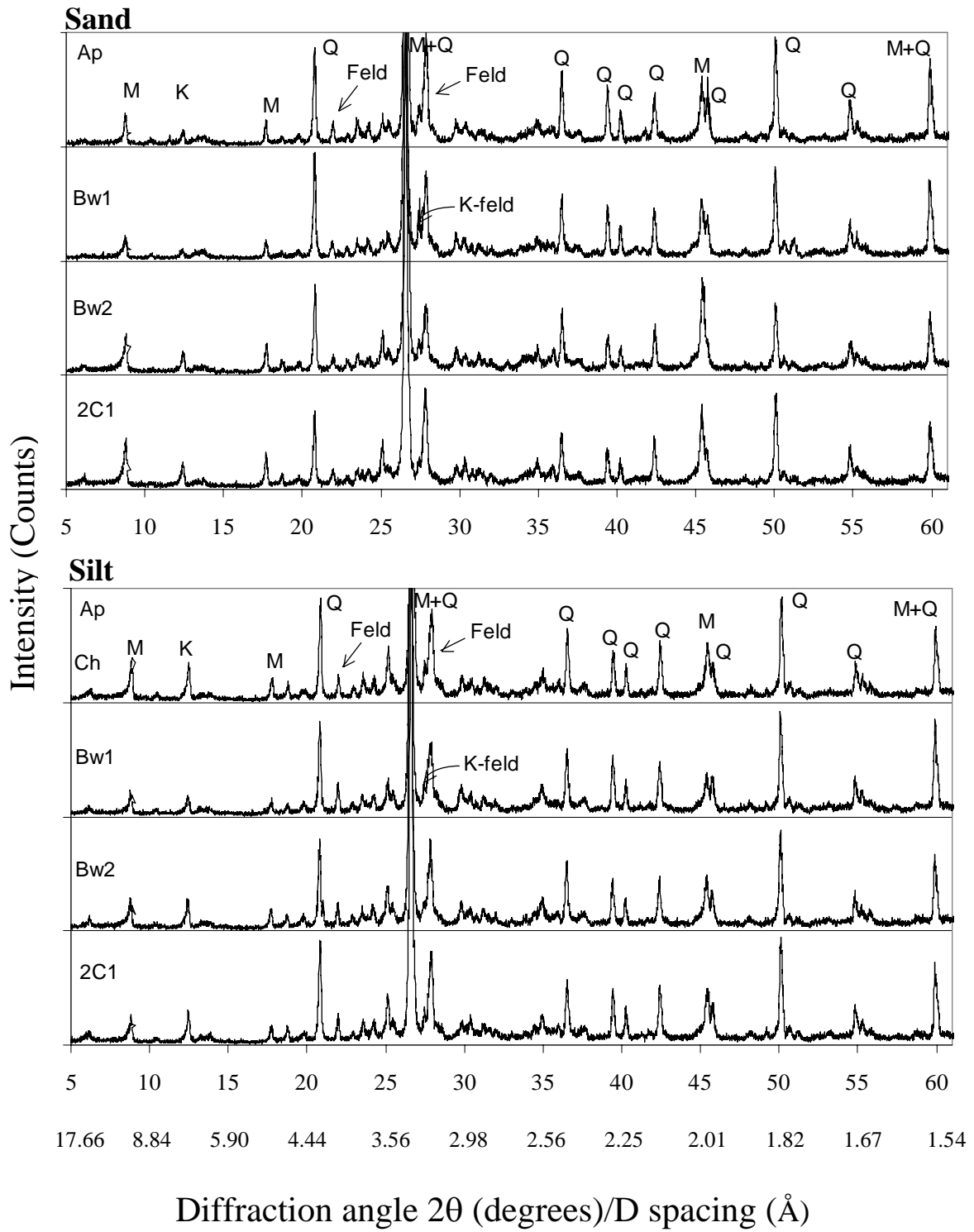
Appendix III

X-ray diffraction pattern of sand ($>50\ \mu\text{m}$) and silt ($2\text{-}50\ \mu\text{m}$) fractions taken from four horizons (two horizons in case of German soils) of each soil profile investigated: Q, quartz; Feld, feldspar; K-feld, potassium feldspar; M, mica; Ch, chlorite.

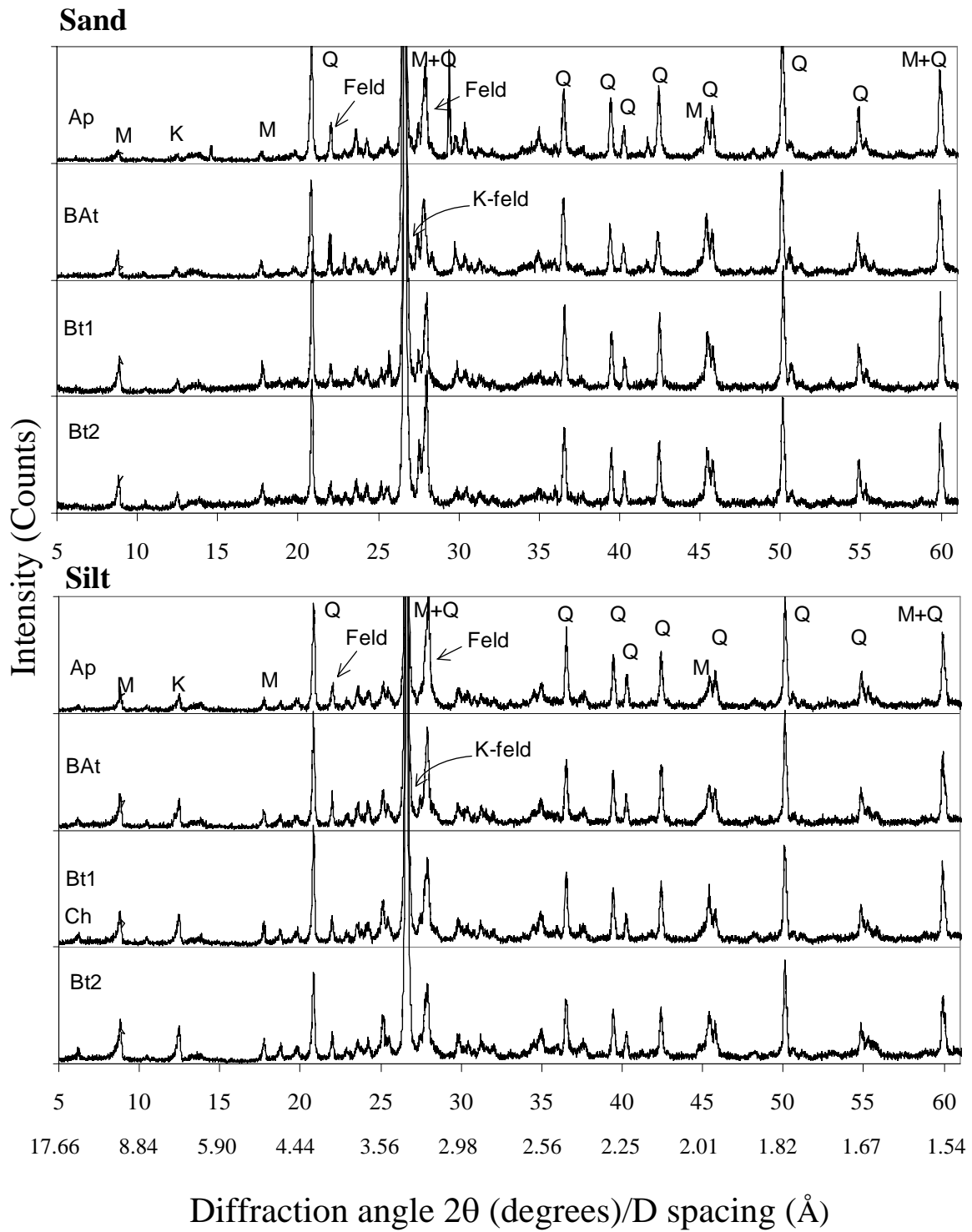
Shahdara profile



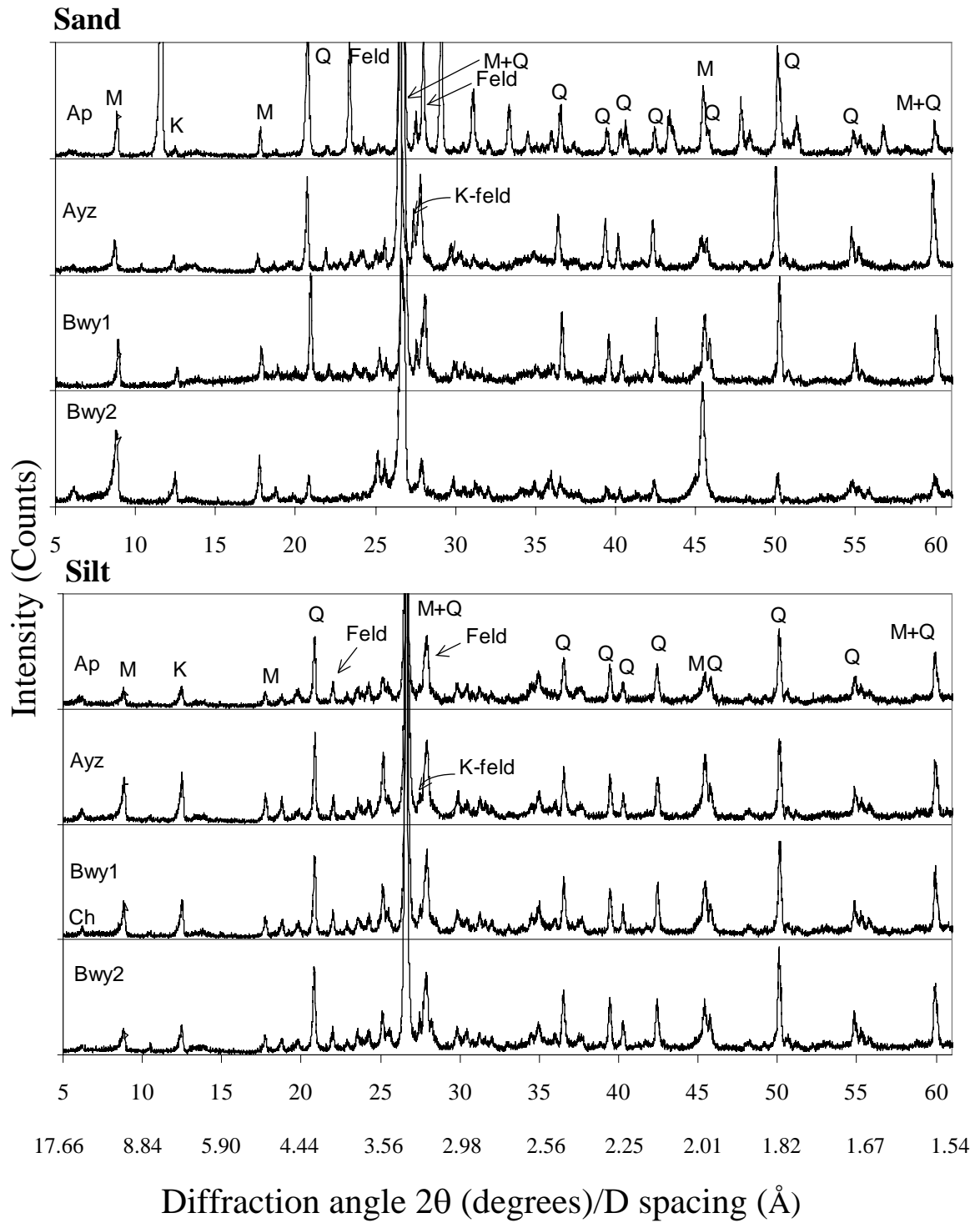
Sultanpur profile



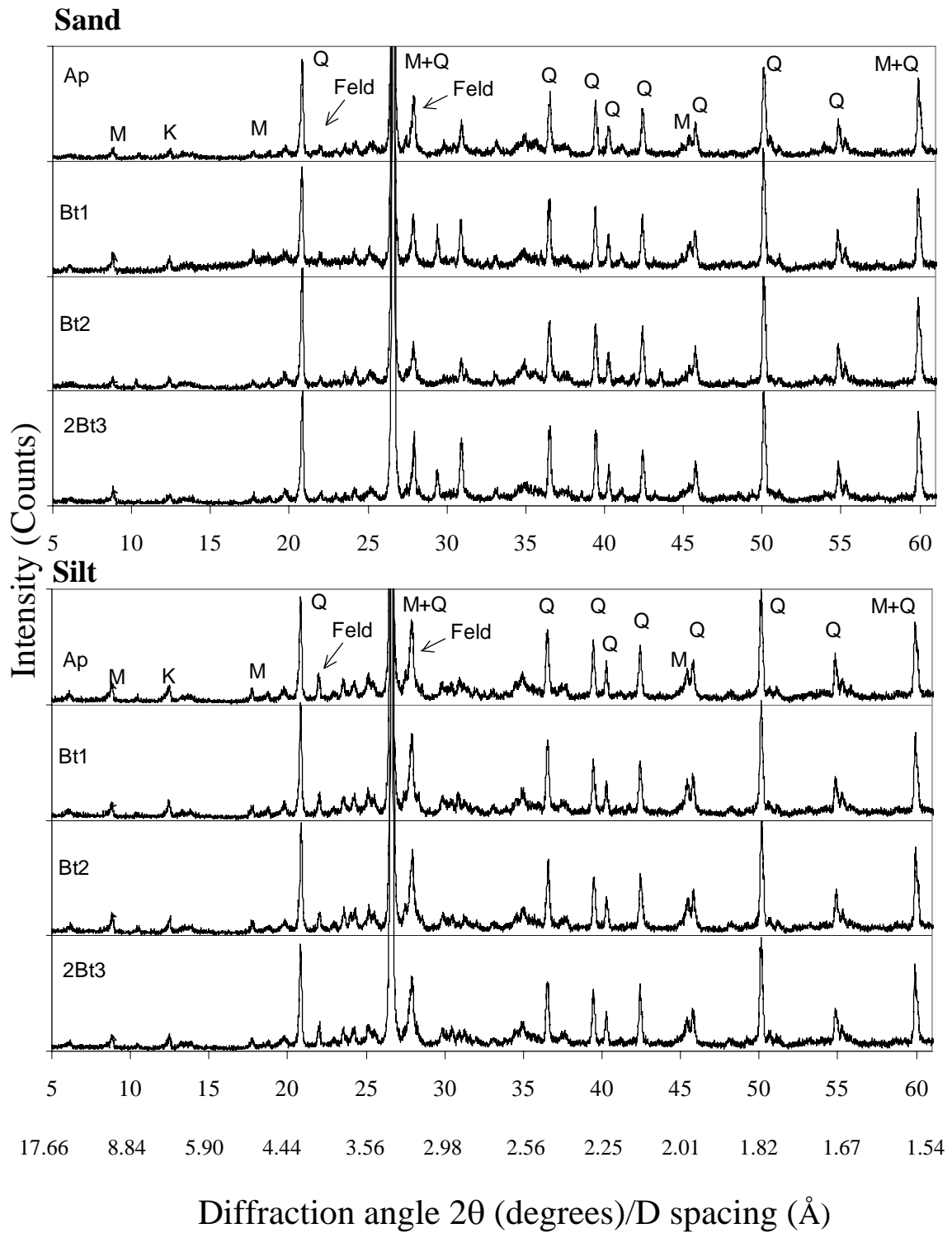
Pacca profile



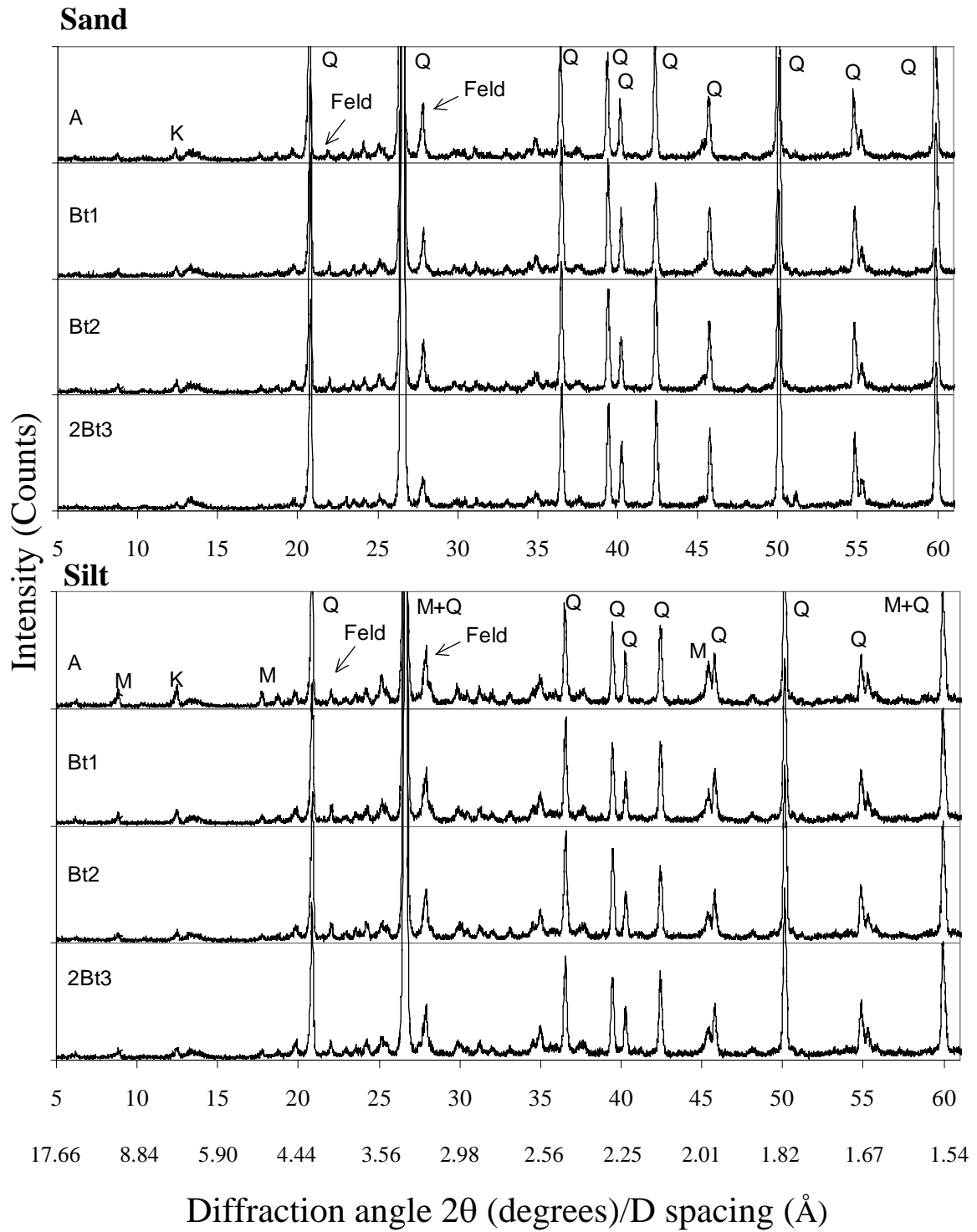
Pitafi profile



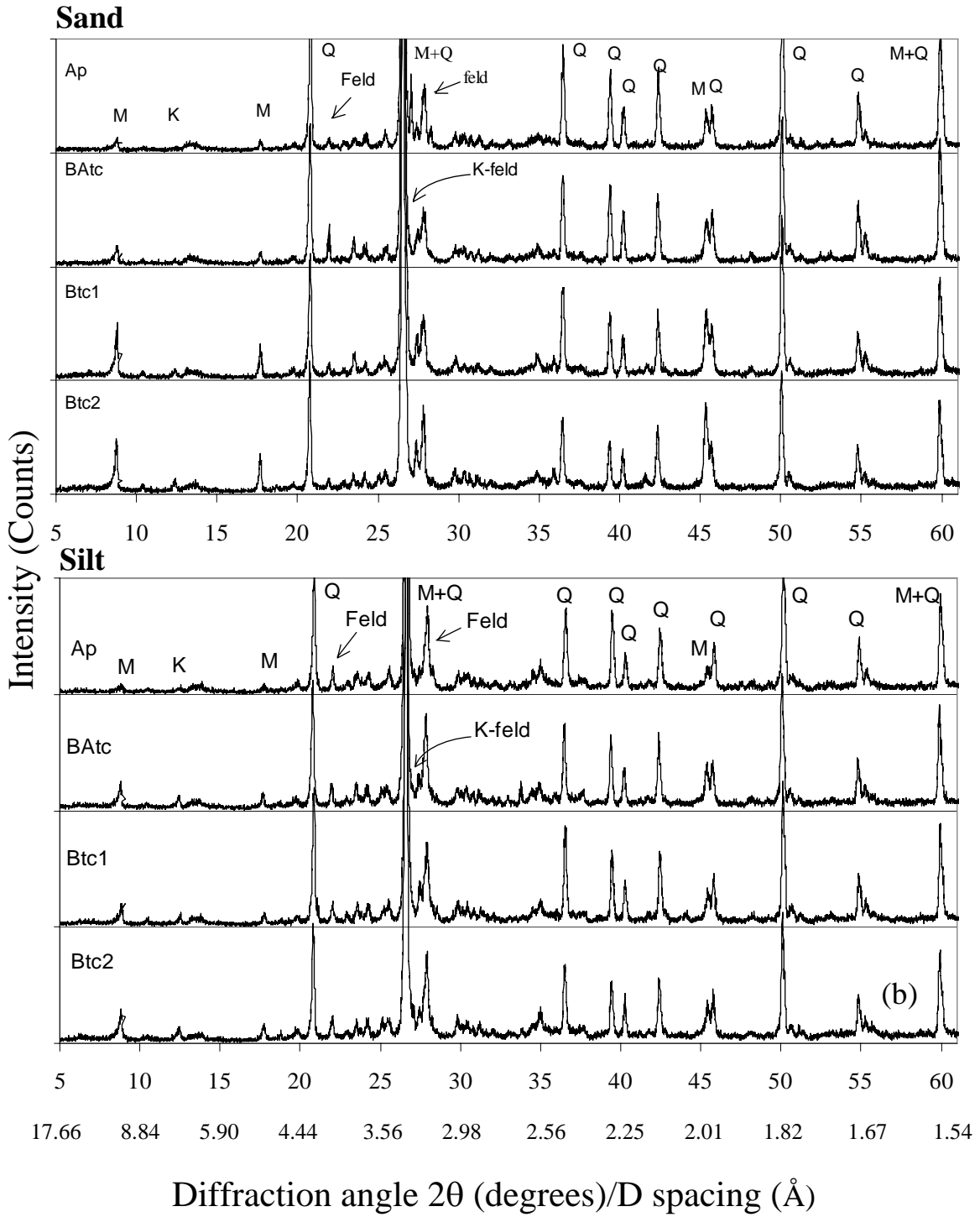
Peshawar profile



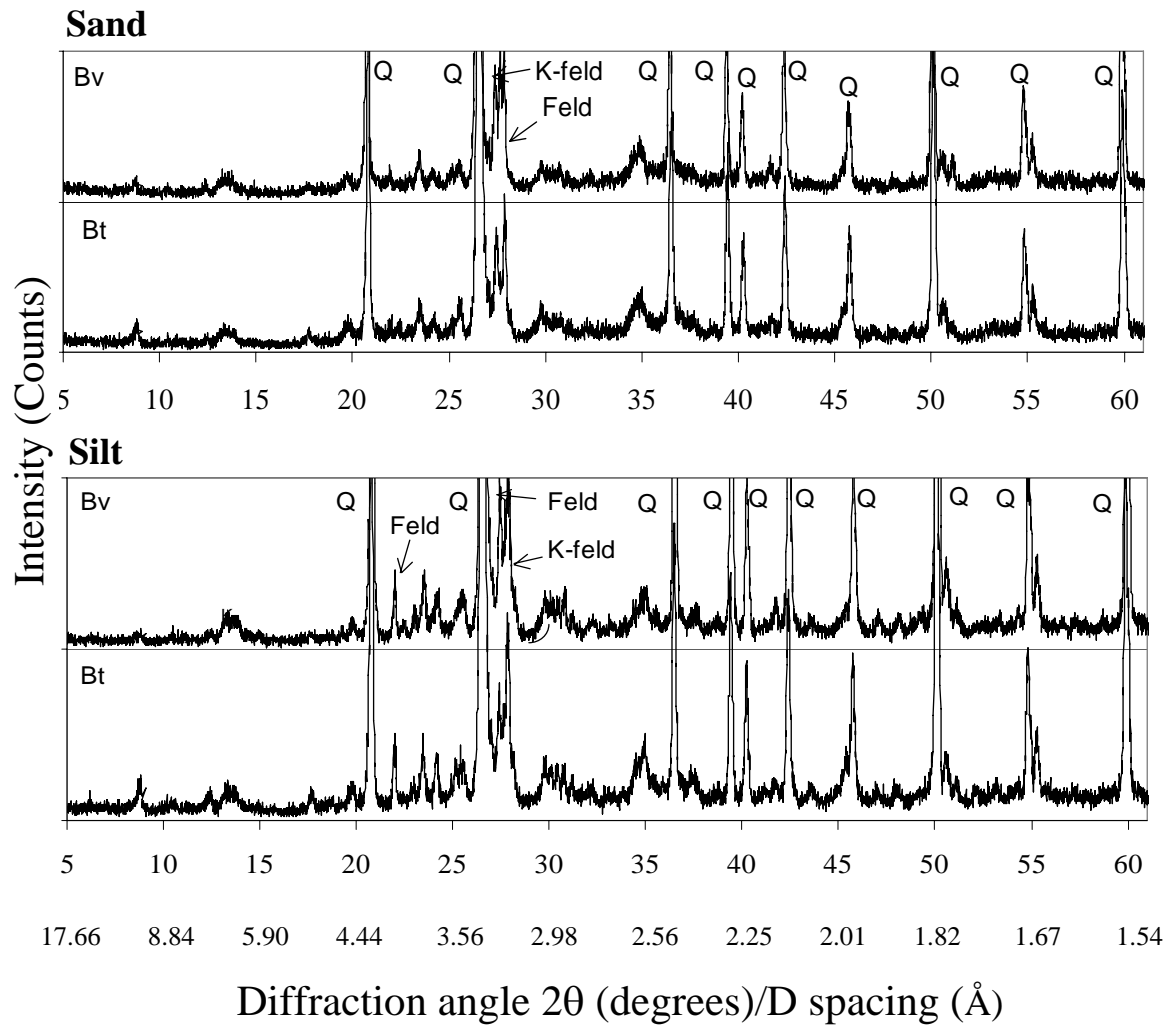
Murree profile



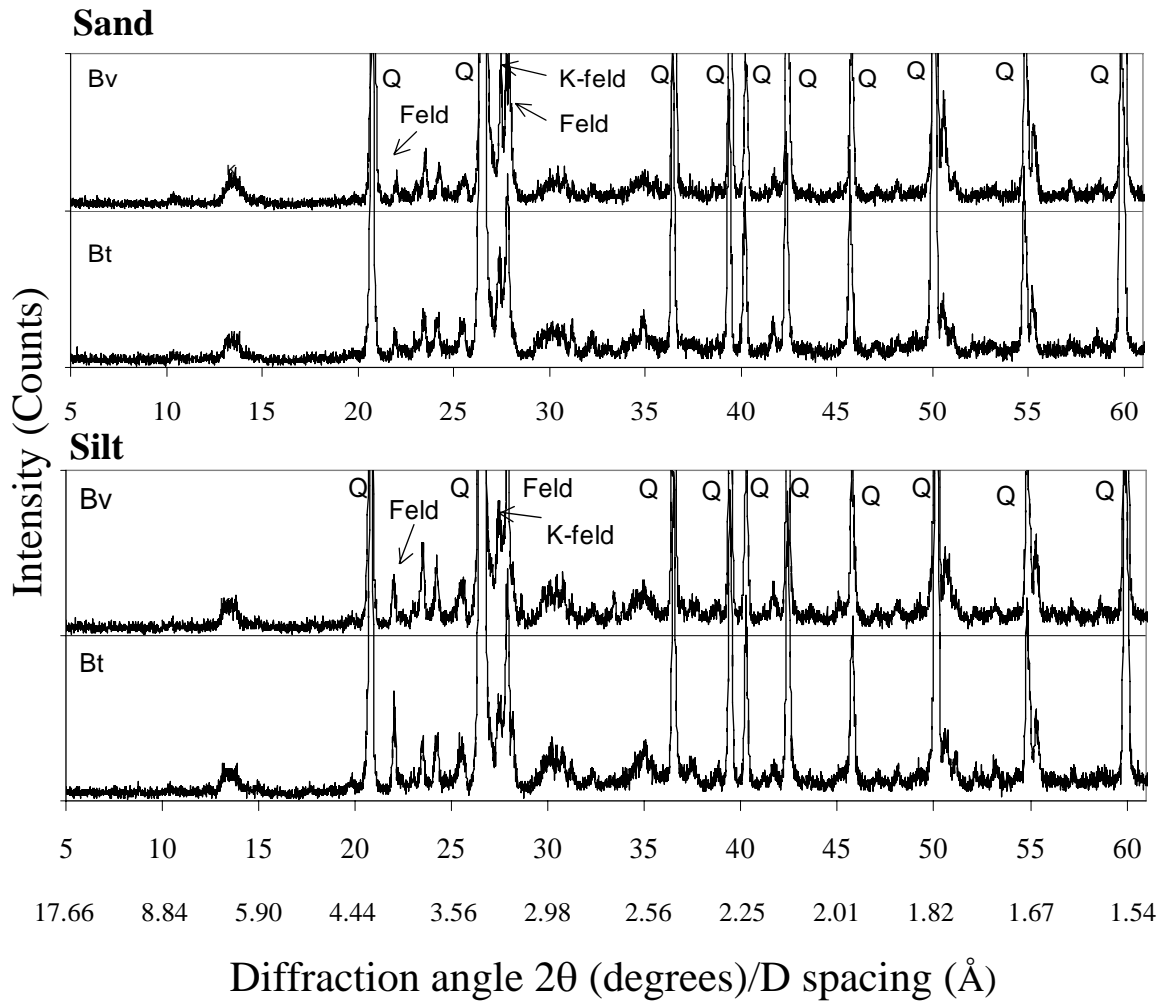
Guliana profile



Parabraunerde from Osterburken



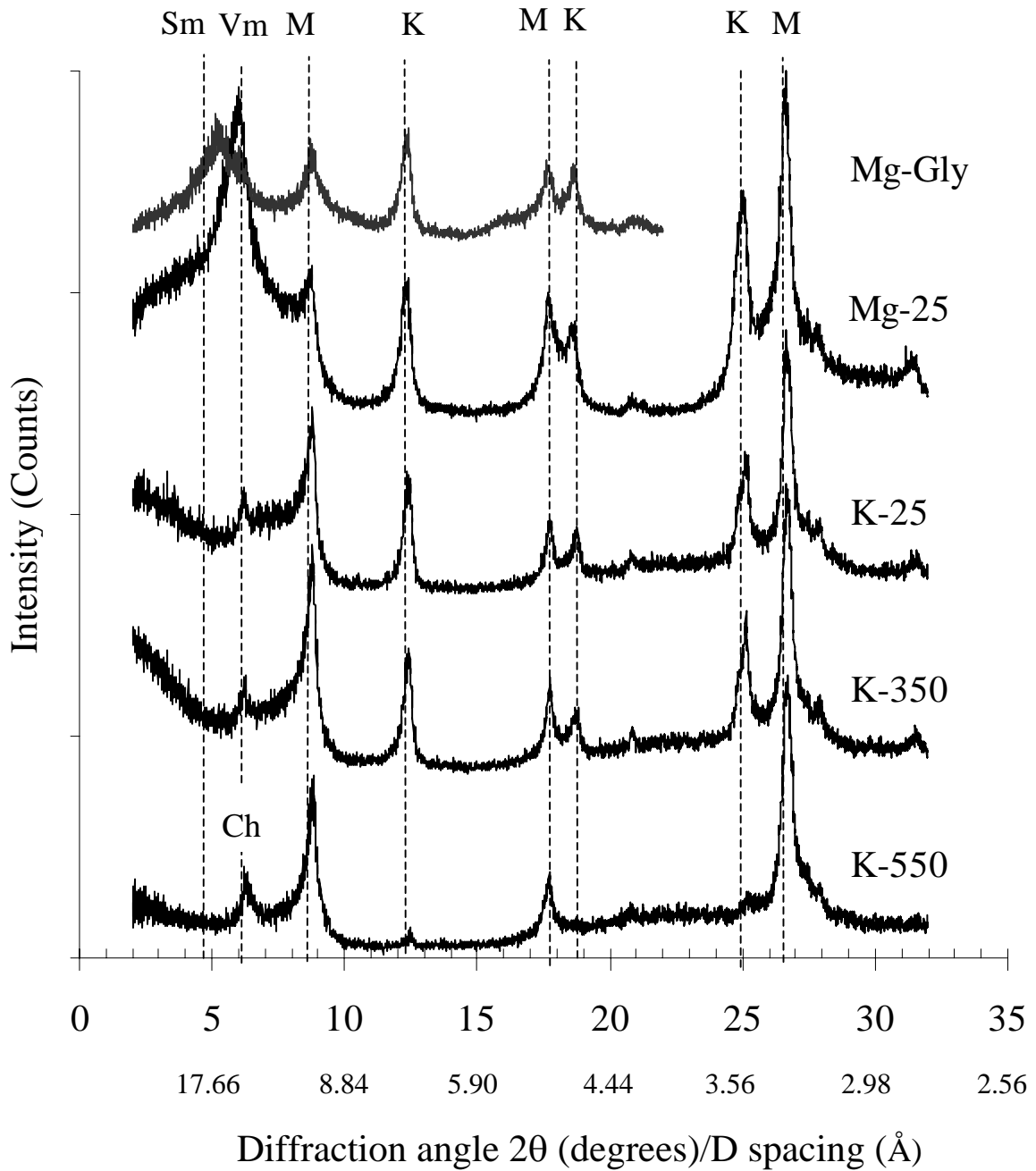
Parabraunerde from Weingarten

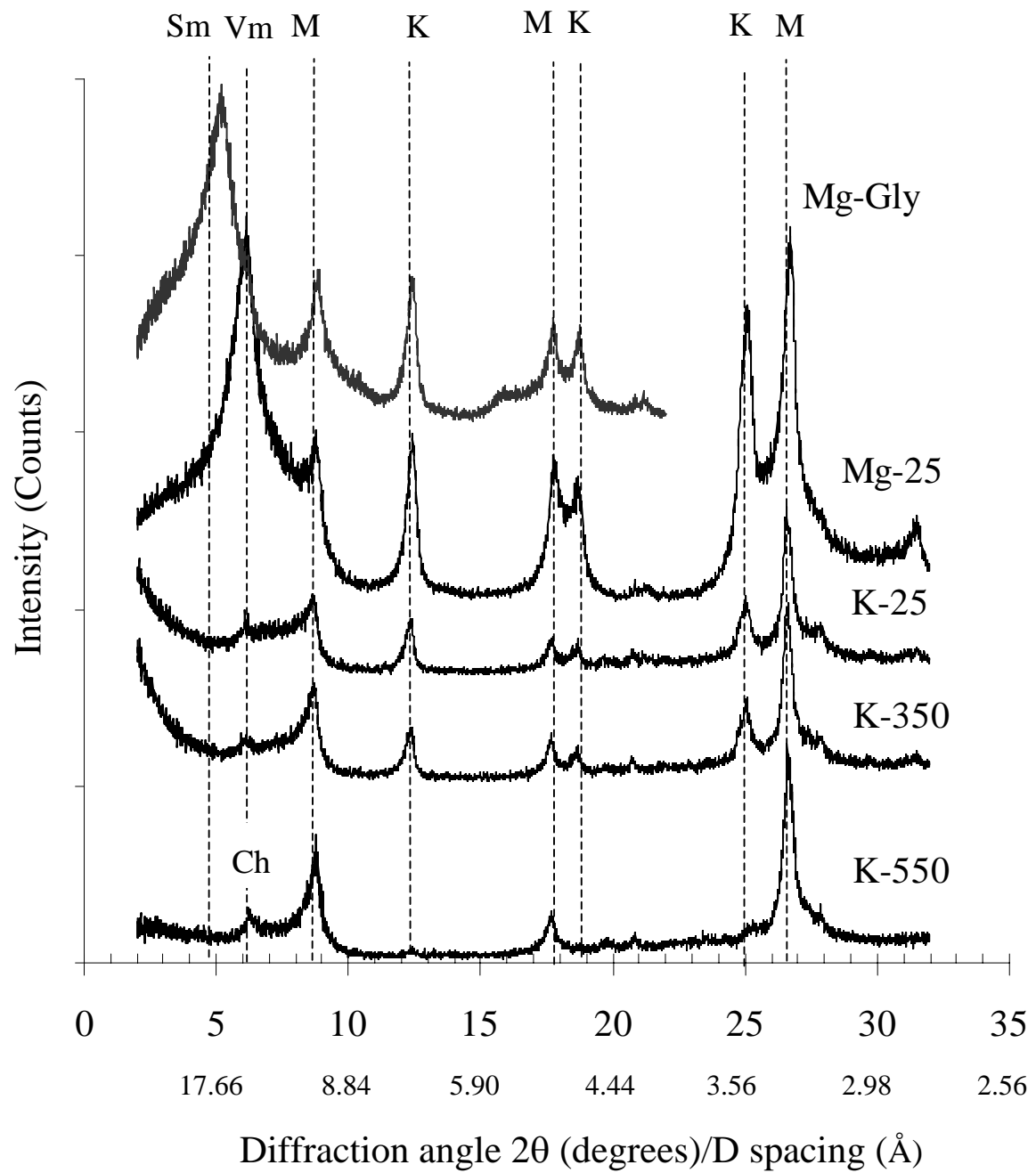


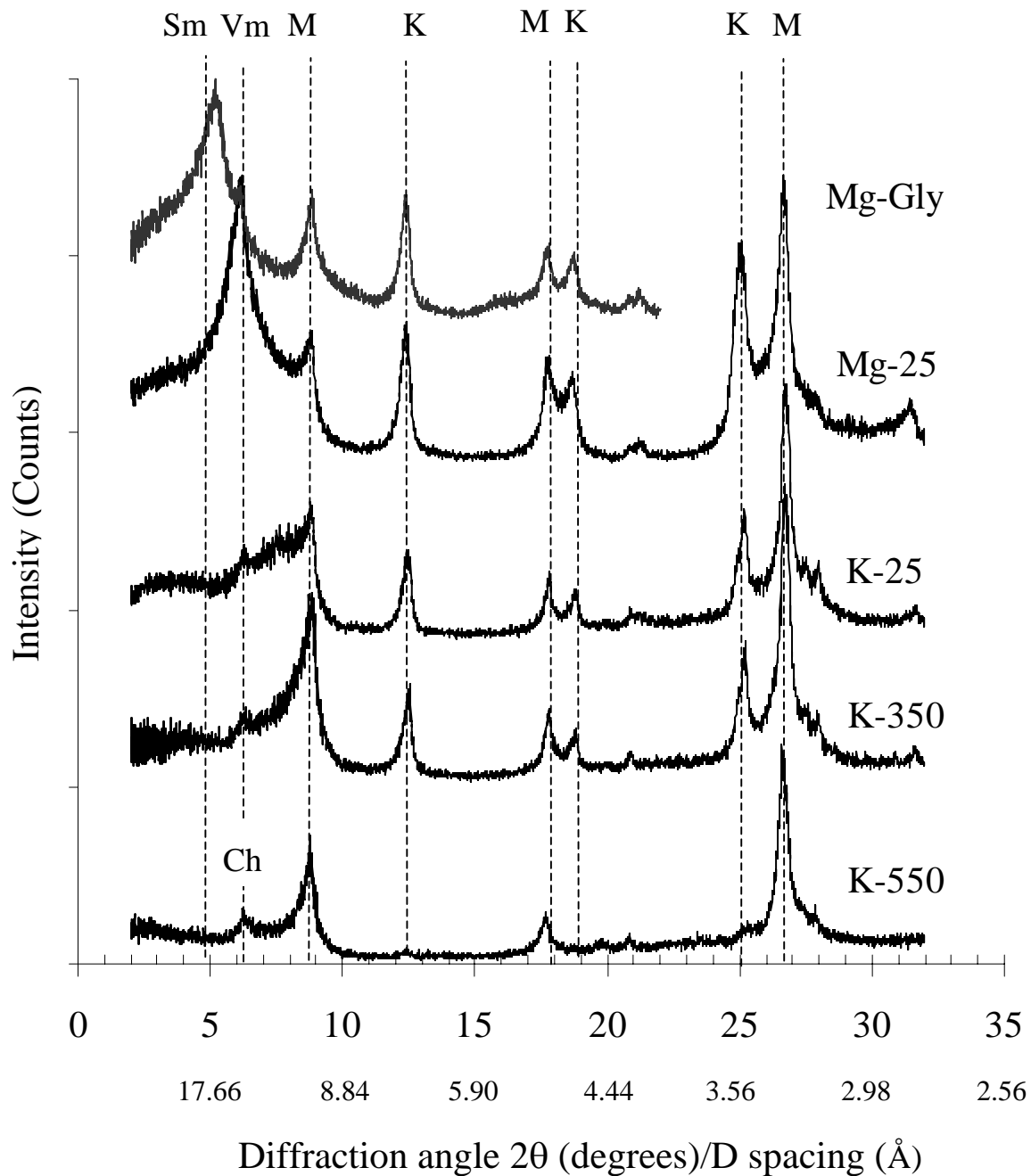
Appendix IV

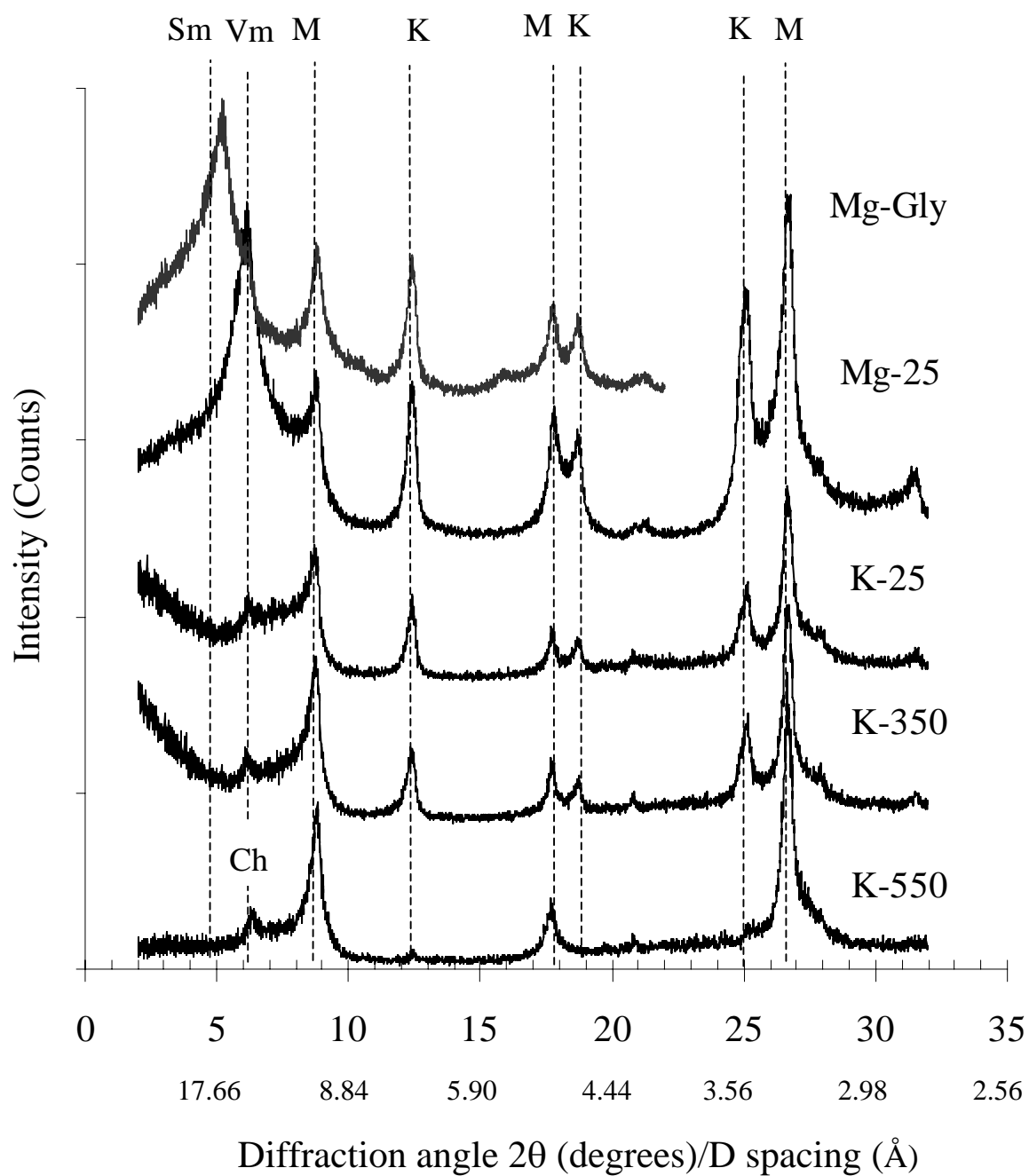
X-ray diffraction pattern for clay (<2 μ m) size fractions taken from four horizons (two horizons in case of German soils) of each soil profile investigated: Mg-Gly., Mg saturated and glycolated; Mg-25, Mg saturated and air dried; K-25, K saturated and air dried; K-350, K saturated and heated at 350°C; and K-550, K saturated and heated at 550°C. Sm, Smectite; Vm, vermiculite; Ch, chlorite; M, mica; K, kaolinite.

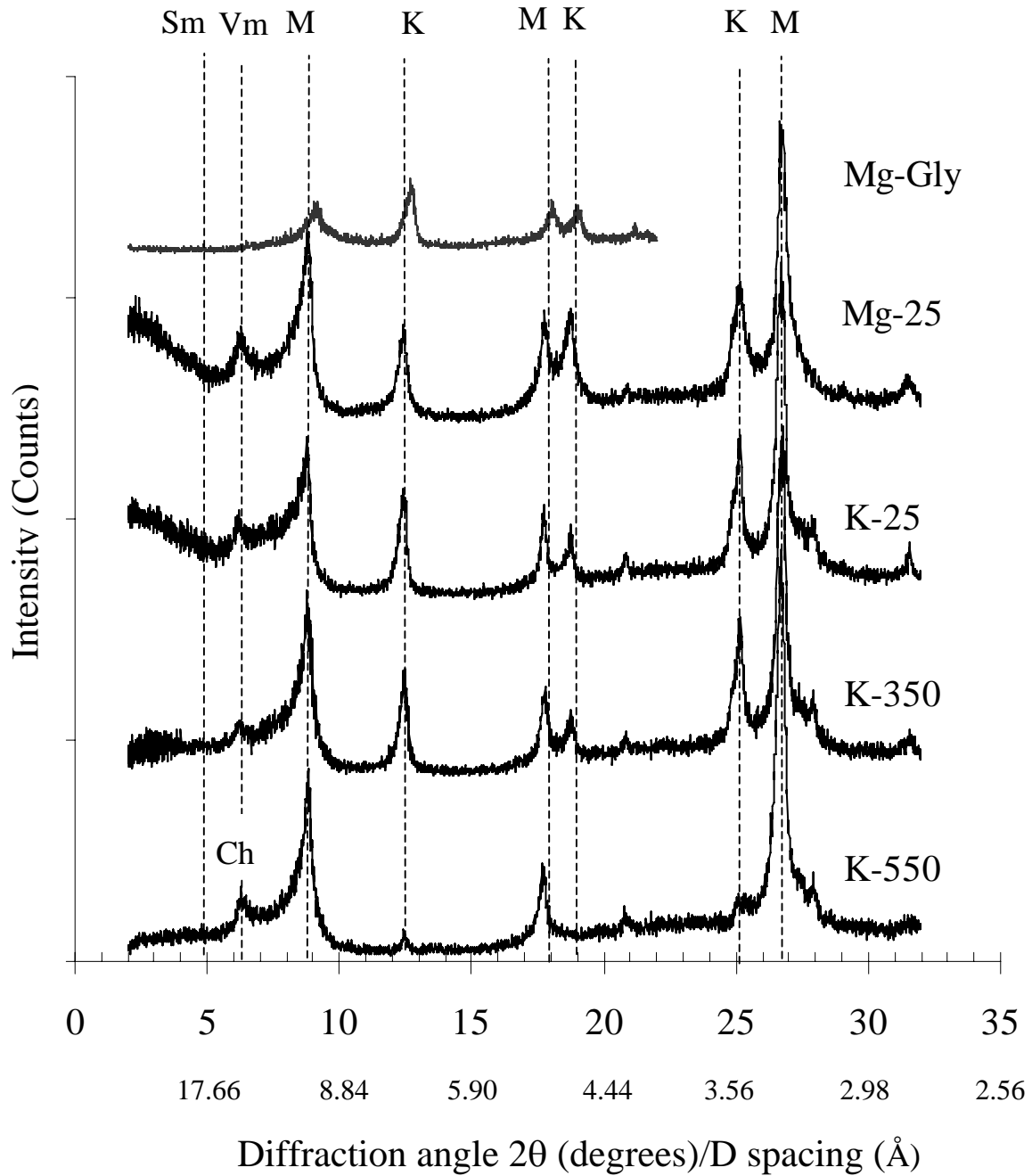
:

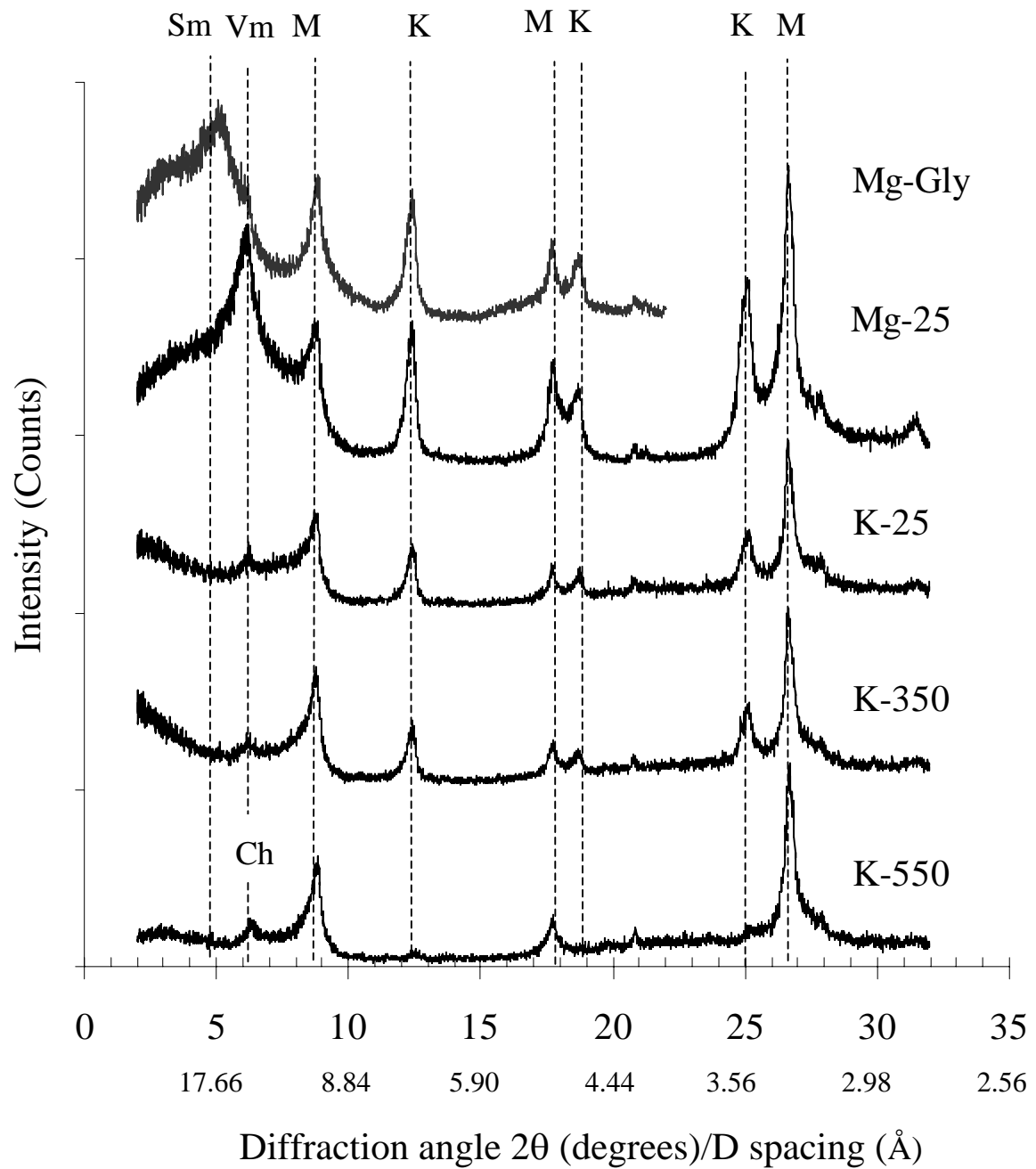
Shahdara soil clay (2 μm) Ap horizon (0-16 cm)

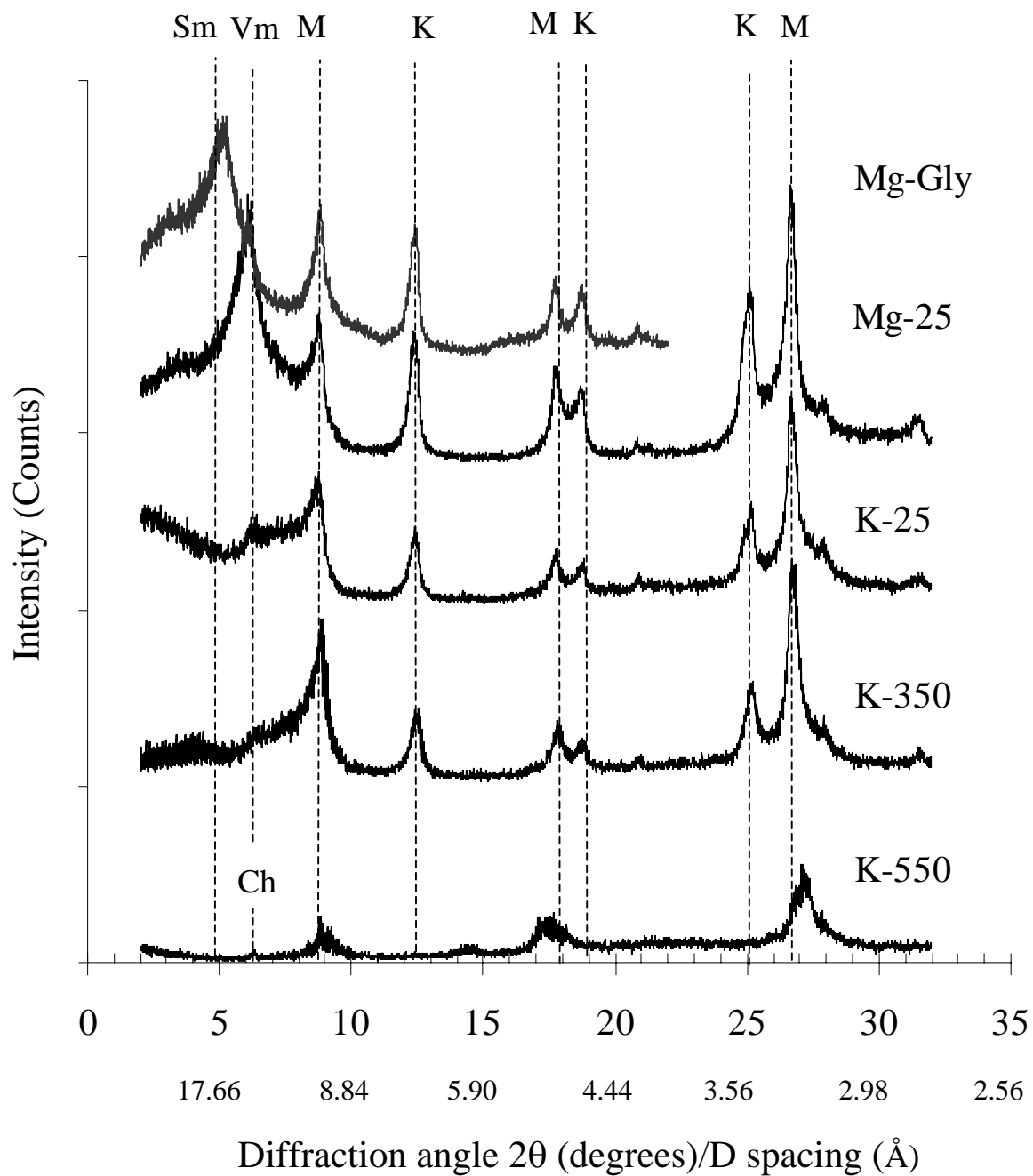
Shahdara soil clay (2 μm) C1 horizon (16-32 cm)

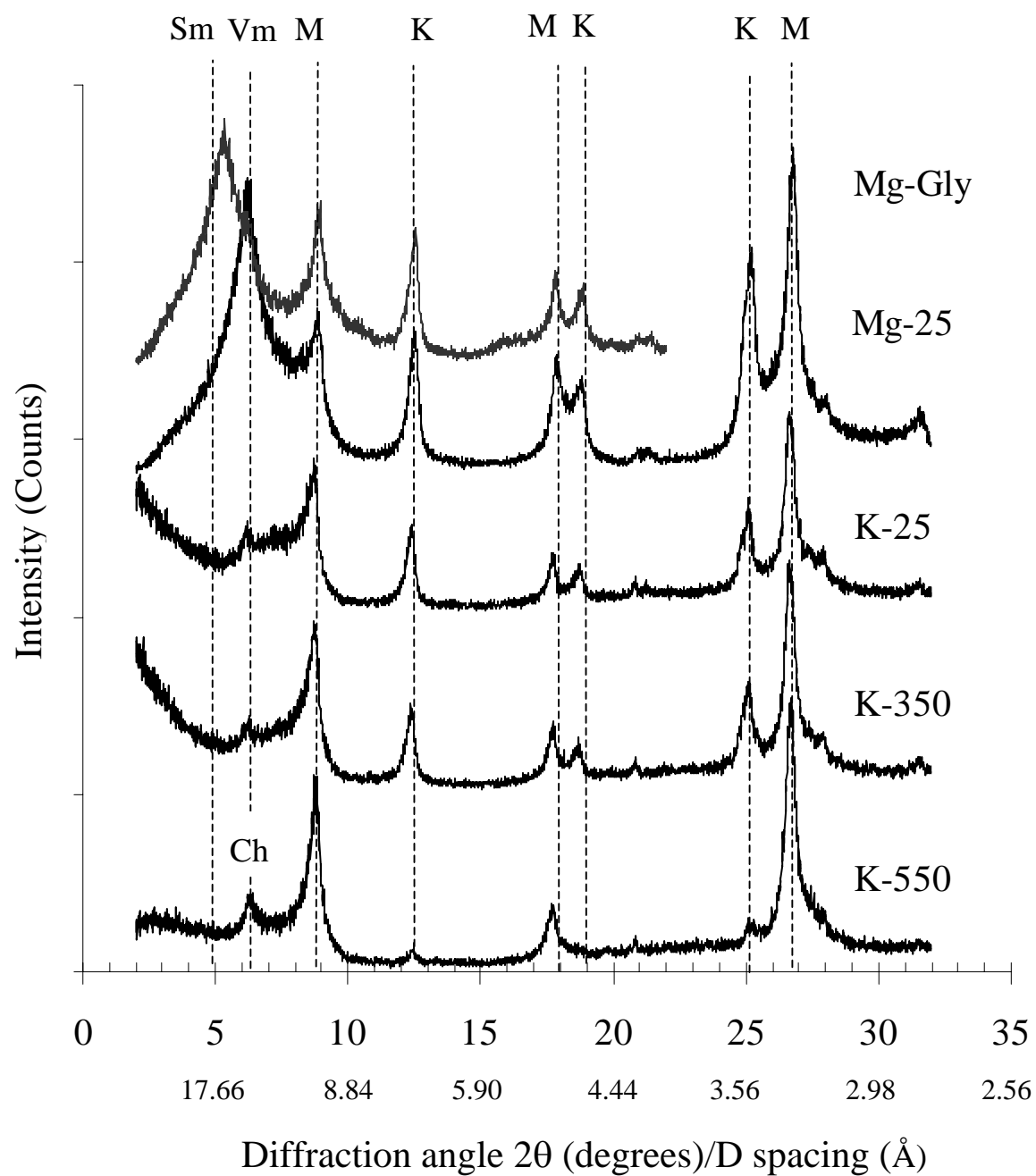
Shahdara soil clay (2 μm) C2 horizon (32-63 cm)

Shahdara soil clay (2 μm) C3 horizon (63-78 cm)

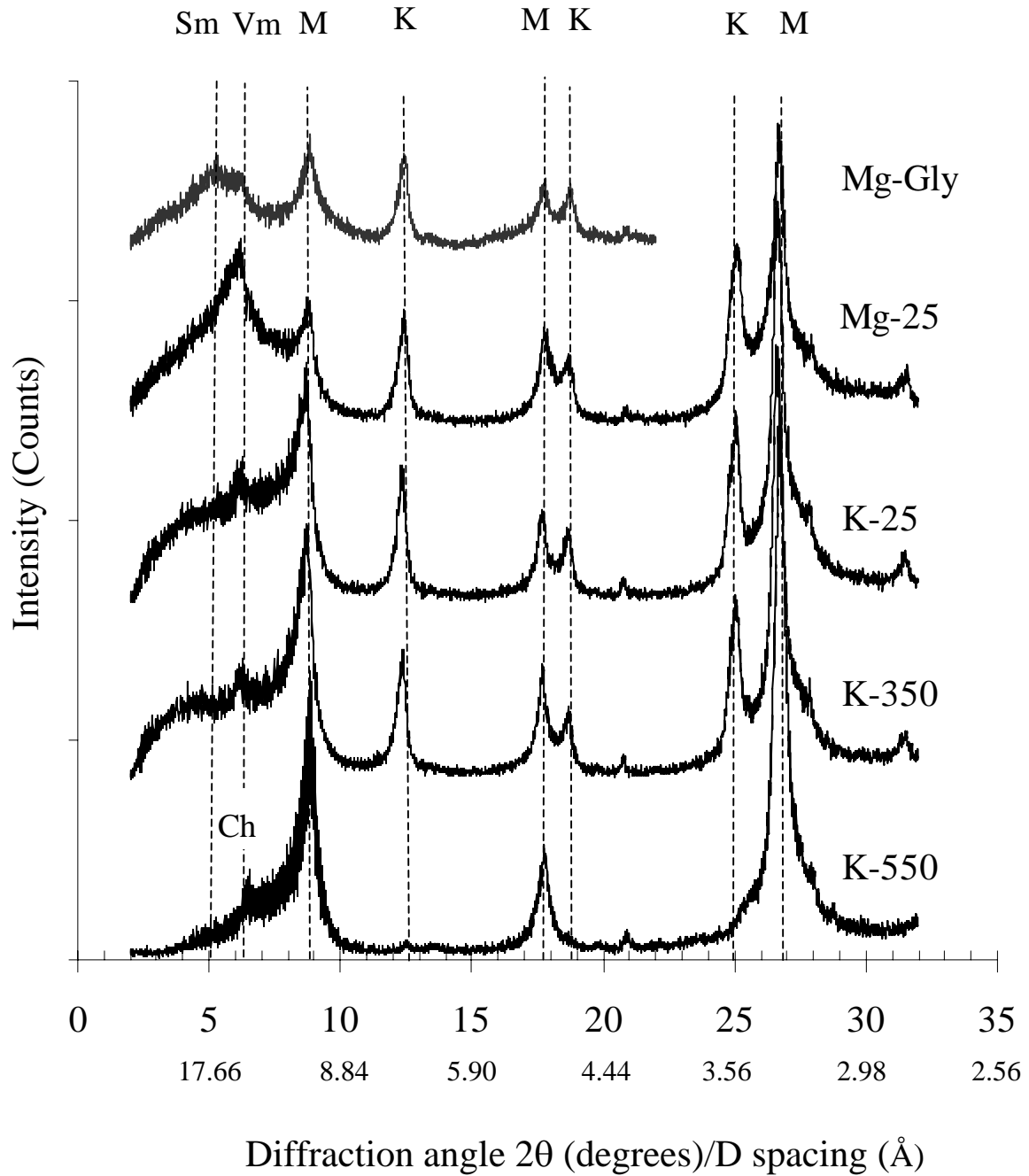
Sultanpur soil clay (2 μm) Ap horizon (0-13 cm)

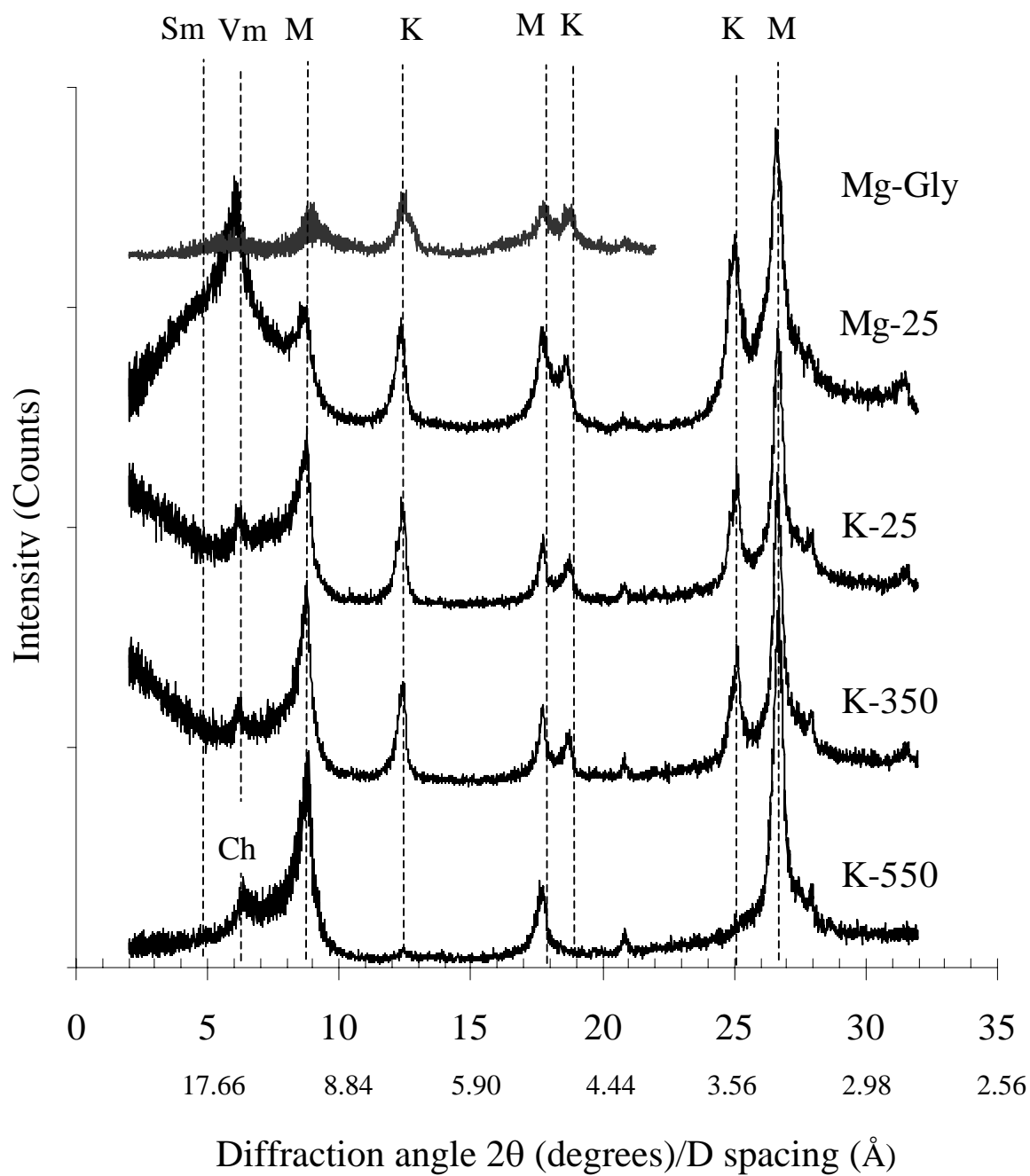
Sultanpur soil clay (2 μm) Bw1 horizon (13-39 cm)

Sultanpur soil clay (2 μm) Bw2 horizon (39-62 cm)

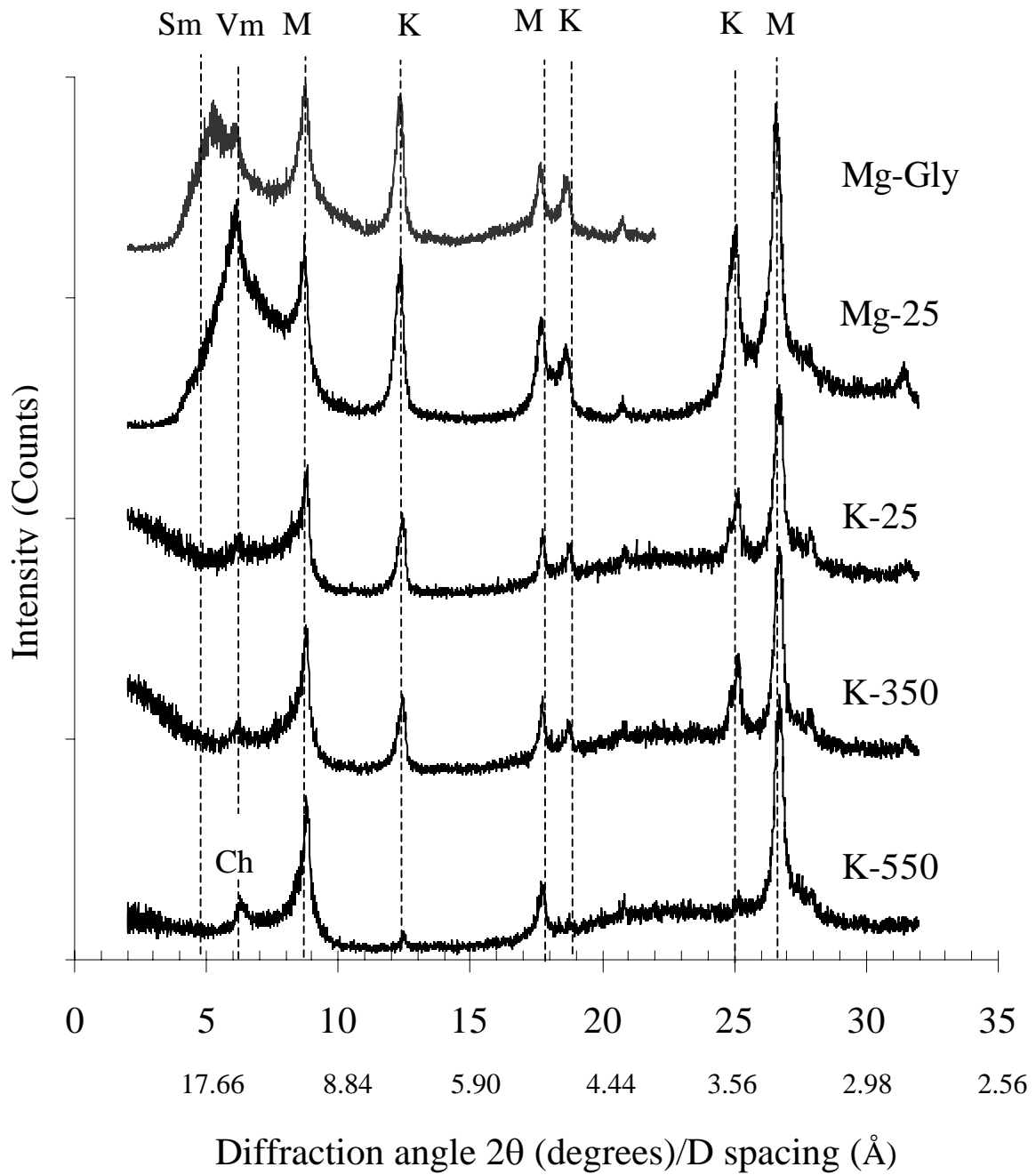
Sultanpur soil clay (2 μm) 2C1 horizon (62-81 cm)

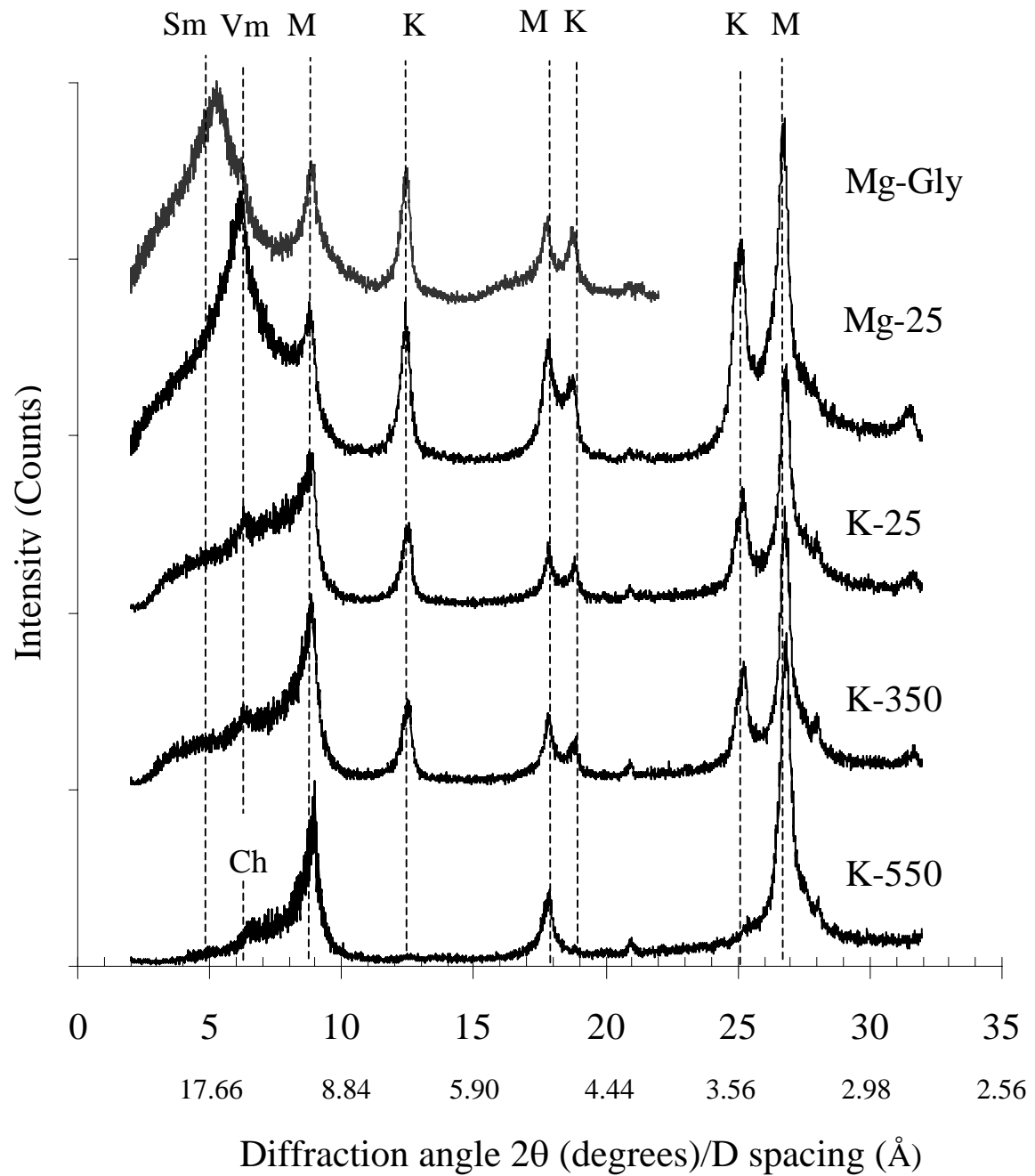
Pacca clay (2 μm) Ap horizon (0-15 cm)



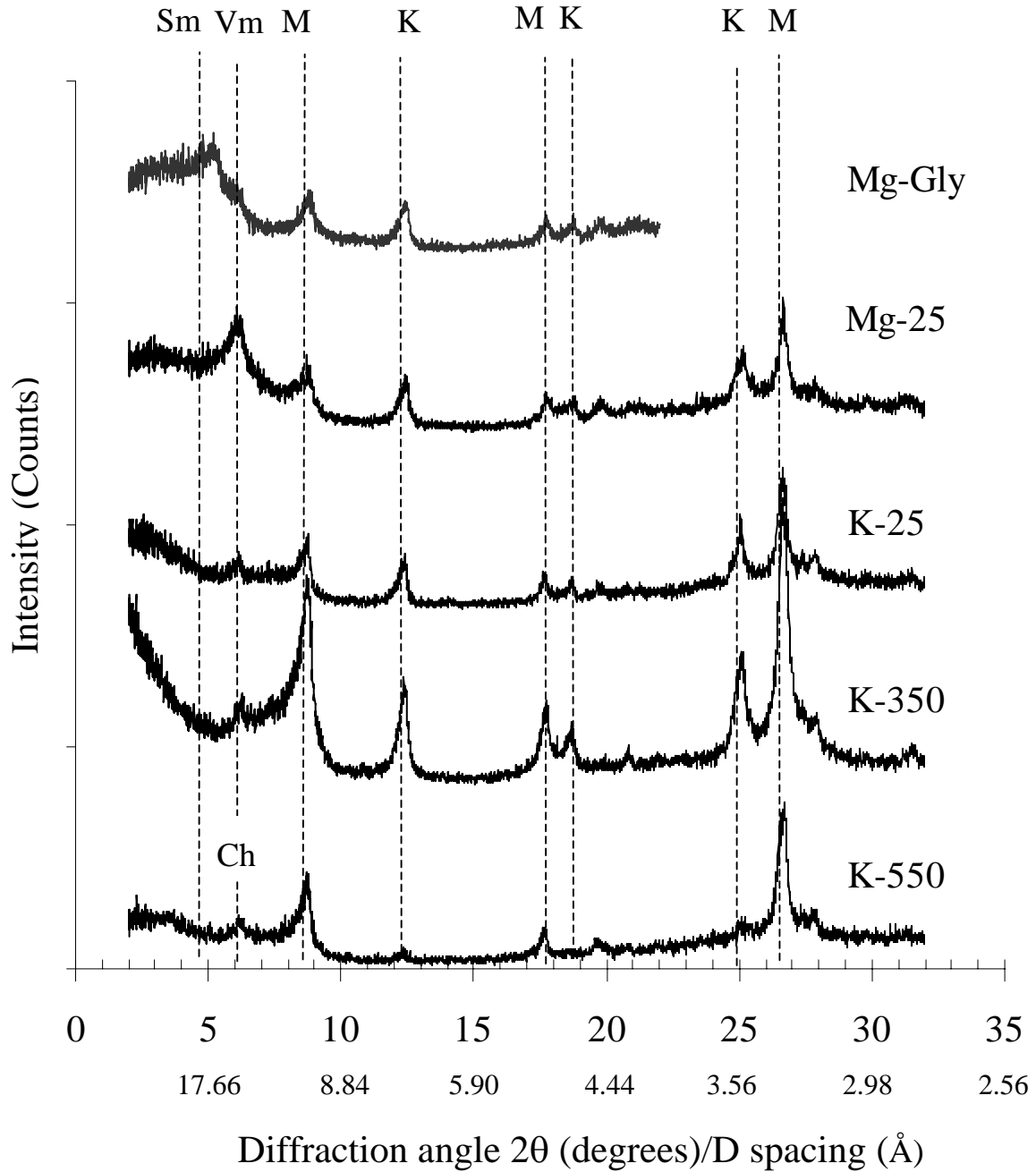
Pacca clay (2 μm) BA horizon (15-32 cm)

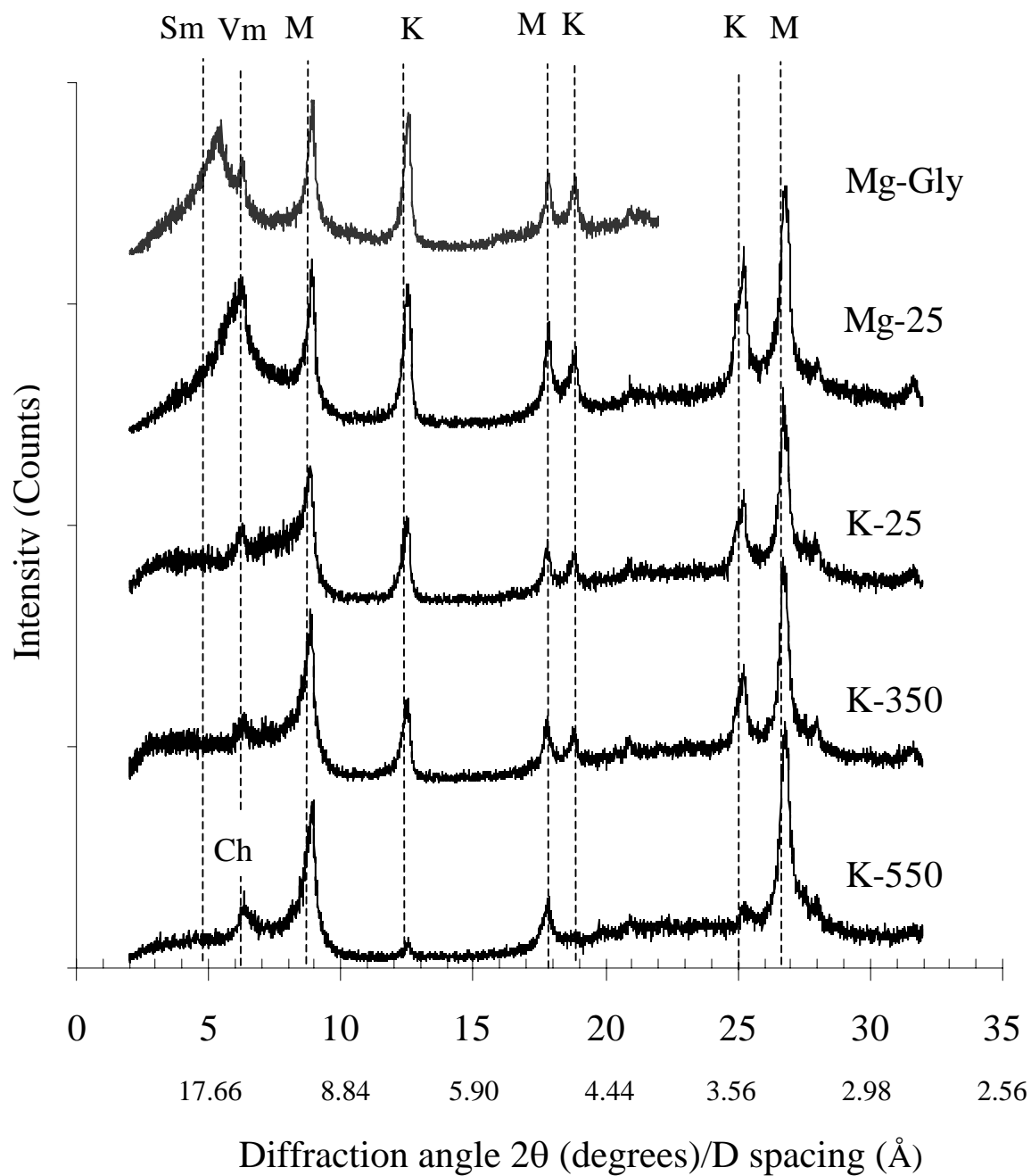
Pacca clay (2 μm) Bt1 horizon (32-53 cm)

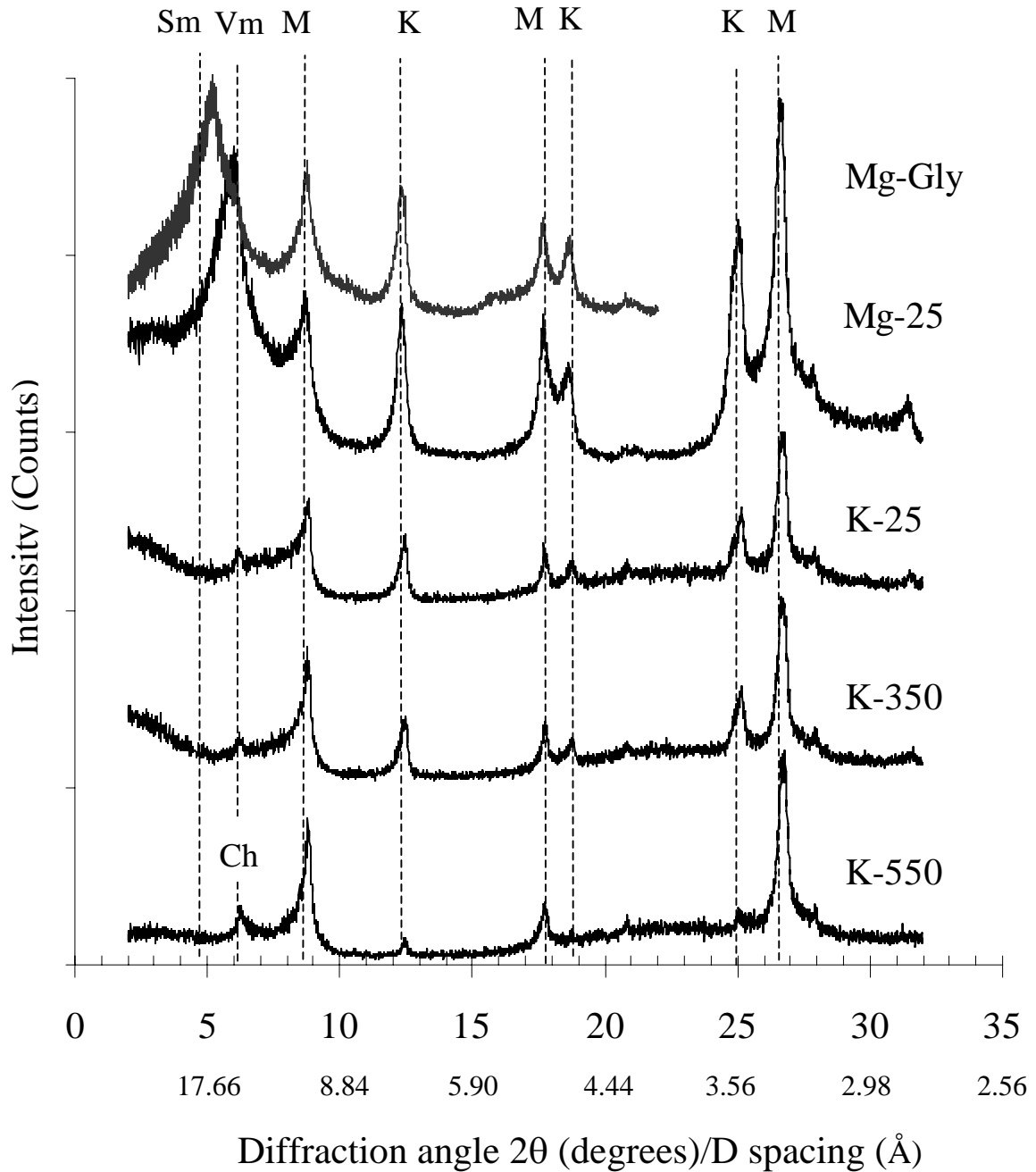


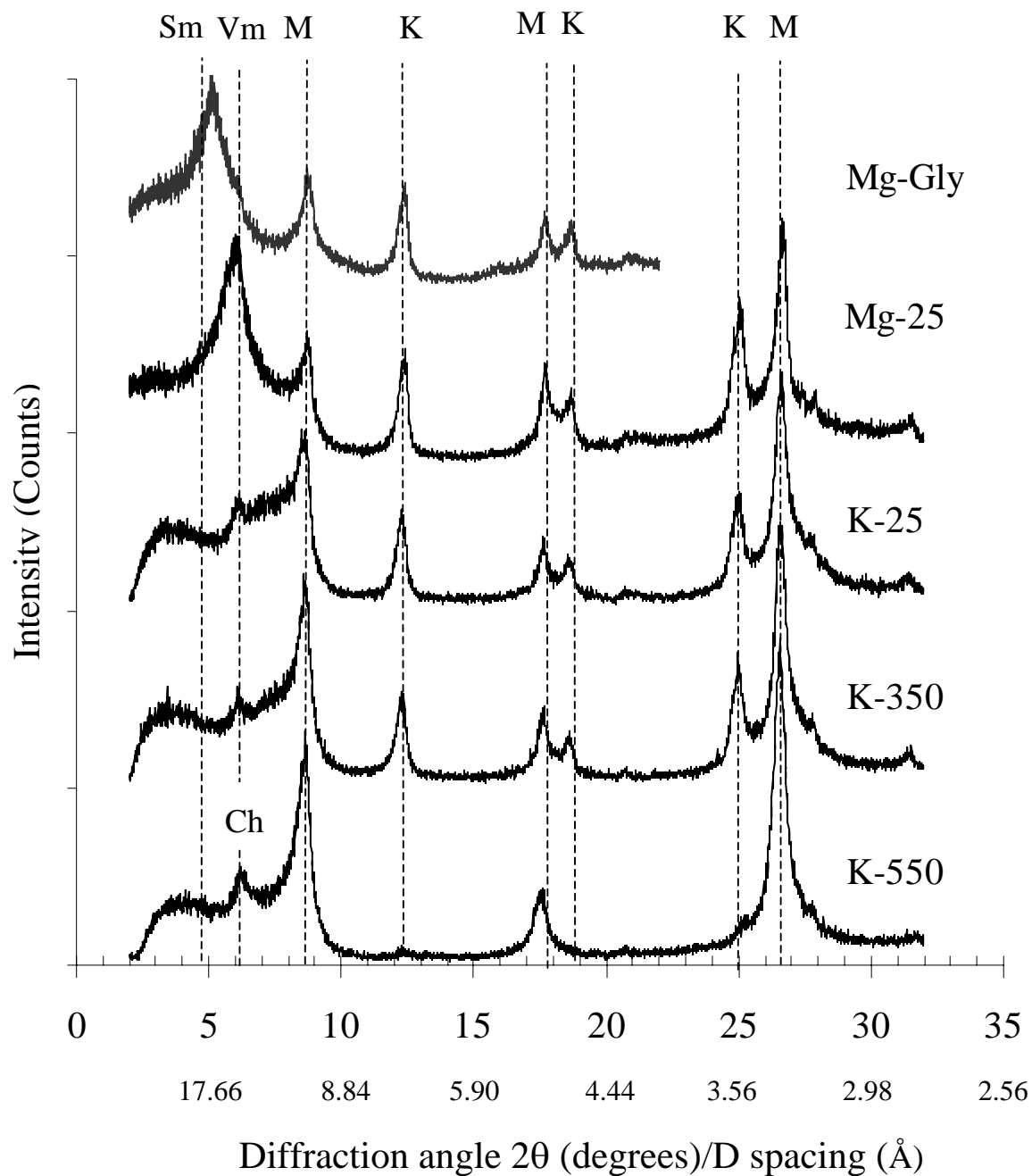
Pacca clay (2 μm) Bt2 horizon (53-92 cm)

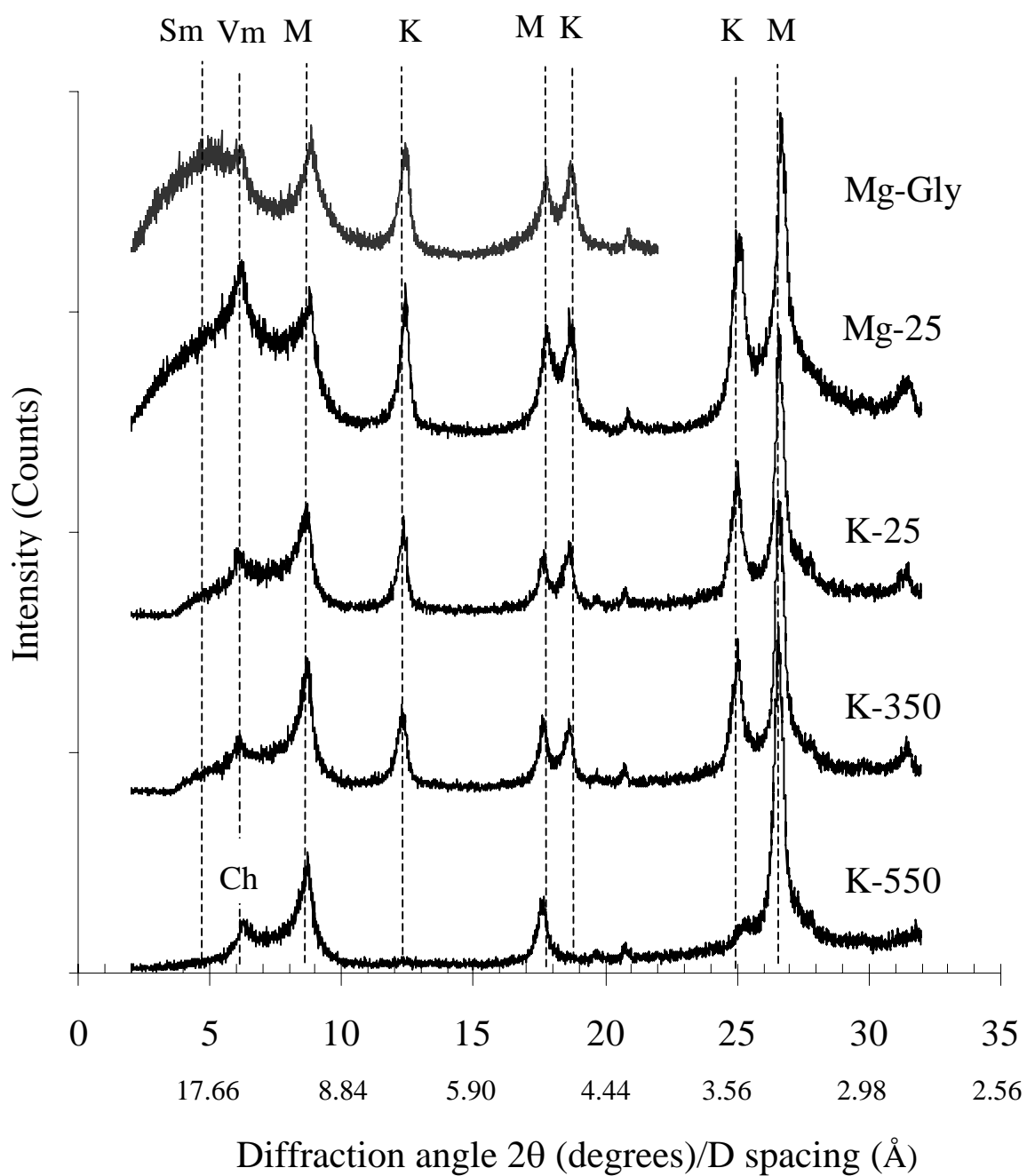
Pitafi clay (2 μm) Ap horizon (0-15 cm)

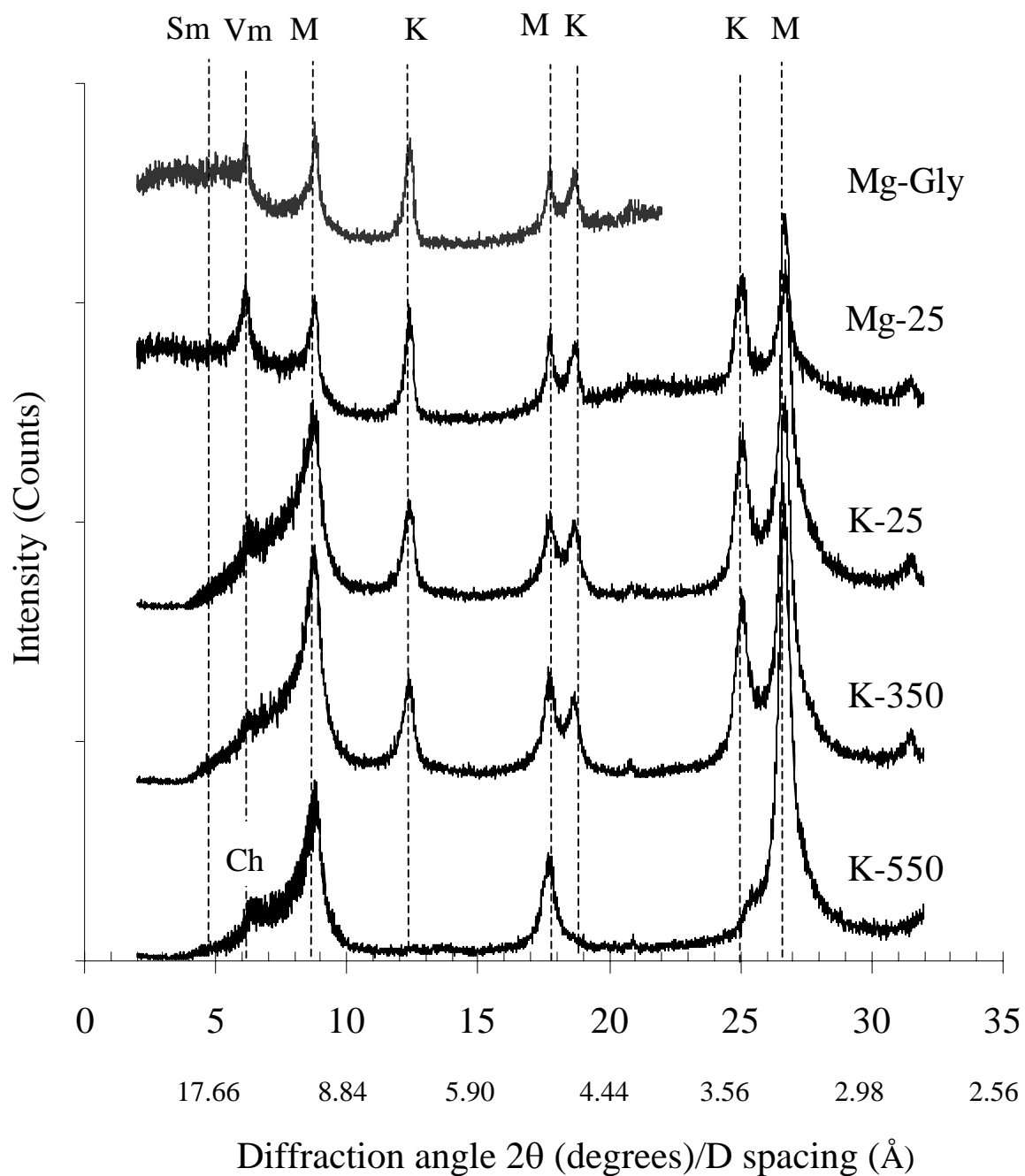


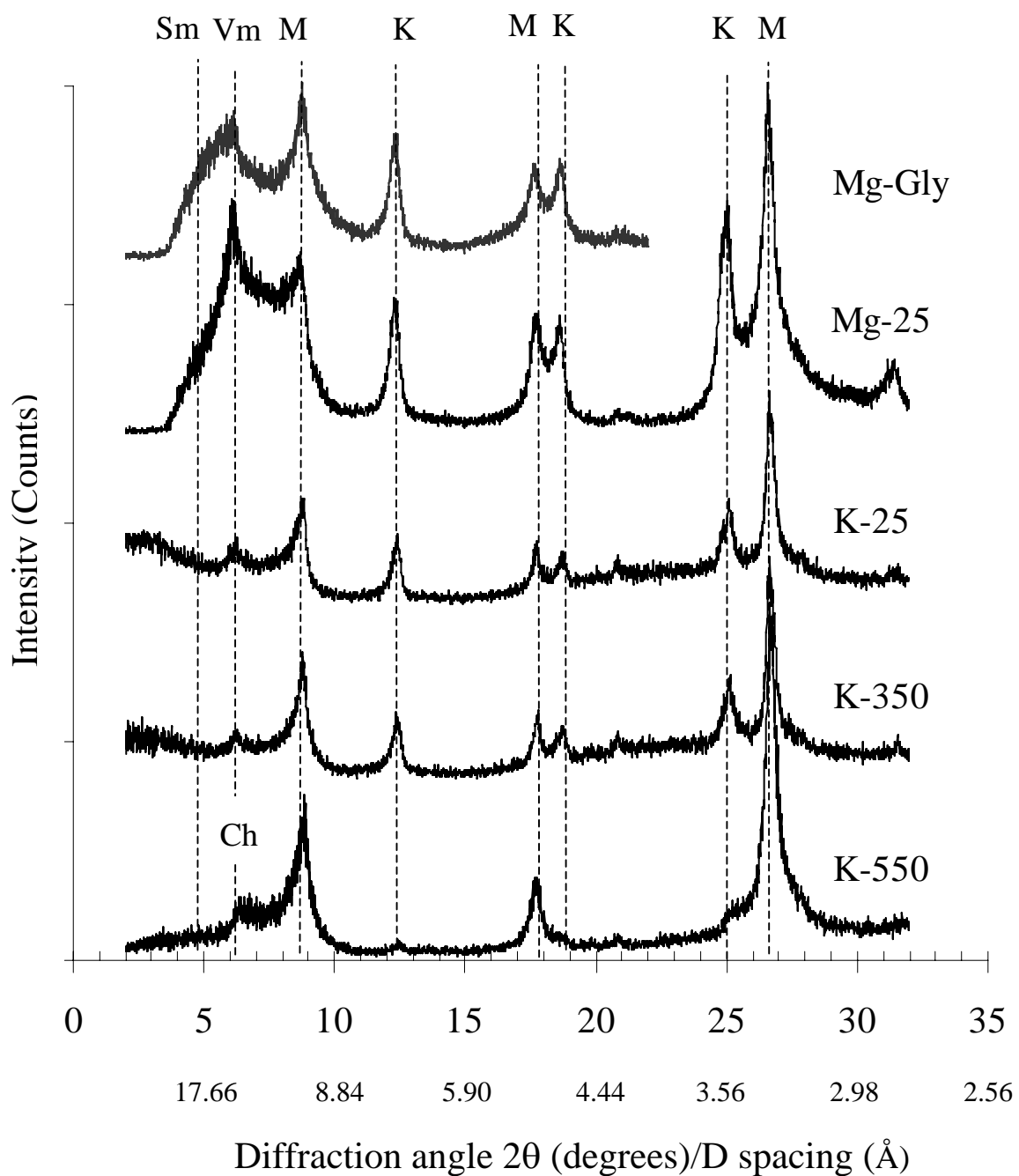
Pitafi clay (2 μm) Avz horizon (15-41 cm)

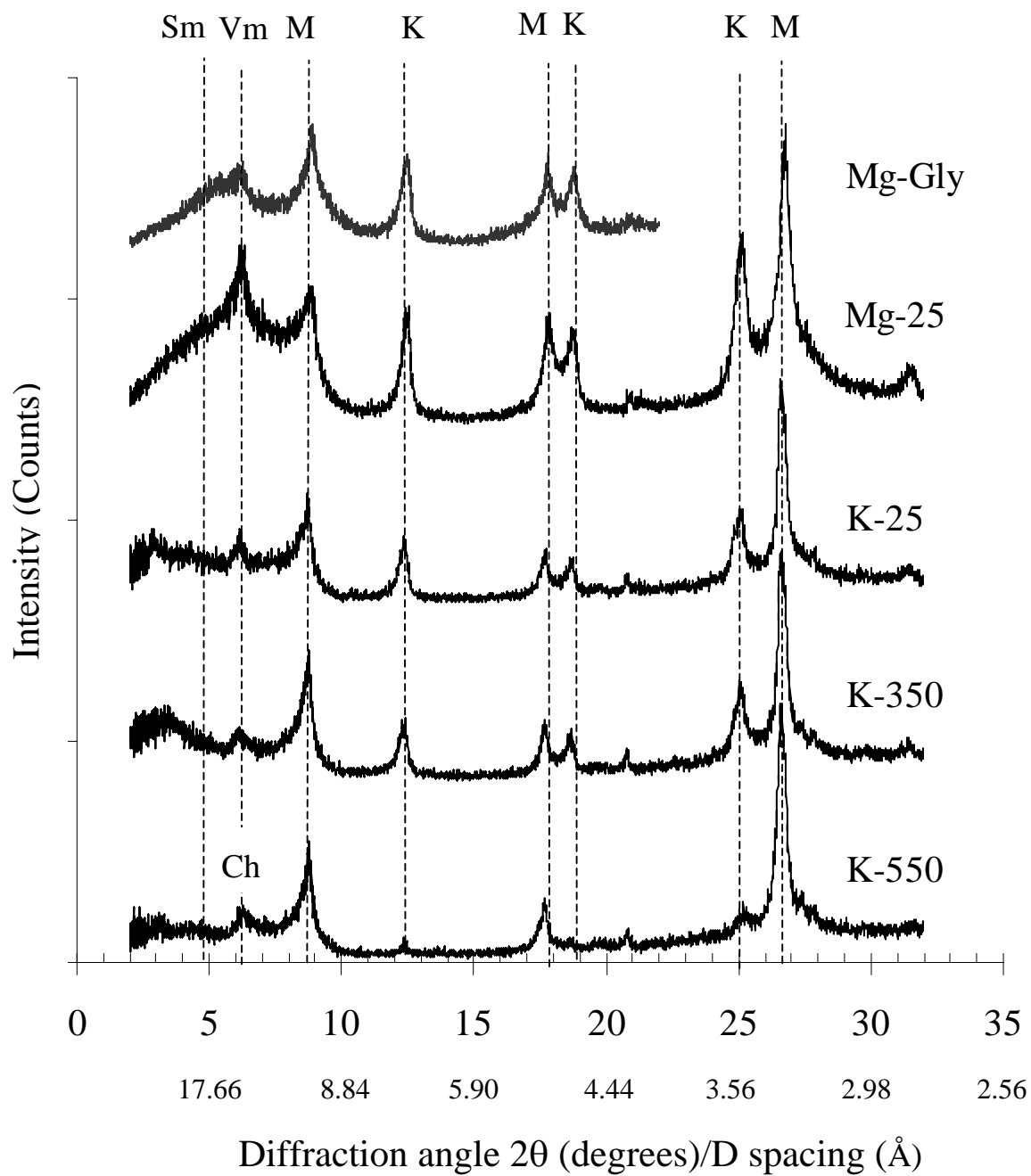
Pitafi clay (2 μm) Bwy1 horizon (41-57 cm)

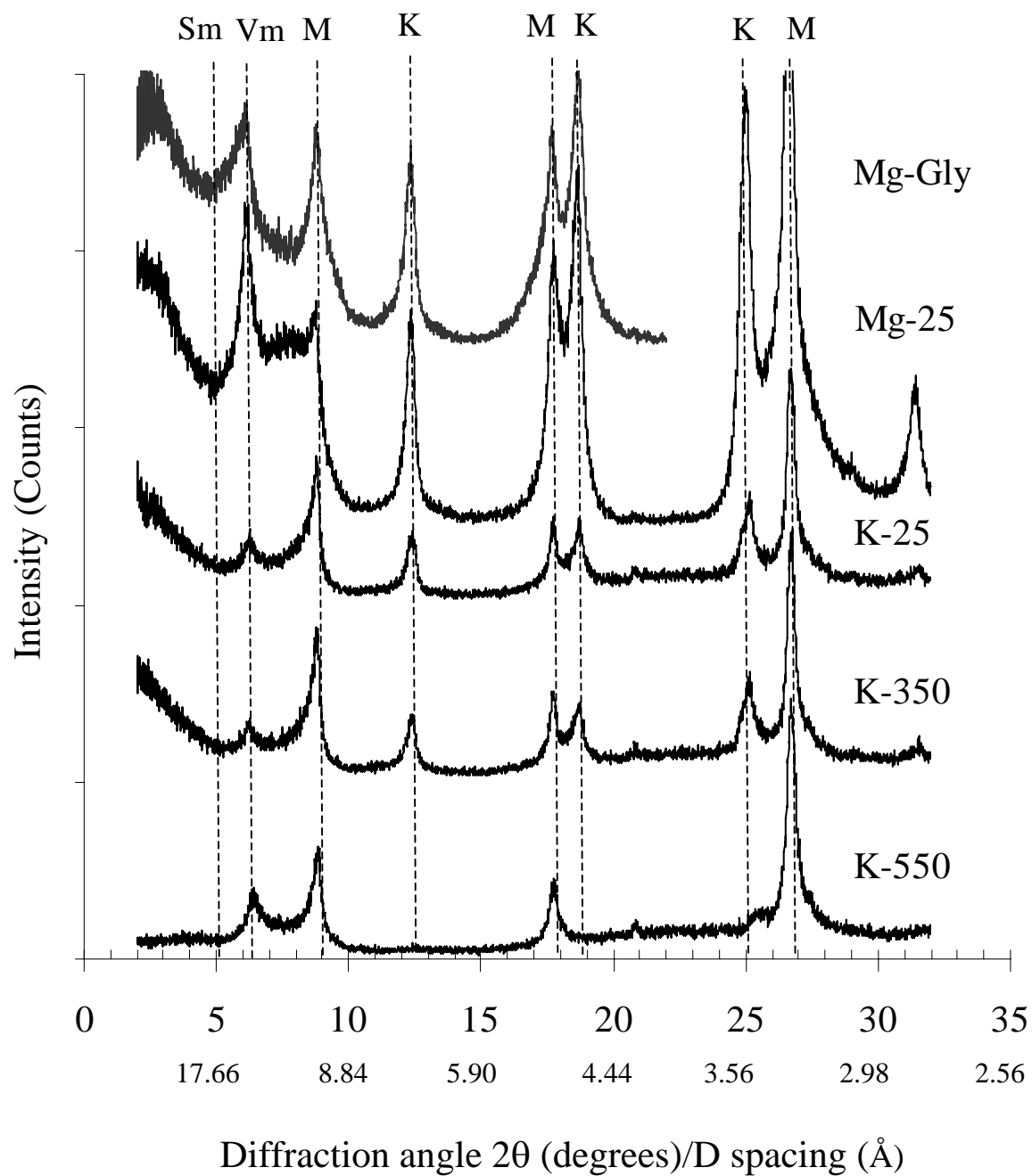
Pitafi clay (2 μm) Bwy2 horizon (63-111 cm)

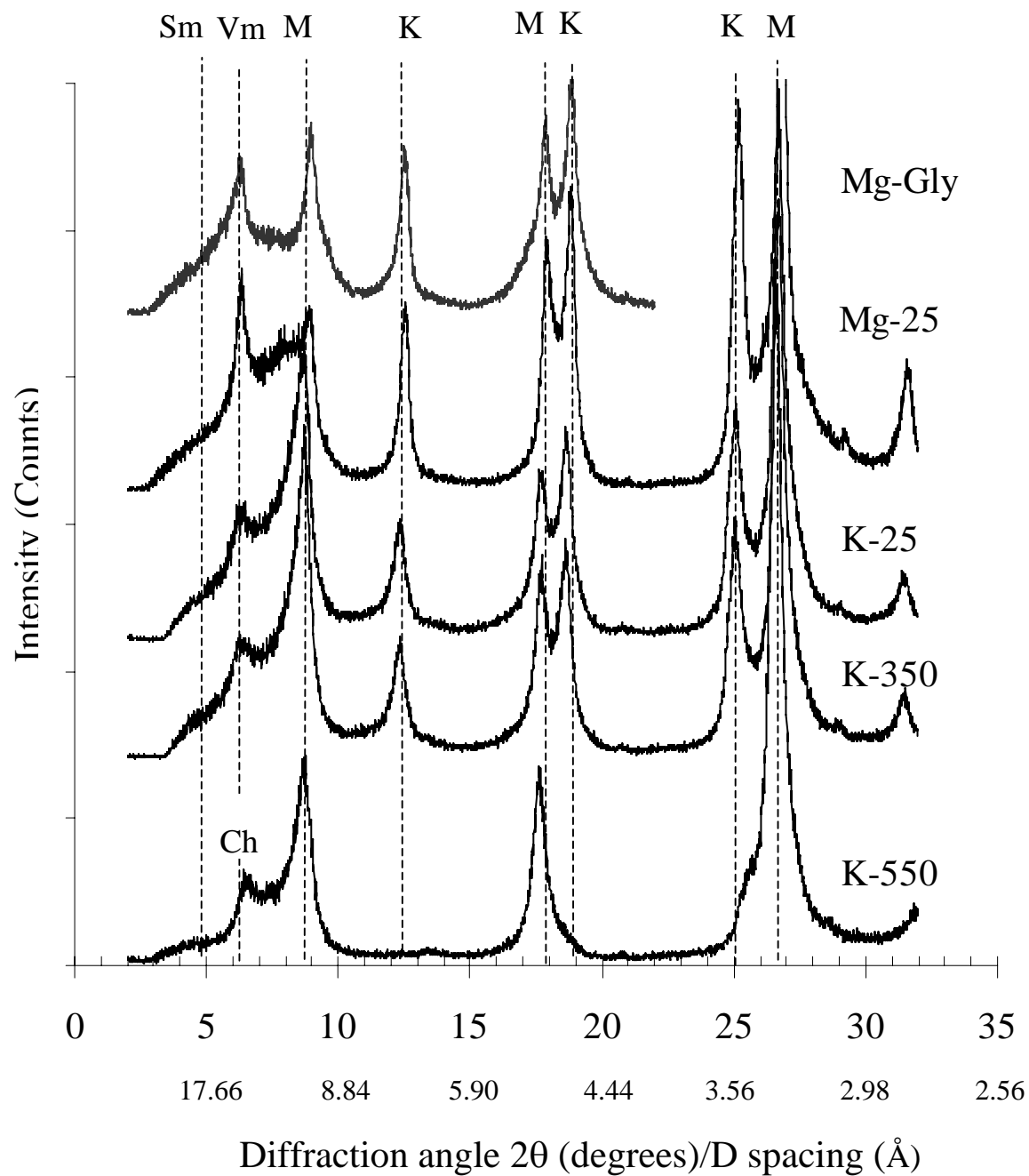
Peshawar clay (2 μm) Ap horizon (0-11 cm)

Peshawar clay (2 μm) Bt1 horizon (11-43 cm)

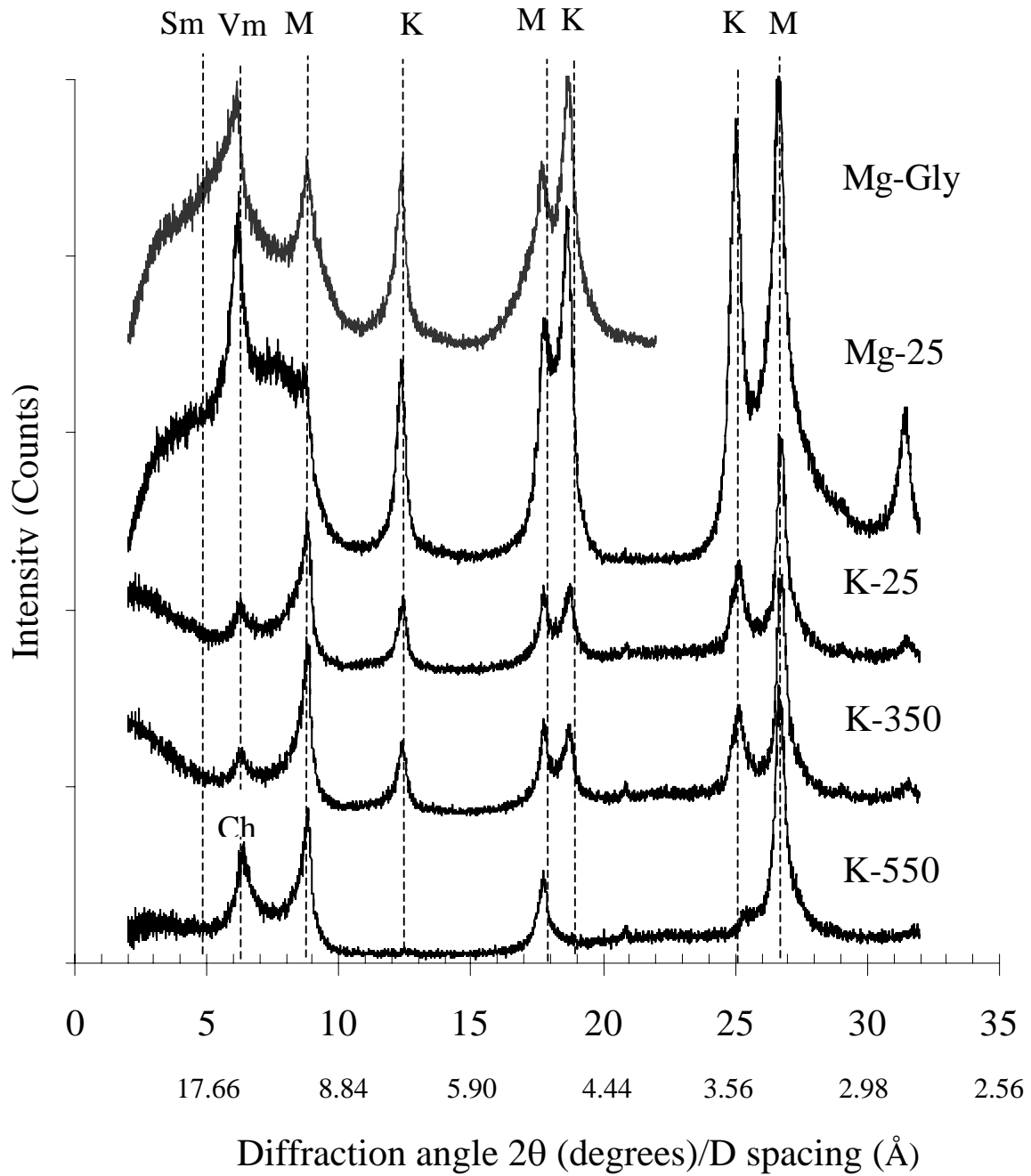
Peshawar clay (2 μm) Bt2 horizon (43-66 cm)

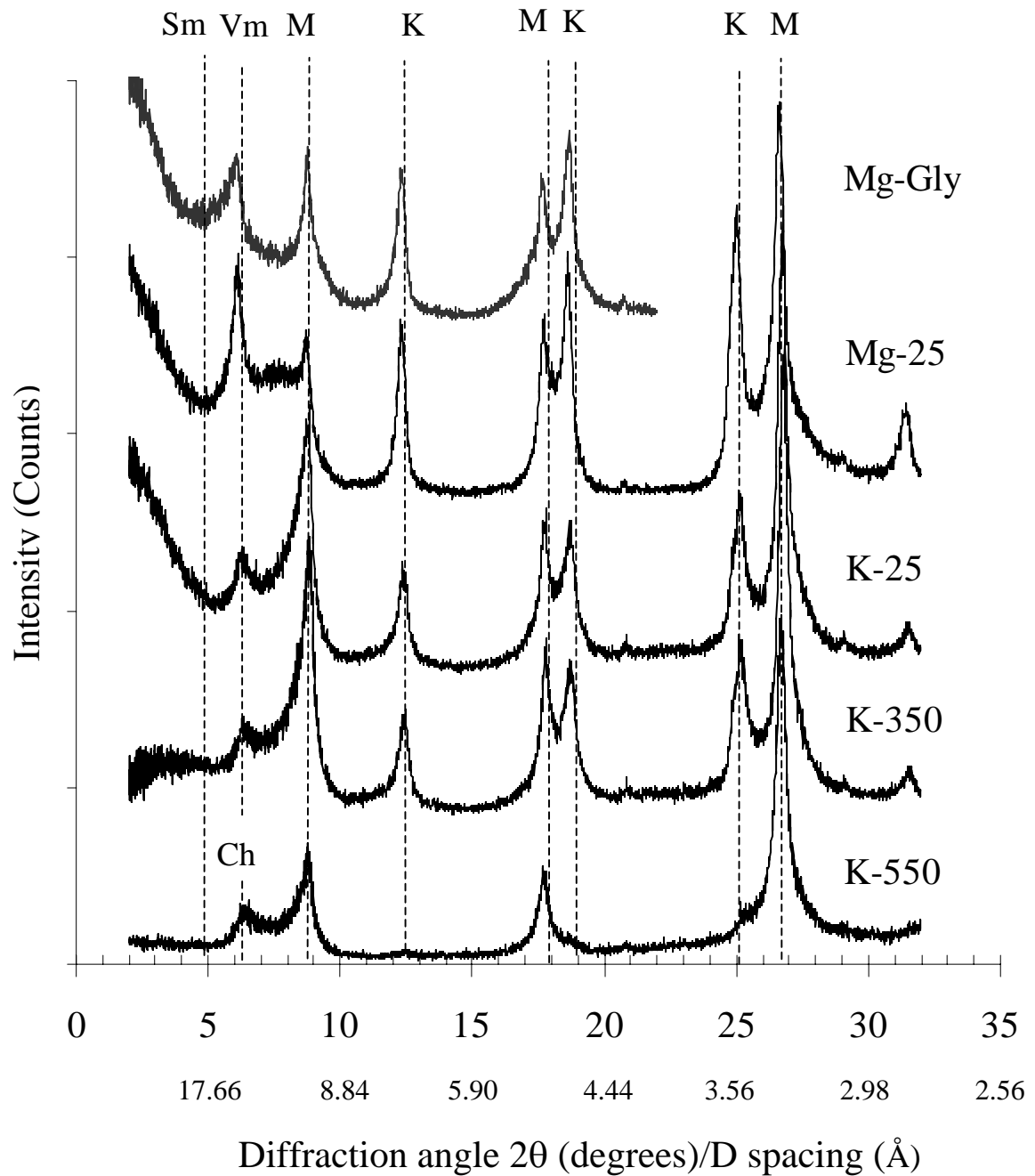
Peshawar clay (2 μm) 2Btb horizon (66-98 cm)

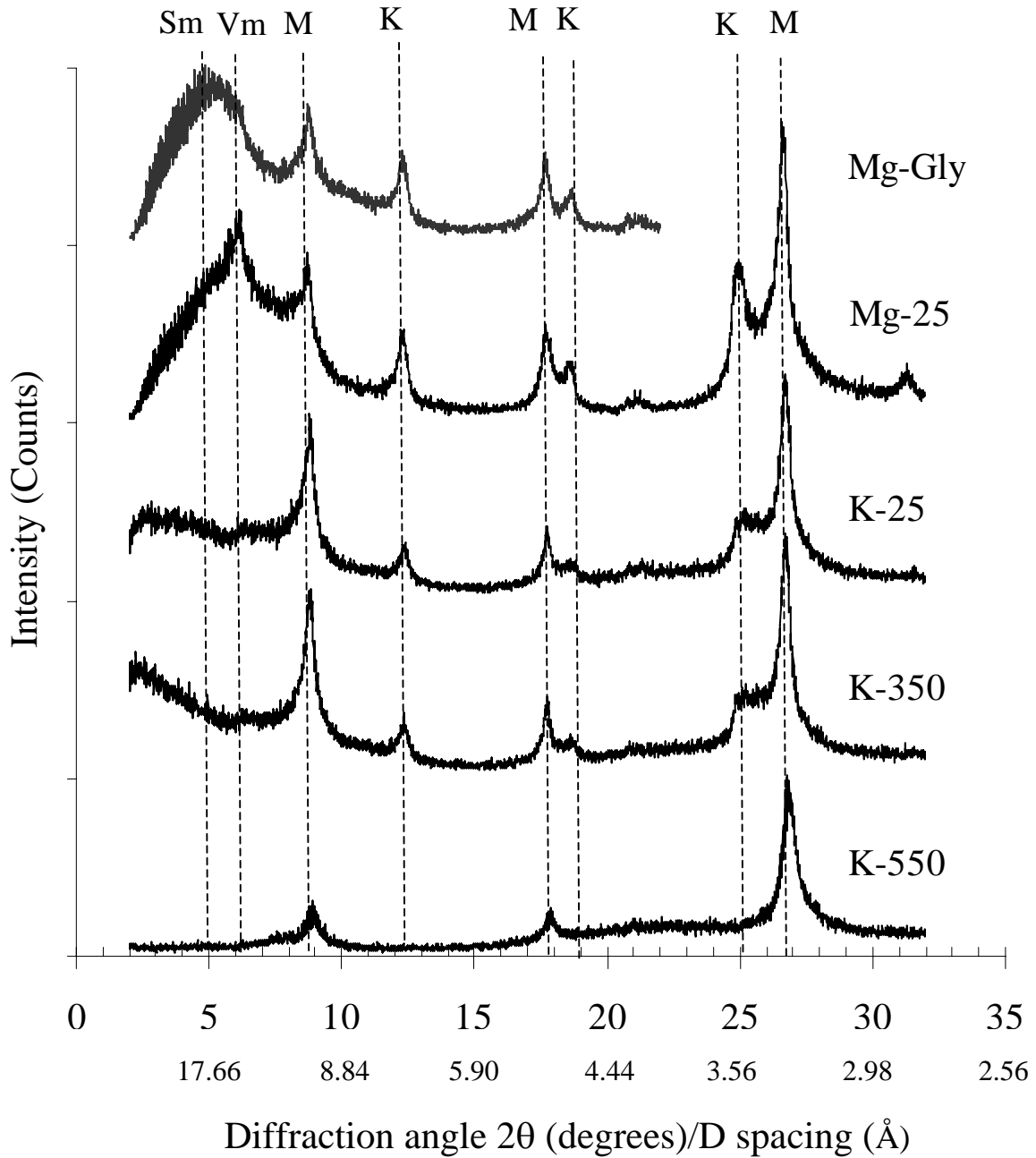
Murree clay (2 μm) A horizon (0-11 cm)

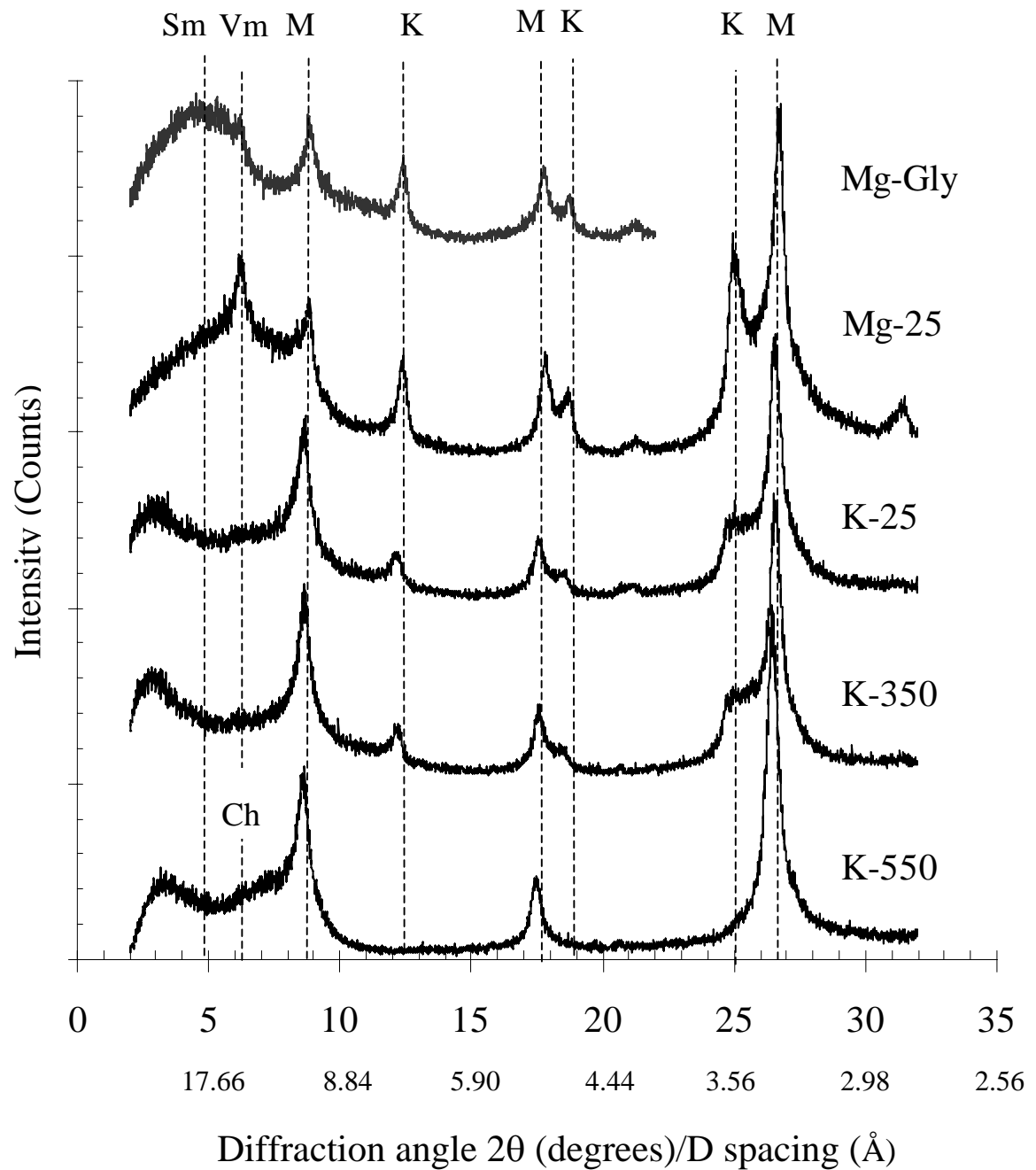
Murree clay (2 μm) Bt1 horizon (11-30 cm)

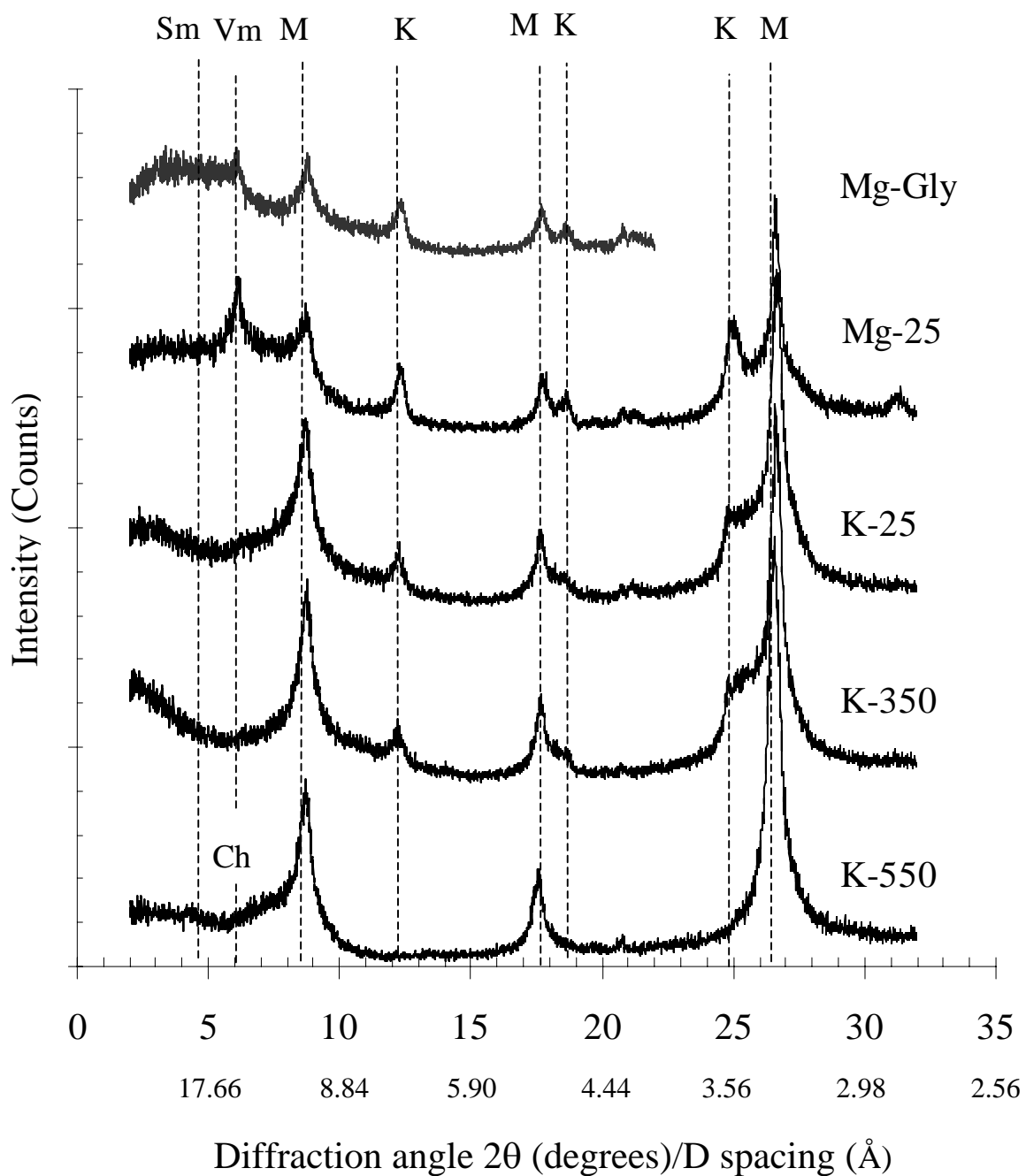
Murree clay (2 μm) Bt2 horizon (30-52 cm)

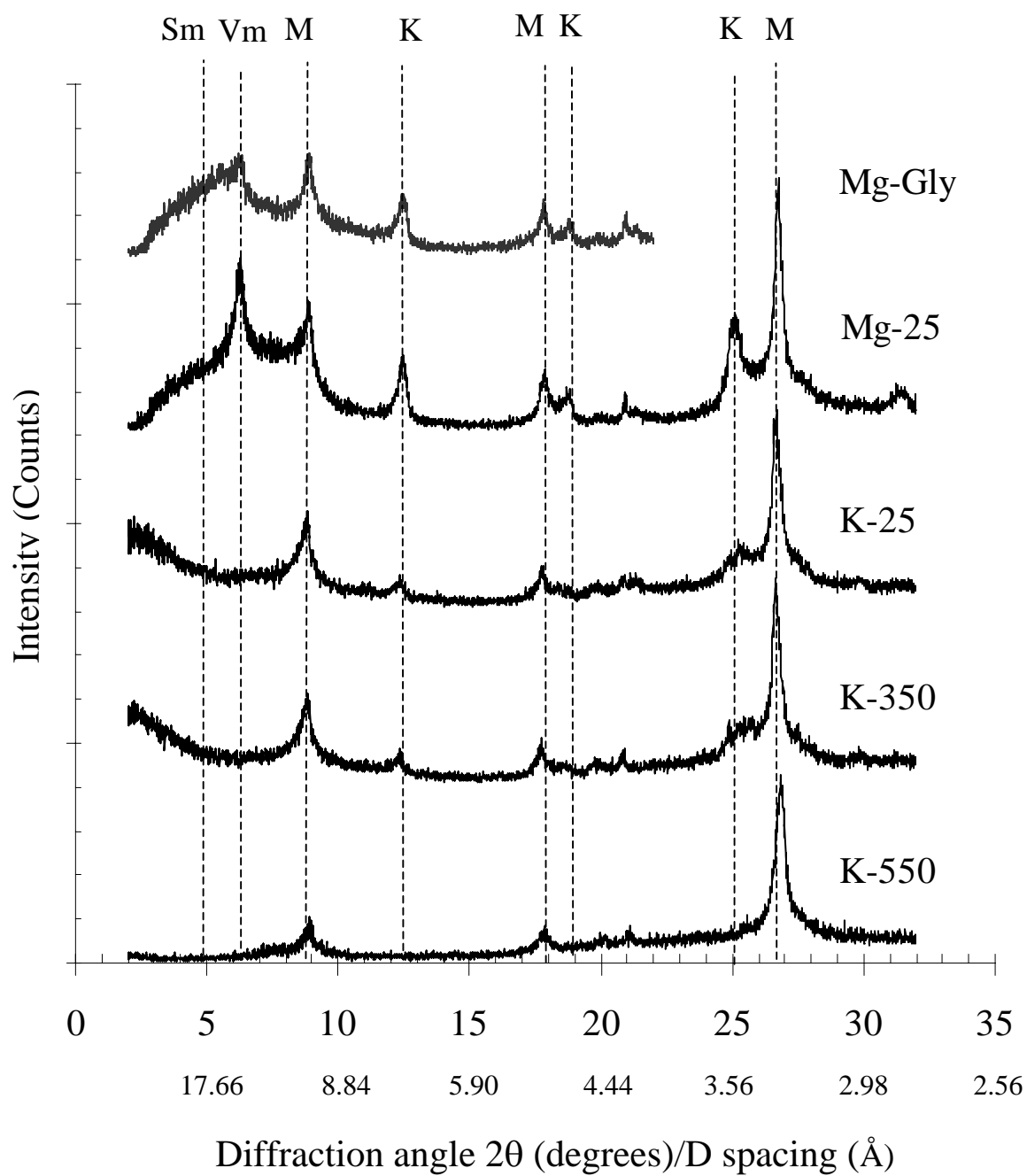


Murree clay (2 μm) 2Bt3 horizon (52-58 cm)

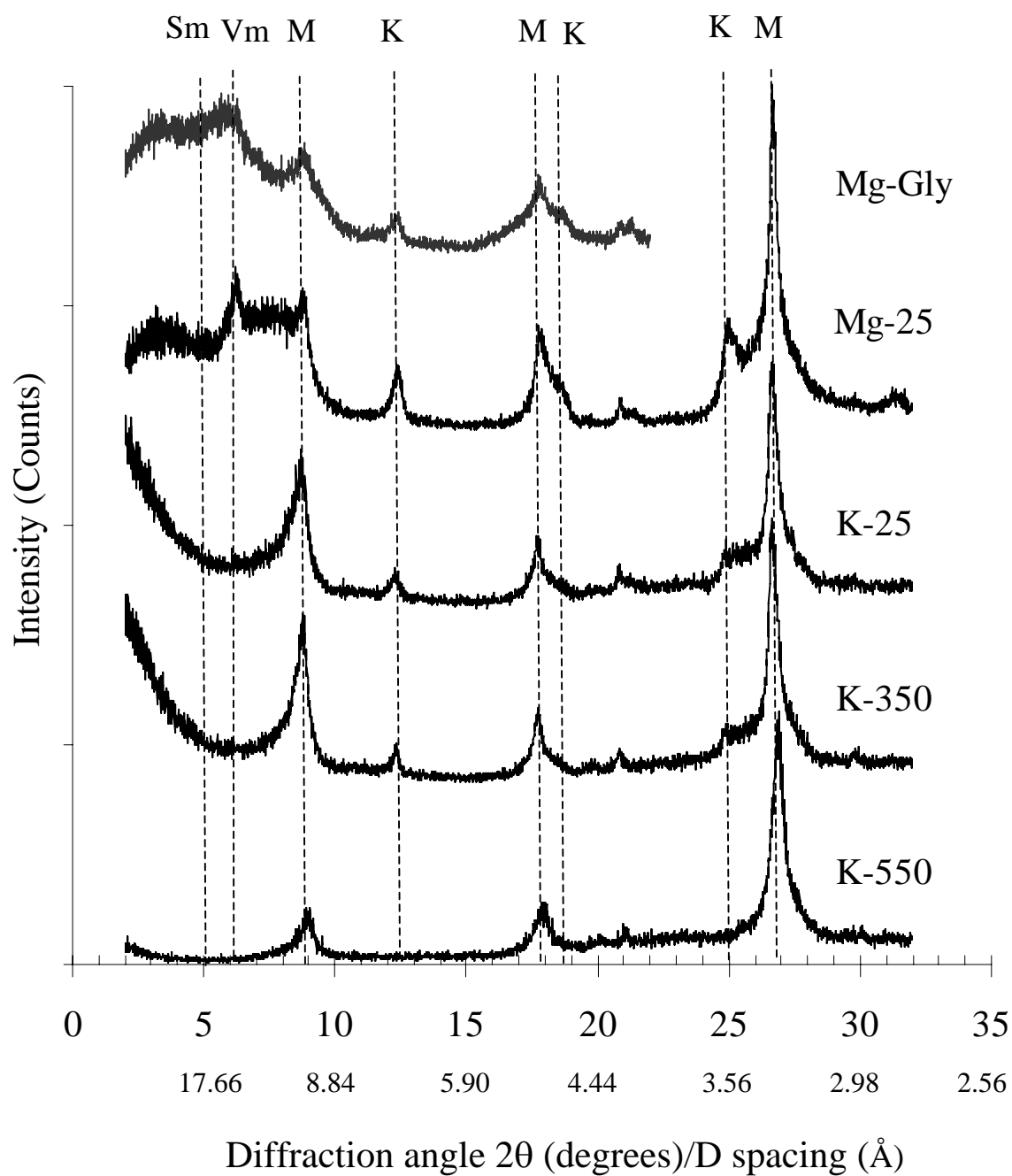
Guliana clay (2 μm) Ap horizon (0-12 cm)

Guliana clay (2 μm) Batc horizon (12-25 cm)

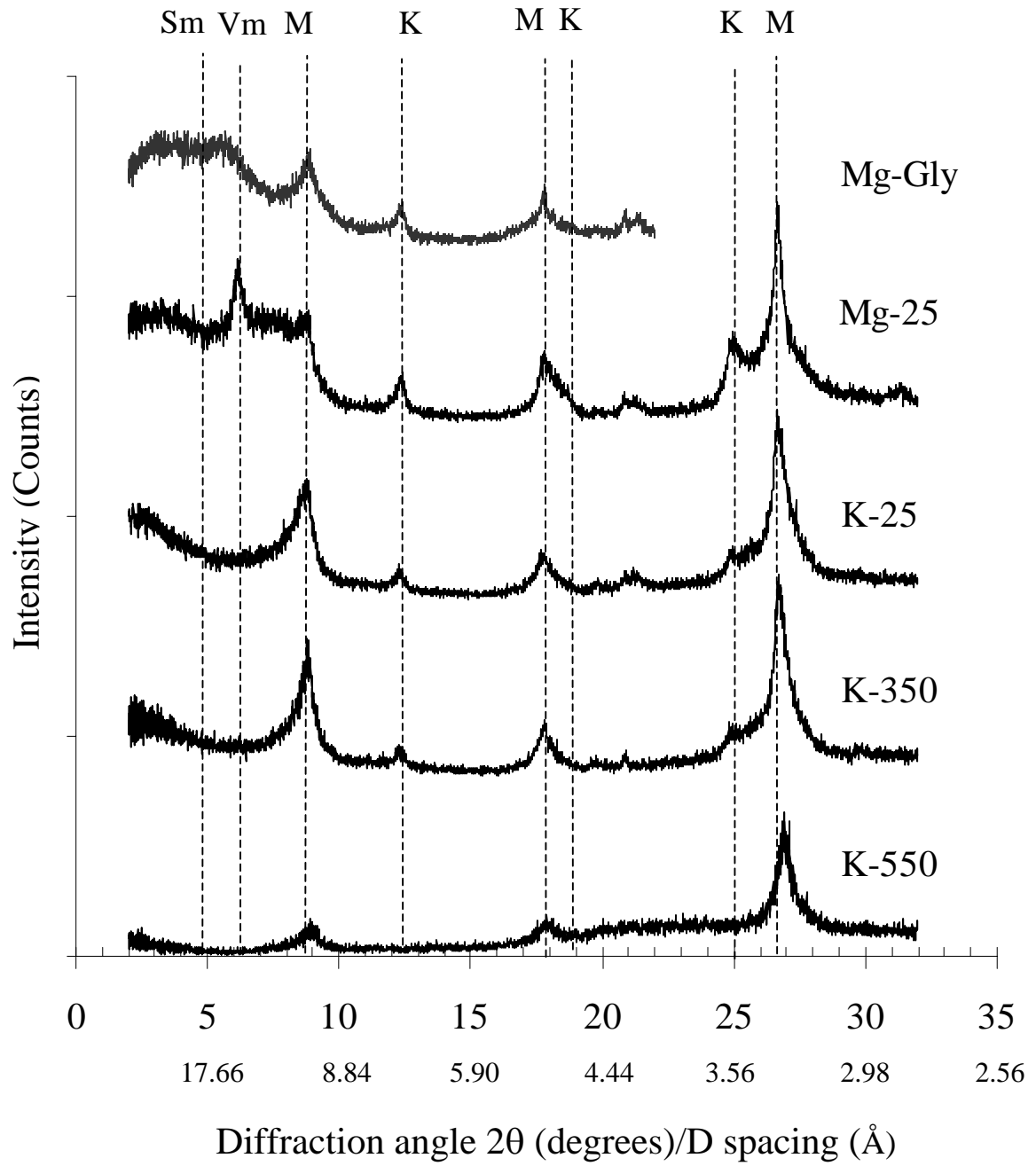
Guliana clay (2 μm) Btc1 horizon (25-56 cm)

Guliana clay (2 μm) Btc2 horizon (56-83 cm)

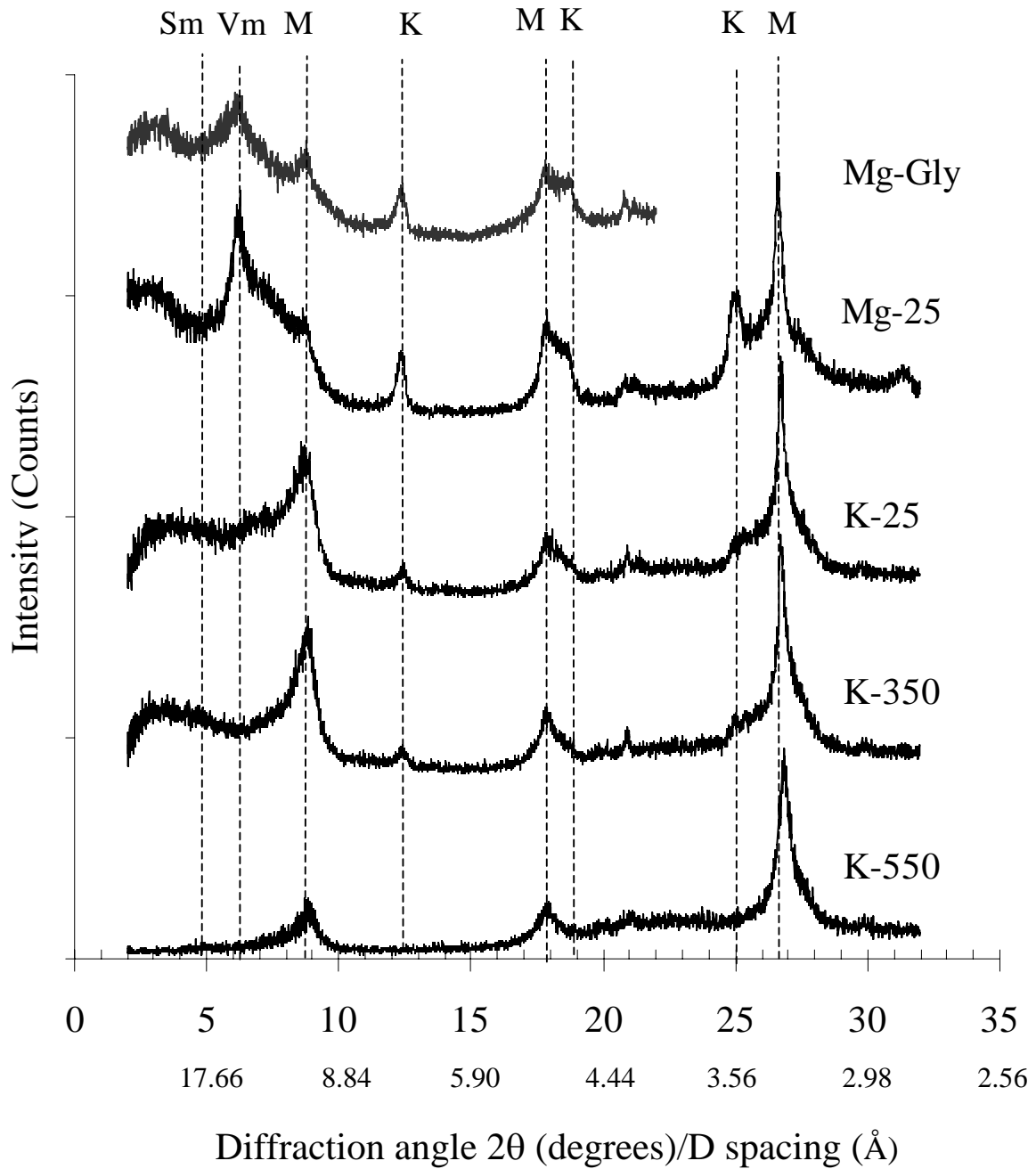
**Parabraunerde from Osterburken clay (2 μm)
Bv horizon (4-25 cm)**



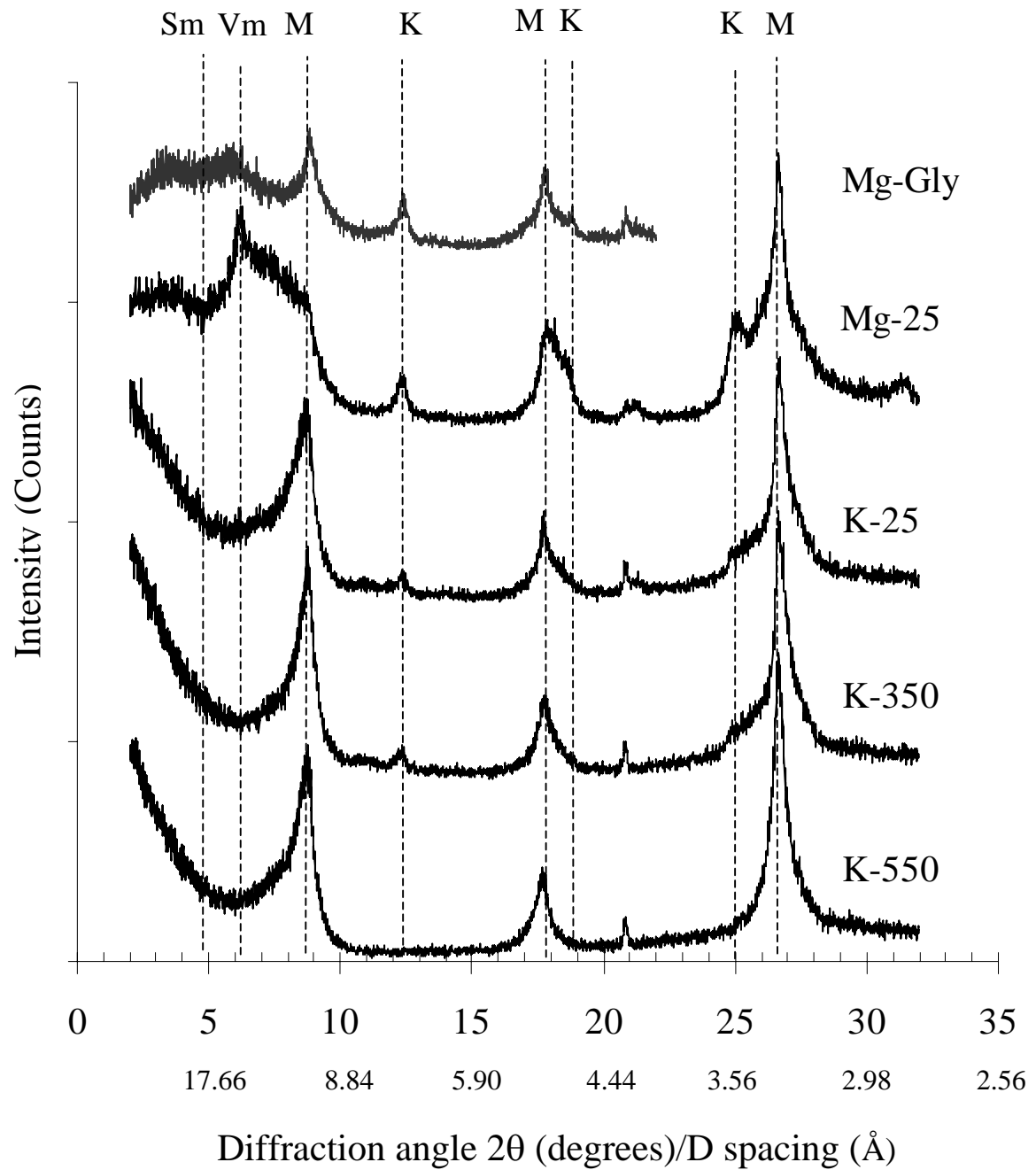
Parabraunerde from Osterburken clay (2 μm)
Bt horizon (25-50 cm)



Parabraunerde from Weingarten clay (2 μm)
Bv horizon (4-25 cm)

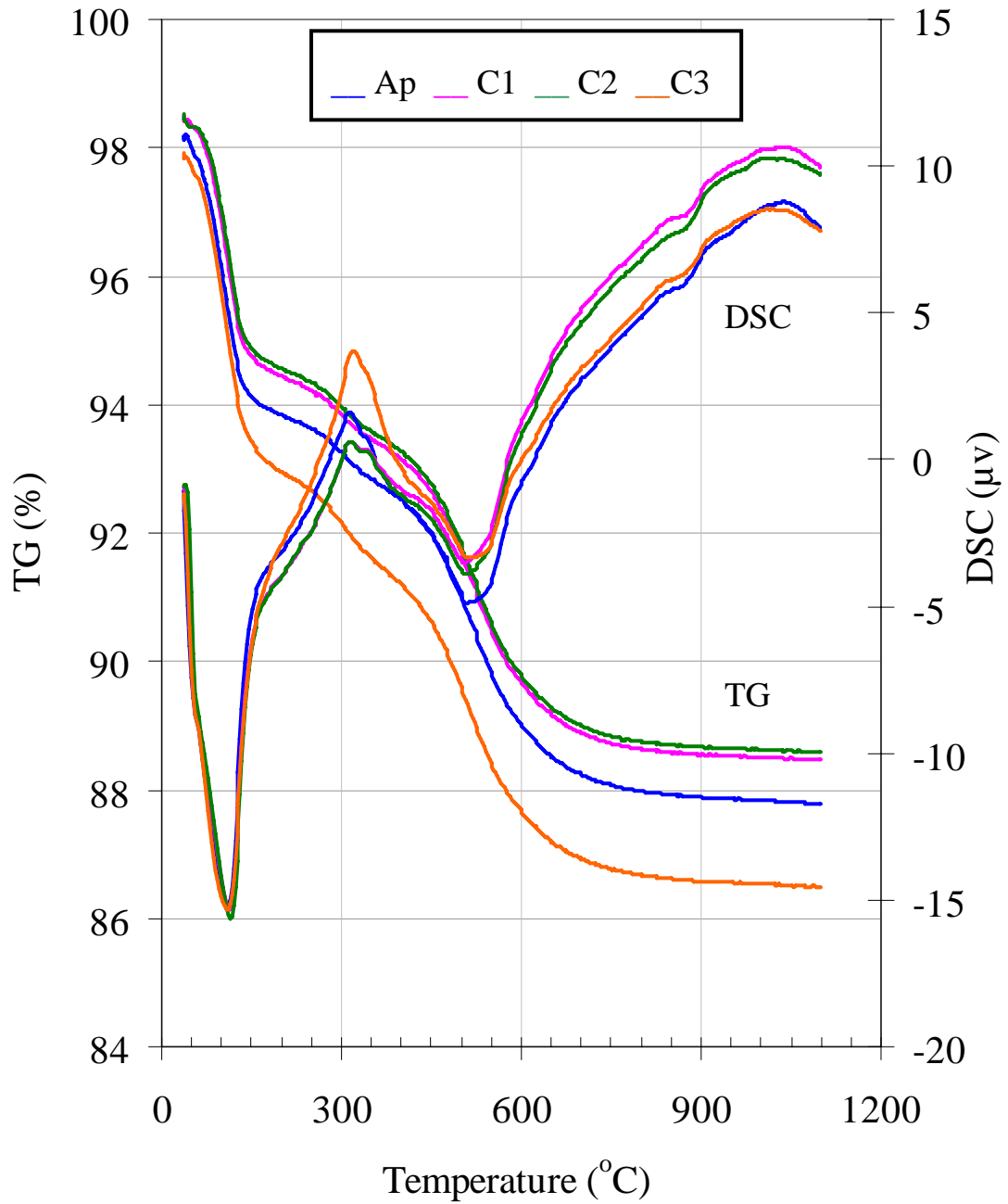


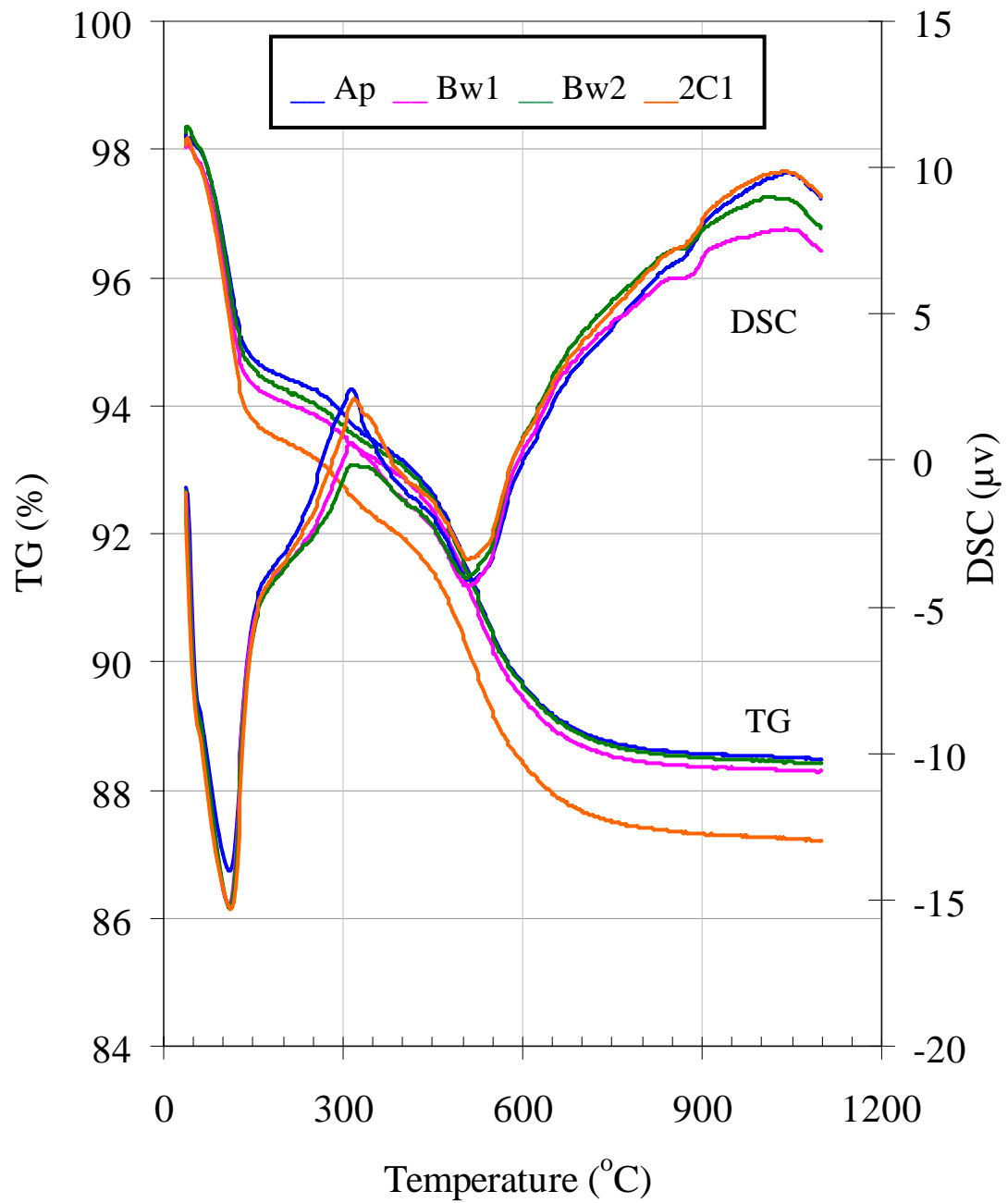
Parabraunerde from Weingarten clay (2 μm)
Bt horizon (25-45 cm)

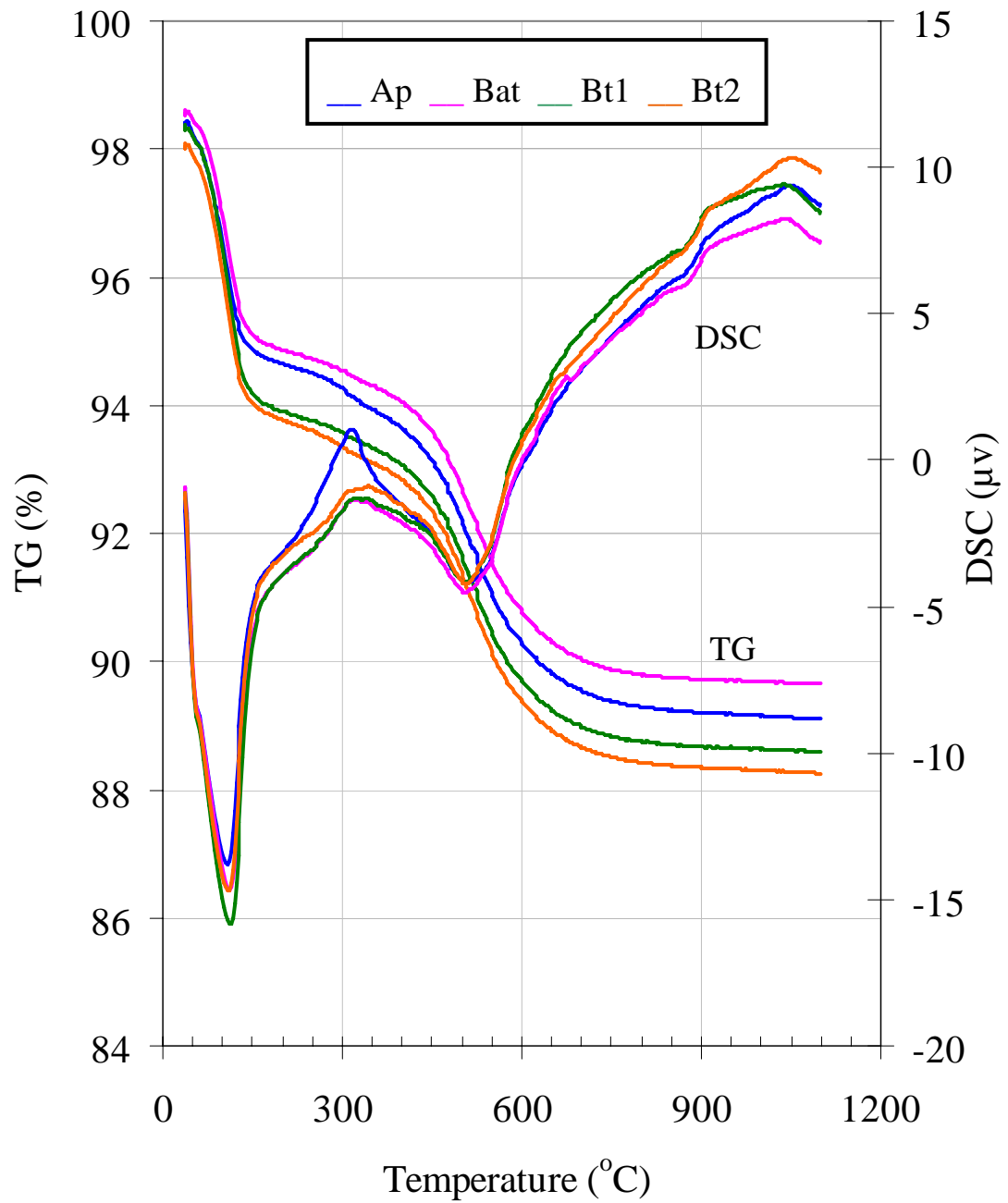


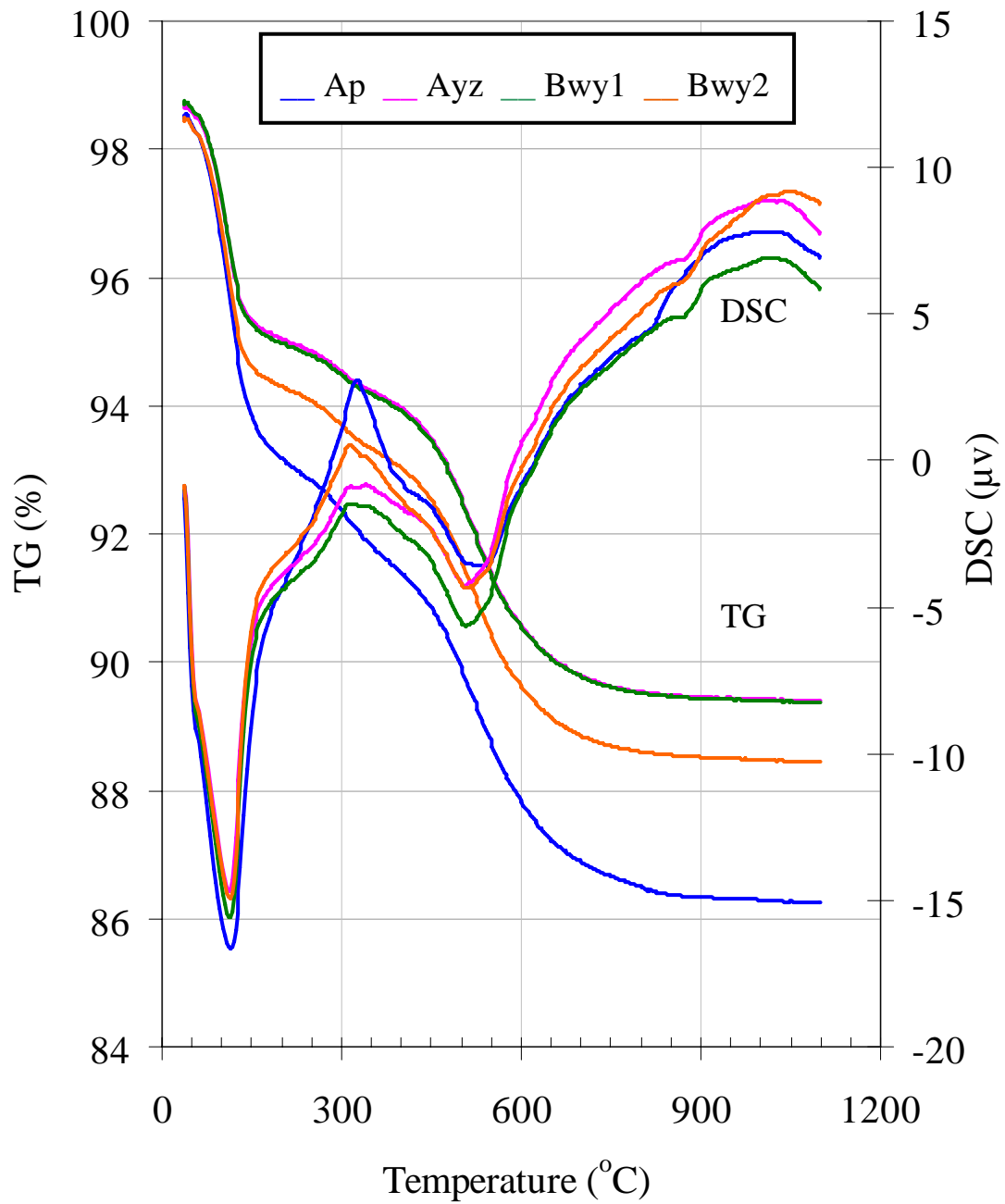
Appendix V

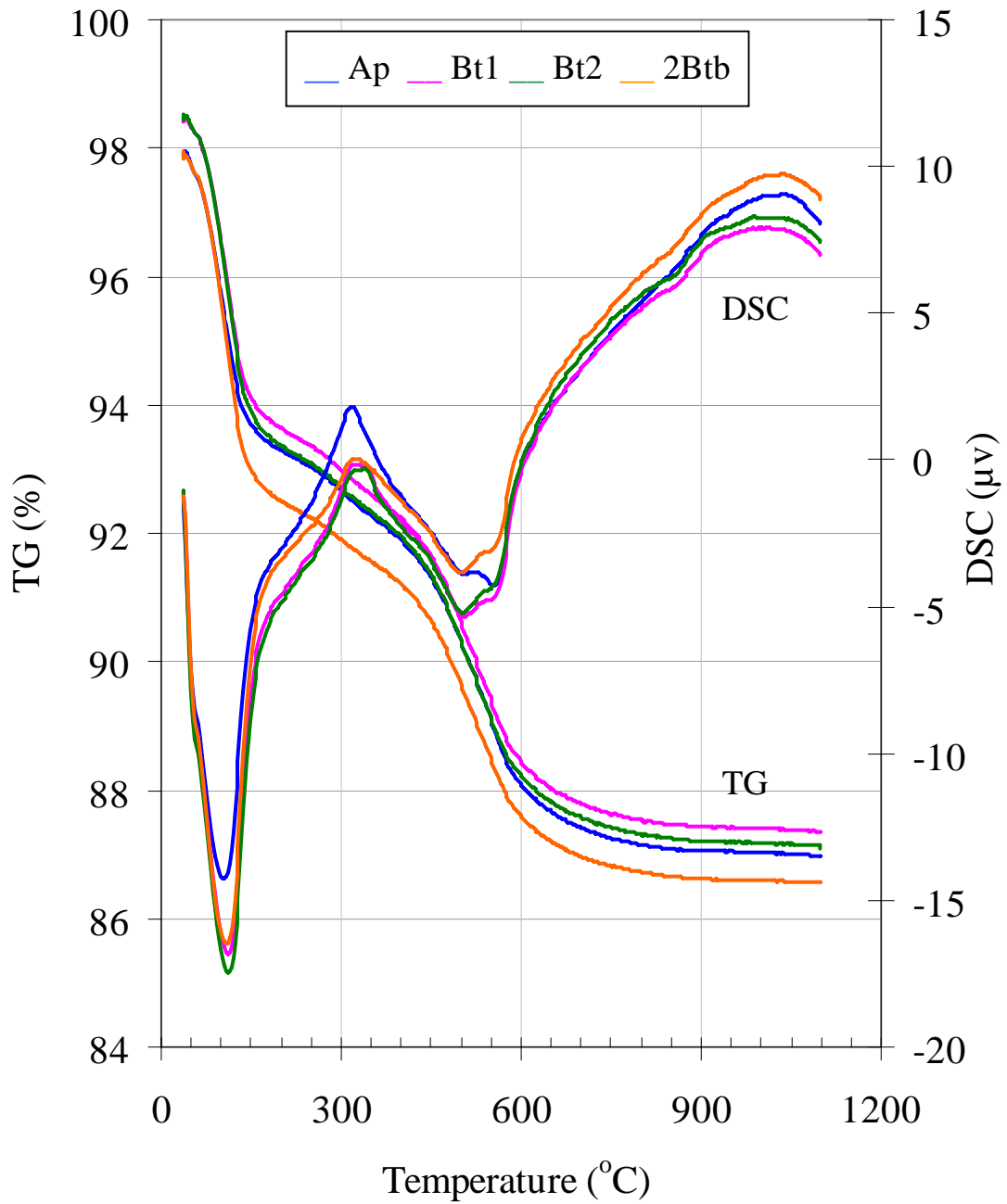
TG /DSC patterns of the soil clay fractions taken from four horizons (two horizons in case of German soils) of each soil profile investigated.

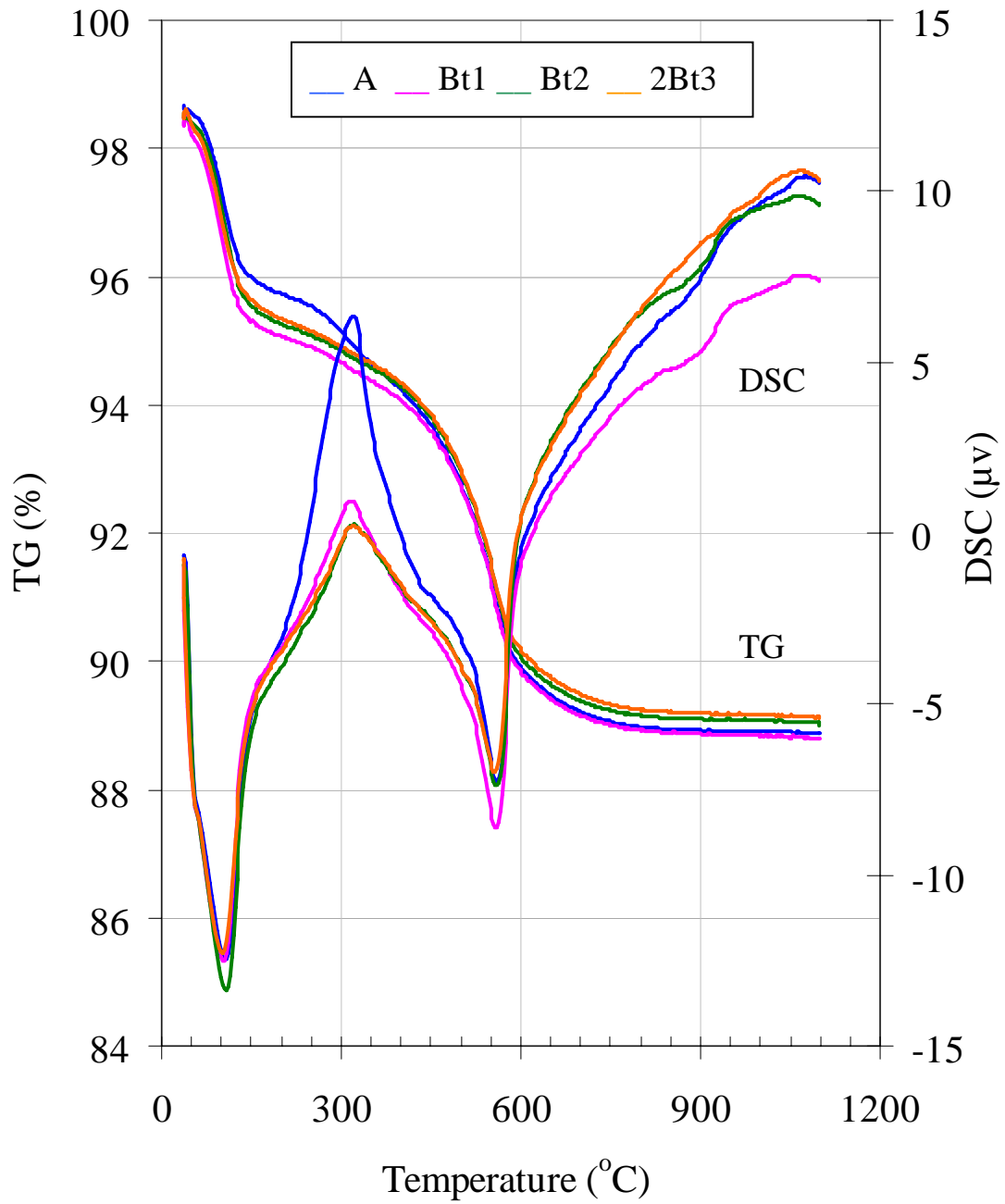
Shahdara soil clay (<2.0 μm)

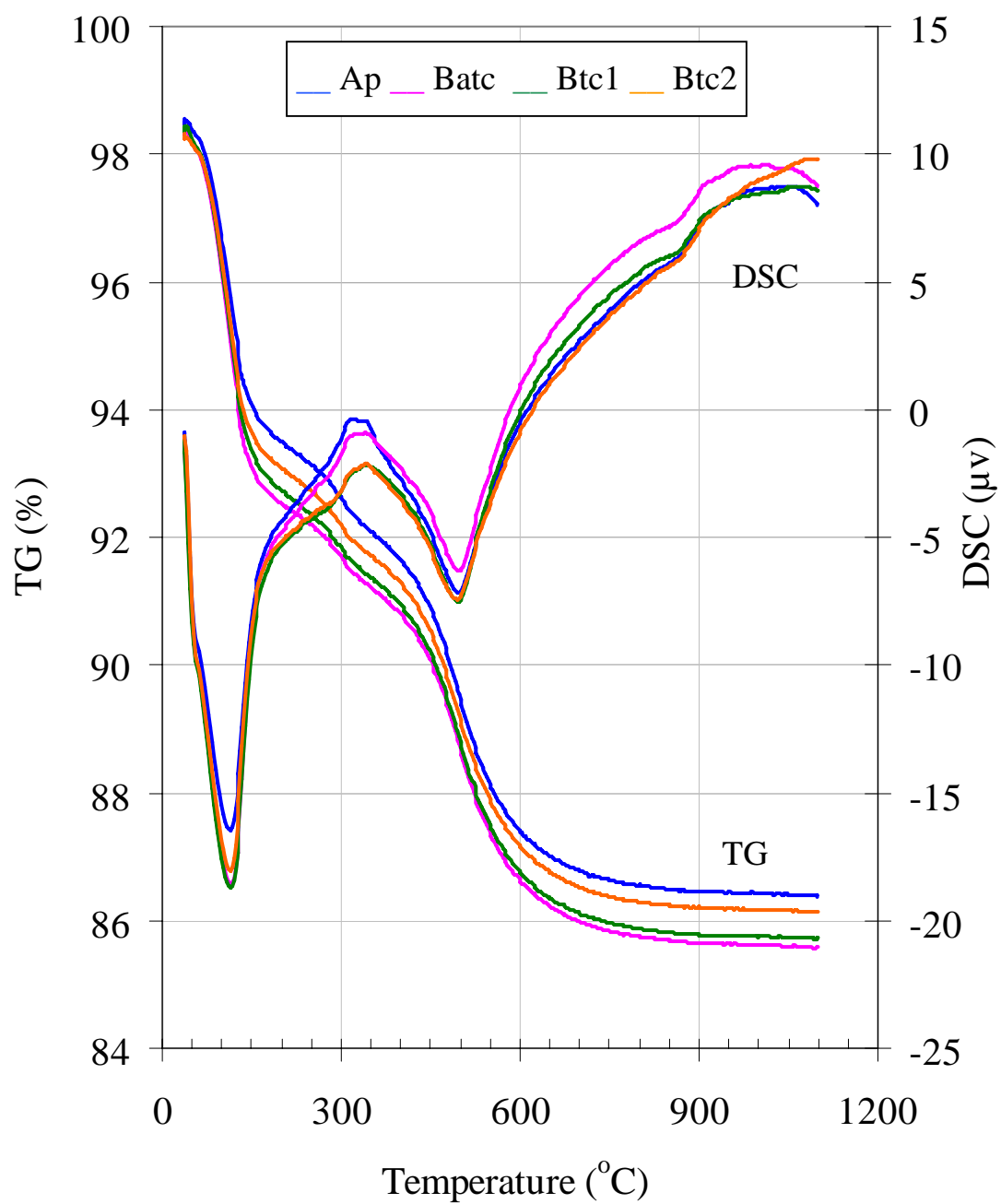
Sultanpur soil clay (<2.0 μm)

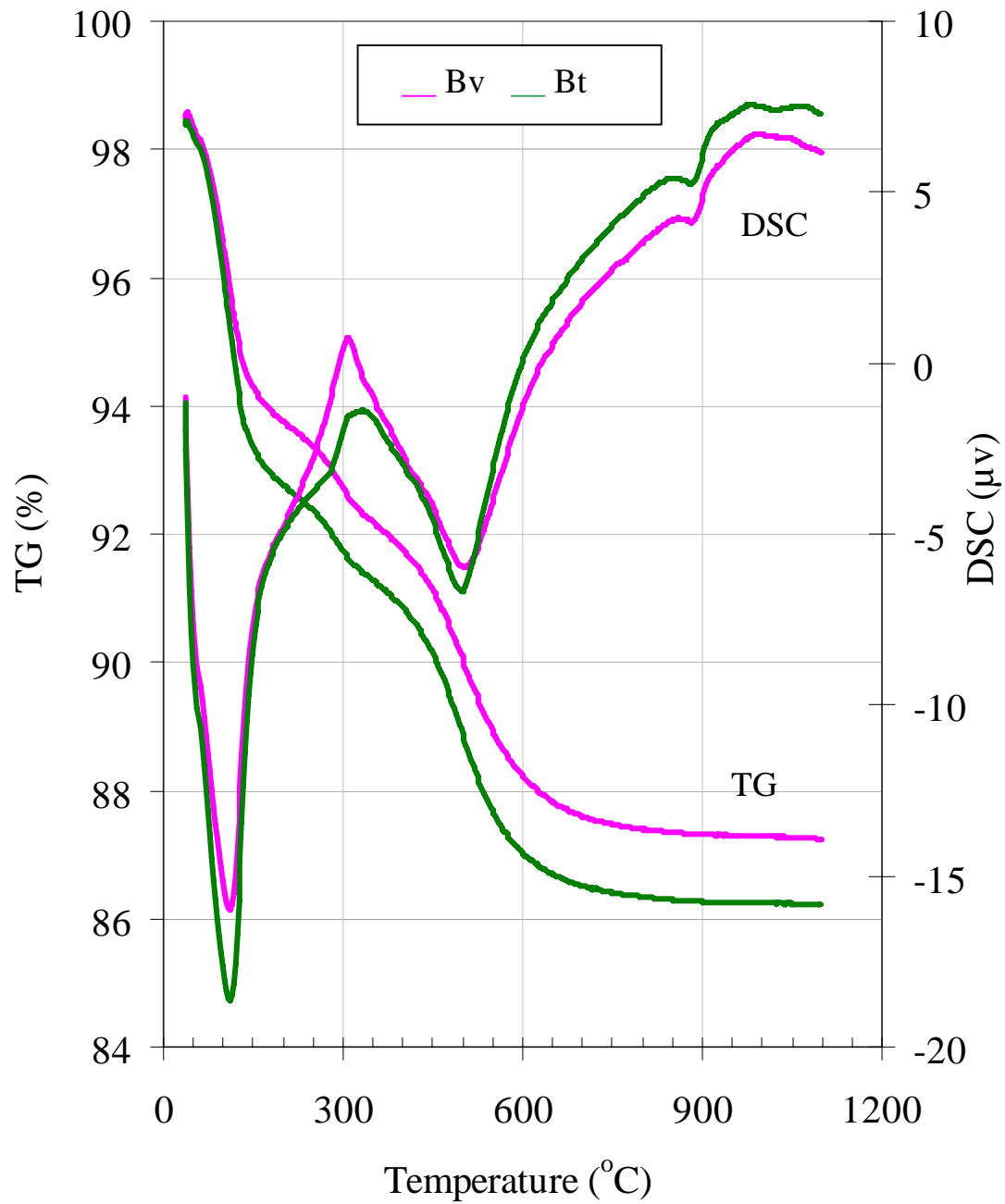
Pacca soil clay (<2.0 μm)

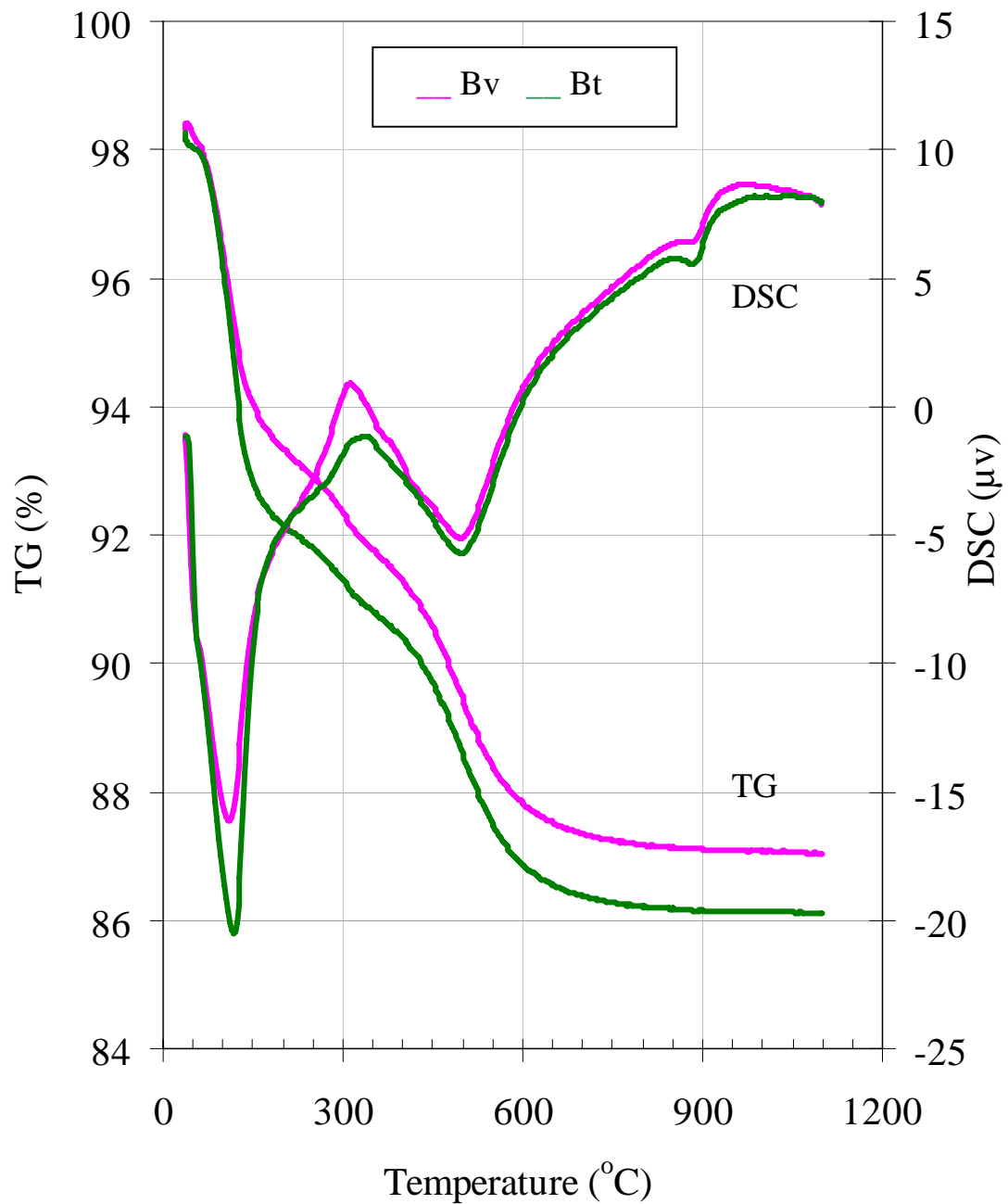
Pitafi soil clay (<2.0 μm)

Peshawar soil clay (<2.0 μm)

Murree soil clay (<2.0 μm)

Guliana soil clay (<2.0 μm)

Prb-Ostb soil clay (<2.0 μm)

Prb-Wein soil clay (<2.0 μm)

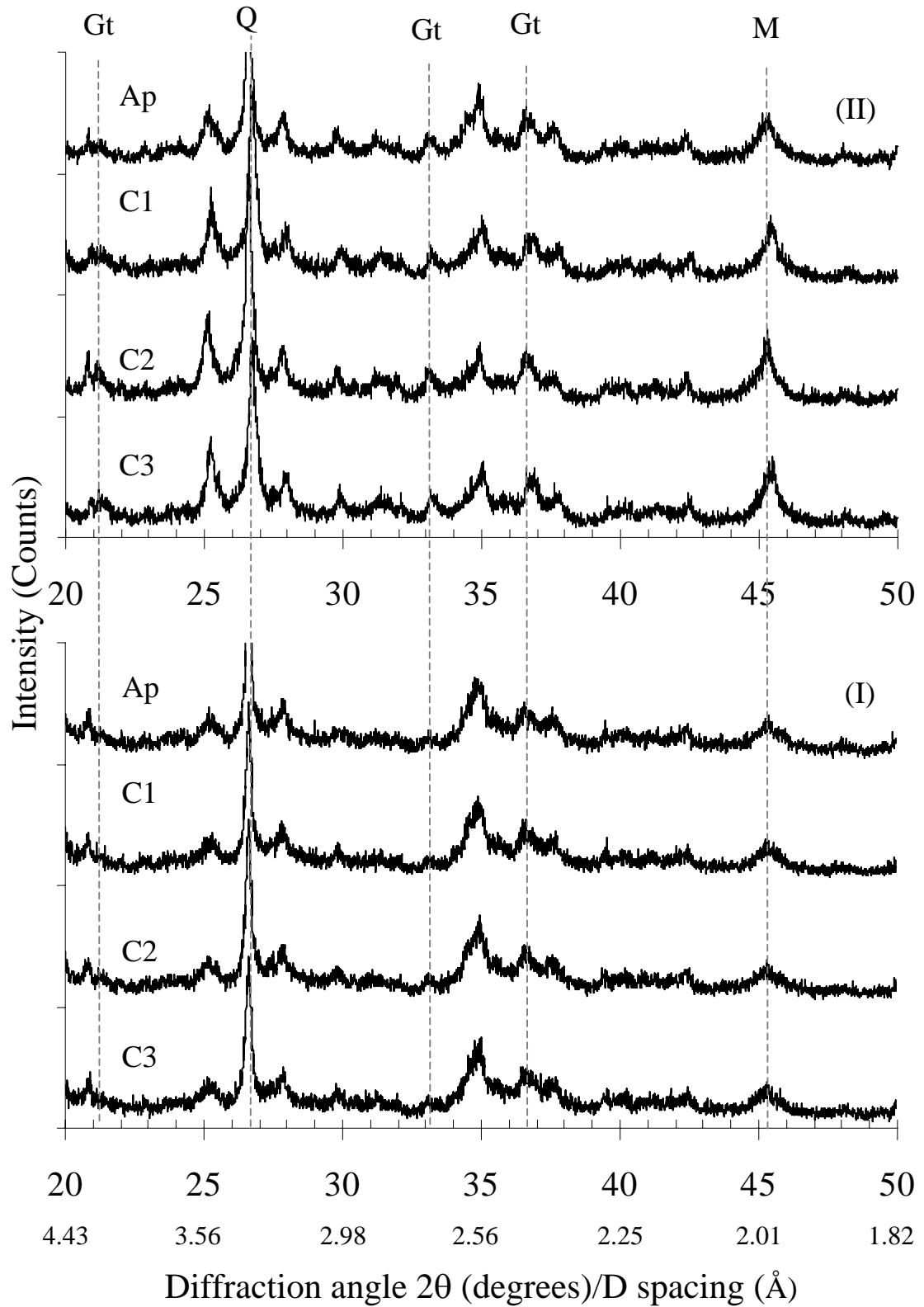
Appendix VI. Vermiculite, smectite, kaolinite, goethite and hematite content of soil clays.

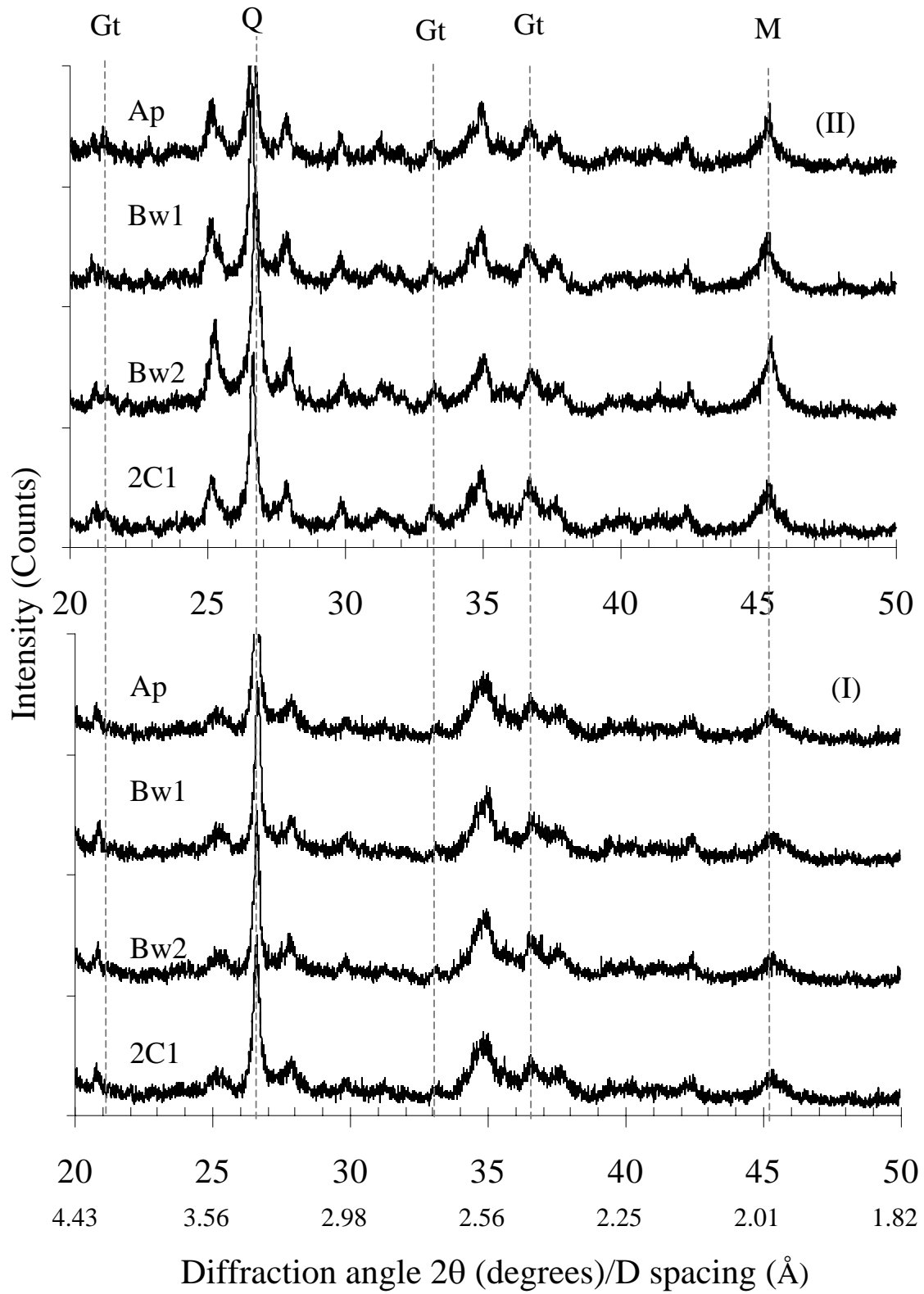
Soil	Horizon	Depth cm	Vm	Sm	K	Gt	Hm	Gt Hm	
								-----g 100 ⁻¹ g clay-----	
Shahdara	Ap	0-16	0.76	19.00	19.10	7.64		13.50	
	C1	16-32	14.73	18.65	18.03	7.08		12.07	
	C2	32-63	0.00	16.97	19.27	7.36		0.81	
	C3	63-78	7.49	16.87	18.51	8.06		4.83	
Sultanpur	Ap	0-13	15.68	17.08	17.87	7.72		16.71	
	Bw1	13-39	13.65	21.77	17.53	7.40		16.80	
	Bw2	39-62	6.71	16.56	18.24	7.34		18.04	
	2C1	62-81	9.48	18.55	18.41	8.43		6.86	
Pacca	Ap	0-15	13.17	16.67	17.34	6.81		28.63	
	Bat	15-32	10.91	17.22	17.13	6.65		28.10	
	Bt1	32-53	4.29	15.90	18.27	4.65		22.02	
	Bt2	53-92	15.13	18.57	17.89	7.68		26.15	
Pitafi	Ap	0-15	13.87	21.53	17.94	3.92		3.49	
	Ayz	15-41	4.67	19.02	18.26	7.11		23.70	
	Bwy1	41-57	9.77	20.45	17.63	7.02		25.09	
	Bwy2	63-111	5.57	18.75	18.13	8.19		13.76	
Peshawar	Ap	0-11	7.62	15.25	20.57	5.94		18.32	
	Bt1	11-43	8.51	14.90	20.33	6.21		19.18	
	Bt2	43-66	12.70	16.21	19.47	6.14		16.83	
	2Btb	66-98	8.96	18.11	18.93	4.58		11.33	
Murree	A	0-11	5.79	13.72	25.44	-	2.76	-	5.21
	Bt1	11-30	4.27	18.25	25.01	-	2.05	-	3.92
	Bt2	30-52	8.10	10.80	25.26	-	2.29	-	4.88
	2Bt3	52-58	4.08	16.39	24.70	-	2.52	-	5.35
Guliana	Ap	0-12	9.69	19.56	32.11	7.84		16.39	
	Batc	12-25	11.67	19.27	32.43	7.53		16.27	
	Btc1	25-56	11.26	15.53	29.29	7.11		20.56	
	Btc2	56-83	18.97	28.88	27.35	7.40		18.48	
Prb-Ostb	Ah	0-4	0.00	15.46	14.01	-			
	Bv	4-25	1.28	18.23	15.50	8.24		20.19	
	Bt	25-50	16.16	22.92	15.98	7.74		34.17	
	C	>50	5.73	16.58	13.59	-			
Prb-Wein	Bv	4-25	17.46	14.38	16.64	7.04		16.76	
	Bt	25-45	12.80	17.14	17.71	7.31		33.71	
	C	>45	7.54	18.38	17.36	-			

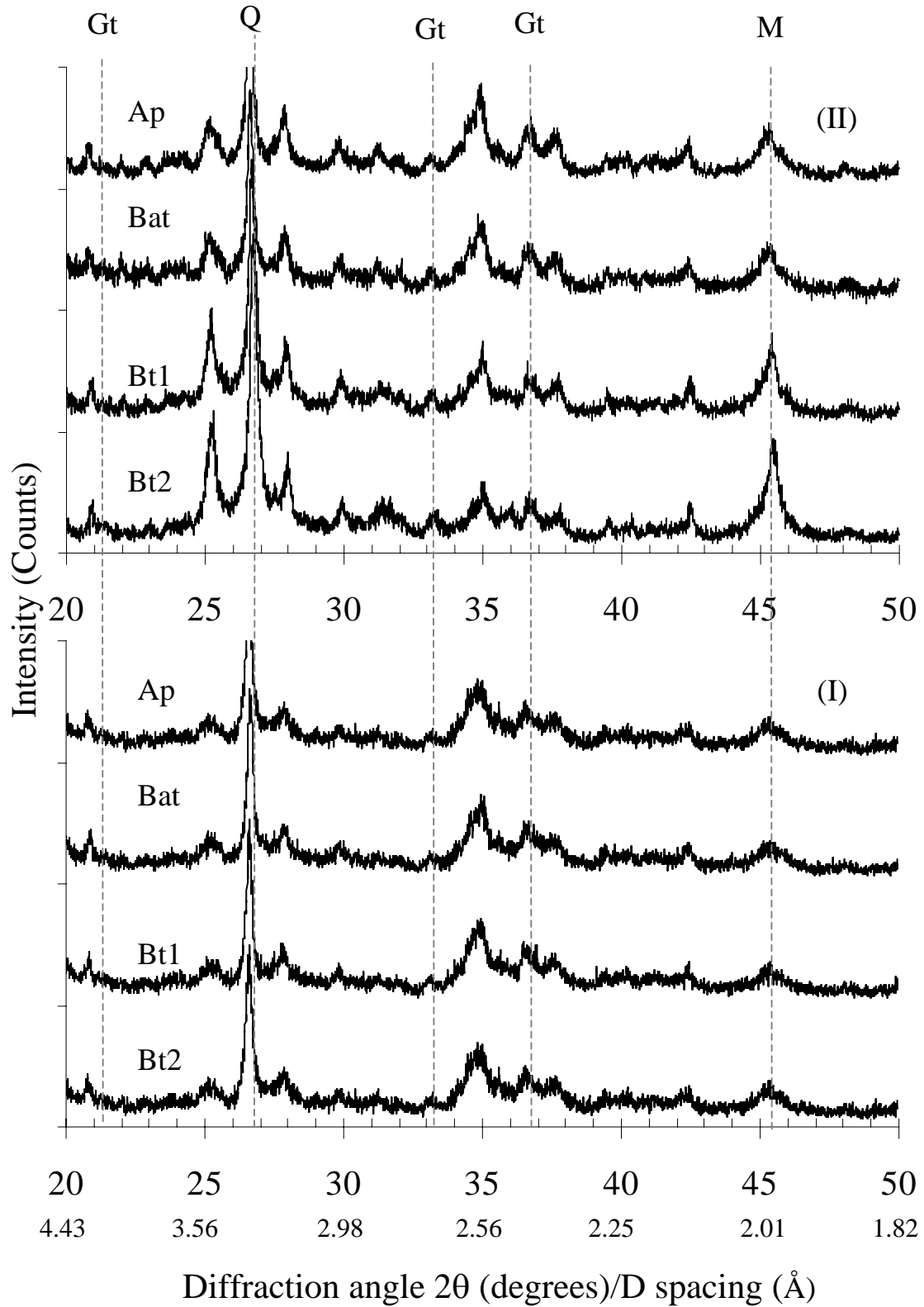
Vm, vermiculite and **Sm**, smectite by Ca/Mg and K/NH₄ CEC; **K**, kaolinite by DTGA; **Gt**, goethite and, **Hm**, hematite by voltammetry.

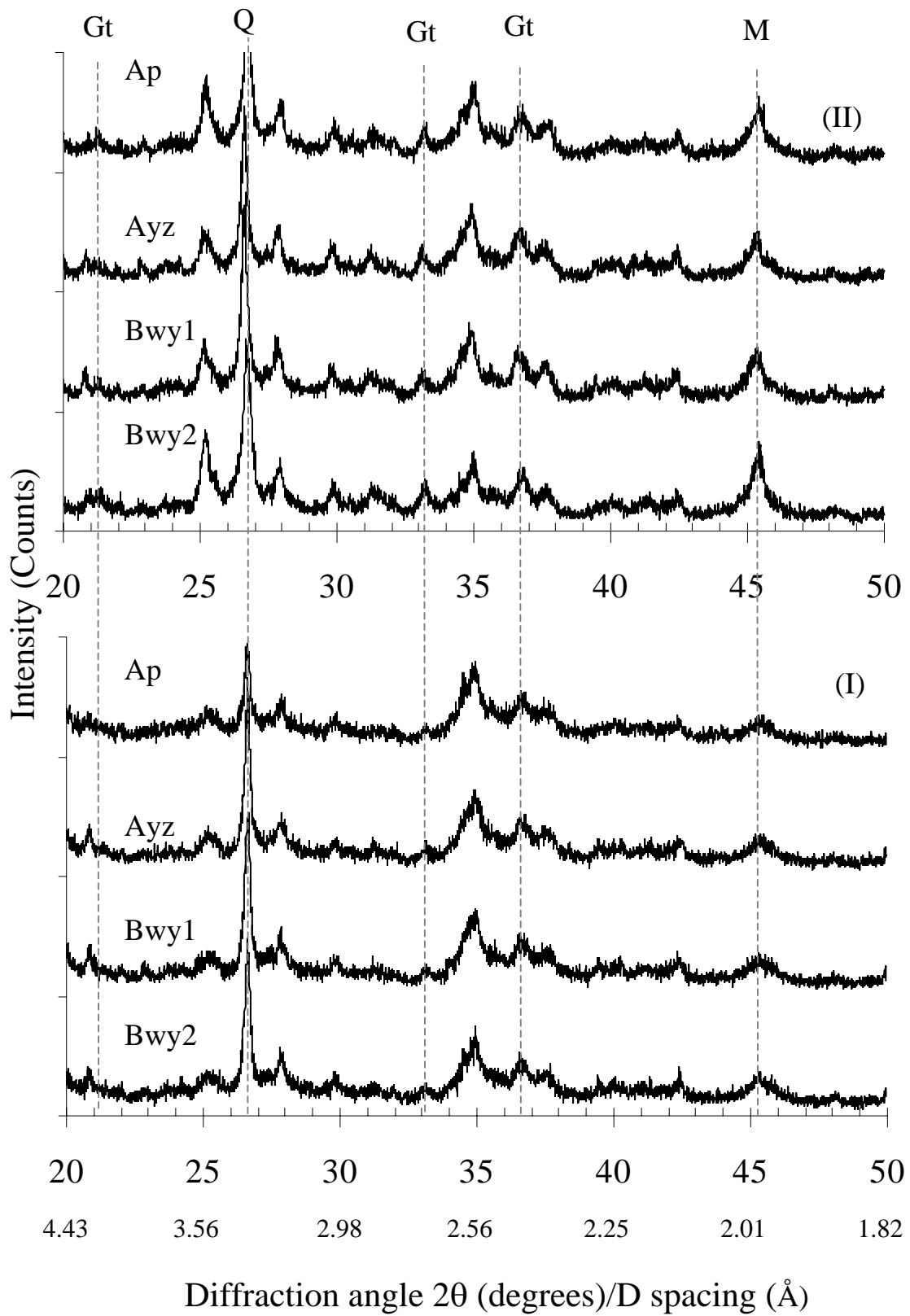
Appendix VII

X-ray diffraction pattern for clay ($<2\mu\text{m}$) size fractions taken from four horizons (two horizons in case of German soils) of each soil profile investigated: before (I) and after (II) pre-concentration treatment showing goethite/hematite. Gt, goethite; Hm; Q, quartz; and M, mica. Goethite is represented by diffraction lines at 4.18, 2.69, and 2.45 Å. Hematite is represented by diffraction lines 2.70, 2.52, 2.21, and 1.84 Å.

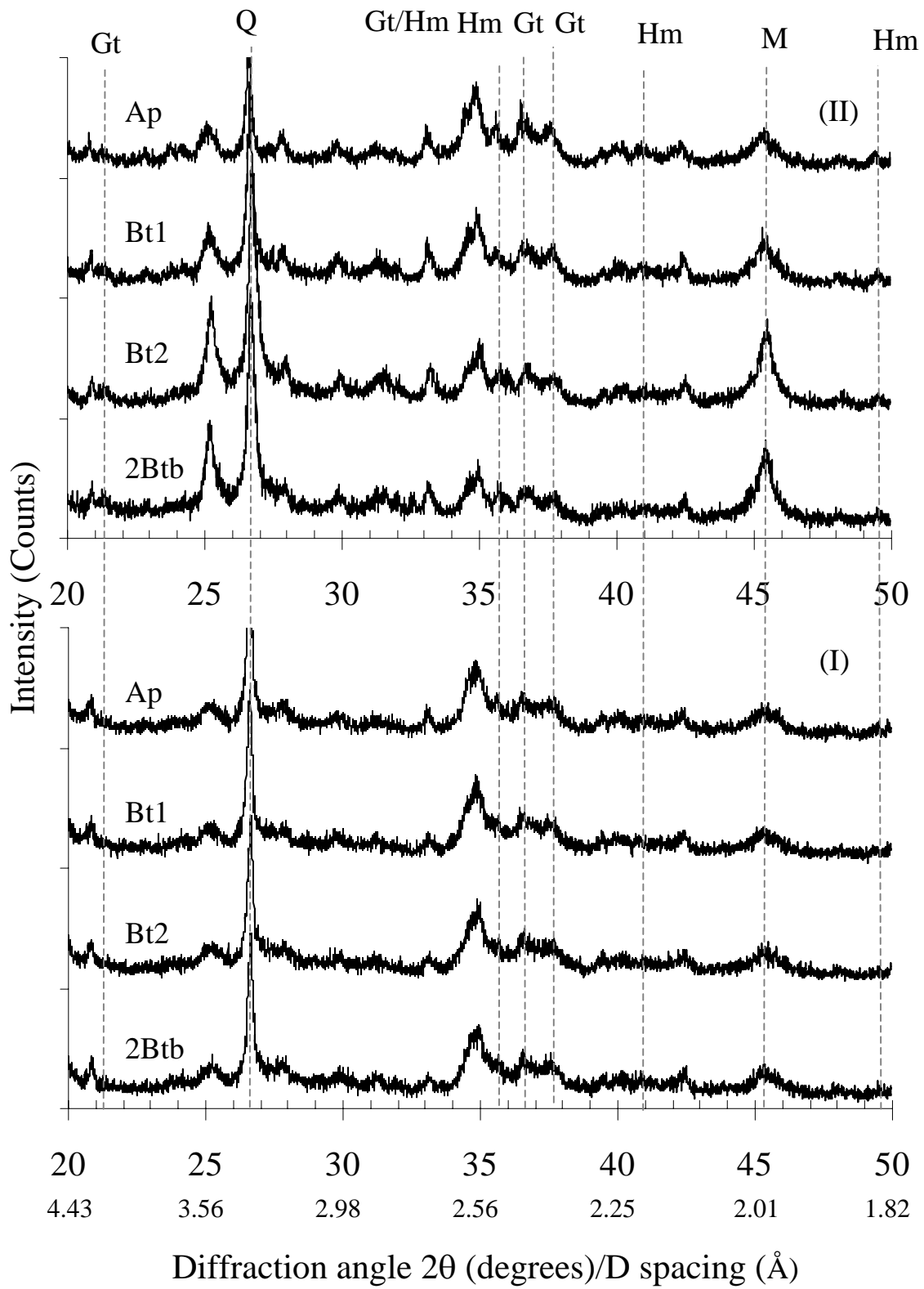
Shahdara soil clay (2 μm)

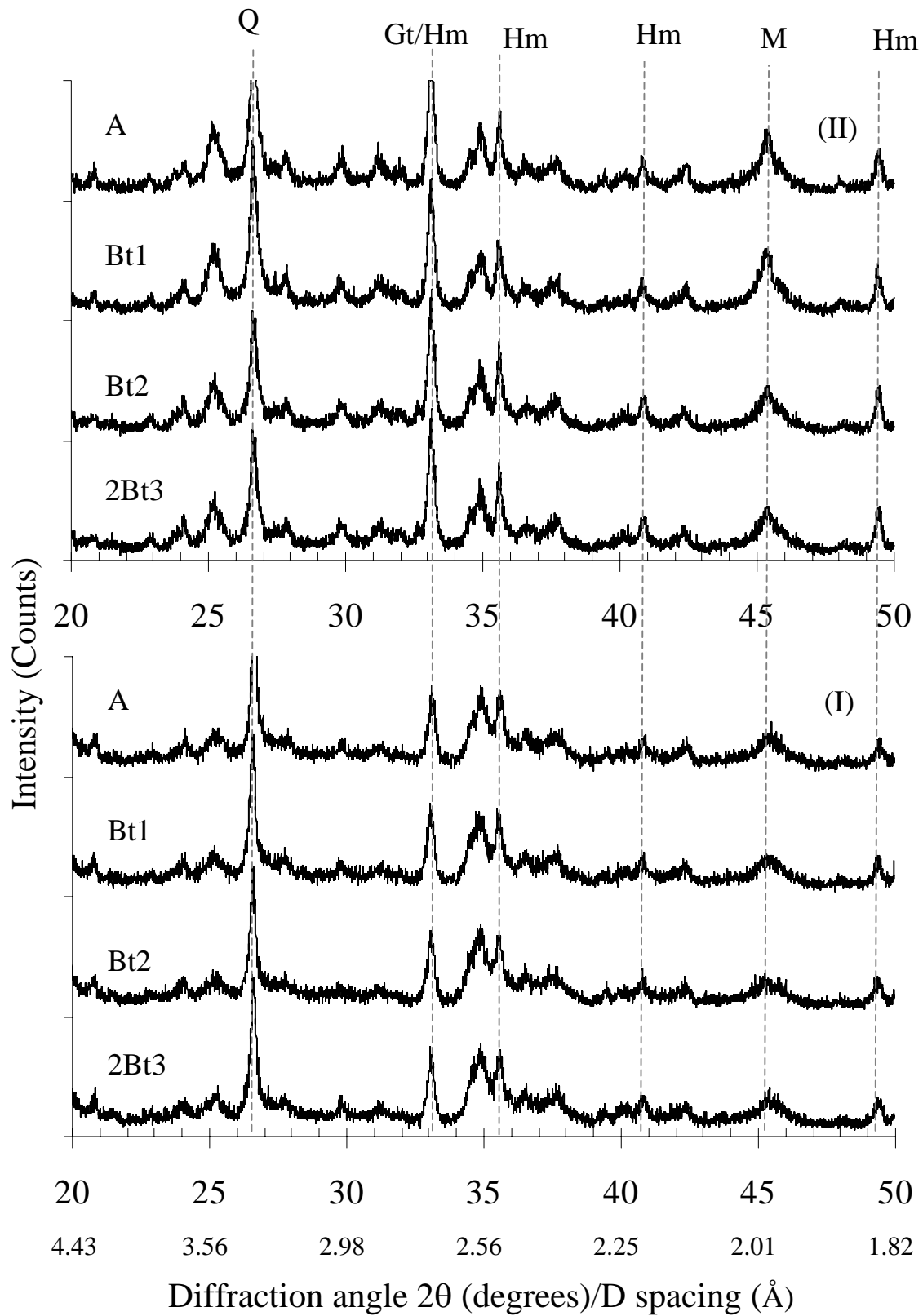
Sultanpur soil clay (2 μm)

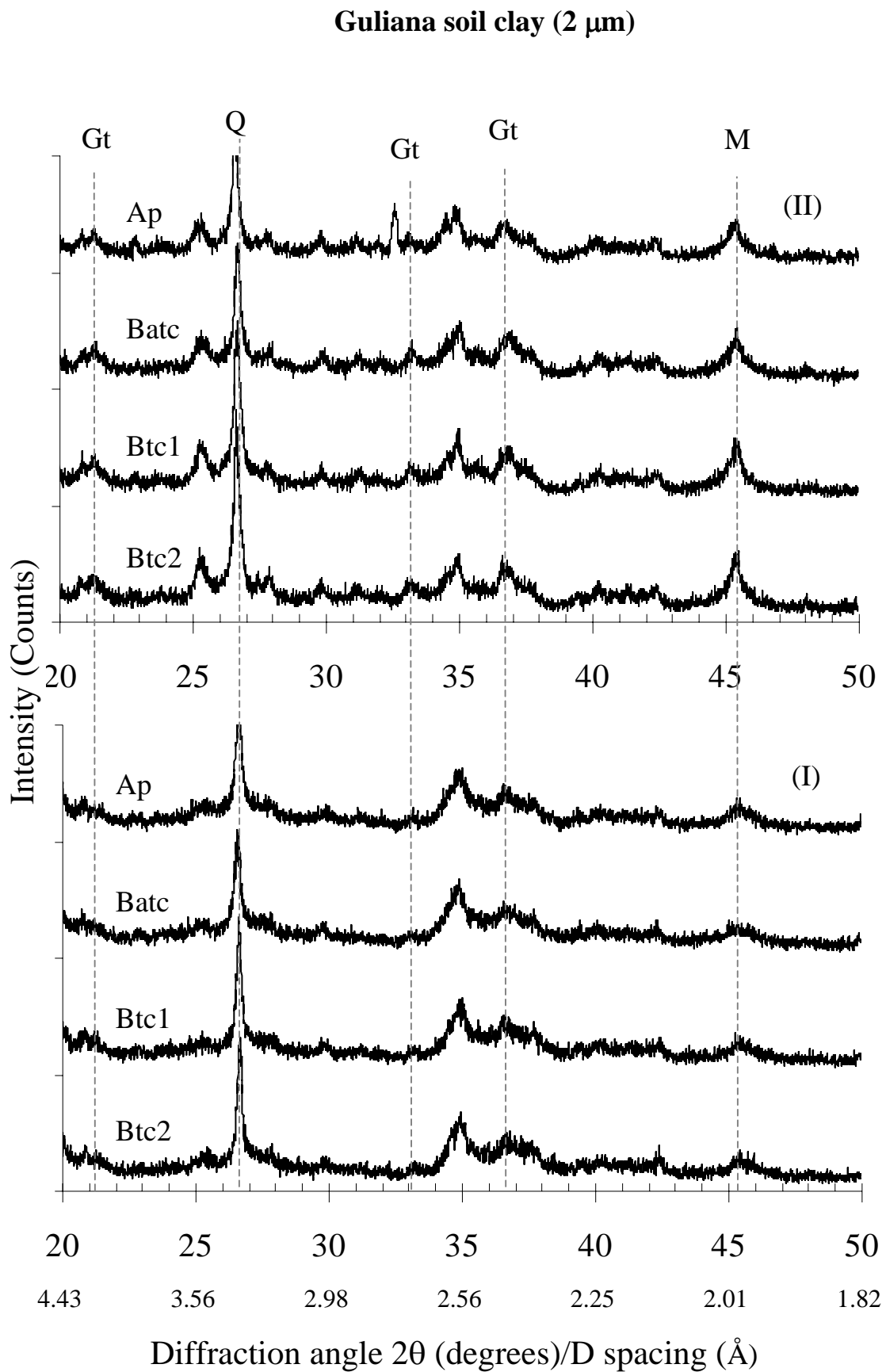
Pacca soil clay (2 μm)

Pitafi soil clay (2 μm)

Peshawar soil clay (2 μm)

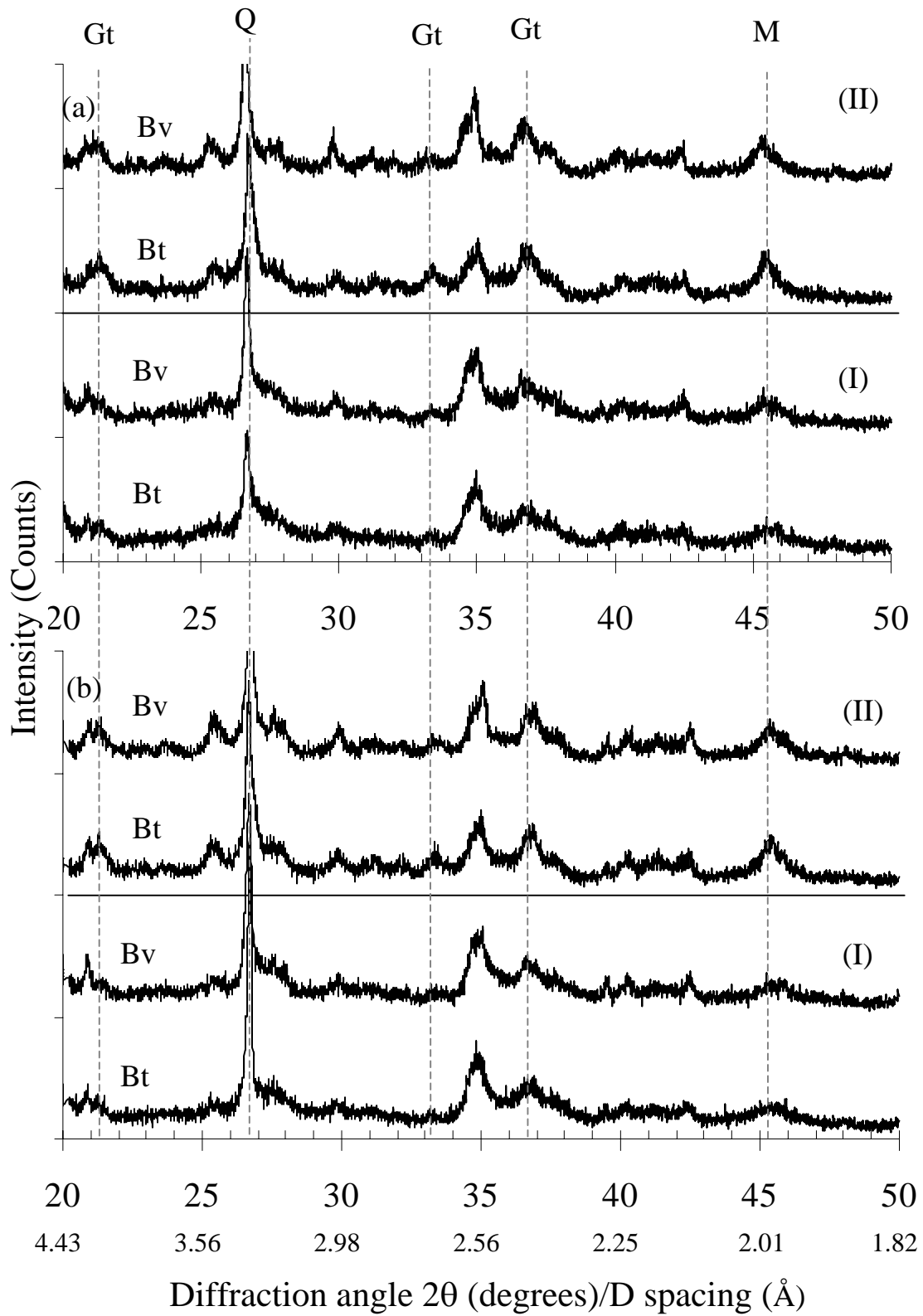


Murree soil clay (2 μm)



Parabraunerde soil clay (2 μm)

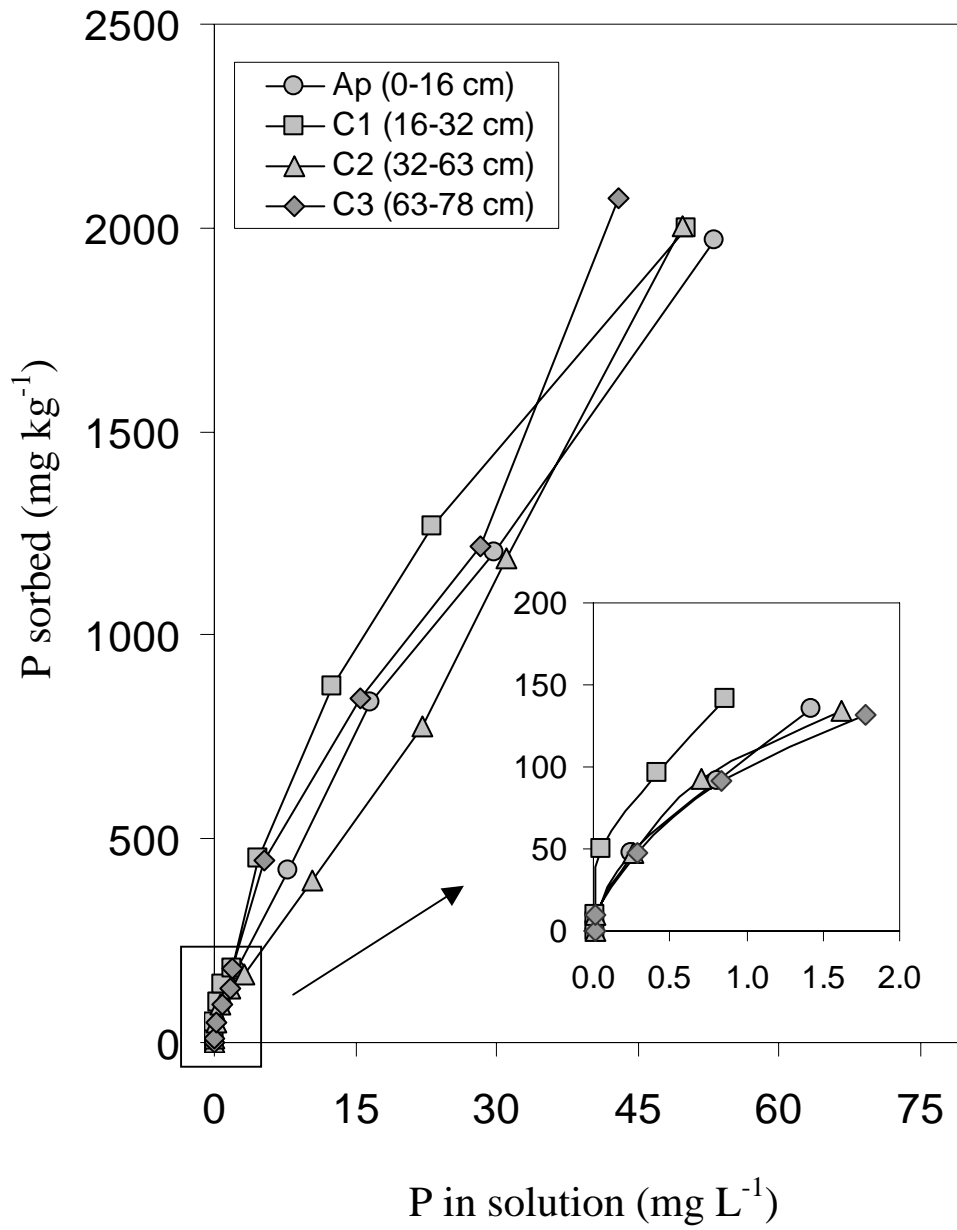
(a) Osterburken (b) Weingarten



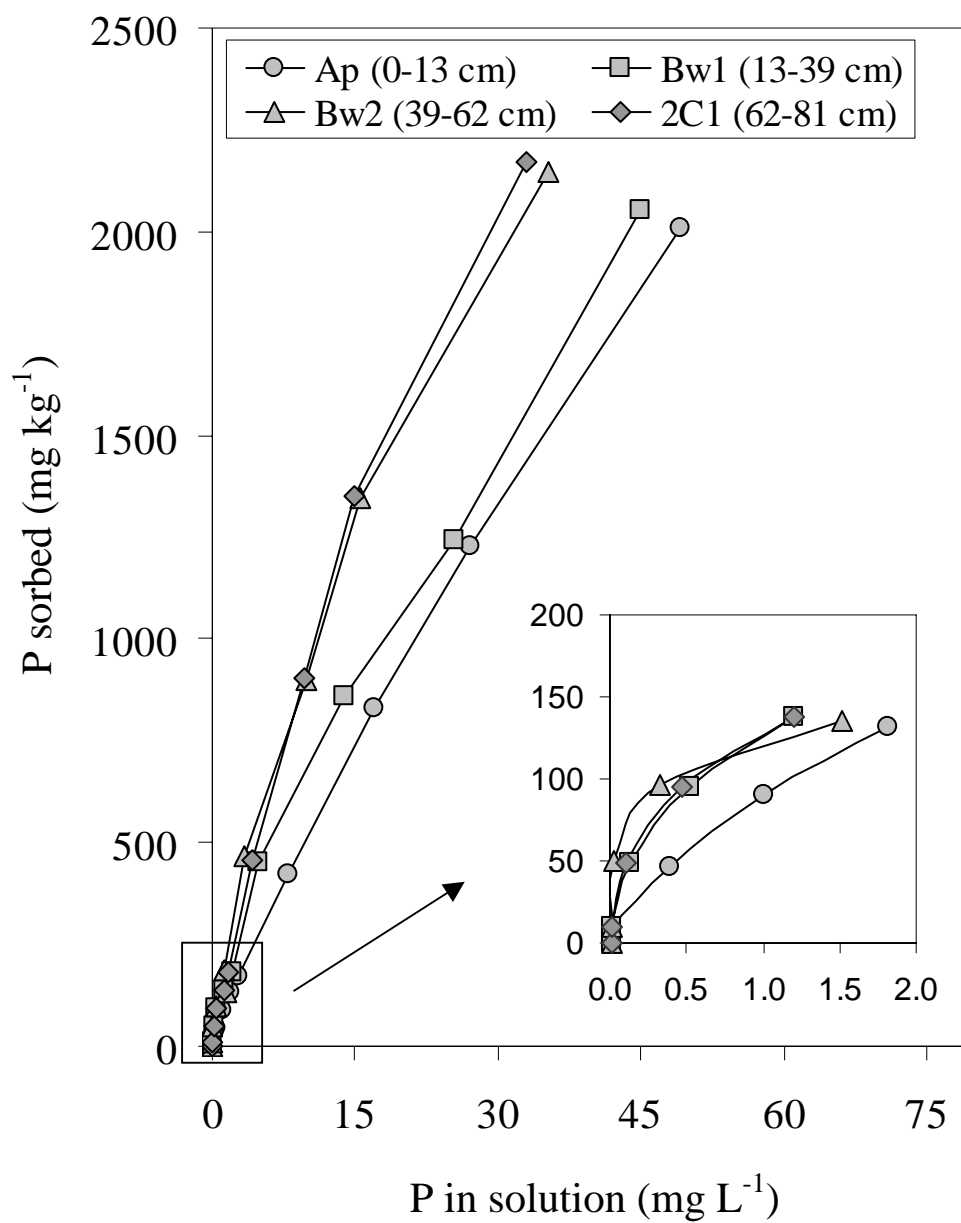
Appendix VIII

Phosphorus adsorption isotherms of soils taken from four horizons (two horizons in case of German soils) of each soil profile investigated: where P adsorbed, ($x/m \text{ mg kg}^{-1}$) is plotted versus equilibrium concentration (mg L^{-1}). The inset in each case depicts the initial part of isotherm.

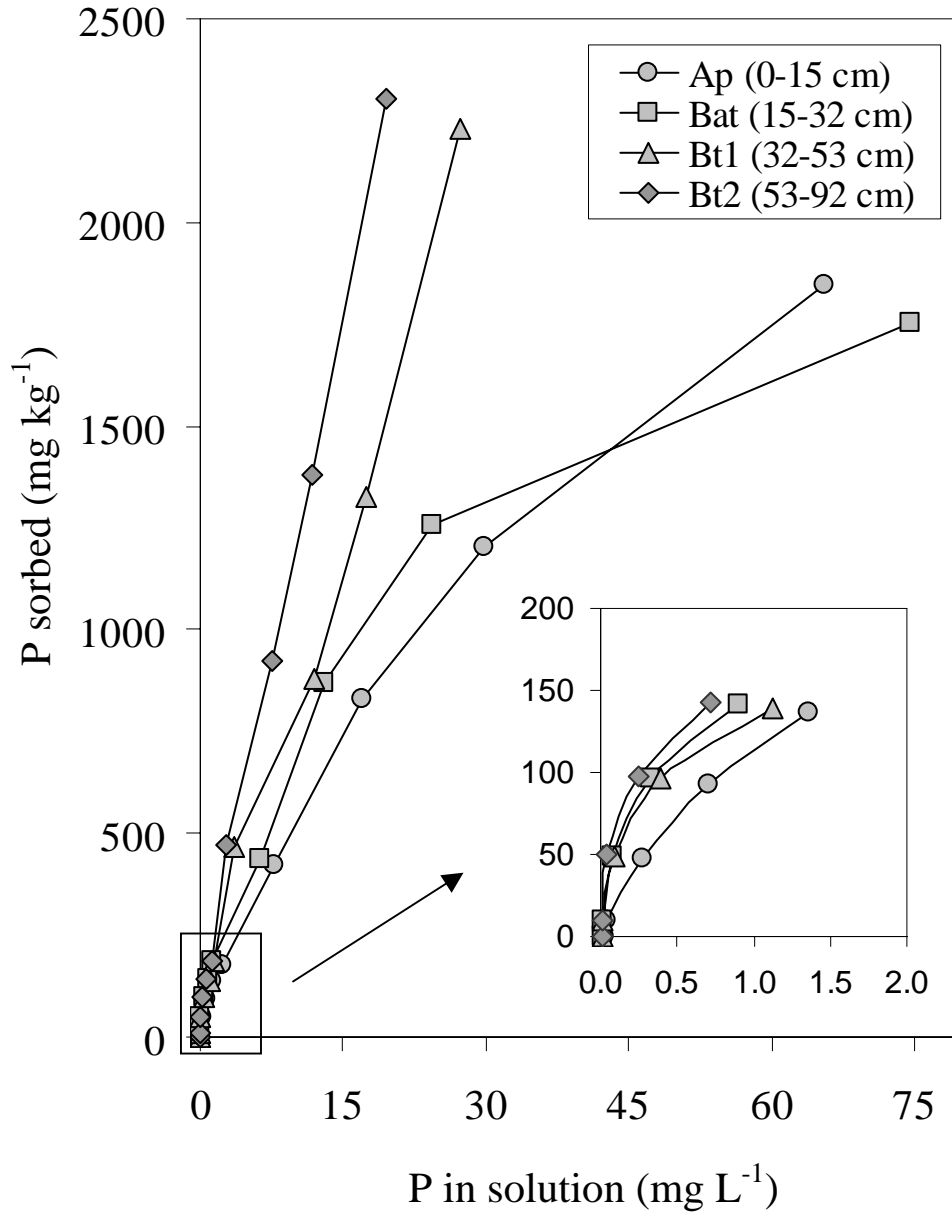
Shahdara soil profile



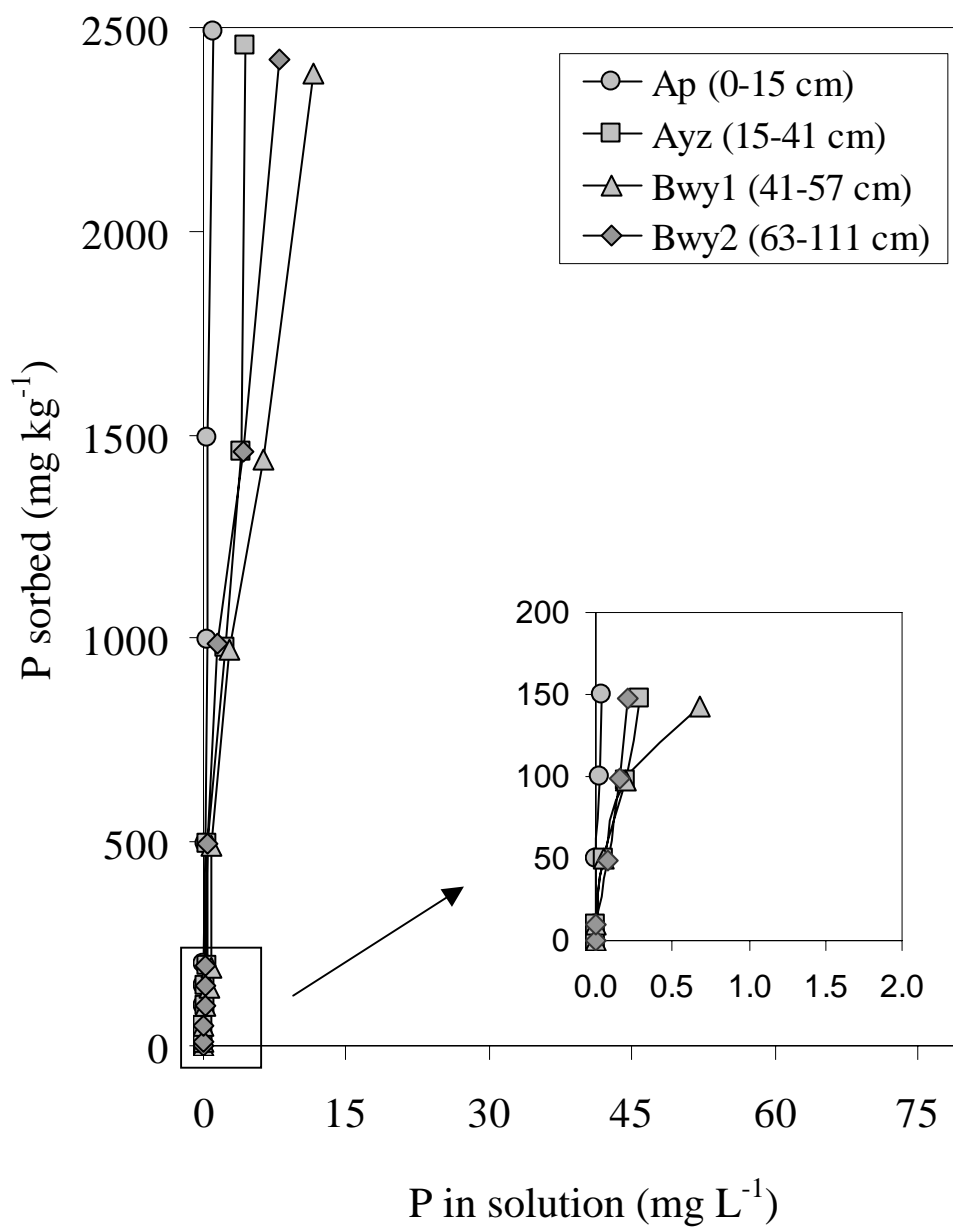
Sultanpur soil profile



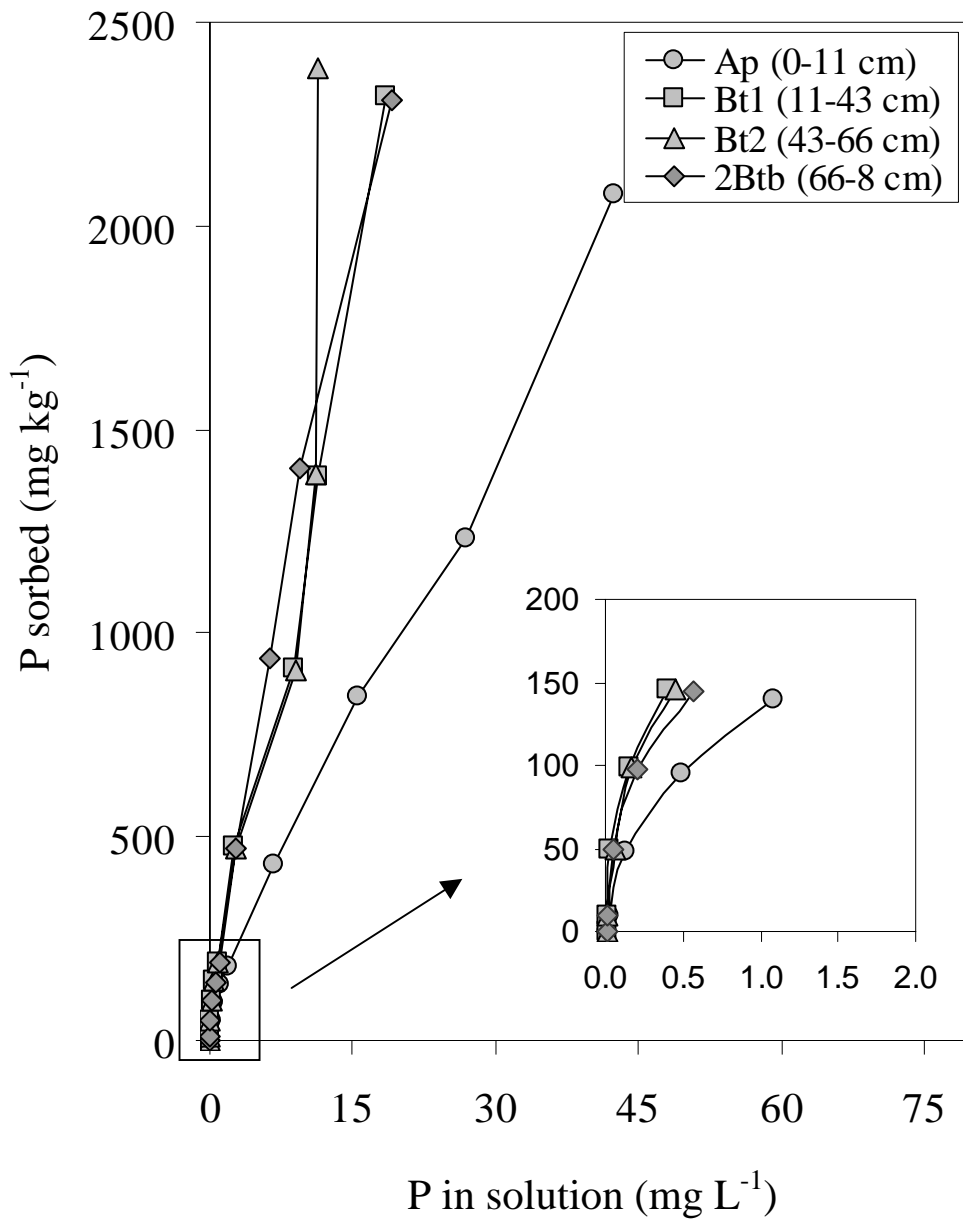
Pacca soil profile

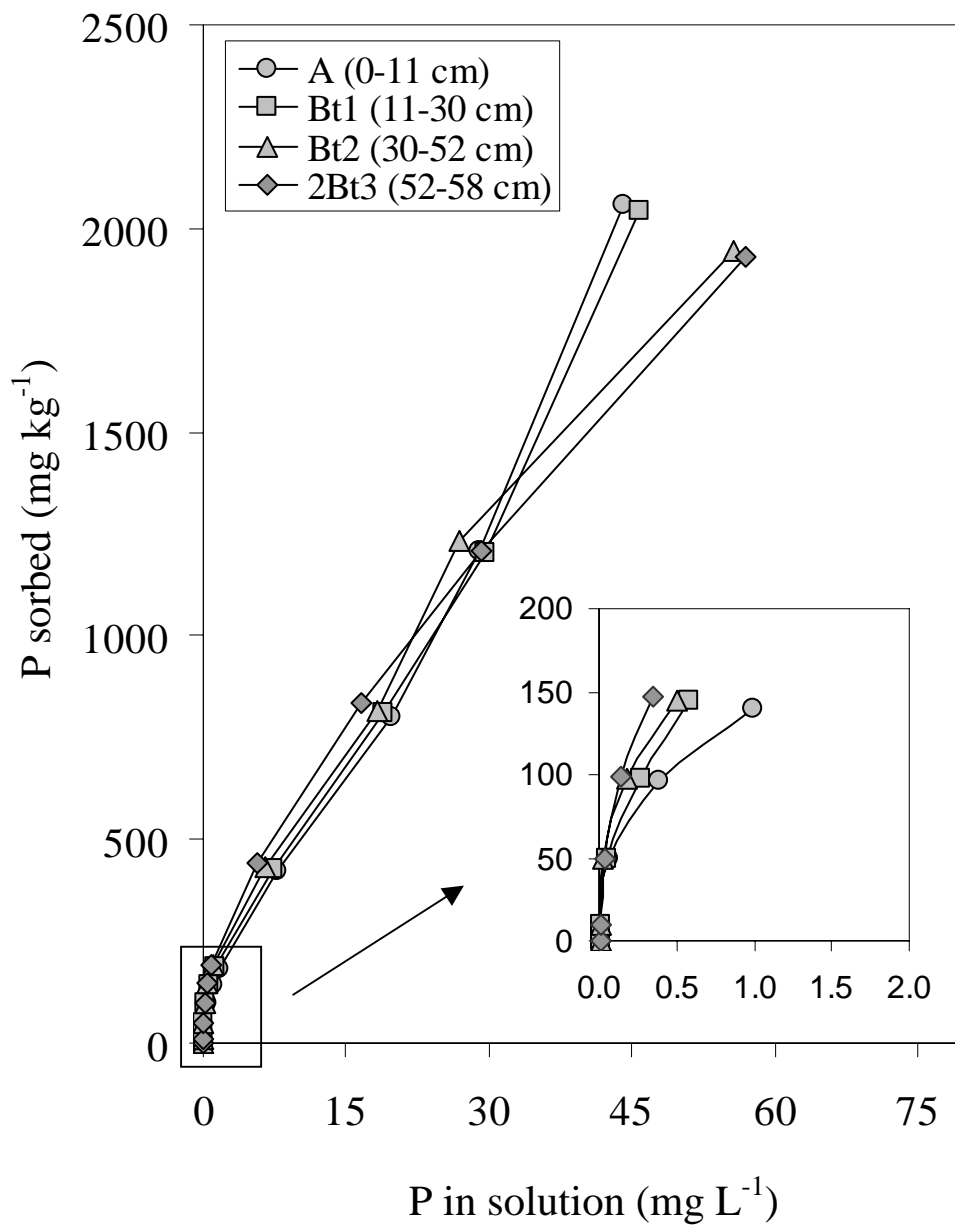


Pitafi soil profile

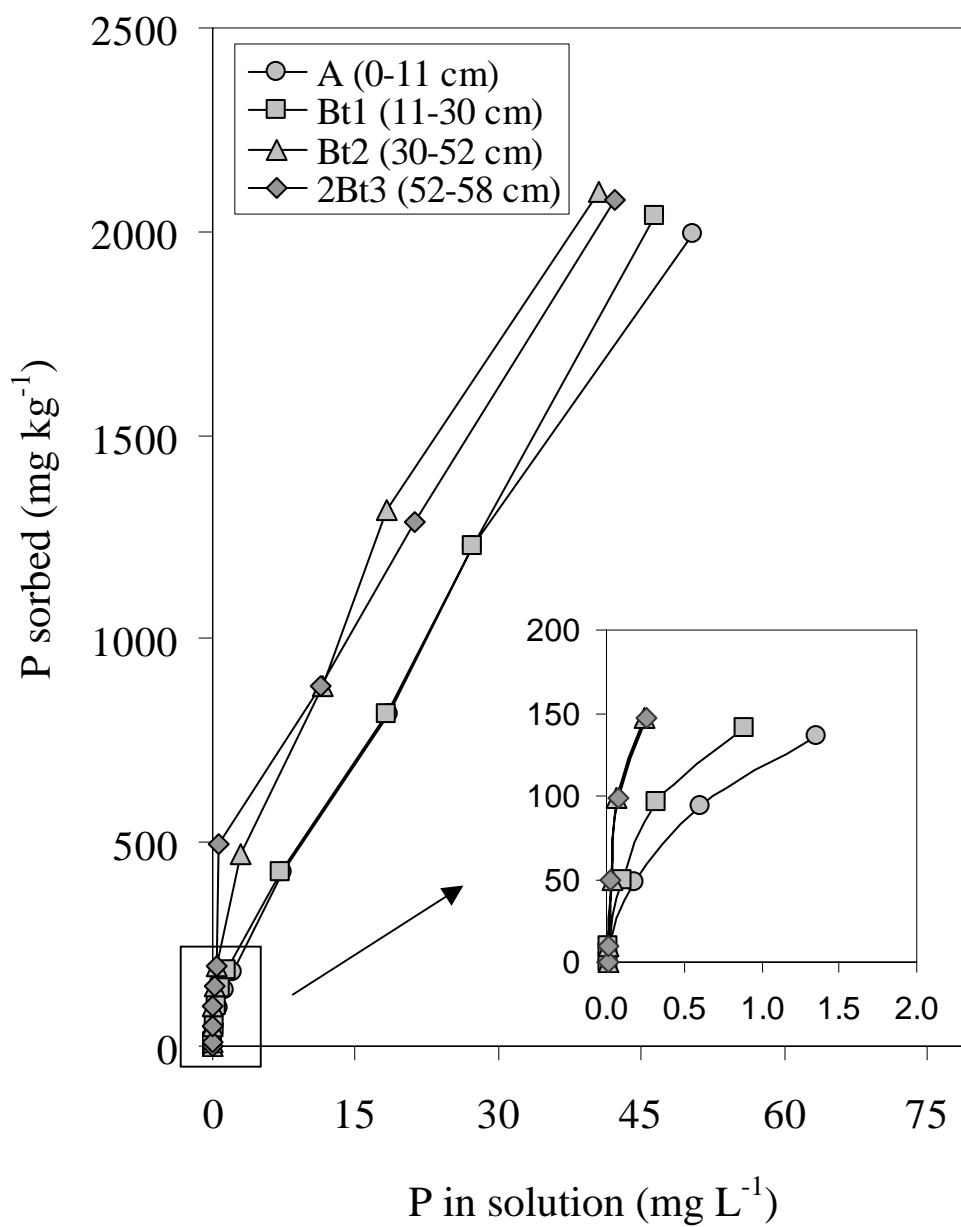


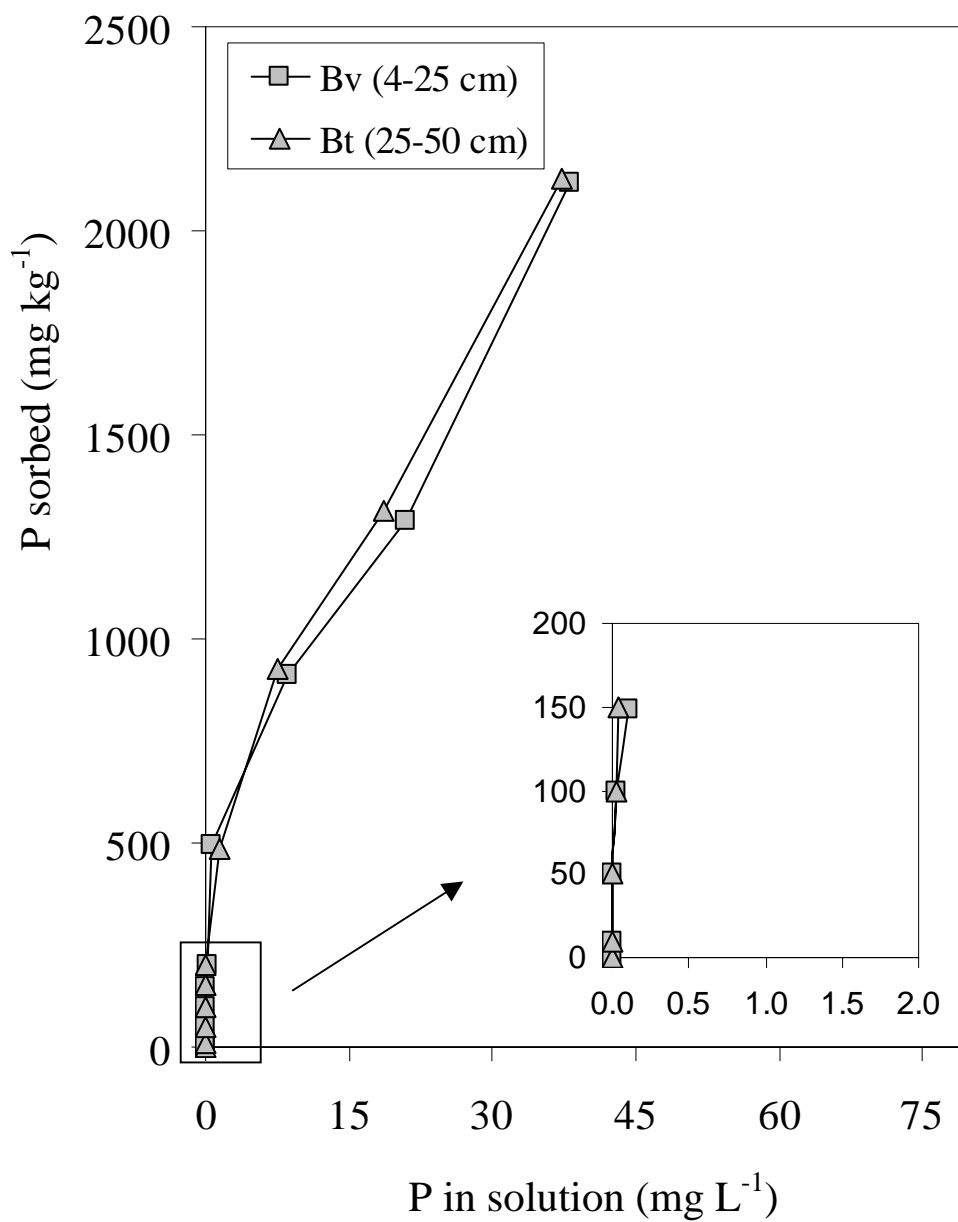
Peshawar soil profile

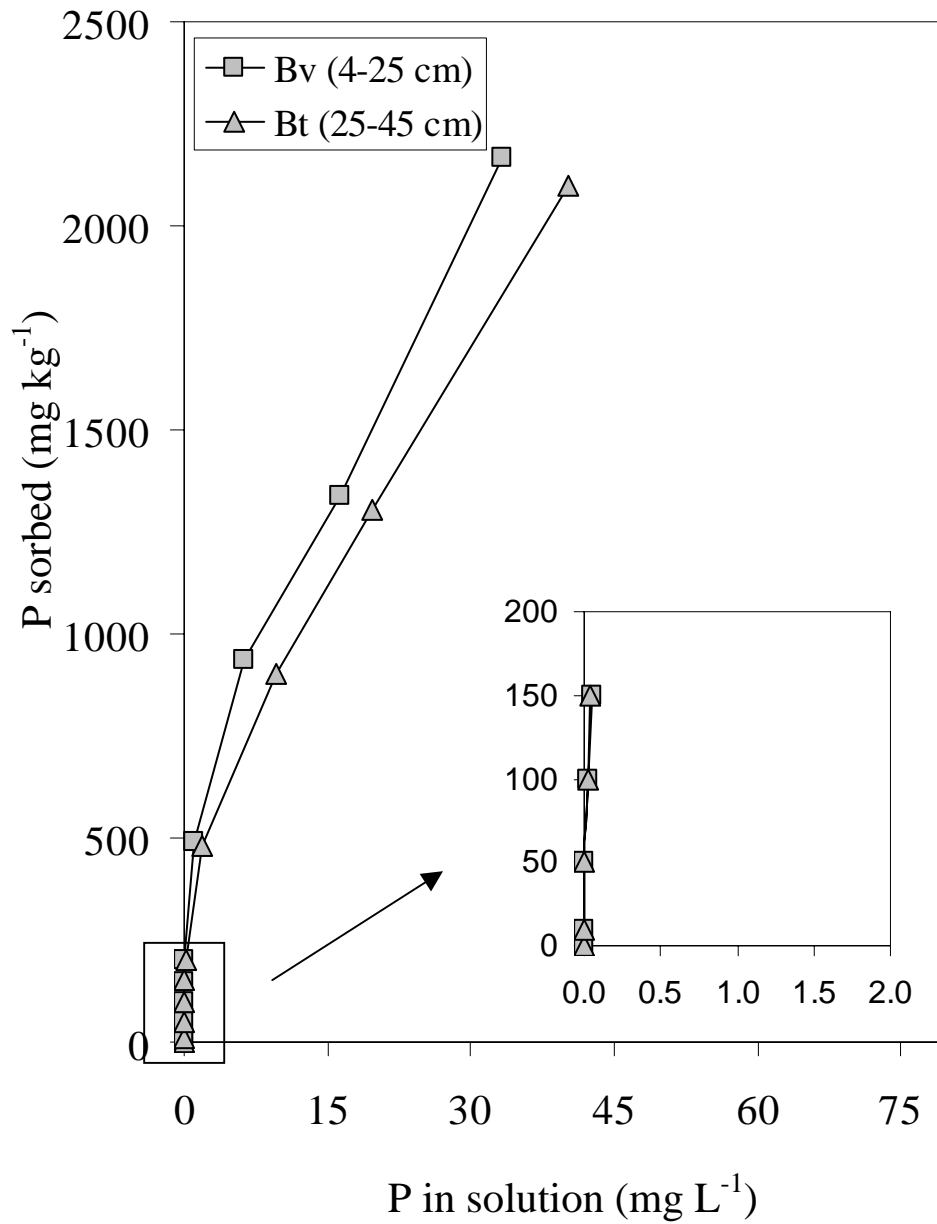


Murree soil profile

Guliana soil profile



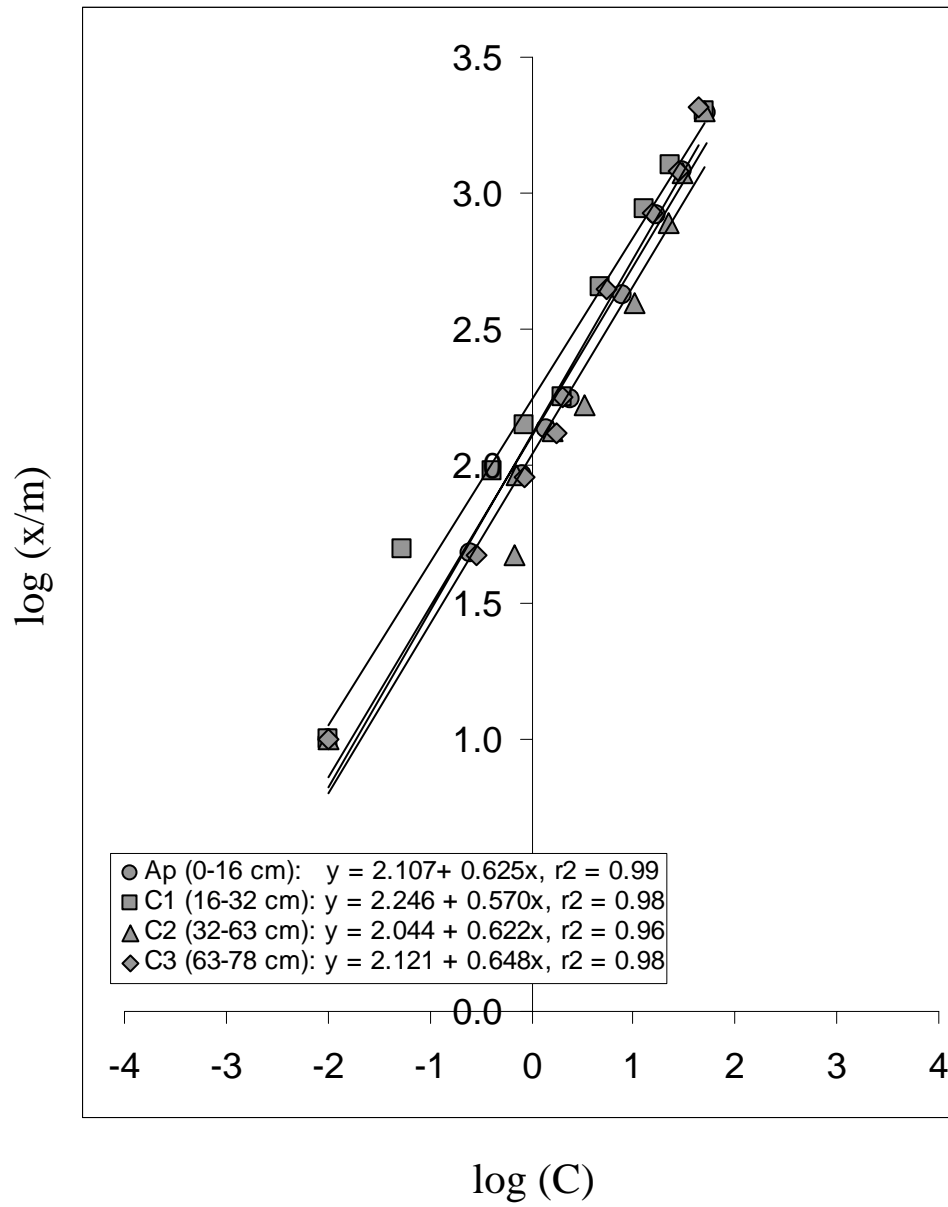
Parabraunerde from Osterburken soil profile

Parabraunerde from Weingarten soil profile

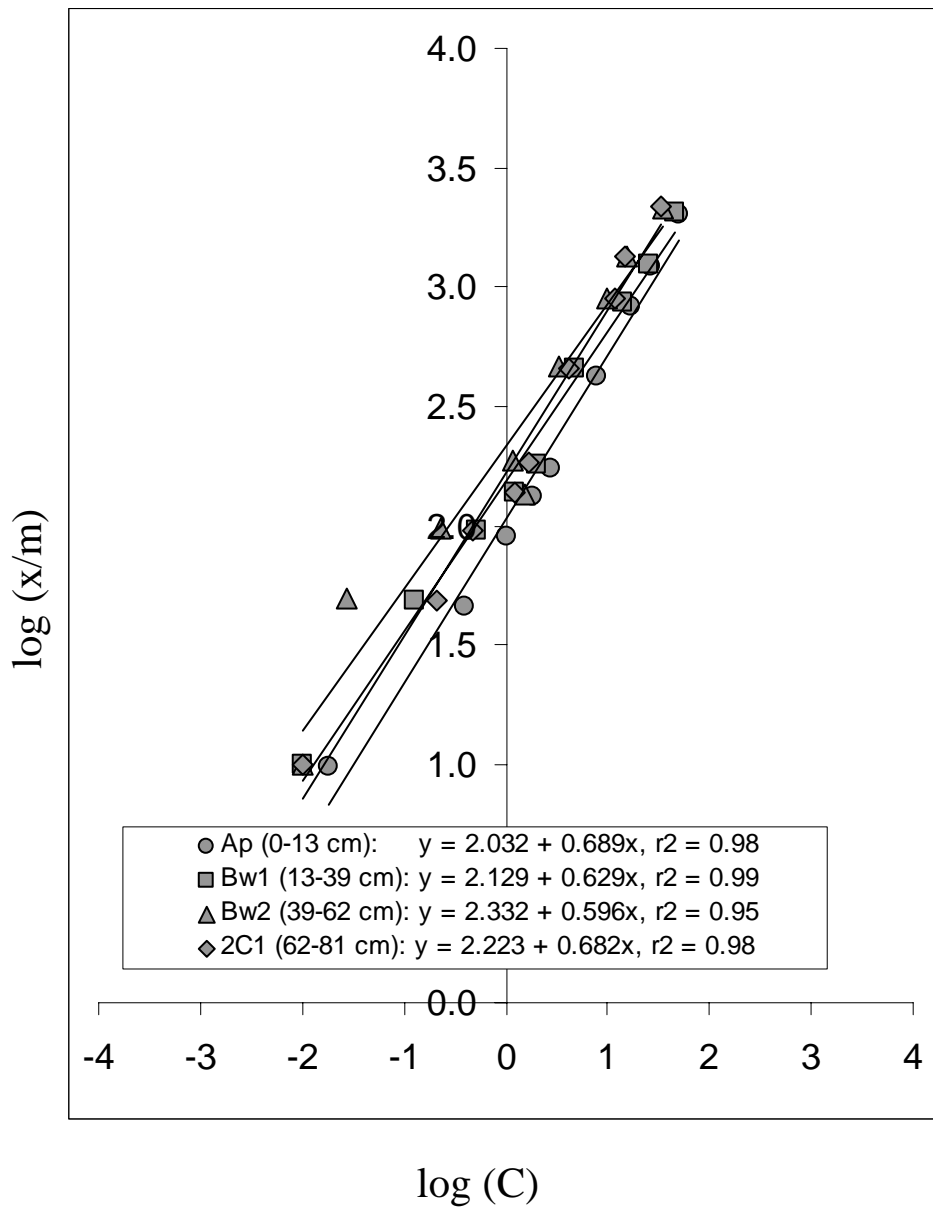
Appendix IX

Phosphorus adsorption isotherms of soils taken from four horizons (two horizons in case of German soils) of each soil profile investigated and fitted to Freundlich equation.

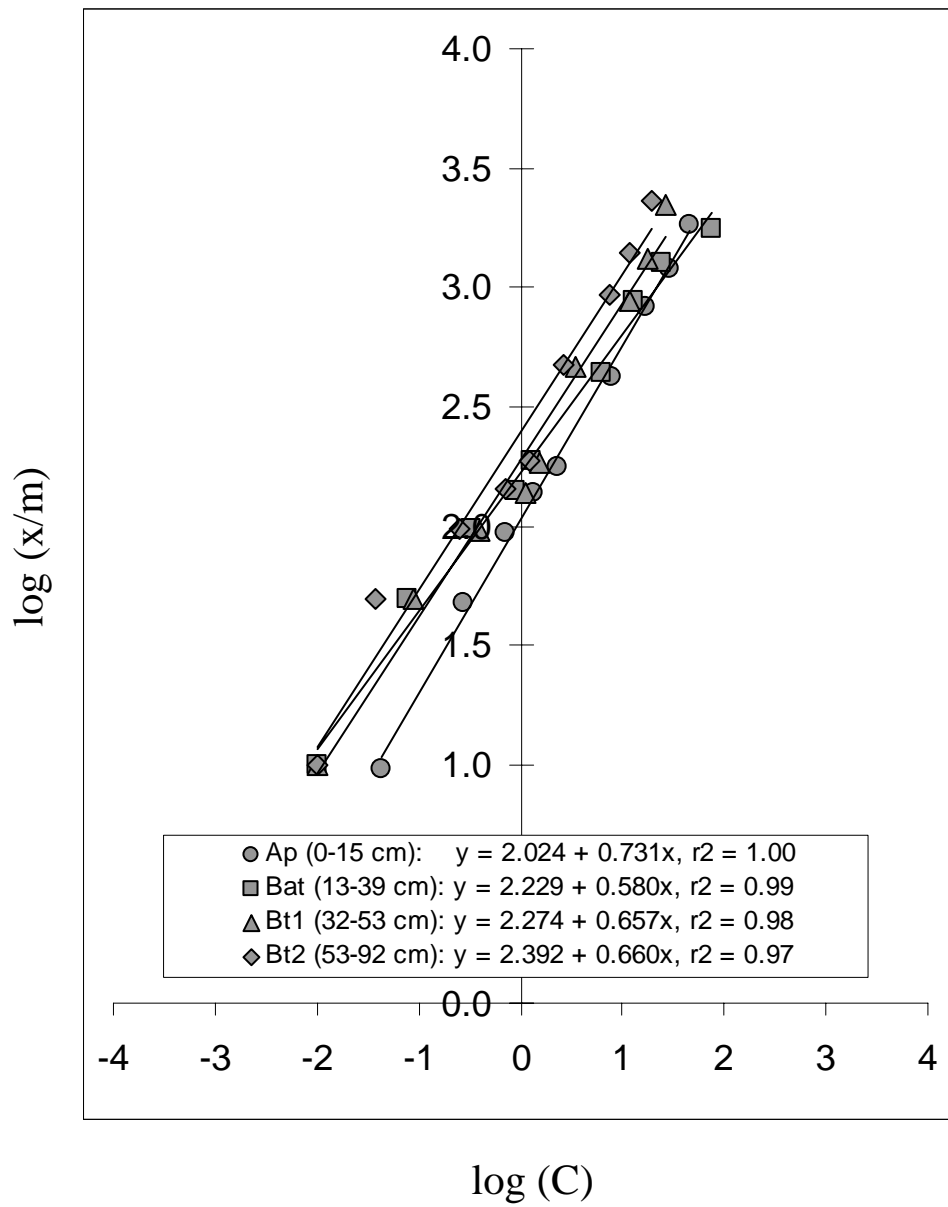
Shahdara soil profile

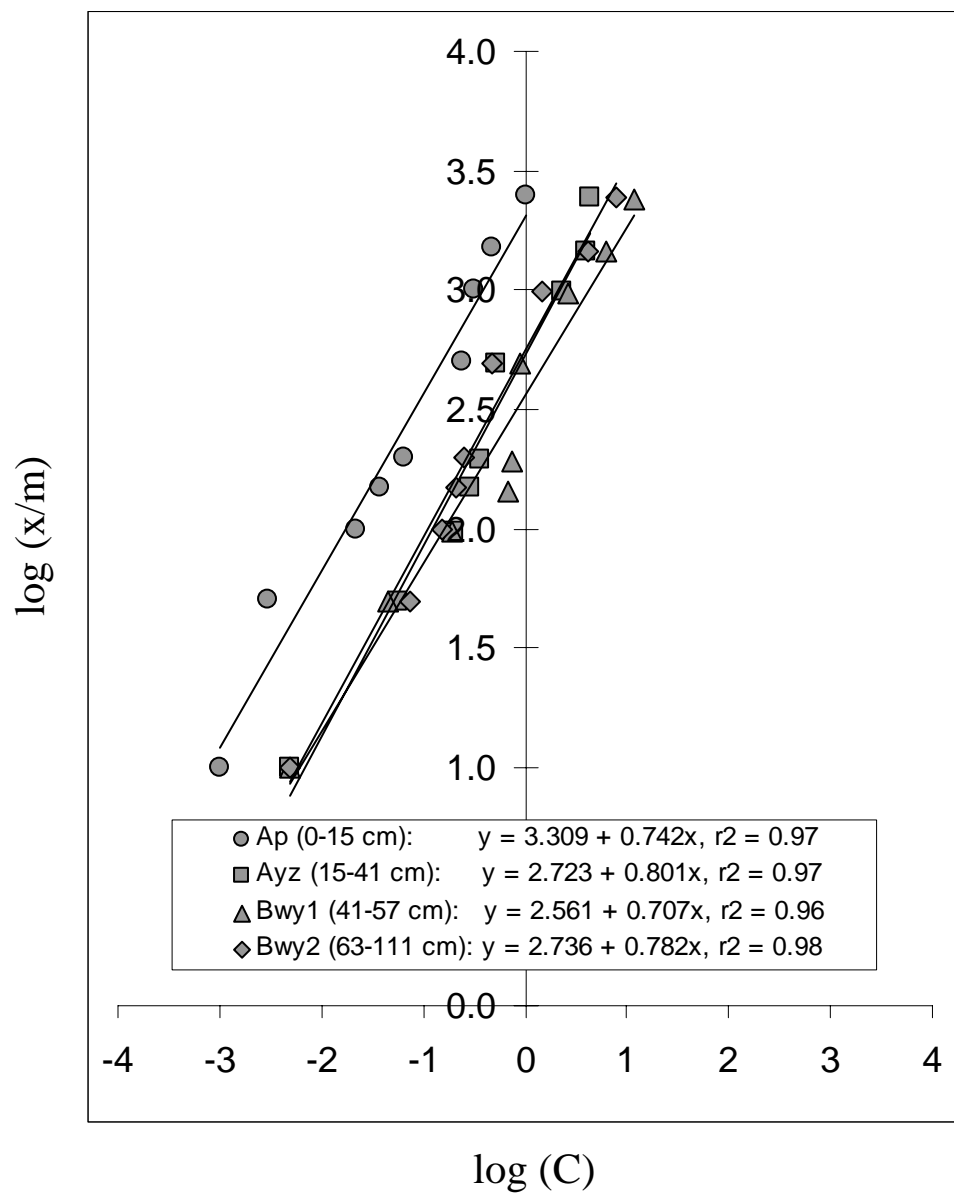


Sultanpur soil profile

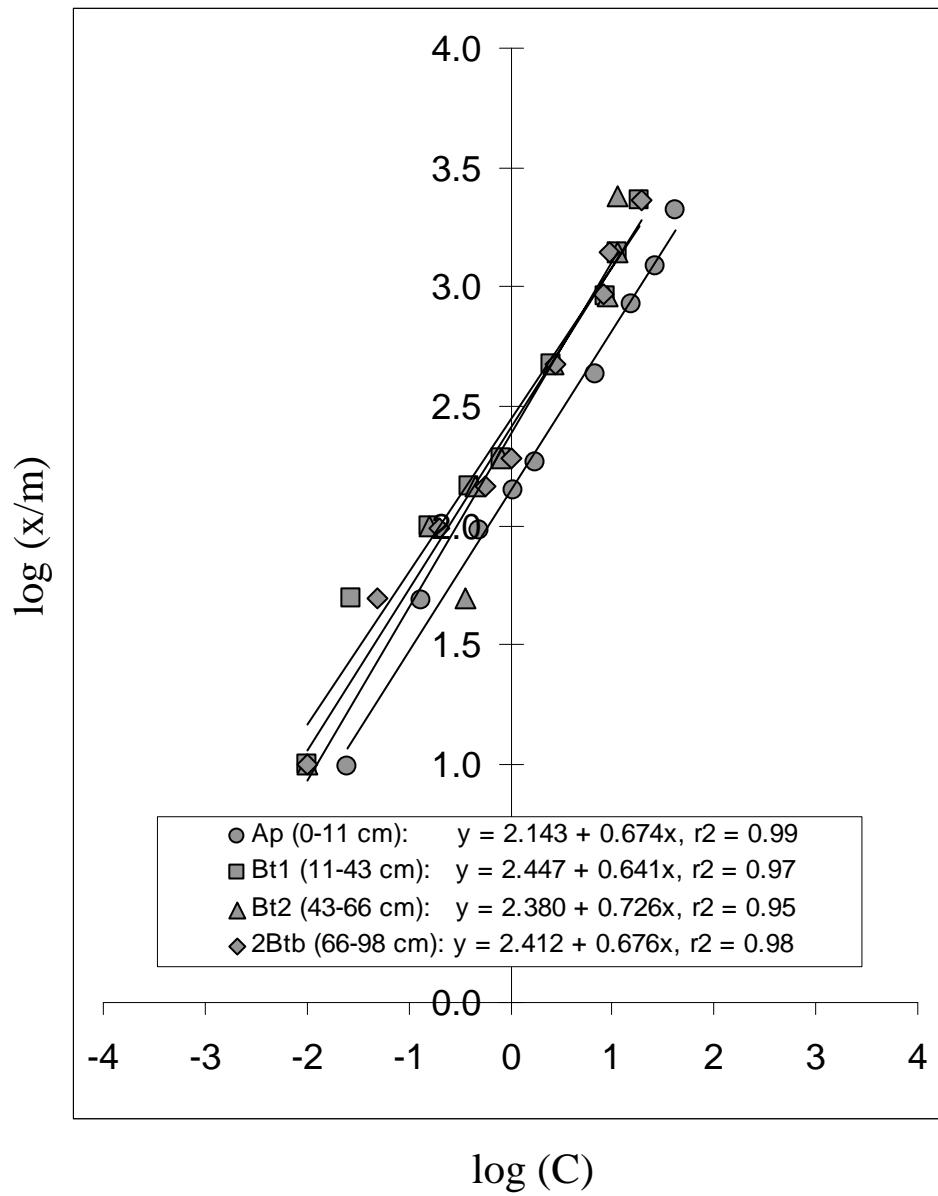


Pacca soil profile

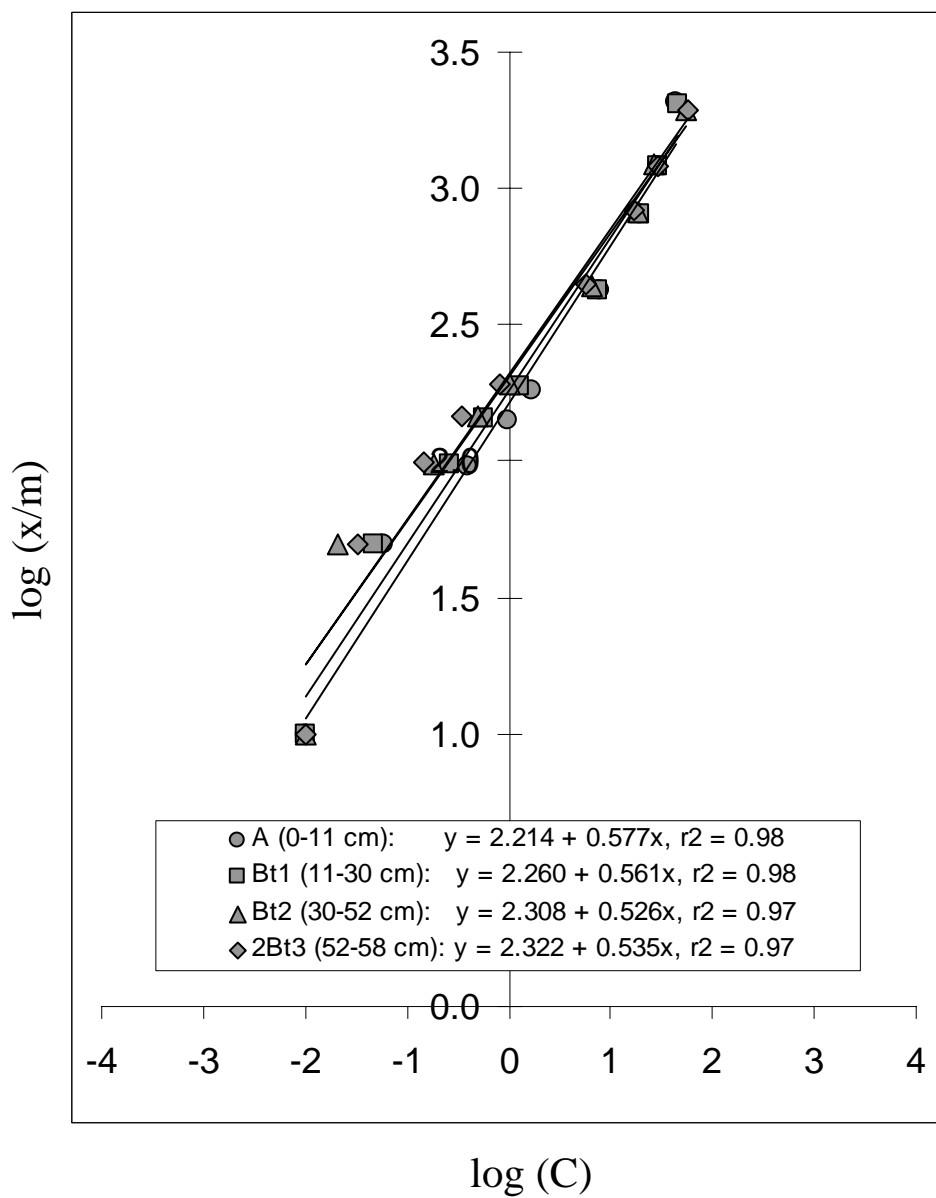


Pitafi soil profile

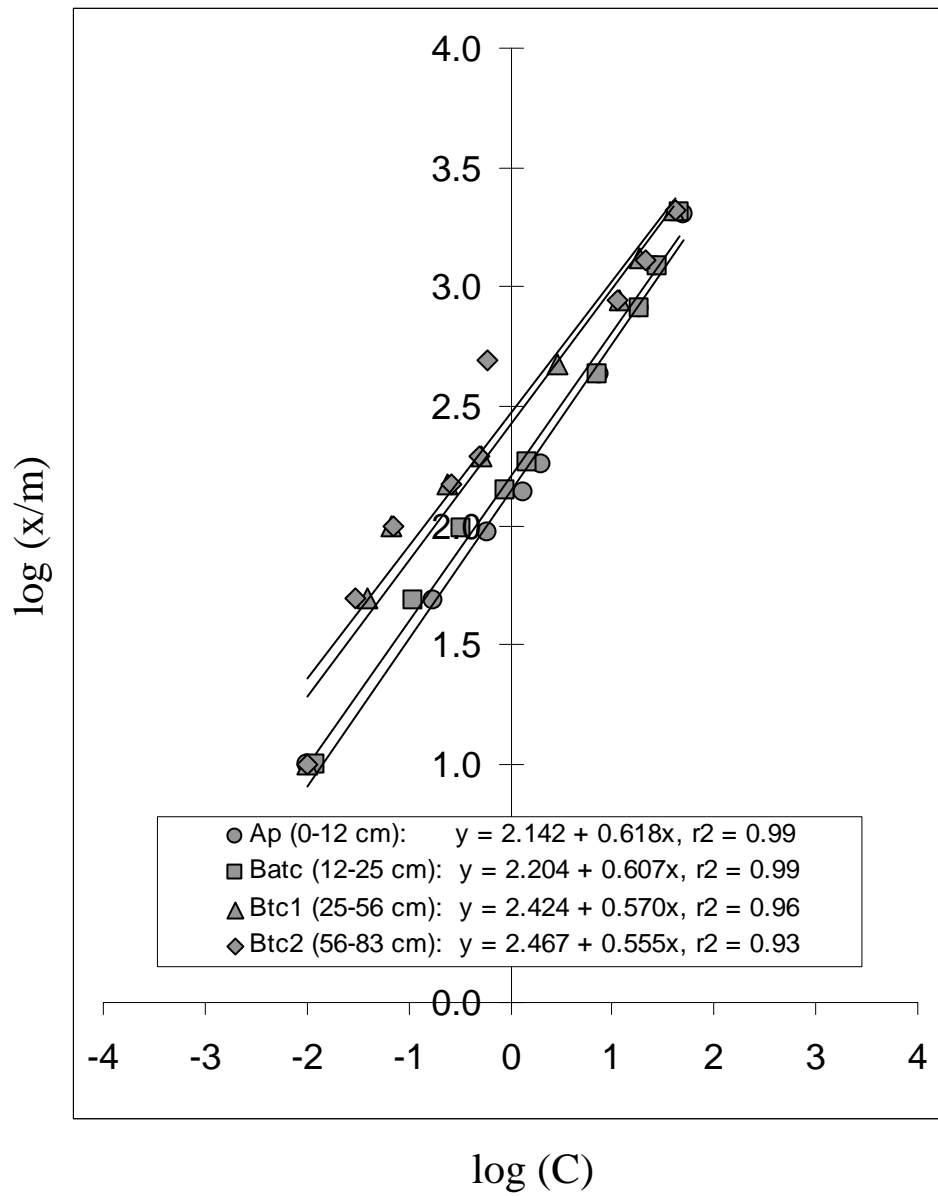
Peshawar soil profile

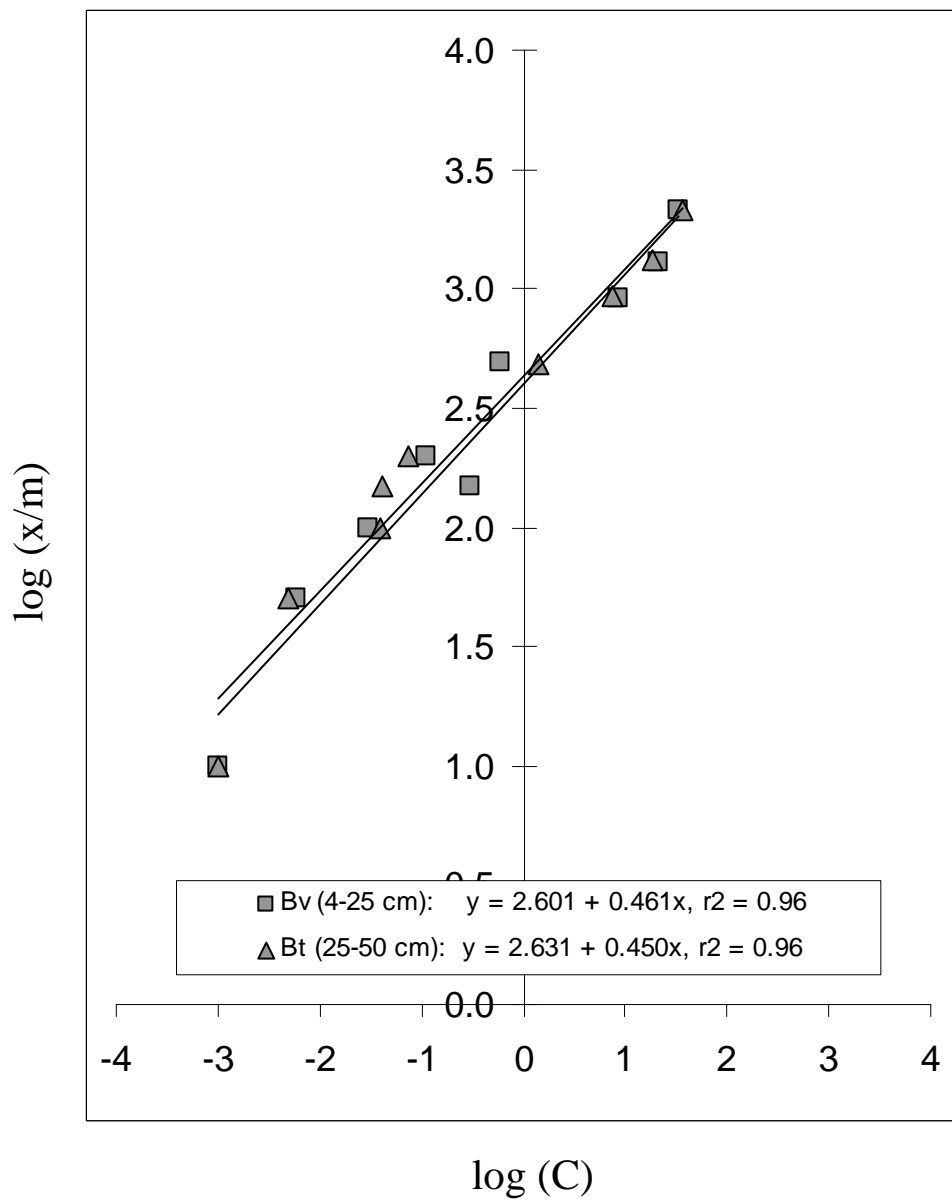


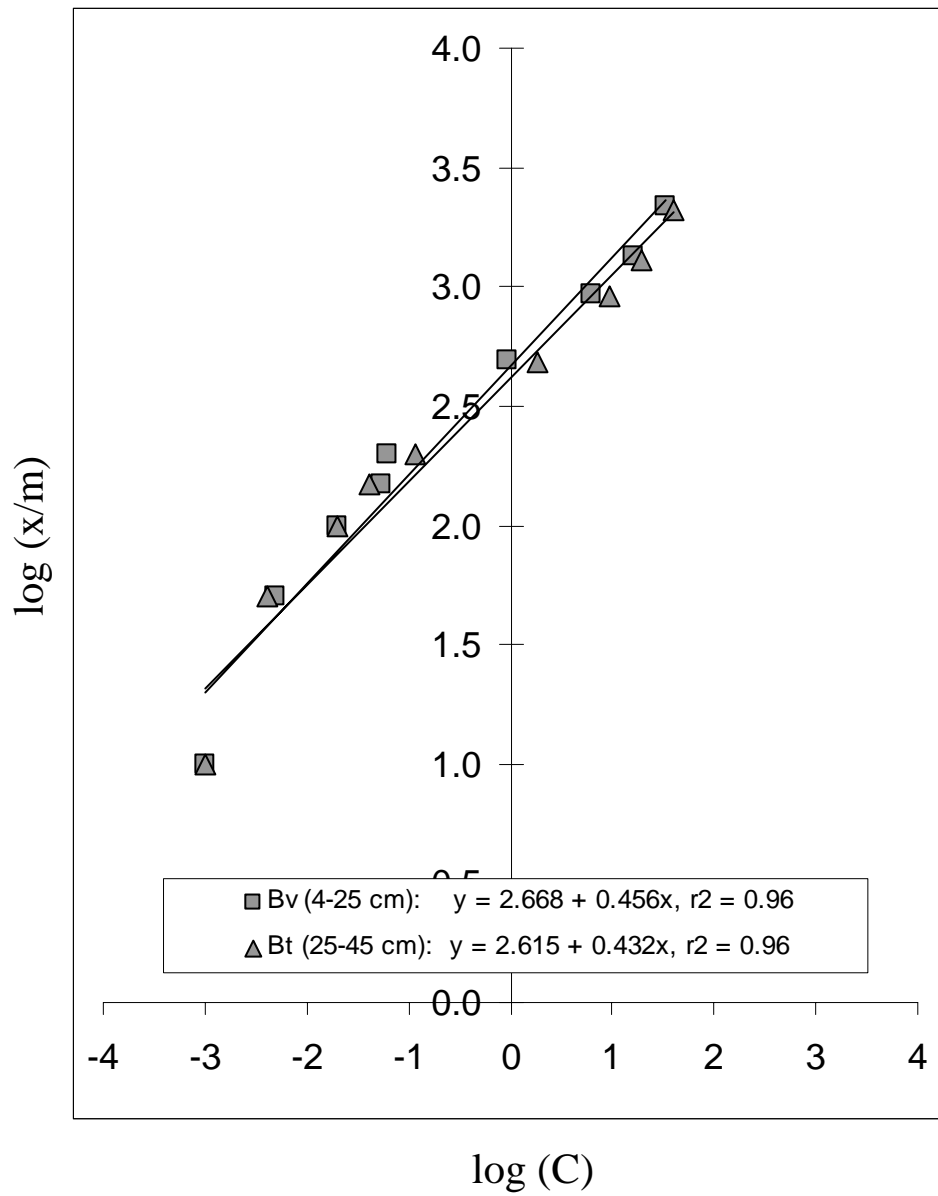
Murree soil profile



Guliana soil profile



Parabraunerde from Osterburken soil profile

Parabraunerde from Weingarten soil profile

Appendix X. Freundlich and Langmuir parameters of soils taken from four horizons (two horizons in case of German soils) of each soil profile investigated.

Soil	Horizon	Depth cm	Freundlich			Langmuir					
			b	k_f	r²	b₁	b₂	k₁	k₂	r²₁	r²₂
						mg kg ⁻¹		L mg ⁻¹			
Shahdara	Ap	0-16	1.60	128	0.99	208	5000	1.55	0.011	0.89	0.92
	C1	16-32	1.68	176	0.97	200	3333	3.57	0.030	0.98	0.98
	C2	32-63	1.61	119	0.97	192	2500	1.73	0.020	0.96	0.83
	C3	63-78	1.54	132	0.99	156	2000	2.37	0.050	0.92	0.99
Sultanpur	Ap	0-13	1.45	108	1.00	167	5000	1.50	0.012	0.84	0.90
	Bw1	13-39	1.59	156	0.98	204	2500	2.45	0.041	0.96	0.96
	Bw2	39-62	1.68	210	0.92	119	3333	14.00	0.045	0.96	0.95
	2C1	62-81	1.47	180	0.97	200	5000	2.78	0.024	0.94	0.98
Pacca	Ap	0-15	1.37	106	1.00	278	3333	0.75	0.019	0.99	1.00
	Bat	15-32	1.72	167	0.99	204	2500	3.50	0.044	0.98	1.00
	Bt1	32-53	1.52	183	0.97	200	2500	3.33	0.055	0.95	0.84
	Bt2	53-92	1.51	236	0.95	167	3333	7.50	0.056	0.99	0.83
Pitafi	Ap	0-15	1.35	1750	0.95	149	5000	22.33	0.074	0.92	0.92
	Ayz	15-41	1.25	490	0.96	133	3333	12.50	0.200	0.97	0.93
	Bwy1	41-57	1.41	364	0.93	132	3333	15.20	0.158	0.99	0.88
	Bwy2	63-111	1.28	545	0.96	145	3333	11.50	0.214	0.76	0.86
Peshawar	Ap	0-11	1.48	139	0.99	233	2500	1.65	0.037	0.98	0.90
	Bt1	11-43	1.56	261	0.97	227	2000	5.50	0.119	0.98	0.98
	Bt2	43-66	1.38	254	0.96	250	1429	3.64	0.189	0.99	1.00
	2Btb	66-98	1.48	264	0.97	222	5000	4.50	0.037	0.98	0.96
Murree	A	0-11	1.73	161	0.96	200	1667	3.57	0.063	0.96	0.82
	Bt1	11-30	1.78	181	0.98	217	1667	4.18	0.062	0.98	0.82
	Bt2	30-52	1.90	203	0.98	217	5000	5.75	0.013	0.97	0.89
	2Bt3	52-58	1.87	210	0.99	233	3333	5.38	0.022	0.99	0.91
Guliana	Ap	0-12	1.62	136	0.99	204	2000	2.04	0.044	0.93	0.84
	Batc	12-25	1.65	157	0.99	217	1667	2.71	0.071	0.98	0.84
	Btc1	25-56	1.76	265	0.99	270	1429	5.29	0.241	0.94	0.91
	Btc2	56-83	1.80	293	0.95	263	1429	5.43	0.368	0.93	0.96
Prb-Ostb	Ah	0-4									
	Bv	4-25	2.17	412	0.98	213	1429	47.00	0.412	0.94	0.97
	Bt	25-50	2.22	438	0.98	263	1429	38.00	0.467	0.98	0.98
	C	>50									
Prb-Wein	Bv	4-25	2.19	464	0.99	244	2000	41.00	0.068	0.92	0.90
	Bt	25-45	2.31	438	0.99	233	2500	47.78	0.073	0.99	0.89
	C	>45									

b and **k_f**, Freundlich constants; **r²**, coefficient of correlation for Freundlich; **b₁**, maximum sorption at high-affinity sites; **b₂**, maximum sorption at low-affinity sites; **k₁**, binding strength at high-affinity sites; **k₂**, binding strength at low-affinity sites; **r²₁**, coefficient of correlation at high-affinity sites; **r²₂**, coefficient of correlation at low-affinity sites.

Appendix XI. Phosphorus fractions (inorganic) as sequentially extracted, sum of inorganic P fractions, organic P and total P of the soils.

Soil	Horizon	Depth cm	-----mg kg ⁻¹ -----								
			Ca ₂ -P	Ca ₈ -P	Ca ₁₀ -P	Al-P	Fe-P	P _{ocl}	ΣP _{in}	P _O	P _T
Shahdara	Ap	0-16	<0.1	9.6	555	33.6	10.6	94.9	704	77.6	781
	C1	16-32	4.3	3.7	501	4.0	4.0	51.7	569	70.2	639
	C2	32-63	6.1	6.1	557	<0.1	<0.1	16.0	589	59.9	649
	C3	63-78	19.8	6.1	561	<0.1	0.8	32.4	622	26.6	649
Sultanpur	Ap	0-13	5.6	13.3	578	25.3	13.1	101.5	737	15.8	753
	Bw1	13-39	<0.1	7.7	703	75.1	<0.1	149.5	943	13.2	956
	Bw2	39-62	<0.1	<0.1	489	4.5	<0.1	62.7	563	12.9	576
	2C1	62-81	13.8	<0.1	434	<0.1	<0.1	39.9	495	92.6	588
Pacca	Ap	0-15	5.9	11.5	585	114.2	16.0	143.1	875	113.9	989
	Bat	15-32	4.2	5.4	532	59.8	9.9	103.5	714	7.1	721
	Bt1	32-53	<0.1	7.8	491	50.2	<0.1	75.4	631	4.4	635
	Bt2	53-92	10.6	6.8	456	11.3	<0.1	71.5	559	4.1	563
Pitafi	Ap	0-15	11.1	5.8	476	14.6	<0.1	96.6	605	42.7	648
	Ayz	15-41	7.4	4.9	523	6.0	<0.1	61.6	603	33.1	636
	Bwyl	41-57	<0.1	5.4	482	6.3	<0.1	83.4	582	36.9	619
	Bwy2	63-111	15.4	4.8	539	<0.1	<0.1	56.1	619	1.5	620
Peshawar	Ap	0-11	<0.1	9.1	602	20.4	16.9	89.8	741	70.8	811
	Bt1	11-43	<0.1	<0.1	503	12.1	<0.1	85.4	610	2.6	613
	Bt2	43-66	8.4	6.7	597	38.2	<0.1	115.9	769	22.2	791
	2Btb	66-98	26.7	8.7	815	80.2	<0.1	133.7	1068	2.5	1070
Murree	A	0-11	10.5	7.1	292	17.8	93.9	15.8	437	100.6	538
	Bt1	11-30	5.5	5.9	329	10.6	50.1	25.2	426	80.6	506
	Bt2	30-52	4.9	5.7	247	8.9	79.6	21.0	367	67.7	435
	2Bt3	52-58	10.1	6.8	232	8.8	94.5	11.0	363	62.2	425
Guliana	Ap	0-12	5.2	6.5	195	29.8	67.1	68.3	372	84.2	456
	Batc	12-25	<0.1	5.4	187	25.6	56.4	58.5	336	54.8	391
	Btc1	25-56	4.3	5.6	147	3.3	50.1	59.6	270	58.0	328
	Btc2	56-83	69.5	4.2	210	4.6	45.6	58.3	393	12.5	405
Prb-Ostb	Ah	0-4	68.6	12.8	51	104.4	337.8	140.6	715	138.4	854
	Bv	4-25	19.4	6.1	43	19.2	193.1	139.3	420	102.2	523
	Bt	25-50	19.9	5.6	342	27.1	178.3	225.1	798	61.7	860
	C	>50	10.8	4.9	701	15.0	47.9	179.2	958	34.4	993
Prb-Wein	Bv	4-25	7.0	5.9	15	<0.1	38.5	30.9	100	63.0	163
	Bt	25-45	5.5	5.2	68	<0.1	39.1	59.5	180	73.4	254
	C	>45	3.2	6.6	434	<0.1	4.1	46.4	494	16.9	511

Ca₂-P, NaHCO₃ extractable P; **Ca₈-P**, ammonium acetate extractable P; **Ca₁₀-P**, H₂SO₄ extractable; **Al-P**, ammonium fluoride extractable; **Fe-P**, NaOH-Na₂CO₃ extractable P; **P_{ocl}**, occluded P extracted by dithionite; **ΣP_{in}**, sum of inorganic P fractions; **P_O**, organic P from the difference of total P to sum of inorganic P fractions; **P_T**, total P by HClO₄ digestion method.

CaCO₃	Ca ₁₀ -P	b _f	P _{om}	Fe-P	Al _o	Al _d	Fe _{NaOH}
	0.66	-0.65	-0.52	-0.50	-0.50	-0.50	-0.49
	0.00	0.00	0.00	0.00	0.00	0.00	0.00
EC	P _{2ppm}	k _f	Ca _{ex}	k ₁	Al _o /Al _d	k _{nonlin}	Fe _o /Fe _d
	0.96	0.93	0.59	0.52	0.50	0.49	0.43
	0.00	0.00	0.00	0.00	0.00	0.00	0.01
P_{Olsen}	Ca ₈ -P	Al-P	P _{oc1}	P _T	OM	P _{tin}	b ₁
	0.69	0.56	0.51	0.49	0.48	0.43	0.38
	0.00	0.00	0.00	0.00	0.00	0.01	0.03
Ca₂-P	Fe-P	b ₁ /b ₂	OM	Al _d	Sm	pH	Al _o
	0.58	0.45	0.43	0.42	0.39	-0.35	0.34
	0.00	0.01	0.01	0.01	0.02	0.04	0.05
Ca₈-P	OM	P _{Olsen}	Al-P	P _T	r _f ²	P _{tin}	k ₂
	0.71	0.69	0.68	0.46	0.42	0.40	-0.34
	0.00	0.00	0.00	0.01	0.02	0.02	0.06
Al-P	Ca ₈ -P	P _T	P _{tin}	P _{oc1}	P _{Olsen}	OM	Fe-P
	0.68	0.65	0.60	0.58	0.56	0.51	0.30
	0.00	0.00	0.00	0.00	0.00	0.00	0.08
Fe-P	b _f	Fe _o	pH	OM	Al _o	P _{om}	Ca ₁₀ -P
	0.71	0.70	-0.68	0.67	0.67	0.62	-0.62
	0.00	0.00	0.00	0.00	0.00	0.00	0.00
P_{oc1}	P _T	P _{tin}	Al-P	P _{Olsen}	KI	Al _o	Clay
	0.71	0.69	0.58	0.51	-0.48	0.47	0.42
	0.00	0.00	0.00	0.00	0.00	0.00	0.01
Ca₁₀-P	P _{tin}	P _T	b _f	pH	CaCO ₃	Fe _{NaOH}	Fe-P
	0.83	0.76	-0.74	0.68	0.66	-0.64	-0.62
	0.00	0.00	0.00	0.00	0.00	0.00	0.00
P_{tin}	P _T	Ca ₁₀ -P	P _{oc1}	Al-P	b _f	KI	Fe _{NaOH}
	0.99	0.83	0.69	0.60	-0.55	-0.50	-0.49
	0.00	0.00	0.00	0.00	0.00	0.00	0.00
P_T	P _{tin}	Ca ₁₀ -P	P _{oc1}	Al-P	b _f	KI	P _{Olsen}
	0.99	0.76	0.71	0.65	-0.52	-0.50	0.49
	0.00	0.00	0.00	0.00	0.00	0.00	0.00
P_{om}	Fe-P	OM	Ca ₁₀ -P	CaCO ₃	Fe _{NaOH}	pH	Fe _o
	0.62	0.56	-0.53	-0.52	0.44	-0.40	0.40
	0.00	0.00	0.00	0.00	0.01	0.02	0.02
Fe_{NaOH}	Ca ₁₀ -P	CaCO ₃	P _{tin}	Fe-P	P _{om}	P _T	KI
	-0.64	-0.49	-0.49	0.47	0.44	-0.43	0.41
	0.00	0.00	0.00	0.00	0.01	0.01	0.01
Fe_{CBD}	Fe _d	Fe _{crs}	Al _o	Al _d	b _f	Clay	Fe _o
	0.96	0.96	0.71	0.68	0.64	0.56	0.55
	0.00	0.00	0.00	0.00	0.00	0.00	0.00
Vm	Gt _S	b ₁	Sm	b ₁ /b ₂	b _{nonlin}	Ca _{ex}	OM
	0.47	0.39	0.38	0.34	-0.33	0.33	-0.29
	0.00	0.03	0.02	0.06	0.06	0.05	0.09
Sm	Gt _C	Ca ₂ -P	Vm	r _f ²	OM	Fe _{NaOH}	P _{2ppm}
	0.40	0.39	0.38	-0.34	-0.30	-0.29	0.29
	0.02	0.02	0.02	0.05	0.09	0.09	0.11
KI	P _{tin}	P _T	Fe _o /Fe _d	P _{oc1}	b _{nonlin}	Fe _{NaOH}	Ca ₁₀ -P
	-0.50	-0.50	-0.50	-0.48	0.42	0.41	-0.36
	0.00	0.00	0.00	0.00	0.02	0.01	0.03
Ca_{ex}	P _{2ppm}	k _f	Al _o /Al _d	EC	k _{nonlin}	pH	Vm
	0.66	0.63	0.63	0.59	0.36	0.36	0.33
	0.00	0.00	0.00	0.00	0.04	0.03	0.05

Gt_c	Gt _S	OM	Al _o /Al _d	Sm	P _{ocl}	Fe _{crs}	b _{nonlin}
	0.60	-0.57	-0.55	0.40	0.37	-0.34	-0.34
Al_o	Al _d	Fe _o	pH	b _f	Fe _d	Fe _{CBD}	Fe _{crs}
	0.89	0.85	-0.77	0.77	0.72	0.71	0.68
Al_d	Al _o	b _f	Fe _o	Fe _d	pH	Fe _{crs}	Fe _{ocl-P}
	0.89	0.76	0.71	0.71	-0.70	0.68	0.68
k_{nonlin}	k ₂	P _{2ppm}	k _f	EC	r _f ²	Fe _o /Fe _d	K ₁
	0.83	0.67	0.65	0.49	-0.41	0.37	0.37
b_{nonlin}	Kl	Fe _o /Fe _d	k ₁	Gt _c	Vm	Fe _o	b _f
	0.42	-0.41	-0.36	-0.34	-0.33	-0.32	-0.30
	0.02	0.02	0.04	0.06	0.06	0.07	0.10